Expanding Applications of Portable Biological Systems:

Enhancements to Mammalian Gene Editing and

Bacterial Quorum Sensing Networks

by

René Daer

A Dissertation Presented in Partial Fulfillment
of the Requirements for the Degree
Doctor of Philosophy

Approved September 2017 by the
Graduate Supervisory Committee:

Karmella Haynes, Chair
David Brafman
David Nielsen
Samira Kiana

ARIZONA STATE UNIVERSITY

December 2017

ABSTRACT

The portability of genetic tools from one organism to another is a cornerstone of synthetic biology. The shared biological language of DNA-to-RNA-to-protein allows for expression of polypeptide chains in phylogenetically distant organisms with little modification. The tools and contexts are diverse, ranging from catalytic RNAs in cell-free systems to bacterial proteins expressed in human cell lines, yet they exhibit an organizing principle: that genes and proteins may be treated as modular units that can be moved from their native organism to a novel one. However, protein behavior is always unpredictable; drop-in functionality is not guaranteed.

My work characterizes how two different classes of tools behave in new contexts and explores methods to improve their functionality: 1. CRISPR/Cas9 in human cells and 2. quorum sensing networks in *Escherichia coli*.

1. The genome-editing tool CRISPR/Cas9 has facilitated easily targeted, effective, high throughput genome editing. However, Cas9 is a bacterially derived protein and its behavior in the complex microenvironment of the eukaryotic nucleus is not well understood. Using transgenic human cell lines, I found that gene-silencing heterochromatin impacts Cas9's ability to bind and cut DNA in a site-specific manner and I investigated ways to improve CRISPR/Cas9 function in heterochromatin.

2. Bacteria use quorum sensing to monitor population density and regulate group behaviors such as virulence, motility, and biofilm formation. Homoserine lactone (HSL) quorum sensing networks are of particular interest to synthetic biologists because they can function as "wires" to connect multiple genetic circuits. However, only four of these networks have been widely implemented in engineered systems. I selected ten quorum sensing networks based on their HSL production profiles and confirmed their functionality in *E. coli*, significantly expanding the quorum sensing toolset available to synthetic biologists.

To my husband,
for pushing me when the days were tedious,
for pulling me away when they were overwhelming.
For your unwavering support and partnership.
Thank you.

To my family,
for your patience and support
and for making our time together fun and fulfilling.

To my parents,
who exemplify hard work and commitment.
Who give to, support, and love their children unconditionally.
Whose pride I don't deserve
but will continue to strive to earn.

To my friend and teammate, Katherine,
for your support and friendship,
without which I would have been lost
and probably still drafting some email from 2013.

ACKNOWLEDGMENTS

TABLE OF CONTENTS

LIST OF TABLES

Chapter 1

INTRODUCTION

1.1 Part I: Cas9 and Chromatin

1.1.1 Chromatin

Chromatin is the DNA, protein, and RNA complex that compacts and organizes genomic DNA into eukaryotic nuclei and controls gene expression. It was first described by Walther Flemming in 1879 after he developed staining solutions to visualize cell division.[1] He named the rod-like structures he observed during mitosis "chromatin," meaning stainable material.[2]

Chromatin can be divided into two types: 1. Euchromatin is characterized by having an "open" or not-compacted structure often with activating chemical modifications and associated proteins Figure 1.1. It is accessible to DNA binding proteins like RNA polymerase and is therefore permissive to transcription; 2. Heterochromatin is characterized by a "closed" or tightly compacted structure with silencing marks and proteins Figure 1.1. It is generally not accessible to DNA binding proteins and thus does not allow for gene expression.

Heterochromatin can be further divided into constitutive heterochromatin and facultative heterochromatin Figure 1.1. Constitutive heterochromatin is found mostly in the pericentromeric regions of chromosomes and on the telomeres. These regions are very stable and contain long repeat sequences with few protein coding sequences. Constitutive heterochromatin clusters near the nuclear membrane. Facultative heterochromatin is more dynamic than constitutive and is responsible for silencing genes and controlling differential gene expression, as is seen in different tissue types or allele-specific silencing. It also controls expression of genes at the appropriate times and concentrations during development of multicellular organisms.

The basic building block of chromatin is the nucleosome, a DNA-protein complex composed of 147 basepair of DNA wrapped around an octamer of histone proteins Figure 1.2 a. Some of the amino acids in histone proteins have unstructured tails that can be chemically modified with either activating or silencing marks. The chromatin state at a particular locus is characterized by the presence of nucleosomes, their proximity to each other, and the chemical modification(s) found on them. The protein complexes that affect these characteristics are called chromatin modifying protein groups. In our work, we focus on one class of facultative heterochromatin regulated by a class of proteins called Polycomb group (PcG) proteins.

1
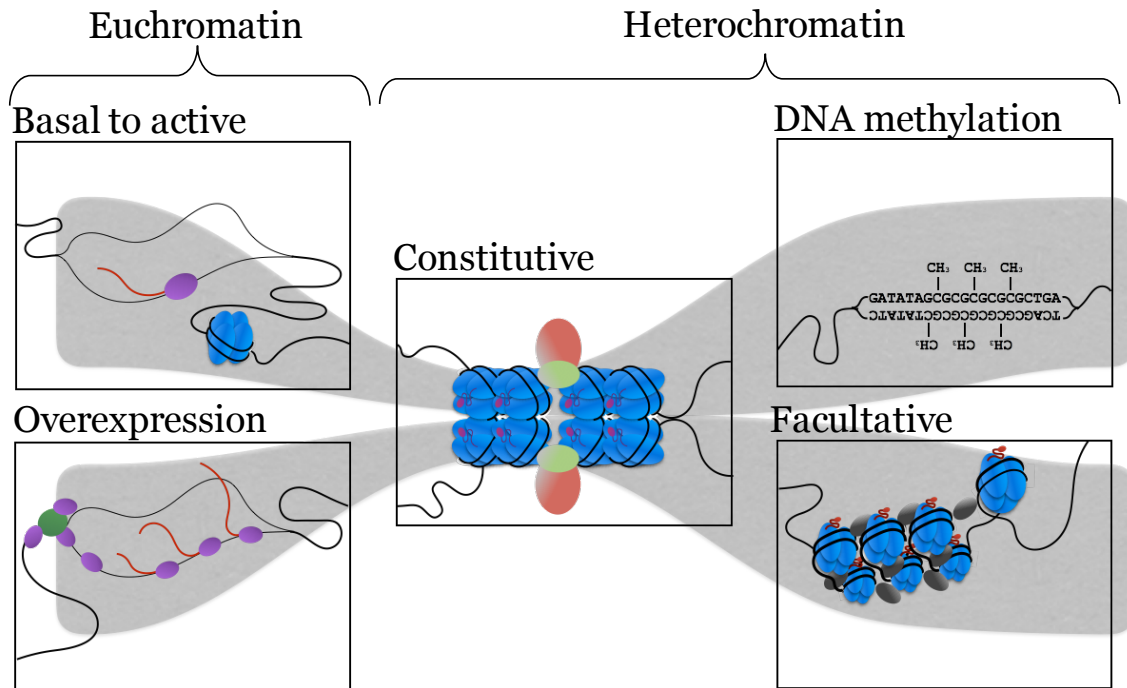
Figure 1.1. Classes of human chromatin. Human chromatin can be divided into two classes: euchromatin and heterochromatin. Euchromatin is decompacted and permissive to RNA Polymerase and thus can have different levels of transcriptional activity. Heterochromatin is tightly compacted and can be further divided based on the associated proteins and histone modifications. For example, constitutive heterochromatin is found in the pericentromeric regions, DNA methylation is associated with CpG rich regions, and facultative heterochromatin controls expression of genes during development and differentiation.[3]

1.1.2 Polycomb Group Proteins

In 1977, Pamela Lewis first identified a *Drosophila* gene coding for a protein called Polycomb.[4] The following year, Ed Lewis described Polycomb as a "regulator of regulators" and proposed it was responsible for controlling the segmentation of the bodies of *Drosophila*.[5] A series of studies in the 1980's revealed that two protein groups, PcG and Trithorax group (TrxG), act antagonistically to control expression of genes responsible for body segmentation, growth, and other crucial steps during *Drosophila* embryonic development.[6–9] It was proposed that these gene expression states are inherited as a form of cellular memory.[10]

While the early work was done in *Drosophila*, PcG and TrxG protein homologs are found in all metazoans. van der Lugt et al. and Coré et al. made Polycomb protein knockout lines to demonstrate that PcG proteins regulate Hox genes in mice.[11,12] In addition to controlling
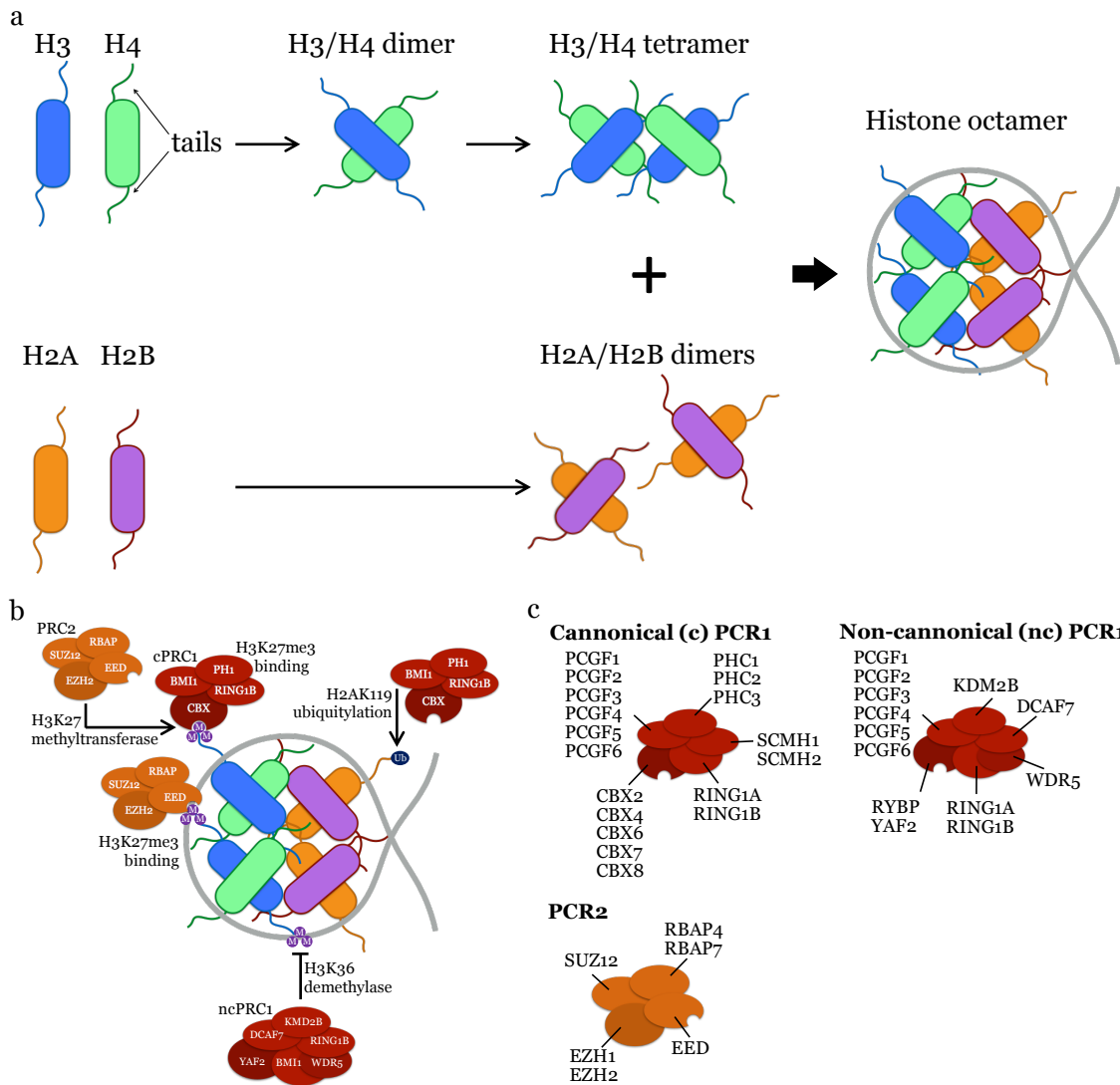
Figure 1.2. Composition of nucleosomes and the role of Polycomb group proteins in regulating them. (a) A nucleosome is a DNA-protein complex with 147 basepair of genomic DNA wrapped around a multimer of eight histone proteins: one H3-H4-H3-H4 tetramer and two H2A-H2B dimers. Histones have unstructured amino acid tails that can be modified to effect the chromatin state. (b) Polycomb repressive complexes 1 and 2 (PRC1 and PRC2) modify and bind to histone tails. The EZH2 protein of PRC2 writes the histone 3 lysine 27 trimethylation (H3K27me3) silencing marks while the EED protein binds to them. In canonical PRC1 (cPRC1), the CBX subunit binds to H3K27me3 while BMI1 writes histone 2A lysine 119 ubiquitilation (H2AK119ub). In non-canonical PRC1 (ncPRC1), KMD2B demethylates histone 3 lysine 36 (H3K36). (c) List of the proteins that can compose different PRC1 and PRC2 variants. For each list, one protein from the group is included in the complex.

gene expression during development, they are responsible for regulating expression of many important cellular processes like senescence, proliferation, and memory of expression states during mitosis.[10,13] Misregulation of PcG and TrxG proteins can lead to cancer.[14–16] Extensive research has been done to understand their function during normal development and how their misregulation results in disease.

1.1.3 Mechanism of Polycomb-Mediated Gene Silencing

Polycomb-mediated gene silencing is controlled by two major PcG complexes: Polycomb repressive complex 1 (PRC1) and Polycomb repressive complex 2 (PRC2). PRC2 can both write and bind to the silencing mark histone 3 lysine 27 trimethylation (H3K27me3) (Figure 1.2 b.[17–20] PRC1 can also bind to H3K27me3[21] as well as ubiquitilate H2AK119 (Figure 1.2 b).[22] In mammals, there are multiple variants of PRC1 and PRC2 (Figure 1.2 c). Expression of different PcG variants and accessory proteins adds an additional level of gene expression control during differentiation. PRC2 accessory proteins change PRC2 function and are hypothesized to control differential gene expression in different tissues (for a review of composition and expression of PcG variants see Schuettengruber et al.).

Until recently, chromatin silencing by PcG proteins was theorized to be hierarchical: PRC2 deposits H3K27me3 followed by PRC1 recruitment and binding to H3K27me3, compacting chromatin and propagating the silencing mark. However, new data suggest that there is not a single model for PcG control of chromatin;[3,23] there are examples of loci that are silenced by only PRC1[24,25] or only PRC2.[26] While these mechanisms are still being investigated, it is clear that localization of PcG proteins and deposition of H3K27me3 results in nucleosome compaction and gene silencing. This compaction blocks access to local DNA by polymerase, activating protein groups, and nucleosome remodeling proteins, causing heritable silencing of local chromatin.

PcG proteins also control chromatin packaging on a genomic scale. Chromatin organizes into higher order structures of active or silenced gene expression called topologically associating domains (TADs).[27,28] These compartments contain regions separated by megabases on the same chromosome or regions from different chromosomes, pulled together by interactions between chromatin-associated proteins. Early observations showed PcG proteins were localized into clusters inside nuclei.[29,30] It was later discovered that silent TADs contain high levels of H3K27me3, the silencing mark deposited by PRC2.[31,32] Furthermore, exogenously introducing H3K27me3 results in TAD formation.[33] Taken together, these observations suggest that PcG proteins regulate higher-order chromatin compaction.[34,35] While the mechanism for this compaction is not completely understood, current research is beginning to shed more light. For example, PRC1 interacts across long distances with

other PRC1 complexes.[35−38] While PRC2 is also involved, only PRC1 is necessary to form TADs.[31,36] For a full review of the role of Polycomb in long range chromatin interactions, see Entrevan et al.

1.1.3.1 Recruitment

While there has been significant effort in this area, it is still unclear how PcG complexes are recruited to a target site in mammalian genomes. *Drosophila* contain Polycomb response elements (PREs) that recruit PcG proteins, even in the absence of nucleosomes.[39−41] However, in mammalian nuclei, the evidence is less clear and sometimes appears conflicting. A model for mammalian recruitment proposes that PRC2 deposits the silencing mark H3K27me3, which both PRC1 and PRC2 bind to (reviewed in Simon et al.). PRC2 binding recruits more PRC2 complexes, propagating the silencing mark. PRC1 complexes bind H3K27me3 and interact with each other, pulling nucleosomes closer together and compacting the chromatin. However, there are other factors that are known to recruit PcG proteins. For example, PcG-recruiting non-coding RNAs (ncRNAs) have been identified.[43] CpG islands are also proposed as PcG protein recruiters, though some evidence suggests that only silent CpG islands recruit Polycomb.[44] Some evidence suggests ncPRC1 ubiquitilation of H2A recruits both PRC1 and PRC2.[22,45] However, there is also evidence that the ubiquitilation activity of PRC1 is not required for PcG-mediated silencing.[46,47] It is likely that there are several forms of PcG recruitment in mammalian genomes, possible utilized at different steps of development and differentiation, adding yet another level of transcriptional control. For a full review of the current research on PcG recruitment, see Schuettengruber et al.

In summary, human chromatin is dynamic and complex, and we are still years away from having a full understanding of it. As synthetic biology moves into more complicated organisms, it is crucial to appreciate this fact while not being deterred by it. We can apply our current understanding of chromatin to investigate how exogenous tools like CRISPR/Cas9 interact with the complexity of mammalian chromatin.

1.1.4 Engineered CRISPR/Cas9 Systems and Chromatin

CRISPR/Cas9, a nucleic acid modifying system borrowed from prokaryotes, is a popular tool for editing eukaryotic DNA. Gene editing efforts have been successful in many cases, but the complex structure of chromatin and its variation in different cells still pose a barrier to reliable and consistent use. Since Jinek et al. first demonstrated the programmability of the CRISPR/Cas9 system, it has rapidly become a popular tool for rapid, high-throughput

genome engineering.[48] In 2013, Gilbert et al. showed that Cas9 is able to efficiently bind and edit mammalian genomes.[49] However, as Cas9 is bacterially derived, it remained unclear whether Cas9 could efficiently edit target sites located in heterochromatin, the dynamic network of non-coding RNA, scaffolding proteins, and protein-modifying enzymes that organizes the packaging of DNA and regulates the expression of genes in eukaryotic nuclei (subsection 1.1.1).[50–52]

In chapter 2, we used a transgenic cell line that allows us to control the chromatin state at a transgenic *luciferase* reporter.[53,54] Addition of the small molecule drug doxycyclin (dox) initiates direct Polycomb-mediated silencing at a *luciferase* transgene, as confirmed with luciferase assay and chromatin immunoprecipitation (ChIP) assay.[54] We compared Cas9 binding through chromatin immunoprecipitation (ChIP) and editing through cleavage-induced non-homologous end-joining repair (NHEJ) in both open and closed chromatin along a single locus. We found that Cas9 editing was completely blocked by heterochromatin at four of nine gRNA targets and that editing was reduced at two sites. Editing at three of the target sites showed no reduction in binding or editing,[54] which suggests that inhibition of Cas9 is discontinuous across regions of closed chromatin.

Our study added to a rapidly growing body of work that support the hypothesis that chromatin states have a strong influence on the accessibility of DNA to Cas9 (Figure 1.3). Several studies have found that off-target binding of non-cleaving deactivated Cas9 (dCas9) is highly correlated with open chromatin, as characterized by DNaseI hypersensitivity.[55–58] Furthermore, Cas9 off-target binding prediction tools that incorporate chromatin state information as a parameter outperform those that do not.[58] Additional studies used libraries of gRNAs targeted across genomes to demonstrate Cas9's preference for regions of open chromatin via CRISPRi-mediated transcriptional regulation[59–62] or Cas9-mediated cleavage.[63,64]

In a series of in vitro studies, researchers provided the first evidence of a mode of chromatin inhibition of Cas9. Using reconstituted nucleosomes complexed with a synthetic DNA sequence, Hinz et al.,[65] Isaac et al.,[66] and Horlbeck et al.[59] showed that Cas9-mediated binding and cleaving of the DNA sequence is completely blocked when it is complexed with the nucleosome. It is important to note that this synthetic sequence associates more tightly with nucleosomes than natural sequences.[67,68] Utilizing transgenic cell lines, Chen et al. showed that ectopic constitutive HP1-mediated heterochromatin compaction inhibits Cas9 binding and editing in HEK293T cells.[69] They targeted the KRAB domain to two transgenes and compared gRNA editing efficiency at each locus in the open or closed state.[69] Of eight target sites within 1500 bp of the nucleation sites, none showed complete inhibition but all showed greater than 1.5-fold reduction in editing efficiencies in the closed state compared to open.[69]
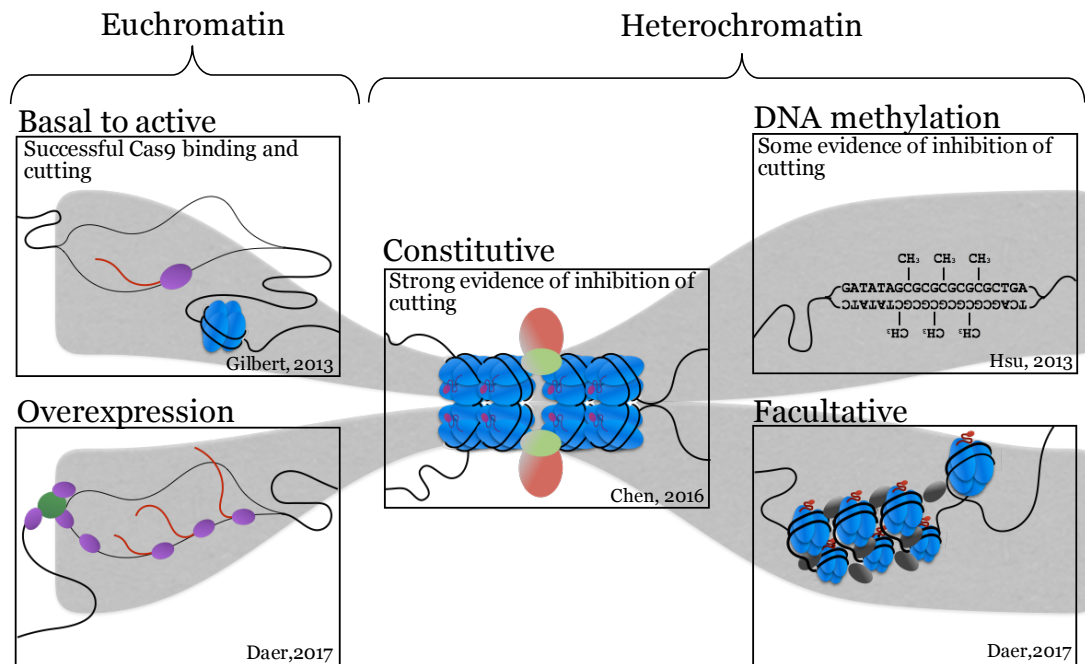
Figure 1.3. Summary of current literature on Cas9 inhibition by human chromatin. Since Gilbert et al., many studies have demonstrated that Cas9 efficiently cuts target sites in open chromatin.[49] Overexpression can evict repressive chromatin (chapter 3) but also hamper Cas9 activity.[54] Hsu et al. provided indirect evidence of inhibition of Cas9 by DNA methylation.[74] Chen et al. and Daer et al. provided direct evidence of inhibtion of Cas9 by constitutive[69] and facultative[54] heterochromatin.

There also exists conflicting evidence that suggests that Cas9 is not impeded by chromatin compaction. Some studies have found that Cas9 is able to efficiently access target sites located in closed chromatin.[70–73] We propose that this is not conflicting evidence, but rather that these data support the hypothesis that Cas9's interaction with chromatin is complex, with the level of inhibition seeming to depend on target site.

Cas9 is rapidly becoming an important tool for bioengineering applications. Therefore, it is becoming increasingly important to solve the problem of inconsistent, site-specific inaccessibility and varying Cas9 efficiency. The relationship between chromatin states, gene expression, and Cas9 editing in cells warrants further investigation. To this end, in chapter 3 we propose methods for improving Cas9 editing at previously inhibited sites by artificially opening chromatin. In our previous work, we demonstrated that artificial conversion of closed chromatin towards a more transcription-permissive state via siRNA-mediated knockdown of the repressive Polycomb protein Suz12 was accompanied by an increase in Cas9-mediated editing efficiency.[54] It is difficult to control the consistency and

magnitude of siRNA delivery. Therefore, we explored alternative methods to induce an open, Cas9-accessible state at closed chromatin.

In chapter 3, we expanded our investigation to two methods for disrupting closed chromatin: a chromatin-disrupting drug (Figure 3.2) and site-directed chromatin modification with targeted transcriptional activators (Figure 3.5). Transcription-activating fusion proteins have been shown to change chromatin accessibility.[72] Furthermore, Isaac et al. and Horlbeck et al. used nucleosome-sliding enzymes to improve Cas9 cleavage of DNA complexed with nucleosomes in vitro.[59,66] Together, these works suggest that targeting silenced chromatin for remodeling could improve Cas9 editing in human cells. To test this hypothesis, we determined the effect of our global and targeted chromatin reopening approaches on transgene expression and chromatin profile. We next analyzed Cas9 editing at a set of sites located downstream from the nucleation site of ectopic chromatin formation. Finally, we investigated whether chemically modified sgRNAs affect Cas9 editing in silenced chromatin. We found that strong induction of transcription from a nearby promoter followed by culturing for several days to allow recovery of a generally permissive chromatin state improved editing at some target sites. Preliminary data suggest our synthetic sgRNA approach could be a promising alternative for editing in challenging loci. Our results inform a general approach for overcoming challenges associated with site-specific Cas9 inaccessibility.

1.2 Part II: Quorum Sensing

1.2.1 Overview of Quorum Sensing Systems

Quorum sensing networks enable bacteria to monitor and respond to changes in population density by coupling gene regulation with diffusible chemical signals from neighboring bacteria.[75] Some species of bacteria use this signaling to control group behaviors such as virulence, biofilm formation, and motility.[76] One class of these chemical signals, known as HSLs*, are produced by a family of synthase enzymes.[77−79] Accumulation of HSLs results in activation of a regulator protein that controls expression of group behaviors. Homologous HSL networks have been identified in over 100 species of bacteria and more networks are regularly being discovered.[80,81] Each network includes an HSL synthase protein that catalyzes the synthesis of specific HSL signaling molecules, a regulator that is allosterically regulated by the HSL ligand, and a promoter that typically contains a palindromic sequence that is bound by the regulator as a monomer or homomultimer (Figure 1.4).[82,83]

---

*These chemicals have traditionally been referred to as N-acyl homoserine lactones (AHLs). However, some synthases produce non-acyl chain homoserine lactones (HSLs) so we use the more inclusive HSL.
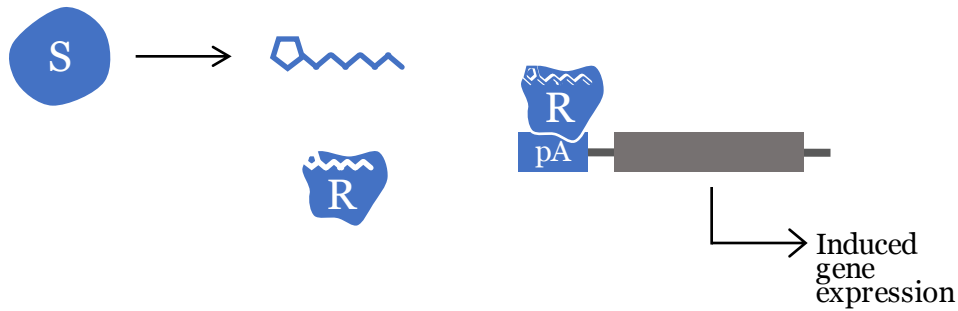
Figure 1.4. General HSL signaling network. An HSL synthase protein produces the HSL signaling molecule. The regulator protein is activated after binding to the HSL and binds to its DNA binding domain. Binding of the HSL-regulator complex activates transcription of genes associated with group behaviors.[75,76]

There are some exceptions to this network architecture. In *Pantoea stewartii*, the regulator EsaR binds to DNA in the absence of its HSL and blocks polymerase from transcribing downstream genes.[84] Accumulation of its HSL releases EsaR and results in upregulation of associated genes.

1.2.2   Quorum Sensing Applications

Scientists have taken advantage of the simplicity of this system to incorporate signal processing pathways into gene circuits as genetic wires to convert an output from one computation into an input of another. In an engineered system, the synthase protein can be considered a "sender module" which produces the input for a "receiver module" comprised of the regulator and the inducible promoter upstream of an output, such as GFP.[85] Engineered quorum sensing networks are used for a variety of applications including metabolic engineering, computational circuits, and medicine. For example, Gupta et al. used the Esa network to build a valve that can control dynamic flux to improve titers of *myo*-inositol, glucaric acid, and shikimate.[86] Chen et al. used two quorum sensing networks, Cin and Rhl, to couple two strains that communicate to control synchronized oscillation.[87] This kind of system could be used to split production of a fermentation product across two strains and tune growth and expression for more efficient bioproduction. Growth can be controlled by expressing a self-lysing gene in response to a threshold population density.[88] Other examples are discussed in detail in chapter 4, including digital and analog computation,[89] edge detection,[90] and engineered biofilm formation.[91]

1.2.3 Limits to Engineering with Quorum Sensing

Most examples of engineered quorum sensing systems use synthetic HSLs added exogenously, limiting the potential complexity of the genetic circuit. Engineered quorum sensing systems that incorporate HSL senders can achieve more complex computation and behavioral cooperation across populations in co-culture or on agar plates. However, promiscuity of the synthase and regulator proteins limits potential complexity. In spite of the natural diversity of quorum sensing networks and their utility to bioengineers, only three—Lux, Las, and Rhl—have been extensively used in reported synthetic systems.

HSL molecules contain a variable R-group that extends from a homoserine lactone ring; the chemistry of the R-group contributes to network diversity (Figure 1.5 and reviewed in chapter 4).[92] Variability arises from the chain length (from 3 to 18 carbons), the saturation of the chain, and the presence of modifications such as methyl or phenol groups. In most cases, regulator proteins bind and respond to the specific HSL produced by the synthase protein. However, since the space of possible HSLs is limited, there are species that produce and respond to the same HSLs. Furthermore, many synthases produce more than one HSL and there are species which have regulator proteins without a synthase protein.[93,94] This results in overlap in signal production and response which manifests as crosstalk and eavesdropping. There are examples of both competitive and cooperative eavesdropping.[77] *Pseudomonas aeruginosa* and *Burkholderia cepacia* coordinate virulence in co-infections.[95] Others, such as *B. thailandensis* and *Chromobacterium violaceum*, produce antibiotics to disrupt biofilm formation of neighboring strains.[96]

1.2.4 Crosstalk Between Quorum Sensing Networks

As in nature, these networks exhibit crosstalk with each other in engineered systems (Figure 1.6): synthases produce many species of HSLs (Figure 1.6b); the HSLs produced by one synthase activates a regulator from a different system (Figure 1.6c); and regulators bind to promoters from different systems (Figure 1.6d). The promiscuity of the most commonly used regulator, LuxR, was explored by Canton et al. who reported LuxR-activated expression of a GFP reporter in response to a range of HSLs.[97] Others have identified promoter crosstalk—wherein the regulator from one system can bind and activate expression at a promoter from another system—as an additional level of crosstalk limiting the potential complexity of genetic circuits.[84,98−100]

Generic HSL structure
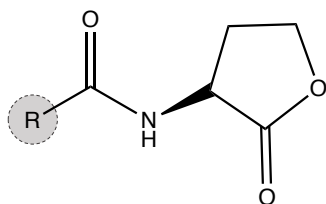
N-(3-oxohexanoyl)-L-HSL
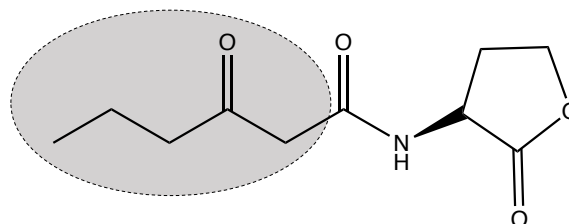
N-Isovaleryl-L-HSL
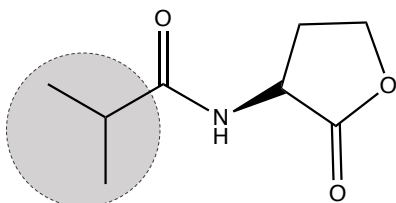
N-(4-Coumaroyl)-L-HSL
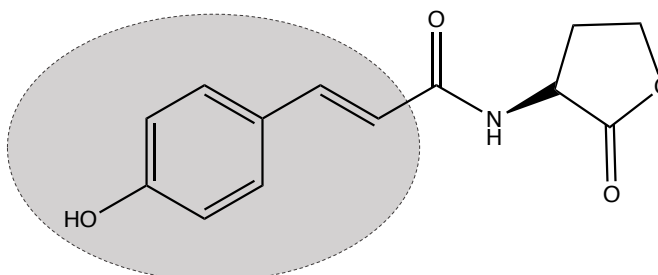
Figure 1.5. Example structures of homoserine lactone (HSL) molecules. HSL molecules are composed of a lactone ring with a variable R-group. The variability in HSL networks is due to different chain length, saturation, and modification of the R-groups.

1.2.5 Progress Toward Overcoming Crosstalk

In chapter 4, we proposed that a major limitation of engineering with quorum sensing networks is a lack of characterized orthogonal pathways, that is, networks that do not cross-induce one another. We compiled a comprehensive list of the known synthase proteins and the HSLs they produce. We compared the secondary structures of several regulator proteins and suggest likely candidates for orthogonal networks.

Recently, several groups have begun characterizing and, in some cases, mutating some of these quorum sensing networks to increase the number of systems available for engineering. Scott et al. screened nine quorum sensing networks for potential orthogonality.[88] While most of them did not function in their chassis, they added the Rpa receiver and, with one mutation, the Tra receiver to the quorum sensing toolbox. In a subsequent paper, they added the RpaI synthase to the toolbox and demonstrated the functional orthogonality of the Lux and Rpa networks.[101] Chen et al. were the first to use the Cin network in an engineering application.[87] They split their circuit across two populations and used the Rhl and Cin networks to control coordinated oscillations of fluorescent protein expression. Tashiro
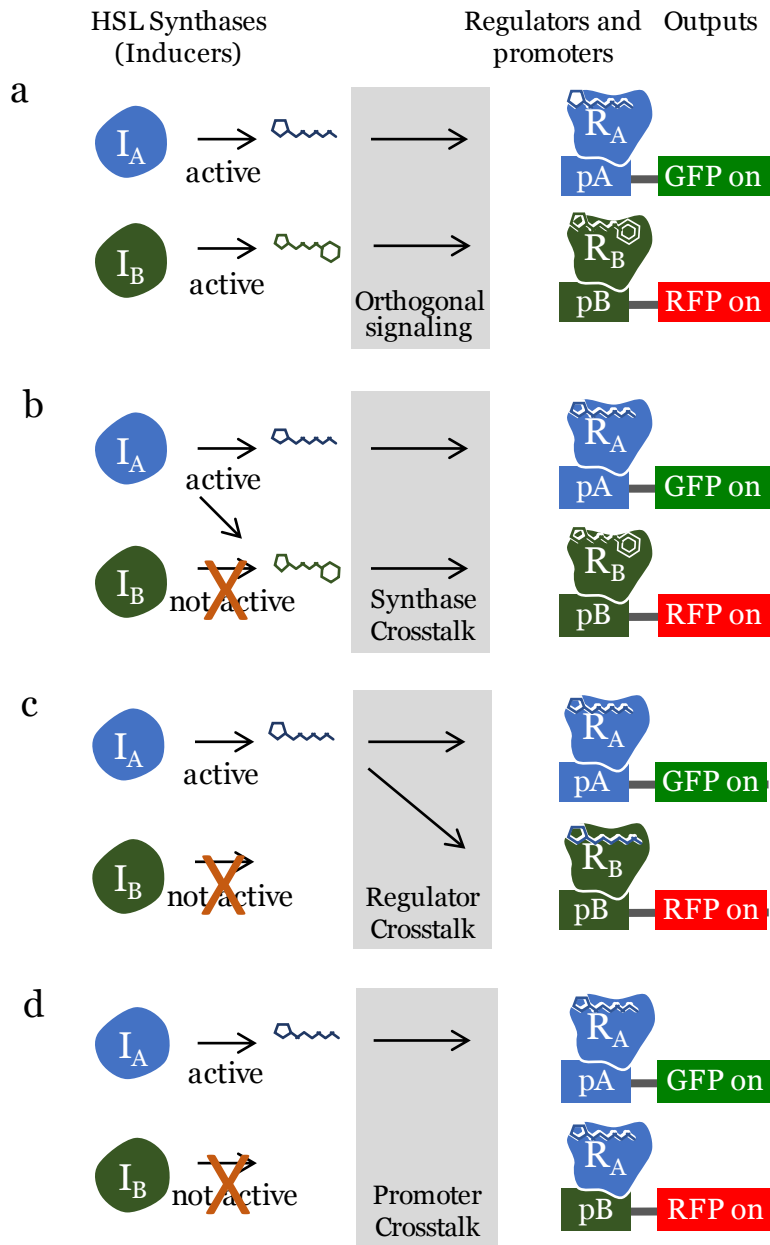
Figure 1.6. Classes of engineered quorum sensing crosstalk. (a) Synthases with narrow HSL profiles induce only their cognate regulators. Regulators are activated by the cognate HSL molecule. Regulators bind only to their cognate promoter. (b) Promiscuous synthase I_A induces both receivers. (c) Promiscuous regulator R_B is activated by a non-cognate HSL. (d) Promiscuous regulator R_A binds at an off-target promoter pB.

et al. evolved the promiscuous LuxR, which is known to respond to its cognate HSL, *N*-(3-oxo-hexanoyl)-ʟ-homoserine lactone (3-oxo-C6-HSL), as well as *N*-(3-oxo-octanoyl)-ʟ-homoserine lactone (3-oxo-C8-HSL) and others, to be more selective.[102] First, they evolved it to maintain wild type sensitivity to 3-oxo-C8-HSL but be 1000 times less sensitive to its cognate HSL, 3-oxo-C6-HSL. Next, they evolved LuxR to be insensitive to 3-oxo-C8-HSL with some reduction in sensitivity to 3-oxo-C6-HSL. While they only used synthetic HSLs for their experiments, these mutated regulators could be used orthogonally with a set of similarly selective synthases. Tackling the problem of promoter crosstalk, Grant et al. mutated the LuxR promoter binding site to reduce binding of LasR and improve binding of LuxR.[103] Taken together, these works have greatly expanded the number of available quorum sensing tools and, importantly, the number of pairs of networks that can be used orthogonally.

1.2.6 Building a Library of Senders

This recent progress in engineering receiver modules has brought us closer to using more than two networks in a single circuit. We propose that building a library of senders that produce narrow profiles of HSLs will allow more complex circuits to be built. However, as discussed above, many synthase proteins produce more than one HSL. Selective receivers are only useful if sender inputs are equally specific. In chapter 5, we present our progress toward building and characterizing a library of senders. We selected synthase proteins that are known to produce one HSL and cover a wide range of tail lengths and modifications and tested their functionality using the promiscuous LuxR regulator protein in *E. coli*. This work complements the recent progress in receiver module development and will enable researchers to engineer increasingly complex multi-strain circuits.

References

(*1*)   Flemming, W., (1879). Beitrage zur kenntnis der zelle und ihrer lebenserscheinungen I. *Archiv für mikroskopische Anatomie 16*, 302–436.

(*2*)   Paweletz, N., (2001). Walther Flemming: pioneer of mitosis research. *Nature reviews. Molecular cell biology 2*, 72–75, DOI: 10.1038/35048077.

(*3*)   Schuettengruber, B., Bourbon, H. M., Di Croce, L., and Cavalli, G., (2017). Genome regulation by Polycomb and Trithorax: 70 years and counting. *Cell 171*, 34–57, DOI: 10.1016/j.cell.2017.08.002.

(*4*)   Lewis, P., (1947). New mutants report. *Drosophila Information Service 21*, 69.

(*5*)   Lewis, E., (1978). A gene complex controlling segmentation in Drosophila. *Nature 276*, 565–570.

(*6*)   Ingham, P. W., (1983). Differential expression of bithorax complex genes in the absence of the extra sex combs and trithorax genes. *Nature 306*, 591–593, DOI: 10.1038/306591a0.

(*7*)   Ingham, P. W., (1985). Genetic control of the spatial pattern of selector gene expression in Drosophila. *Cold Spring Harbor Symposia on Quantitative Biology 50*, 201–208.

(*8*)   Struhl, G., and Akam, M., (1985). Altered distributions of Ultrabithorax transcripts in extra sex combs mutant embryos of Drosophila. *The EMBO journal 4*, 3259–3264.

(*9*)   Kennison, J. A., and Tamkun, J. W., (1988). Dosage-dependent modifiers of polycomb and antennapedia mutations in Drosophila. *Proceedings of the National Academy of Sciences 85*, 8136–8140, DOI: 10.1073/pnas.85.21.8136.

(*10*)   Ingham, P. W., (1985). A clonal analysis of the requirement for the trithorax gene in the diversification of segments in Drosophila. *Journal of embryology and experimental morphology 89*, 349–365.

(*11*)   van der Lugt, N. M., Domen, J., Linders, K., van Roon, M., Robanus-Maandag, E., te Riele, H., van der Valk, M., Deschamps, J., Sofroniew, M., and van Lohuizen, M., (1994). Posterior transformation, neurological abnormalities, and severe hematopoietic defects in mice with a targeted deletion of the bmi-1 proto-oncogene. *Genes & Development 8*, 757–69.

(*12*)   Coré, N., Bel, S., Gaunt, S. J., Aurrand-Lions, M., Pearce, J., Fisher, A., and Djabali, M., (1997). Altered cellular proliferation and mesoderm patterning in Polycomb-M33-deficient mice. *Development 124*, 721–729, DOI: 10.1038/374724a0.

(*13*)   Jacobs, J. J., Kieboom, K., Marino, S., DePinho, R. A., and van Lohuizen, M., (1999). The oncogene and Polycomb-group gene bmi-1 regulates cell proliferation and senescence through the ink4a locus. *Nature 397*, 164–168, DOI: 10.1038/16476.

(*14*)   van Lohuizen, M., Frasch, M., Wientjens, E., and Berns, A., (1991). Sequence similarity between the mammalian bmi-1 proto-oncogene and the Drosophila regulatory genes Psc and Su(z)2. *Nature 353*, 353–355, DOI: 10.1038/353353a0.

(*15*)   Djabali, M., Selleri, L., Parry, P., Bower, M., Young, B. D., and Evans, G. a., (1992). A trithorax-like gene is interrupted by chromosome 11q23 translocations in acute leukaemias. *Nature genetics 2*, 113–118, DOI: 10.1038/ng1092-113.

(*16*)   Jacobs, J. L., Scheijen, B., Voncken, J. W., Kieboom, K., Berns, A., and van Lohuizen, M., (1999). Bmi-1 collaborates with c-Mycin tumorigenesis by inhibiting c-Myc-induced apoptosis via INK4a/ARF. *Genes {&} Development*, 2678–2690, DOI: 10.1101/gad.13.20.2678.

(*17*)   Cao, R., Wang, L., Wang, H., Xia, L., Erdjument-Bromage, H., Tempst, P., Jones, R. S., and Zhang, Y., (2002). Role of histone H3 lysine 27 methylation in Polycomb-group silencing. *Science 298*, 1039–1043, DOI: 10.1126/science.1076997.

(*18*)   Czermin, B., Melfi, R., McCabe, D., Seitz, V., Imhof, A., and Pirrotta, V., (2002). Drosophila enhancer of Zeste/ESC complexes have a histone H3 methyltransferase activity that marks chromosomal Polycomb sites. *Cell 111*, 185–196, DOI: 10.1016/ S0092-8674(02)00975-3.

(*19*)   Kuzmichev, A., Nishioka, K., Erdjument-Bromage, H., Tempst, P., and Reinberg, D., (2002). Histone methyltransferase activity associated with a human multiprotein complex containing the Enhancer of Zeste protein. *Genes & Development 16*, 2893– 2905, DOI: 10.1101/gad.1035902.

(*20*)   Müller, J., Hart, C. M., Francis, N. J., Vargas, M. L., Sengupta, A., Wild, B., Miller, E. L., O'Connor, M. B., Kingston, R. E., and Simon, J. A., (2002). Histone methyl-transferase activity of a Drosophila Polycomb group repressor complex. *Cell 111*, 197–208, DOI: 10.1016/S0092-8674(02)00976-5.

(*21*)   Fischle, W., Wang, Y., Jacobs, S. A., Kim, Y., Allis, C. D., and Khorasanizadeh, S., (2003). Molecular basis for the discrimination of repressive methyl-lysine marks in histone H3 by Polycomb and HP1 chromodomains. *Genes & Development 17*, 1870–1881, DOI: 10.1101/gad.1110503.

(*22*)   Cooper, S., Dienstbier, M., Hassan, R., Schermelleh, L., Sharif, J., Blackledge, N. P., De Marco, V., Elderkin, S., Koseki, H., Klose, R., Heger, A., and Brockdorff, N., (2014). Targeting Polycomb to pericentric heterochromatin in embryonic stem cells reveals a role for H2AK119u1 in PRC2 recruitment. *Cell Reports 7*, 1456–1470, DOI: 10.1016/j.celrep.2014.04.012.

(*23*)   Blackledge, N. P., Rose, N. R., and Klose, R. J., (2015). Targeting Polycomb systems to regulate gene expression: modifications to a complex story. *Nature Reviews Molecular Cell Biology 16*, 643–649, DOI: 10.1038/nrm4067.

(*24*)   Schaaf, C. A., Misulovin, Z., Gause, M., Koenig, A., Gohara, D. W., Watson, A., and Dorsett, D., (2013). Cohesin and Polycomb proteins functionally interact to control transcription at silenced and active genes. *PLoS Genetics 9*, DOI: 10.1371/ journal.pgen.1003560.

(*25*)   Loubiere, V., Delest, A., Thomas, A., Bonev, B., Schuettengruber, B., Sati, S., Mar-tinez, A.-M., and Cavalli, G., (2016). Coordinate redeployment of PRC1 proteins suppresses tumor formation during Drosophila development. *Nature Genetics 48*, 1436–1442, DOI: 10.1038/ng.3671.

(*26*)   Margueron, R., Li, G., Sarma, K., Blais, A., Zavadil, J., Woodcock, C. L., Dynlacht, B. D., and Reinberg, D., (2008). Ezh1 and Ezh2 maintain repressive chromatin through different mechanisms. *Molecular Cell 32*, 503–518, DOI: 10.1016/j.molcel. 2008.11.004.

(*27*) Osborne, C. S., Chakalova, L., Brown, K. E., Carter, D., Horton, A., Debrand, E., Goyenechea, B., Mitchell, J. A., Lopes, S., Reik, W., and Fraser, P., (2004). Active genes dynamically colocalize to shared sites of ongoing transcription. *Nature Genetics 36*, 1065–1071, DOI: 10.1038/ng1423.

(*28*) Simonis, M., Klous, P., Splinter, E., Moshkin, Y., Willemsen, R., de Wit, E., van Steensel, B., and de Laat, W., (2006). Nuclear organization of active and inactive chromatin domains uncovered by chromosome conformation capture–on-chip (4C). *Nature Genetics 38*, 1348–1354, DOI: 10.1038/ng1896.

(*29*) Buchenau, P., Hodgson, J., Strutt, H., and Arndt-Jovin, D. J., (1998). The distribution of Polycomb-group proteins during cell division and development in Drosophila embryos- Impact on models for silencing. *Cell 141*, 469–481, DOI: 10.1083/jcb.141.2.469.

(*30*) Saurin, A. J., Shiels, C., Williamson, J., Satijn, D. P., Otte, A. P., Sheer, D., and Freemont, P. S., (1998). The human Polycomb group complex associates with pericentromeric heterochromatin to form a novel nuclear domain. *Journal of Cell Biology 142*, 887–898, DOI: 10.1083/jcb.142.4.887.

(*31*) Denholtz, M., Bonora, G., Chronis, C., Splinter, E., de Laat, W., Ernst, J., Pellegrini, M., and Plath, K., (2013). Long-range chromatin contacts in embryonic stem cells reveal a role for pluripotency factors and Polycomb proteins in genome organization. *Cell Stem Cell 13*, ed. by Nixon, A. E., 602–616, DOI: 10.1016/j.stem.2013.08.013.

(*32*) Vieux-Rochas, M., Fabre, P. J., Leleu, M., Duboule, D., and Noordermeer, D., (2015). Clustering of mammalian Hox genes with other H3K27me3 targets within an active nuclear domain. *Proceedings of the National Academy of Sciences 112*, 4672–4677, DOI: 10.1073/pnas.1504783112.

(*33*) Wijchers, P. J., Krijger, P. H., Geeven, G., Zhu, Y., Denker, A., Verstegen, M. J., Valdes-Quezada, C., Vermeulen, C., Janssen, M., Teunissen, H., Anink-Groenen, L. C., Verschure, P. J., and de Laat, W., (2016). Cause and consequence of tethering a SubTAD to different nuclear compartments. *Molecular Cell 61*, 461–473, DOI: 10.1016/j.molcel.2016.01.001.

(*34*) Entrevan, M., Schuettengruber, B., and Cavalli, G., (2016). Regulation of genome architecture and function by Polycomb proteins. *Trends in Cell Biology 26*, 511–525, DOI: 10.1016/j.tcb.2016.04.009.

(*35*) Wani, A. H., Boettiger, A. N., Schorderet, P., Ergun, A., Münger, C., Sadreyev, R. I., Zhuang, X., Kingston, R. E., and Francis, N. J., (2016). Chromatin topology is coupled to Polycomb group protein subnuclear organization. *Nature Communications 7*, 10291, DOI: 10.1038/ncomms10291.

(*36*) Schoenfelder, S., Sugar, R., Dimond, A., Javierre, B.-m., Armstrong, H., Mifsud, B., Dimitrova, E., Matheson, L., Tavares-Cadete, F., Furlan-Magaril, M., Segonds-Pichon, A., Jurkowski, W., Wingett, S. W., Tabbada, K., Andrews, S., Herman, B.,

LeProust, E., Osborne, C. S., Koseki, H., Fraser, P., Luscombe, N. M., and Elderkin, S., (2015). Polycomb repressive complex PRC1 spatially constrains the mouse embryonic stem cell genome. *Nature Genetics 47*, 1179–1186, DOI: 10.1038/ng.3393.

(*37*)   Kundu, S., Ji, F., Sunwoo, H., Jain, G., Lee, J. T., Sadreyev, R. I., Dekker, J., and Kingston, R. E., (2017). Polycomb Repressive Complex 1 generates discrete compacted domains that change during differentiation. *Molecular Cell 65*, 432–446.e5, DOI: 10.1016/j.molcel.2017.01.009.

(*38*)   Isono, K., Endo, T. A., Ku, M., Yamada, D., Suzuki, R., Sharif, J., Ishikura, T., Toyoda, T., Bernstein, B. E., and Koseki, H., (2013). SAM domain polymerization links subnuclear clustering of PRC1 to gene silencing. *Developmental Cell 26*, 565–577, DOI: 10.1016/j.devcel.2013.08.016.

(*39*)   Simon, J., Chiang, A., Bender, W., Shimell, M. J., and O'Connor, M., Elements of the Drosophila bithorax complex that mediate repression by Polycomb group products., 1993, DOI: 10.1006/dbio.1993.1174.

(*40*)   Fauvarque, M.-o., and Dura, J.-m., (1993). Polyhomeotic regulatory sequences induce developmental regulator- dependent variegation and targeted P- element insertions in Drosophila. *Genes & Development 7*, 1508–1520.

(*41*)   Müller, J., and Bienz, M., (1991). Long range repression conferring boundaries of Ultrabithorax expression in the Drosophila embryo. *The EMBO journal 10*, 3147–3155.

(*42*)   Simon, J. A., and Kingston, R. E., (2013). Occupying chromatin: Polycomb mechanisms for getting to genomic targets, stopping transcriptional traffic, and staying put. *Molecular Cell 49*, 808–824, DOI: 10.1016/j.molcel.2013.02.013.

(*43*)   Plath, K., Fang, J., Mlynarczyk-Evans, S., Cao, R., Worringer, K., Wang, H., de la Cruz, C., Otte, A., Panning, B., and Zhang, Y., (2003). Role of histone H3 lysine 27 methylation in X inactivation. *Science 300*, 131–135, DOI: 10.1126/science.1084274.

(*44*)   Mendenhall, E. M., Koche, R. P., Truong, T., Zhou, V. W., Issac, B., Chi, A. S., Ku, M., and Bernstein, B. E., (2010). GC-rich sequence elements recruit PRC2 in mammalian ES cells. *PLoS Genetics 6*, ed. by Madhani, H. D., e1001244, DOI: 10.1371/journal.pgen.1001244.

(*45*)   Blackledge, N. P., Farcas, A. M., Kondo, T., King, H. W., McGouran, J. F., Hanssen, L. L., Ito, S., Cooper, S., Kondo, K., Koseki, Y., Ishikura, T., Long, H. K., Sheahan, T. W., Brockdorff, N., Kessler, B. M., Koseki, H., and Klose, R. J., (2014). Variant PRC1 complex-dependent H2A ubiquitylation drives PRC2 recruitment and Polycomb domain formation. *Cell 157*, 1445–1459, DOI: 10.1016/j.cell.2014.05.004.

(*46*)   Illingworth, R. S., Moffat, M., Mann, A. R., Read, D., Hunter, C. J., Pradeepa, M. M., Adams, I. R., and Bickmore, W. A., (2015). The E3 ubiquitin ligase activity

of RING1B is not essential for early mouse development. *Genes & Development 29*, 1897−1902, DOI: 10.1101/gad.268151.115.

(*47*)   Pengelly, A. R., Kalb, R., Finkl, K., and Müller, J., (2015). Transcriptional repression by PRC1 in the absence of H2A monoubiquitylation. *Genes & Development 29*, 1487−1492, DOI: 10.1101/gad.265439.115.

(*48*)   Jinek, M., Chylinski, K., Fonfara, I., Hauer, M., Doudna, J. a., and Charpentier, E., (2012). A Programmable Dual-RNA-Guided DNA Endonuclease in Adaptive Bacterial Immunity. *Science 337*, 816−821, DOI: 10.1126/science.1225829.

(*49*)   Gilbert, L. A., Larson, M. H., Morsut, L., Liu, Z., Brar, G. A., Torres, S. E., Stern-Ginossar, N., Brandman, O., Whitehead, E. H., Doudna, J. A., Lim, W. A., Weissman, J. S., and Qi, L. S., (2013). CRISPR-Mediated Modular RNA-Guided Regulation of Transcription in Eukaryotes. *Cell 154*, 442−451, DOI: 10.1016/j.cell.2013.06.044.

(*50*)   Tiwari, V. K., Cope, L., McGarvey, K. M., Ohm, J. E., and Baylin, S. B., (2008). A novel 6C assay uncovers Polycomb-mediated higher order chromatin conformations. *Genome Research 18*, 1171−1179, DOI: 10.1101/gr.073452.107.

(*51*)   Bell, O., Tiwari, V. K., Thomä, N. H., and Schübeler, D., (2011). Determinants and dynamics of genome accessibility. *Nature Reviews Genetics 12*, 554−564, DOI: 10.1038/nrg3017.

(*52*)   Aoto, T., Saitoh, N., Sakamoto, Y., Watanabe, S., and Nakao, M., (2008). Polycomb group protein-associated chromatin is reproduced in post-mitotic G 1 phase and is required for S phase progression. *Journal of Biological Chemistry 283*, 18905−18915, DOI: 10.1074/jbc.M709322200.

(*53*)   Hansen, K. H., Bracken, A. P., Pasini, D., Dietrich, N., Gehani, S. S., Monrad, A., Rappsilber, J., Lerdrup, M., and Helin, K., (2008). A model for transmission of the H3K27me3 epigenetic mark. *Nature Cell Biology 10*, 1291−1300, DOI: 10.1038/ncb1787.

(*54*)   Daer, R. M., Cutts, J. P., Brafman, D. A., and Haynes, K. A., (2017). The Impact of Chromatin Dynamics on Cas9-Mediated Genome Editing in Human Cells. *ACS Synthetic Biology 6*, 428−438, DOI: 10.1021/acssynbio.5b00299.

(*55*)   Wu, X., Scott, D. A., Kriz, A. J., Chiu, A. C., Hsu, P. D., Dadon, D. B., Cheng, A. W., Trevino, A. E., Konermann, S., Chen, S., Jaenisch, R., Zhang, F., and Sharp, P. A., (2014). Genome-wide binding of the CRISPR endonuclease Cas9 in mammalian cells. *Nature Biotechnology 32*, 670−676, DOI: 10.1038/nbt.2889.

(*56*)   Kuscu, C., Arslan, S., Singh, R., Thorpe, J., and Adli, M., (2014). Genome-wide analysis reveals characteristics of off-target sites bound by the Cas9 endonuclease. *Nature Biotechnology 32*, 677−683, DOI: 10.1038/nbt.2916.

(*57*)   O'Geen, H., Henry, I. M., Bhakta, M. S., Meckler, J. F., and Segal, D. J., (2015). A genome-wide analysis of Cas9 binding specificity using ChIP-seq and targeted sequence capture. *Nucleic Acids Research 43*, 3389–3404, DOI: 10.1093/nar/gkv137.

(*58*)   Singh, R., Kuscu, C., Quinlan, A., Qi, Y., and Adli, M., (2015). Cas9-chromatin binding information enables more accurate CRISPR off-target prediction. *Nucleic Acids Research 43*, e118, DOI: 10.1093/nar/gkv575.

(*59*)   Horlbeck, M. A., Witkowsky, L. B., Guglielmi, B., Replogle, J. M., Gilbert, L. A., Villalta, J. E., Torigoe, S. E., Tjian, R., and Weissman, J. S., (2016). Nucleosomes impede cas9 access to DNA in vivo and in vitro. *eLife 5*, 1–21, DOI: 10.7554/eLife.12677.

(*60*)   Horlbeck, M. A., Gilbert, L. A., Villalta, J. E., Adamson, B., Pak, R. A., Chen, Y., Fields, A. P., Park, C. Y., Corn, J. E., Kampmann, M., and Weissman, J. S., (2016). Compact and highly active next-generation libraries for CRISPR-mediated gene repression and activation. *eLife 5*, 1–20, DOI: 10.7554/eLife.19760.

(*61*)   Radzisheuskaya, A., Shlyueva, D., Müller, I., and Helin, K., (2016). Optimizing sgRNA position markedly improves the efficiency of CRISPR/dCas9-mediated transcriptional repression. *Nucleic Acids Research 44*, DOI: 10.1093/nar/gkw583.

(*62*)   Smith, J. D., Suresh, S., Schlecht, U., Wu, M., Wagih, O., Peltz, G., Davis, R. W., Steinmetz, L. M., Parts, L., and St.Onge, R. P., (2016). Quantitative CRISPR interference screens in yeast identify chemical-genetic interactions and new rules for guide RNA design. *Genome Biology 17*, 45, DOI: 10.1186/s13059-016-0900-9.

(*63*)   Chari, R., Mali, P., Moosburner, M., and Church, G. M., (2015). Unraveling CRISPR-Cas9 genome engineering parameters via a library-on-library approach. *Nature Methods 12*, 823–826, DOI: 10.1038/nmeth.3473.

(*64*)   Jensen, K. T., Fløe, L., Petersen, T. S., Huang, J., Xu, F., Bolund, L., Luo, Y., and Lin, L., (2017). Chromatin accessibility and guide sequence secondary structure affect CRISPR-Cas9 gene editing efficiency. *FEBS Letters 591*, 1892–1901, DOI: 10.1002/1873-3468.12707.

(*65*)   Hinz, J. M., Laughery, M. F., and Wyrick, J. J., (2015). Nucleosomes Inhibit Cas9 Endonuclease Activity in Vitro. *Biochemistry 54*, 7063–7066, DOI: 10.1021/acs.biochem.5b01108.

(*66*)   Isaac, R. S., Jiang, F., Doudna, J. A., Lim, W. A., Narlikar, G. J., and Almeida, R., (2016). Nucleosome breathing and remodeling constrain CRISPR-Cas9 function. *eLife 5*, 1–14, DOI: 10.7554/eLife.13450.

(*67*)   Anderson, J., and Widom, J., (2000). Sequence and position-dependence of the equilibrium accessibility of nucleosomal DNA target sites 1 1Edited by T. Richmond. *Journal of Molecular Biology 296*, 979–987, DOI: 10.1006/jmbi.2000.3531.

(*68*)   Partensky, P. D., and Narlikar, G. J., (2009). Chromatin Remodelers Act Globally, Sequence Positions Nucleosomes Locally. *Journal of Molecular Biology 391*, 12–25, DOI: 10.1016/j.jmb.2009.04.085.

(*69*)   Chen, X., Rinsma, M., Janssen, J. M., Liu, J., Maggio, I., and Gonçalves, M. A., (2016). Probing the impact of chromatin conformation on genome editing tools. *Nucleic Acids Research 44*, 6482–6492, DOI: 10.1093/nar/gkw524.

(*70*)   Yang, L., Guell, M., Byrne, S., Yang, J. L., De Los Angeles, A., Mali, P., Aach, J., Kim-Kiselak, C., Briggs, A. W., Rios, X., Huang, P. Y., Daley, G., and Church, G., (2013). Optimization of scarless human stem cell genome editing. *Nucleic Acids Research 41*, 9049–9061, DOI: 10.1093/nar/gkt555.

(*71*)   Perez-Pinera, P., Kocak, D. D., Vockley, C. M., Adler, A. F., Kabadi, A. M., Polstein, L. R., Thakore, P. I., Glass, K. A., Ousterout, D. G., Leong, K. W., Guilak, F., Crawford, G. E., Reddy, T. E., Gersbach, C. A., Kabadi, M., Polstein, L. R., Thakore, P. I., Glass, K. A., Ousterout, D. G., Leong, K. W., Guilak, F., Crawford, G. E., Reddy, T. E., and Gersbach, C. A., (2013). RNA-guided gene activation by CRISPR-Cas9–based transcription factors. *Nature Methods 10*, 973–976, DOI: 10.1038/nmeth.2600.

(*72*)   Polstein, L. R., Perez-pinera, P., Kocak, D. D., Vockley, M., Bledsoe, P., Song, L., Safi, A., Crawford, G. E., Reddy, T. E., Gersbach, C. a., Carolina, N., and Surgery, O., (2015). Genome-wide specificity of DNA binding , gene regulation , and chromatin remodeling by TALE- and CRISPR / Cas9-based transcriptional activators. *Genome research 25*, 1158–1169, DOI: 10.1101/gr.179044.114..

(*73*)   Knight, S. C., Xie, L., Deng, W., Guglielmi, B., Witkowsky, L. B., Bosanac, L., Zhang, E. T., El Beheiry, M., Masson, J.-B., Dahan, M., Liu, Z., Doudna, J. A., and Tjian, R., (2015). Dynamics of CRISPR-Cas9 genome interrogation in living cells. *Science 350*, 823–826, DOI: 10.1126/science.aac6572.

(*74*)   Hsu, P. D., Scott, D. a., Weinstein, J. a., Ran, F. A., Konermann, S., Agarwala, V., Li, Y., Fine, E. J., Wu, X., Shalem, O., Cradick, T. J., Marraffini, L. a., Bao, G., and Zhang, F., (2013). DNA targeting specificity of RNA-guided Cas9 nucleases. *Nature Biotechnology 31*, 827–832, DOI: 10.1038/nbt.2647.

(*75*)   Ruby, E. G., and Nealson, K. H., (1976). Symbiotic Association of Photobacterium Fischeri with the Marine Luminous Fish Monocentris Japonica: A Model Of Symbiosis Based on Bacterial Studies. *The Biological Bulletin 151*, 574–586, DOI: 10.2307/1540507.

(*76*)   Eberl, L., (1999). N-acyl homoserinelactone-mediated gene regulation in gram-negative bacteria. *Systematic and applied microbiology 22*, 493–506, DOI: 10. 1016/S0723-2020(99)80001-0.

(*77*)   Fuqua, C., Winans, S. C., and Greenberg, E. P., (1996). Census and consensus in bacterial ecosystems: the LuxR-LuxI family of quorum-sensing transcriptional regulators. *Annual review of microbiology 50*, 727–51, DOI: 10.1146/annurev. micro.50.1.727.

(*78*)   Williams, P., Winzer, K., Chan, W. C., and Camara, M., (2007). Look who's talking: communication and quorum sensing in the bacterial world. *Philosophical Transactions of the Royal Society B: Biological Sciences 362*, 1119–1134, DOI: 10.1098/rstb.2007.2039.

(*79*)   Dickschat, J. S., (2010). Quorum sensing and bacterial biofilms. *Natural product reports 27*, 343–69, DOI: 10.1039/b804469b.

(*80*)   Case, R. J., Labbate, M., and Kjelleberg, S., (2008). AHL-driven quorum-sensing circuits: their frequency and function among the Proteobacteria. *The ISME journal 2*, 345–9, DOI: 10.1038/ismej.2008.13.

(*81*)   Nasuno, E., Kimura, N., Fujita, M. J., Nakatsu, C. H., Kamagata, Y., and Hanada, S., (2012). Phylogenetically Novel LuxI/LuxR-Type Quorum Sensing Systems Isolated Using a Metagenomic Approach. *Applied and Environmental Microbiology 78*, 8067–8074, DOI: 10.1128/AEM.01442-12.

(*82*)   Engebrecht, J., and Silverman, M., (1984). Identification of genes and gene products necessary for bacterial bioluminescence. *Proceedings of the National Academy of Sciences of the United States of America 81*, 4154–8.

(*83*)   Kaplan, H. B., and Greenberg, E. P., (1987). Overproduction and purification of the luxR gene product: Transcriptional activator of the Vibrio fischeri luminescence system. *Proceedings of the National Academy of Sciences of the United States of America 84*, 6639–43.

(*84*)   von Bodman, S., Ball, J., Faini, M., Herrera, C., Minogue, T., Urbanowski, M., and Stevens, A., (2003). The quorum sensing negative regulators EsaR and ExpREcc, homologues within the LuxR family, retain the ability to function as activators of transcription. *Journal of bacteriology 185*, 7001–7007, DOI: 10.1128/JB.185.23.7001.

(*85*)   Miller, M. B., and Bassler, B. L., (2001). Quorum sensing in bacteria. *Annual review of microbiology 55*, 165–99, DOI: 10.1146/annurev.micro.55.1.165.

(*86*)   Gupta, A., Reizman, I. M. B., Reisch, C. R., and Prather, K. L. J., (2017). Dynamic regulation of metabolic flux in engineered bacteria using a pathway-independent quorum-sensing circuit. *Nature Biotechnology 35*, 273–279, DOI: 10.1038/nbt.3796.

(*87*)   Chen, Y., Kim, J. K., Hirning, A. J., and Bennett, Matthew, R., (2016). Emergent genetic oscillations in a synthetic microbial consortium. *Science 349*, 986–989, DOI: 10.1126/science.aaa3794.Emergent.

(*88*)   Scott, S. R., and Hasty, J., (2016). Quorum Sensing Communication Modules for Microbial Consortia. *ACS Synthetic Biology 5*, 969–977, DOI: 10.1021/acssynbio.5b00286.

(*89*)   Daniel, R., Rubens, J. R., Sarpeshkar, R., and Lu, T. K., (2013). Synthetic analog computation in living cells. *Nature 497*, 619–23, DOI: 10.1038/nature12148.

(*90*) Tabor, J. J., Salis, H. M., Simpson, Z. B., Chevalier, A. a., Levskaya, A., Marcotte, E. M., Voigt, C. a., and Ellington, A. D., (2009). A Synthetic Genetic Edge Detection Program. *Cell 137*, 1272–1281, DOI: 10.1016/j.cell.2009.04.048.

(*91*) Brenner, K., Karig, D. K., Weiss, R., and Arnold, F. H., (2007). Engineered bidirectional communication mediates a consensus in a microbial biofilm consortium. *Proceedings of the National Academy of Sciences of the United States of America 104*, 17300–4, DOI: 10.1073/pnas.0704256104.

(*92*) Davis, R. M., Muller, R. Y., and Haynes, K. A., (2015). Can the Natural Diversity of Quorum-Sensing Advance Synthetic Biology? *Frontiers in Bioengineering and Biotechnology 3*, 1–10, DOI: 10.3389/fbioe.2015.00030.

(*93*) Hudaiberdiev, S., Choudhary, K. S., Vera Alvarez, R., Gelencsér, Z., Ligeti, B., Lamba, D., and Pongor, S., (2015). Census of solo LuxR genes in prokaryotic genomes. *Frontiers in cellular and infection microbiology 5*, 20, DOI: 10.3389/fcimb.2015.00020.

(*94*) Passos da Silva, D., Patel, H. K., González, J. F., Devescovi, G., Meng, X., Covaceuszach, S., Lamba, D., Subramoni, S., and Venturi, V., (2015). Studies on synthetic LuxR solo hybrids. *Frontiers in cellular and infection microbiology 5*, 52, DOI: 10.3389/fcimb.2015.00052.

(*95*) Lewenza, S., Visser, M. B., and Sokol, P. a., (2002). Interspecies communication between Burkholderia cepacia and Pseudomonas aeruginosa. *Canadian Journal of Microbiology 48*, 707–716, DOI: 10.1139/w02-068.

(*96*) Chandler, J. R., Heilmann, S., Mittler, J. E., and Greenberg, E. P., (2012). Acyl-homoserine lactone-dependent eavesdropping promotes competition in a laboratory co-culture model. *The ISME journal 6*, 1–10, DOI: 10.1038/ismej.2012.69.

(*97*) Canton, B., Labno, A., and Endy, D., (2008). Refinement and standardization of synthetic biological parts and devices. *Nature biotechnology 26*, 787–93, DOI: 10.1038/nbt1413.

(*98*) Saeidi, N., Wong, C. K., Lo, T.-M., Nguyen, H. X., Ling, H., Leong, S. S. J., Poh, C. L., and Chang, M. W., (2011). Engineering microbes to sense and eradicate Pseudomonas aeruginosa, a human pathogen. *Molecular systems biology 7*, 1–11, DOI: 10.1038/msb.2011.55.

(*99*) Shong, J., Huang, Y.-M., Bystroff, C., and Collins, C. H., (2013). Directed evolution of the quorum-sensing regulator EsaR for increased signal sensitivity. *ACS Chemical Biology 8*, 789–95, DOI: 10.1021/cb3006402.

(*100*) Wu, F., Menn, D. J., and Wang, X., (2014). Article Circuits : From Unimodality to Trimodality. *Chemistry & Biology 21*, 1629–1638, DOI: 10.1016/j.chembiol.2014.10.008.

(*101*)   Scott, S. R., Din, M. O., Bittihn, P., Xiong, L., Tsimring, L. S., and Hasty, J., (2017). A stabilized microbial ecosystem of self-limiting bacteria using synthetic quorum-regulated lysis. *Nature Microbiology 2*, 17083, DOI: 10.1038/nmicrobiol.2017.83.

(*102*)   Tashiro, Y., Kimura, Y., Furubayashi, M., Tanaka, A., Terakubo, K., Saito, K., Kawai-Noma, S., and Umeno, D., (2016). Directed evolution of the autoinducer selectivity of Vibrio fischeri LuxR. *The Journal of General and Applied Microbiology 247*, 1–8, DOI: 10.2323/jgam.2016.04.005.

(*103*)   Grant, P. K., Dalchau, N., Brown, J. R., Federici, F., Rudge, T. J., Yordanov, B., Patange, O., Phillips, A., and Haseloff, J., (2016). Orthogonal intercellular signaling for programmed spatial behavior. *Molecular Systems Biology 12*, 849–849, DOI: 10.15252/msb.20156590.

Chapter 2

THE IMPACT OF CHROMATIN DYNAMICS ON
CAS9-MEDIATED GENOME EDITING IN HUMAN CELLS[†]

In order to efficiently edit eukaryotic genomes, it is critical to test the impact of chromatin dynamics on CRISPR/Cas9 function and develop strategies to adapt the system to eukaryotic contexts. So far, research has extensively characterized the relationship between the CRISPR endonuclease Cas9 and the composition of the RNA–DNA duplex that mediates the system's precision. Evidence suggests that chromatin modifications and DNA packaging can block eukaryotic genome editing by custom-built DNA endonucleases like Cas9; however, the underlying mechanism of Cas9 inhibition is unclear. Here, we demonstrate that closed, gene-silencing-associated chromatin is a mechanism for the interference of Cas9-mediated DNA editing. Our assays use a transgenic cell line with a drug-inducible switch to control chromatin states (open and closed) at a single genomic locus. We show that closed chromatin inhibits binding and editing at specific target sites and that artificial reversal of the silenced state restores editing efficiency. These results provide new insights to improve Cas9-mediated editing in human and other mammalian cells.
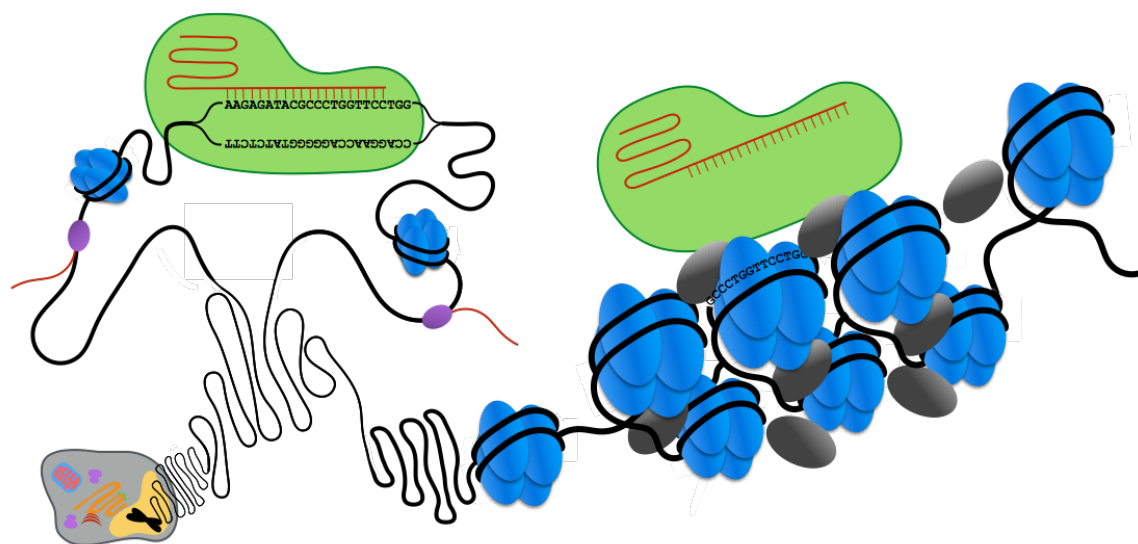
2.1 Introduction

Extensive characterization and engineering is driving the CRISPR/Cas9 system to the forefront of biomedical research, human gene therapy, and tissue regeneration.[104–107] Realizing the full potential of CRISPR/Cas9 editing in eukaryotic cells will require efficient access to target sites within chromatin, the ubiquitous DNA-protein complexes that organize eukaryotic genomes, regulate gene expression, and render DNA less accessible to nucleases.[50–52] While some evidence suggests that chromatin modifications and DNA packaging can block eukaryotic genome editing by custom-built DNA endonucleases,[55,69,105,108,109] the underlying mechanism of Cas9 interference is unknown. Here, we present direct evidence that closed, gene-silencing-associated chromatin inhibits Cas9-mediated DNA editing. These results establish closed chromatin as a target for improving CRISPR/Cas9 efficiency in human and other eukaryotic cells.

There is conflicting evidence on whether chromatin interferes with Cas9 binding and nuclease activity in human cells. Chromatin immunoprecipitation (ChIP) mapping of dCas9, which lacks nuclease activity, showed preferential binding at off-target sites across the human genome with characteristics of open chromatin: high levels of DNase-hypersensitivity and protein-coding gene sequences.[55,56,58] Wu et al. reported reduced DNA cleavage at off-target sites near closed chromatin versus on-target sites near open chromatin.[55] While Cas9-mediated editing is not completely blocked at the silenced SERPINB5 locus, which contains methylated DNA, the reported editing frequency was only ~8%.[105] Taken together, these data suggest Cas9 may be inhibited by closed chromatin. However, Chen et al. showed that pericentromeric heterochromatin inhibited INDEL formation.[69] Perez-Pinera et al. found that dCas9-based activators were functional at sites within closed chromatin, suggesting binding was not prevented.[71] So far, no study has compared Cas9 activity and binding at a single site for both open and Polycomb-mediated closed chromatin.

2.2 Results and Discussion

Here, we use a model silencing system developed in Hansen et al. to control the chromatin state at a single site, a stably integrated *firefly luciferase* transgene.[53] We directly measured the impact of closed chromatin on Cas9-mediated DNA editing by targeting Cas9 to sites within the *luciferase* gene in unsilenced, partially silenced, and fully silenced chromatin states. The Gal4EED HEK293 cell line contains a doxycycline (dox)-inducible transgene that expresses Gal4EED, which binds upstream of *luciferase* and recruits endogenous Polycomb Repressive Complexes (PRCs), key regulators of facultatively closed chromatin (Figure 2.1a, see Methods for detail).[42] PRCs target hundreds of genes and play a critical role in gene

25
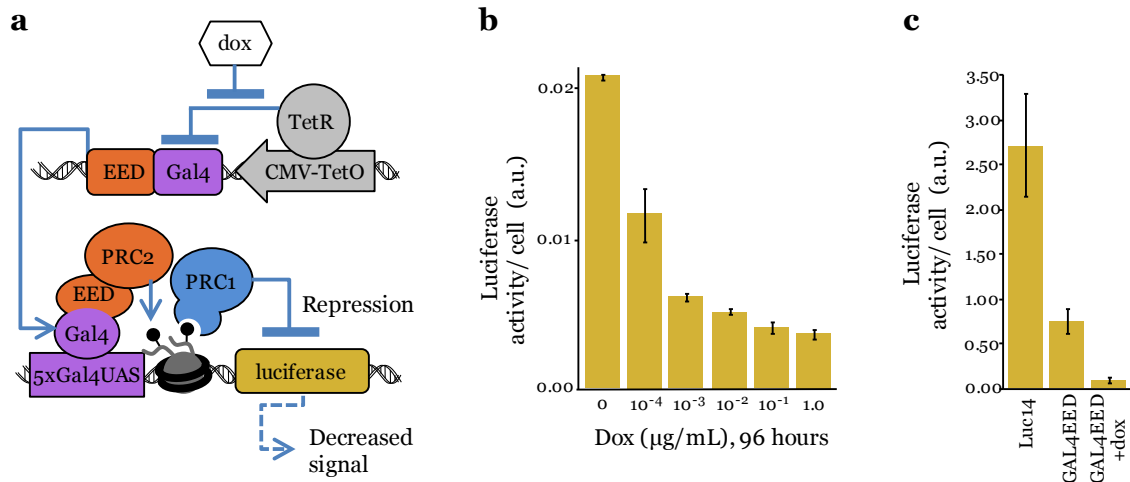
Figure 2.1. A closed chromatin state at *luciferase* is regulated by doxycycline (dox) in GAL4EED cells. (a) The GAL4EED circuit diagram illustrates how dox regulates the expression of the Gal4EED fusion protein, which mediates accumulation of Polycomb Repressive Complex 1 (PRC1) and closed chromatin at the *luciferase* reporter. (b) A repressed expression state at *luciferase* is stimulated by dox in GAL4EED cells. (c) Comparison of *luciferase* expression in cells that lack a *Gal4EED* gene (Luc14), and GAL4EED cells before and after treatment with dox. a.u.: arbitrary units from luminescence readings. Error bars indicate s.d. for *n* = 3 technical replicates.

silencing, embryonic development, stem cell maintenance and differentiation, and tumor suppression,[110–114] and thus, understanding whether differences in PRC accumulation influence Cas9 activity is necessary for advancing biomedical applications.

GAL4EED cells grown with 1 μg/ml dox for 96 h show maximal levels of repression (Figure 2.1b). We observed that the GAL4EED cell line shows less *luciferase* expression than the parental Luc14 cell line, which lacks the *Gal4EED* transgene, perhaps due to leaky Gal4EED expression and a partially silenced chromatin state (Figure 2.1c). The chromatin states in GAL4EED are stable over time and in the presence of transfected plasmids. Once initiated by Gal4EED, the silenced state remains stable up to 96 h after dox is removed and Gal4EED expression is no longer activated.[53] In our previous work, we showed that control plasmids that express fluorescent proteins do not alter the expression levels of active or Gal4EED-silenced *luciferase*.[115]

We constructed a series of plasmids expressing Cas9 and a short guide RNA (sgRNA) designed to target 1 of 23 sites within *Gal4UAS-TK-luciferase*. Editing efficiencies were determined using a SURVEYOR digestion assay and a Bioanalyzer (Figure 2.2a). The target sites are distributed across 900 basepairs (bp) of the transgene located downstream of the Gal4EED binding site (5xGal4UAS in Figure 2.2b). The sgRNAs showed a wide
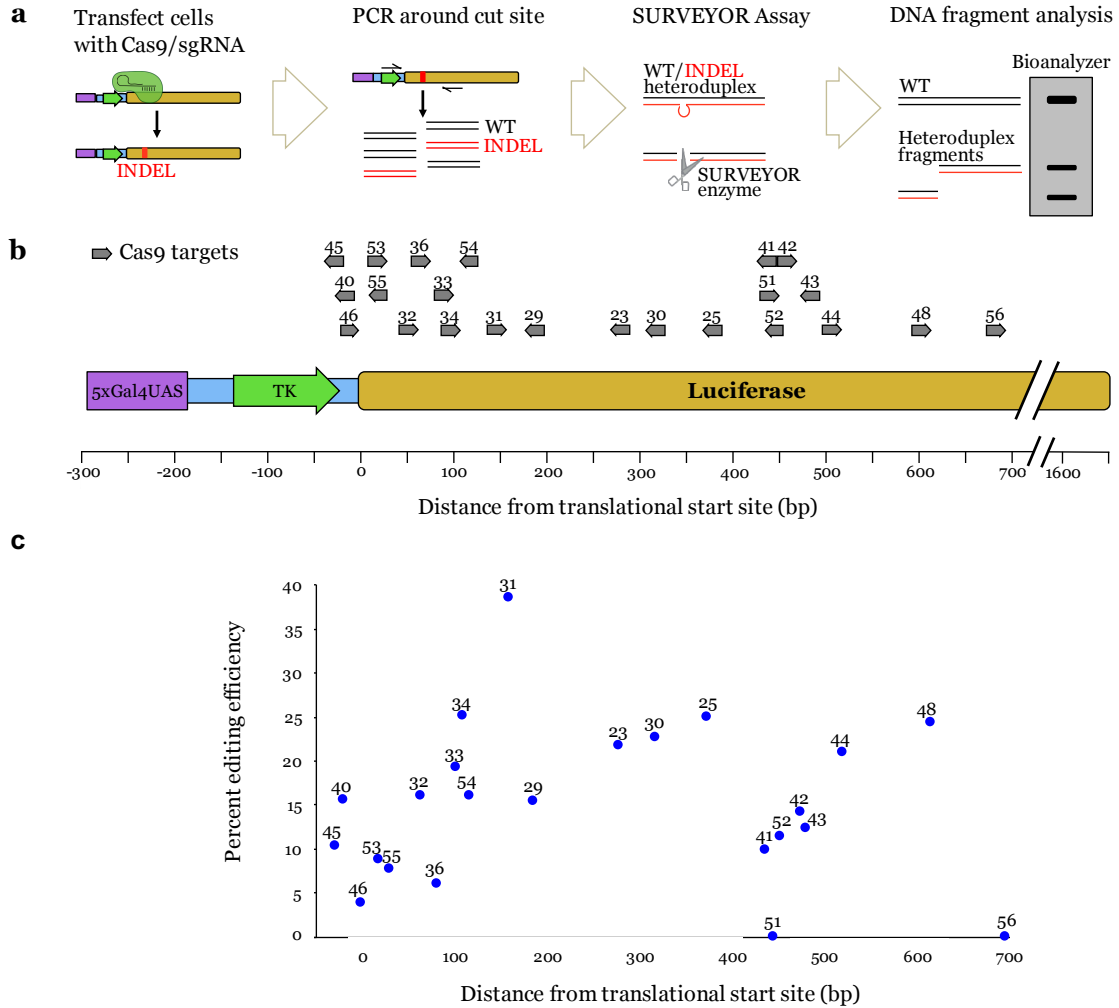
Figure 2.2. Editing efficiency at different Cas9/sgRNA target sites detected by SURVEYOR assays. (a) Diagram of the SURVEYOR assay. INDELS: Insertions and deletions; WT: wildtype. (b) Map of all sgRNAs tested in this study. Arrows show Cas9/sgRNA binding sites. (c) SURVEYOR results from a screen to identify sgRNAs with detectable editing rates at the *UAS-TK-luciferase* reporter in Luc14 cells.

variability of INDEL frequency from zero (below detection limits) to almost 40% in Luc14 cells (Figure 2.2c).

To determine the effect of facultative closed chromatin on Cas9-mediated editing, we compared the editing efficiencies of Cas9 in cells where the luciferase target was set to different expression states: unsilenced (Luc14), partially silenced (GAL4EED), and fully silenced (GAL4EED + dox) (Figure 2.1c). For this analysis, we used the five sgRNAs that showed the highest editing efficiencies in preliminary tests (Figure 2.2c) in Luc14 cells: sg034, sg031, sg025, sg044, and sg048. We also tested four additional sgRNAs, located farther upstream (sg046, sg055, sg032, sg054) in order to investigate Cas9 interference closer to the initiation site of chromatin compaction. In order to control for varying transfection and expression levels across cell lines and conditions, we added an enhanced green fluorescent protein (EGFP) reporter gene to the Cas9 plasmid (Figure 2.3a). In this plasmid, EGFP expression is driven by the same promoter as Cas9, but the T2A signal allows EGFP to be translated as a separate peptide to avoid interference with Cas9 function. We used the percentage of GFP-positive cells (Figure 2.3b) to normalize editing efficiency values across different experiments.

Cas9-mediated editing was reduced at target sites in fully silenced chromatin compared to unsilenced chromatin for six of the nine sgRNAs we tested (Figure 2.3c). The greatest significant reductions occurred within 150 bp of the transcription start site downstream of the chromatin initiation site at 5xGal4 at sites sg046 ($p = 0.002$), sg055 ($p = 0.092$), sg032 ($p = 0.008$), and sg054 ($p = 0.001$). In the unsilenced state (Luc14), average editing efficiencies at these sites were 7.5 to 55.1% while mutation frequencies were below detection limits in both the partially (GAL4EED) and fully (GAL4EED + dox) silenced states. These results suggests that editing at TSS-proximal sites is sensitive to closed chromatin. Cas9-mediated editing in fully silenced chromatin was reduced, but not completely inhibited, farther downstream at sg034 ($p = 0.024$) and sg044 ($p = 0.022$) compared to unsilenced chromatin. Interestingly, editing efficiency at sg025, located between sg031 and sg044, and sg048, located downstream of g044, is not decreased in the presence of closed chromatin. This suggests that interference may occur in a Cas9/sgRNA-dependent manner or that the spreading of closed chromatin from the UAS is discontinuous. Overall, our results reveal differences in Cas9 accessibility at a greater resolution than what has been reported to date for a single genomic locus. Furthermore, comparison of open, moderately closed, and fully closed states at several on-target sites along a single locus allowed us to detect different levels of interference that are the direct outcome of the formation of facultative chromatin.

Next, we tested the hypothesis that in addition to reducing editing efficiency, silenced chromatin also affects the types of mutations that are generated at the target site. We analyzed mutations at target site sg034 because at this location the closed state still showed

a Cas9/sgRNA – EGFP plasmid

BbsI cloning site
U6 promoter
U6 terminator
sgRNA scaffold
CBh promoter
NLS
3xFLAG

pU6-(BbsI)_CBh-Cas9-T2A-EGFP

BGH polyA
EGFP
NLS
T2A
Cas9

b Cas9/sgRNA – EGFP plasmid transfection efficiency

	Luc14	GAL4EED	GAL4EED +dox
sg046	51.1 ±7.6	32.4 ±0.2	36.9 ±1.7
sg055	30.1 ±4.1	29.4 ±1.6	38.2 ±2.6
sg032	51.1 ±7.0	33.0 ±1.3	38.0 ±0.2
sg034	32.5 ±3.6	33.2 ±2.5	23.5 ±2.1
sg054	32.3 ±3.9	12.1 ±1.4	12.3 ±0.8
sg031	55.7 ±3.2	32.0 ±1.8	31.9 ±2.0
sg025	50.8 ±6.1	31.8 ±1.1	34.1 ±0.8
sg044	37.1 ±3.0	30.5 ±1.3	34.3 ±2.0
sg048	49.5 ±2.8	35.3 ±2.6	28.3 ±3.2

c

Percent editing efficiency normalized to transfection efficiency

Luc14 / GAL4EED / GAL4EED +dox

Cas9/sgRNA target site: sg046, sg055, sg032, sg034, sg054, sg031, sg025, sg044, sg048

d

Editing reduced at partially and fully silenced site

Editing reduced at fully silenced site

46 32 34 54 44

5xGal4UAS | TK | Luciferase

Distance from translational start site (bp)
-300 -200 -100 0 100 200 300 400 500 600 700 1600

Figure 2.3. Cas9 editing efficiencies at target sites in unsilenced, partially silenced, and fully silenced chromatin states. (a) A map of the Cas9/sgRNA-expressing plasmid. Cas9 and EGFP expression are both driven by the CBh promoter. The T2A signal allows EGFP to be translated as a separate peptide to avoid interference of Cas9 function. (b) Table of average frequencies of EGFP-expressing cells (transfection efficiencies) as determined by flow cytometry of triplicate samples for transfected Luc14, GAL4EED, and GAL4EED cells treated with doxycycline.

29

Figure 2.3. Continued. (c) Mean editing frequencies normalized to transfection efficiency in Luc14, GAL4EED, or GAL4EED + dox cells for Cas9 targeted to sites sg046, sg055, sg032, sg034, sg054, sg031, sg025, sg044, and sg048. * Indicates significantly reduced editing efficiencies at fully silenced chromatin compared to unsilenced chromatin ($p < 0.025$ for 3 biological replicates). Editing frequencies for target sites sg046, sg055, sg032, and sg054 for both GAL4EED or GAL4EED + dox cell types were below detection limits. Error bars indicate s.d. for n = 3 biological replicates. (d) Summary of the data in (c). Cas9 target sites sg046, sg032, and sg054 show a reduction in editing efficiency in both the partially and fully silenced states compared to the unsilenced states (red arrows). Cas9 target sites sg034 and sg044 show a reduction in editing efficiency in the fully silence states compared to the unsilenced states (yellow arrows).

detectable Cas9-mediated editing. Sequencing of cloned mutants from Cas9-edited DNA confirmed lower editing efficiency at a target site in fully silenced chromatin compared to unsilenced chromatin. We then compared the distribution of mutated sequences from unsilenced- and fully silenced-chromatin samples. We detected various mutations that were generated in the absence of a repair template by nonhomologous end joining (NHEJ) at target site sg034. These mutations primarily consisted of deletions ranging from 1 bp to 24 bp (Figure 2.4a). A small number of insertions (1 bp to 205 bp) and single base pair substitutions were also detected. DNA cloned from Cas9/sg034-treated *luciferase* in the unsilenced chromatin state showed a higher frequency and broader range of affected nucleotides compared to the fully silenced chromatin state (Figure 2.4b). The most frequent mutation was a single base pair deletion at the Cas9 cut site in both the unsilenced and fully silenced chromatin states (12.3% and 2.3%, respectively). This result led us to reject our hypothesis. The mutant library sequence data indicate that Cas9-mediated editing is reduced by ~30% in fully silenced chromatin. SURVEYOR assays showed a similar reduction, ~40%. Therefore, the sequencing data and the SURVEYOR data provide corroborating evidence that repressive chromatin interferes with Cas9-mediated editing at site sg034.

In order to investigate inducible chromatin and Cas9 binding, we performed chromatin immunoprecipitation followed by quantitative PCR (ChIP-qPCR) (Figure 2.5a). First, we used an anti-H3K27me3 antibody to map the silencing mark at *luciferase*. H3K27me3 is required for the maintenance of Polycomb-mediated chromatin compaction. We detected 29- to 338-fold increases in mean H3K27me3 enrichment at *luciferase* in GAL4EED cells that were treated with dox for 96 h compared to untreated Luc14 cells. We also detected 4- to 93-fold increases in H3K27me3 enrichment spanning the Cas9/sgRNA target sites in untreated GAL4EED cells relative to Luc14 cells. These data, along with the Luciferase expression assays in Figure 2.1b, validate the dox-induced, facultative silenced chromatin at *luciferase*. Previous work by Hansen et al. showed through ChIP-qPCR that upon addition

Luc14   GAL4EED +dox

```
GGCTATGAAGAGAT-----------------------CTTTTACAGATG          0.7    0.0
GGCTATGAAGAGATAC--------------------GCTTTTACAGATG          0.7    0.0
GGCTATGAAGAGATAC------------------TTGCTTTTACAGATG          0.7    0.0
GGCTATGAAGAGAT----------------ACAATTGCTTTTACAGATG          0.7    0.6
GGCTATGAAGAGATACGCCCTGG------------TGCTTTTACAGATG          0.0    0.6
GGCTATGAAGAGATACGCCCTGG-----------TTGCTaTTACAGATG          0.7    0.0
GGCTATGAAGAGATACGCCCTGGT----------TTGCTTTTACAGATG          0.7    0.0
GGCTATGAAGAGA-----------TCCTGGAACAATTGCTTTTACAGATG         0.7    0.0
GGCTATGAAGAGATACGCCCT--------GAACAATTGCTTTTACAGATG         0.7    0.0
GGCTATGAAGAGATAC--------TCCTGGAACAATTGCTTTTACAGATG         1.3    0.6
GGCTATGAAGAGATACGCCCTGGTTCCTG-------TGCTTTTACAGATG         0.7    0.0
GGCTATGAAGAGATACGC-------CCTGGAACAATTGCTTTTACAGATG         2.0    0.0
GGCTATGAAGAGATACGC------TCCTGGAACAATTGCTTTTACAGATG         1.3    0.0
GGCTATGAAGAGATACG------gTCCTGGAACAATTGCTTTTACAGATG         0.7    0.0
GGCTATGAAGAGATACGCC-----TCCTGGAACAATTGCTTTTACAGATG         0.7    0.0
GGCTATGAAGAGATACGCCCTGGT-----GAACAATTGCTTTTACAGATG         0.7    0.0
GGCTATGAAGAGATACGCCCTGG----TGGAACAATTGCTTTTACAGATG         0.0    0.6
GGCTATGAAGAGATACGCCC---TTCCTGGAACAATTGCTTTTACAGATG         0.0    0.6
GGCTATGAAGAGATACGCCCTG--TCCTGGAACAATTGCTTTTACAGATG         4.0    0.6
GGCTATGAAGAGATACGCCCTGG-TCCTGGAACAATTGCTTTTACAGATG        12.1    2.3
GGCTATGAAGATACGCCCTGGTTCCTGGAACAATTGCTTTTACAGATG          62.4   92.6
GGCTATGAAGAGATACGCCCTGGTnTCCTGGAACAATTGCTTTTACAGATG        4.7    1.1
GGCTATGAAGAGATACGCCCTGGtGTTCCTGGAACAATTGCTTTTACAGATG       0.7    0.0
GGCTATGAAGAGATACGCCCTGGTataTCCTGGAACAATTGCTTTTACAGATG      0.7    0.0
GGCTATGAAGAGATACGCCCTGGT[69]TCCTGGAACAATTGCTTTTACAGATG     0.7    0.0
GGCTATGAAGAGATACGCCCTG[99]GTTCCTGGAACAATTGCTTTTACAGATG     0.7    0.0
GGCTATGAAGAGATACGCCCTG[205]GTTCCTGGAACAATTGCTTTTACAGATG    0.7    0.0
GGCTATGAAGAGATACGCCCTGGTTCCTGGAACAATTGCcTTTACAGATG         0.7    0.0
GGCTATGAAGAGATACGCCCcGGTTCCTGGAACAATTGCTTTTACAGATG         0.0    0.6
```

Deletions · WT · Insertions · Sub.

Legend:
- Target site — Deletion
- ▼ Cleavage site — n Insertion
- PAM — **n** Substitution

b

A T A C G C C C T G G T T C C T G G A A C A A T T G C

Luc14
GAL4EED +dox

0 10 20 30 40

Figure 2.4. Frequencies of mutations in genomic DNA from Cas9/sg034-treated Luc14 or GAL4EED + dox cells. (a) Each row shows the mutated sequence aligned to the wild type sequence (WT). Bar graphs show the percentage of library clones that correspond to the sequence in the same row on the left. (b) The heat map shows the number of times each nucleotide position was affected by a deletion that arose from nonhomologous end joining (NHEJ) repair.

of dox, Polycomb Group 2 (PRC2) protein EZH2, Polycomb Group 1 (PRC1) protein CBX8, and the H3K27me3 mark accumulate at the *luciferase* transgene in GAL4EED cells.[53] We can conclude from their data that when Gal4EED protein binds upstream of *luciferase*, PRC2 is recruited and trimethylates H3K27. H3K27me3 binds PRC1, which is associated with nucleosome compaction and gene silencing.

Next, we used ChIP-qPCR to investigate whether interference of Cas9 activity is associated with a decrease in Cas9 binding. We used deactivated Cas9 (dCas9), which lacks DNA-cutting activity[116] tagged with a C-terminal FLAG sequence to analyze the binding activity of the Cas9/sgRNA complex at unsilenced, partially silenced, and fully silenced chromatin. Formaldehyde-cross-linked chromatin was extracted from dCas9/sgRNA-transfected cells and sheared to ~700 bp. ChIP was carried out in triplicate using an antibody against the FLAG tag. We observed a 3- to 5-fold decrease in mean dCas9 enrichment at sg032 in cells with partial or full silencing at *luciferase* compared to the unsilenced state (Figure 2.5c). This result and the changes in editing efficiency we observed at sg032 (Figure 2.3c) support a mechanism where closed chromatin blocks access of Cas9/sgRNA complexes to the target site. In order to further investigate how Cas9 binding is associated editing efficiency, we investigated two sites where editing was either partially affected or unaffected by the closed chromatin state. Sg034 showed comparable editing in the unsilenced and partially silenced states (Figure 2.3c). The ChIP-qPCR results show comparable enrichment of dCas9 in these two states for sg034. In the fully silenced state where editing efficiency was reduced at sg034, dCas9 enrichment was undetectable. Sg031 showed the least amount of interference (Figure 2.3c). We detected very modest decreases in the mean editing efficiencies for the partially and fully silenced state compared to the unsilenced state. The ChIP-qPCR data followed a similar trend, where dCas9 enrichment was reduced but not eliminated. Perhaps at this site, modest levels of Cas9 binding are sufficient to allow DNA editing. In summary, these results strongly suggest that closed chromatin reduces editing efficiency by blocking access of Cas9 to the target site.

Next, we investigated whether changes in chromatin states (illustrated in Figure 2.6a) could enhance or restore Cas9-mediated editing. In order to induce a hyperactive expression state, we transfected Luc14 cells with a plasmid that expressed the strong transcriptional-activator Gal4-p65. We exposed the *luciferase* transgene to Cas9 editing by cotransfecting these cells with the Cas9/sg034 plasmid. Gal4-p65 induced *luciferase* expression approximately 6-fold compared to the basal expression level in Luc14 cells (Figure 2.6b). SUR-VEYOR showed reduced INDEL formation at hyperactivated *luciferase* compared to the basal level ($p = 0.018$), suggesting that dynamic chromatin remodeling through transcriptional activation or competition with transcription factors interferes with Cas9-mediated INDEL formation. Next, we investigated Cas9 efficiency after restoring the active state
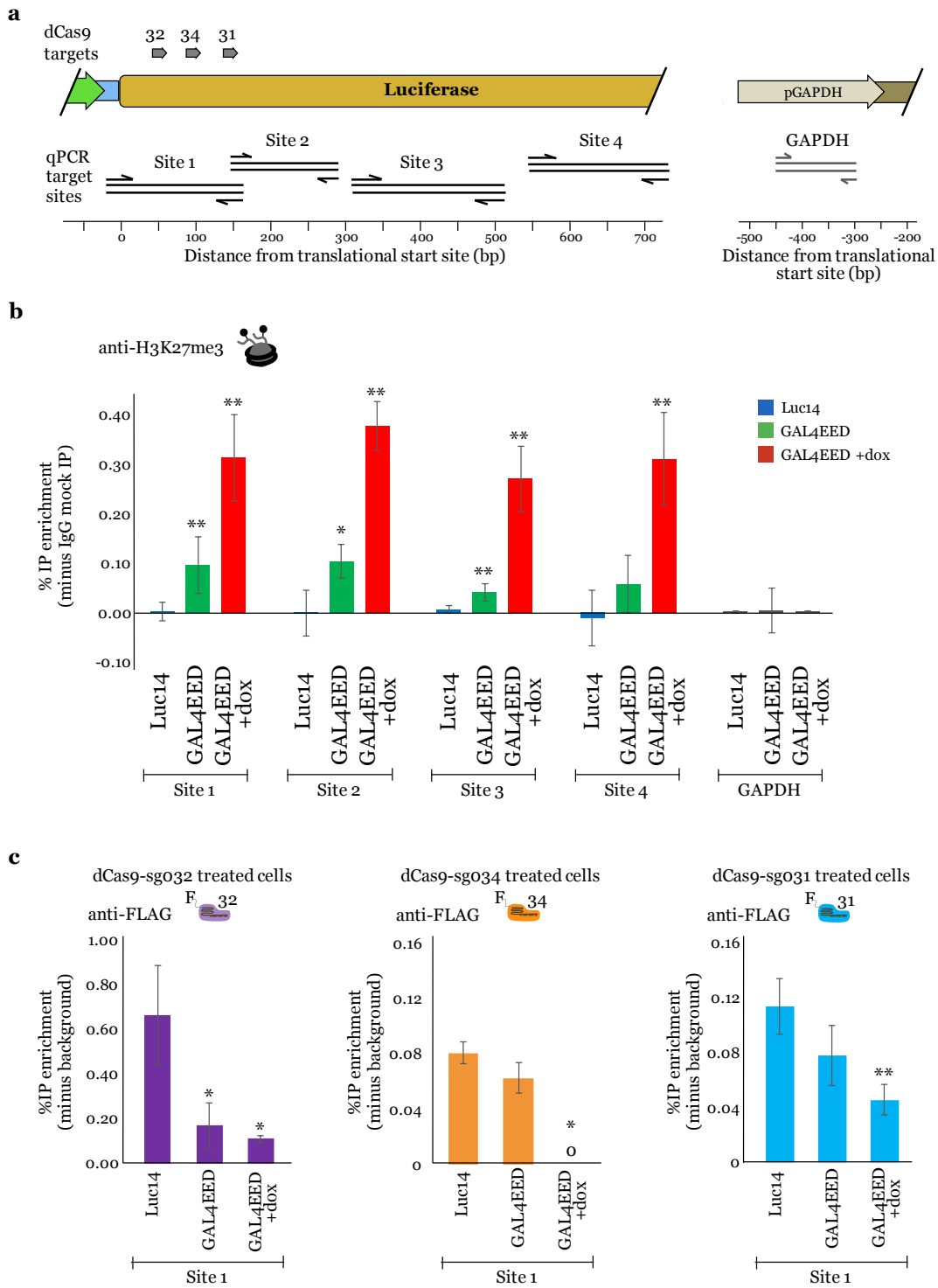
Figure 2.5. Chromatin mapping data show differential enrichment of H3K27me3 and dCas9 at *luciferase* in the open, partially closed, and closed chromatin states.

Figure 2.5. Continued. (a) Cross-linked, sheared chromatin was prepared from Luc14 (unsilenced), GAL4EED (partially silenced), or GAL4EED + dox (fully silenced) cells. An anti-H3K27me3 antibody was used to immunoprecipitate (IP) chromatin from untreated cells. An anti-FLAG antibody was used to IP chromatin from dCas9_gRNA-transfected cells. Quantitative PCR (qPCR) was used to measure IP'ed DNA. Primers (described in Methods) and amplicon sizes are shown in the illustrated maps. A primer pair located at the constitutively active GAPDH promoter was used as a negative control to determine off-target binding. (b) Mean H3K27me3 enrichments for Luc14 (unsilenced), GAL4EED (partially silenced), and GAL4EED + dox (fully silenced) cells at four sites spanning the Cas9/sgRNA target sites. Enrichment is shown as percentages of input minus IgG mock IP. (c) Enrichments of IP DNA for dCas9 are shown for three gRNA target sites, sg032, sg034, and sg031 in three chromatin states, unsilenced, partially silenced, and fully silenced. Enrichments are shown as percentages of input minus background (IgG mock IP and GAPDH) (see Methods). In (b) and (c), error bars indicate s.d. for $n = 3$ replicate IPs from a single chromatin preparation. A one-tailed t test was done to compare Gal4EED or Gal4EED + dox to Luc14 (*$p < 0.5$, **$p < 0.01$).

from a previously silenced state. GAL4EED +dox cells were treated with anti-SuZ12 siRNA to disrupt PRC2 accumulation, or Gal4-p65 to enhance *luciferase* expression. SuZ12, a member of the PRC2 complex, is required for maintaining the H3K27me3 mark.[53] Anti-SuZ12 stimulated partial reactivation compared to the basal expression state and showed full recovery of Cas9 editing efficiency compared to the fully silenced state ($p = 0.045$) (Figure 2.6b and 2.6c). Gal4-p65-treated GAL4EED + dox cells showed full reactivation of *luciferase* compared to the basal expression level and partially restored the frequency of INDEL formation (Figure 2.6b and 2.6c). These results suggest that artificial restoration of gene expression is an effective approach for enhancing Cas9-mediated editing at a target gene.

In conclusion, our results provide direct evidence that at a single genomic locus, Polycomb-mediated chromatin structure impairs Cas9-mediated DNA editing and Cas9 binding at specific sites. Specifically, in the partially and fully repressed chromatin states, the sg032 target site is less accessible to dCas9/sgRNA binding and INDEL formation is reduced. Similarly, at the fully repressed chromatin state, the sg034 target site is less accessible to dCas9/sgRNA binding and INDEL formation is also reduced. Others have investigated the Cas9/sgRNA-target binding step using dCas9 and found off-target binding to be reduced at sites of closed chromatin.[55,56,58] *In vitro* studies suggest that the nucleosome core particle directly contributes to Cas9 interference. Nuclease activity on naked DNA confirmed that Cas9/sgRNA is active *in vitro*.[117] Experiments that used reconstituted chromatin templates demonstrated that nucleosome-occupied regions are blocked from Cas9 binding.[59,66] Our data support these previous observations by demonstrating that closed chromatin inhibits
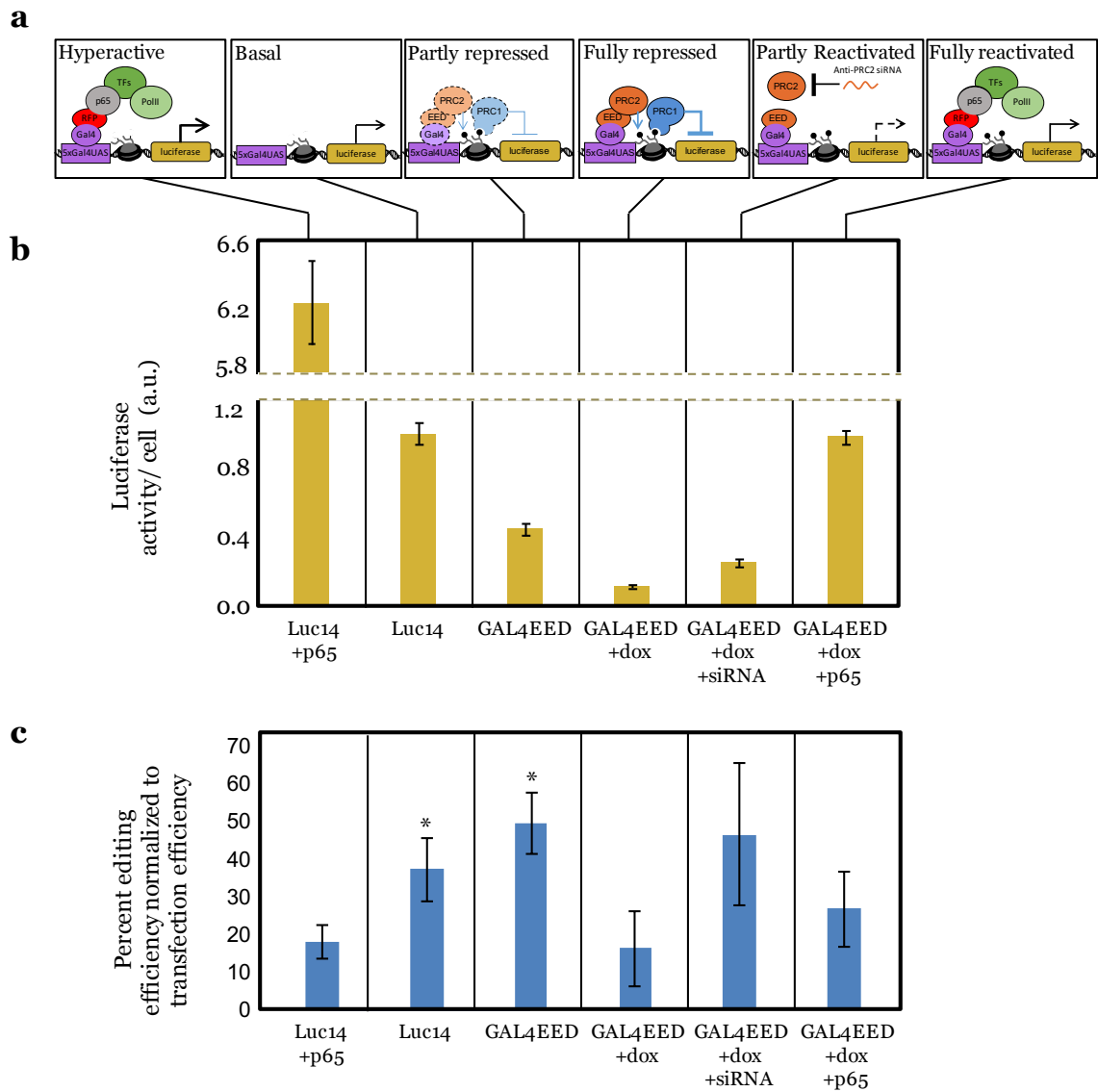
Figure 2.6. Dynamic regulatory states impact Cas9-mediated editing at the *luciferase* transgene. (a) Illustration of the *luciferase* transgene in the basal expression state and in different, artificially regulated states. (b) Background-subtracted Luciferase expression levels per cell were measured 96 h after dox treatment (GAL4EED + dox), immediately before transfection with Gal4-p65 plasmid DNA (+p65), or mock-transfection (vehicle only). Luciferase expression was measured in siRNA-treated cells 336 h after transfection. a.u.: arbitrary units.

Figure 2.6. Continued. (c) Editing efficiency for Cas9/sg034 was determined by SURVEYOR assays. Editing was reduced in the hyperactive expression state (Luc14 + p65) compared to the Luc14 basal state (*p = 0.018) and the GAL4EED partially repressed state (*p = 0.004). Reversal of the closed state via siRNA treatment (GAL4EED + dox + siRNA) was accompanied by an increase in *luciferase* expression and editing efficiency (p = 0.045) compared to the fully repressed state. Editing efficiencies for Luc14, GAL4EED, and GAL4EED + dox shown here are the same data shown in Figure 2.3c.

Cas9/sgRNA-DNA binding at an on-target site. Reduced enrichment of Cas9 is associated with reduced INDEL formation. Taken together, our findings support a mechanism for Cas9 inhibition where chromatin compaction and nucleosome occupancy disrupt Cas9-mediated editing by blocking accessibility of the target site.

Our findings identify repressive chromatin as a critical barrier to efficient Cas9-mediated editing in mammalian cells. In high-throughput applications, such as generating knockout libraries for model organisms, many target sites may be located in closed chromatin in certain cell types. Many sgRNAs may be prone to high failure rates; thus, trial-and-error to achieve gene editing may be impractical. Methods for opening closed chromatin, such as transcriptional activators[118] and inhibitors of heterochromatin proteins[119,120] might enhance Cas9 editing efficiency. We observed that treating cells with siRNA against the silencing protein SuZ12 led to full recovery of editing efficiency comparable to the basal expression state (Figure 2.6). Inducing an active state with a transactivator (Gal4p65) might inhibit Cas9 via competition with the activator and the transcription complex. Therefore, an effective general strategy for restoring an open, Cas9-accessible state at chromatin-regulated target sites may be siRNA-mediated inhibition of closed chromatin. Our study with a switchable Polycomb chromatin system[53] sheds light on the impact of eukaryotic chromatin on Cas9-mediated genome editing and opens new avenues to for enhancing Cas9 function in the context of the human genome.

2.3 Methods

2.3.1 Plasmid DNA Construction

In order to determine transfection efficiencies using flow cytometry, we modified the vectors pX330-U6-Chimeric_BB-CBh-hSpCas9[107] (a gift from Feng Zhang, Addgene plasmid #42230) and pX330A_d-Cas9-1×4[116] (a gift from Takashi Yamamoto, Addgene plasmid #63598) using the T2A peptide skipping sequence to express EGFP from the same mRNA transcript as the Cas9 protein. PX330 or pX330A and the gBlock Gene Fragment (Integrative

DNA Technologies) FseI-NLS-T2A-EGFP-EcoRI containing EGFP were cut with FseI (New England BioLabs) and FastDigest EcoRI (ThermoFisher Scientific) and ligated using T4 DNA Ligase (New England BioLabs). We named this new vector pU6-(BbsI)_CBh-Cas9-T2A-EGFP (DNASU UnSC00746685). SgRNAs used in the study (Table A.1) were designed using the CRISPR design tool at crispr.mit.edu.[74] DNA oligos were synthesized with the overhangs for cloning into pX330g or pX330g_dCas9 (Integrative DNA Technology). Drop-in of sgRNAs followed the cloning protocol described in Cong et al..[107] The Gal4-p65 fusion was expressed from plasmid CMV-Gal4p65_MV1 (DNASU UnSC00746686). Annotated sequences of the plasmids used in this study are available online.[121]

2.3.2 Cell Culturing and Transfections

The Luc14 cell line carries a *firefly luciferase* gene (*Gal4UAS-TK-luciferase*), which is stably integrated into the genome of HEK293 cells.[53] A second cell line, GAL4EED, contains the *firefly luciferase* gene (*Gal4UAS-TK-luciferase*) as well as a *TetO-CMV-Gal4EED* transgene, which carries a Gal4 DNA-binding motif (Gal4) fused to an embryonic ectoderm development (EED) open reading frame driven by TetO-CMV promoter.[53] Expression of the Gal4EED fusion protein-encoding sequence is silenced by a Tetracycline repressor (TetR) (Figure 2.1a). The cell line also contains a puromycin (puro)-inducible anti-Gal4EED miRNA to counter leaky transcription of *TetO-CMV-Gal4EED*. The removal of puro and addition of doxycycline (dox) to cultured GAL4EED cells releases the TetR protein from *TetO-CMV-Gal4EED* and allows the expression of *Gal4EED*. Gal4EED binds to the Gal4UAS site and switches the chromatin state at *luciferase* from active to silenced through accumulation of PRC (Figure 2.1b, Hansen et al.,[53] and Haynes et al.)[115]).

Cells were grown in Gibco DMEM high glucose 1× (Life Technologies) with 10% Tet-free Fetal Bovine Serum (FBS) (Omega Scientific), 0.5 µg/ml puro and 1% penicillin streptomycin (ATCC) at 37 °C in a humidified 5% CO_2 incubator. At time 0 h, puromycin was removed and GAL4EED cells were induced with doxycyclin (dox) (Santa Cruz Biotechnology) at 1 µg/ml. At 72 h, Luc14 cells and dox-induced GAL4EED cells were seeded in 12-well plates such that at 96 h, cells reached 90% confluency. One well from each cell type was collected for Luciferase assay (see below). The remaining wells were used for lipid-mediated transfection. For pX330g/sgRNA transfections, 0.5 µg plasmid was used/well, 3 µl Lipofectamine LTX, and 1 µl Plus Reagent (Life Technologies) per manufacturer's protocol. At 144 h, cells were collected to determine transfection efficiency by flow cytometry and editing efficiency by SURVEYOR Assay (see below).

For p65 CMV-Gal4p65_MV1 transfections, 0.5 µg of each plasmid was used/well, 3 µl Lipofectamine LTX, and 1 µl Plus Reagent (Life Technologies) per manufacturer's protocol.

At 144 h, cells were collected for downstream analyses, including determining transfection efficiency, and performing Luciferase Assay and SURVEYOR Assay (described below).

2.3.3 Luciferase Assay

Cells were washed with 0.5 ml PBS (Irvine Scientific), detached with 0.2 ml trypsin (Life Technologies), collected with the addition of 0.5 ml DMEM, and spun at 100 g. Supernatant was aspirated and the cell pellet was resuspended in 2 ml of FACS buffer (PBS with 1% FBS) and filtered using 35 μm cell strainers (Electron Microscopy Sciences). Twenty μl of cells + FACS buffer were counted and gated using the BD Accuri C6 Flow Cytometer and software (BD Biosciences). The luciferase assay was performed using Steady-Luc Firefly HTS Assay Kit (Biotium) according to manufacturer's protocol. Briefly, 100 μl of cells in FACS buffer from each sample were added to three wells of a Corning and Costar 96-well Cell Culture Plate, black, clear bottom (Bioexpress). One hundred μl of Luciferase working solution was added to each well. Three wells with FACS buffer (without cells) plus Luciferase working solution were read and the highest measured value of the three wells was used as background signal. The plate was incubated for 5 min with orbital shaking and luminescence was read using a Synergy H1 Multi-Mode Reader (Biotek). Luciferase expression per cell was calculated as follows:

$$\text{Sample Luciferase per cell} = \text{Sample Luciferase signal} - \frac{\text{background signal}}{\text{cell count} \times 100\,\mu\text{l}/20\,\mu\text{l}}$$

2.3.4 SURVEYOR Assay

Genomic DNA was extracted using a QIAamp DNA Mini Kit (Qiagen). Cas9/sgRNA target DNA was amplified using Phusion polymerase first with external primers P197 5'–gct-cactcattaggcacccc and P198 5'–ggcgttggtcgcttccggat. PCR products were diluted 1:1000 in water. Nested PCR was performed using primers flanking the Cas9/sgRNA target site (Table A.2 and Table A.3). An annotated map of primers is available online (UAS-TK-luc HEK293).[121] PCR products were purified (GenElute PCR Clean-Up, Sigma) and SURVEYOR assay (IDT) was performed according to the manufacturer's protocol. Briefly, 400 ng of PCR product was mixed with 1.5 μl of annealing buffer (10 mM Tris-HCl (pH 8.8), 1.5 mM MgCl$_2$, and 50 mM KCl), and brought to 15 μl with water. PCR products were melted and reannealed and digested with 1 μl SURVEYOR enzyme and 1 μl Enhancer for 1 h at 42 °C. The concentrations of fragments in each sample were measured on an Agilent 2100 Bio-analyzer. The ratio of uncut wildtype (WT) to cut heteroduplex DNA fragments (HDlarge,

HDsmall) was calculated as follows:

$$\text{Percent editing efficiency} = 100 \times \frac{\text{HDlarge} + \text{HDsmall}}{\text{HDlarge} + \text{HDsmall} + \text{WT}}$$

Genomic DNA from untreated Luc14 and GAL4EED cells and genomic DNA from Cas9/sgRNA treated cells lacking S-nuclease treatment were used as controls to distinguish background noise from actual cut heteroduplex DNA fragments.

The editing efficiencies shown in Figures 3 and 6 were normalized by transfection efficiency. At 72 h post-transfection (12-well plates, ~4×10^5 cells/well), cells were washed with 0.5 ml PBS (Irvine Scientific), detached with 0.2 ml trypsin (Life Technologies), collected with 0.5 ml DMEM, and spun at 100 g for 5 min. Supernatant was aspirated and the cell pellet was resuspended in 2 ml of FACS buffer (1% FBS in 1× PBS) and filtered using 35 μm cell strainers (Electron Microscopy Sciences). Live cells were gated based on forward and side scatter using the BD Accuri C6 Flow Cytometer and software (BD Biosciences). Data was analyzed using FlowJo software. Fluorescence intensity for ten thousand live cells, detected with settings for GFP (488 nm laser, 533/30 filters), was plotted against cell count. The GFP-expression threshold was determined using non-GFP expressing HEK293 cells. Transfection efficiency was calculated as the percent of cells GFP-positive cells in the total live cell population. This value was used to normalize editing efficiencies to cells containing the Cas9/sgRNA plasmid:

$$\text{Percent editing efficiency normalized to transfection efficiency} = \frac{\text{Percent editing efficiency}}{\text{transfection efficiency}}$$

Statistical Analyses. For analyses of SURVEYOR Assay data, standard deviations were calculated for $n = 3$ biological replicates. The differences of means for Luc14/GAL4EED cells and Luc14/GAL4EED + dox cells were calculated using the two sample, one-tailed Student's t test with a confidence of 97.5% for 2 degrees of freedom and a test statistic of $t_{(0.025,2)} = 4.303$.

2.3.5 Mutant Clone Library

The sg034 target region was PCR amplified from genomic DNA and prepared as described above (see "SURVEYOR assay"). Thirty ng (0.072 pmol) of each blunt ~630 bp PCR product was ligated with linear pJET1.2 vector (0.05 pmol ends) in a 10 μl reaction following the manufacturer's protocol (CloneJET PCR Cloning Kit, Life Technologies) with the following modifications: 1× ligation buffer (Roche), T4 DNA ligase (New England Biolabs). Reactions were incubated at room temperature (25 °C) for 5 min, mixed with 50 μl of thawed Turbo competent DH5-alpha *E. coli* (New England Biolabs), and incubated on

ice for 5 min. Transformed cells were plated directly on prewarmed LB agar (100 μg/ml ampicillin) and incubated overnight at 37 °C to grow colonies. Liquid cultures (200 μl LB broth, 100 μg/ml ampicillin) were inoculated in deep round-bottom 96-well plates with single colonies collected via sterile, disposable pipet tips. Plasmid DNA was purified using the Montage Plasmid Miniprep HTS 96 Kit (Millipore). Sanger sequencing was performed using primer P163 (5'–caaaccccgcccagcgtctt). The sequence data were aligned to the pUAS-TK-luc reference sequence in Benchling using MAFFT.[122] Sequence variants were binned manually and counted using Excel software.

2.3.6 Cross-linked chromatin immunoprecipitation (ChIP)

Luc14, GAL4EED, and GAL4EED + dox cells were electroporated with plasmid pX330g_-dCas9/sg031, pX330g_dCas9/sg032, or pX330g_dCas9/sg034 using the Neon Transfection System (Invitrogen) following manufacturers protocols. Electroporation settings were as follows: 100 μl tip, Pulse voltage 1100 V, pulse width 20 ms, 2 pulses, with cell density 5×10^7/ml. Two transfections were plated into each 15 cm plates for each cell type. Transfected cells were grown at 37 °C for 72 h before collection for IPs.

Transfected (for dCas9 IPs) and nontransfected (for H3K27me3 IPs) were collected by trypsin-treatment, and incubated with 20 ml of 1% formaldehyde (Thermo Fisher Scientific)/1× Dulbecco's PBS for 10 min at room temperature. Cross-linking was quenched with 125 mM glycine for 5 min. Cross-linked cells were washed twice with cold 1× PBS buffer + Pierce Protease Inhibitors (Thermo Fisher Scientific) for 5 min with shaking. Cells were washed again with 1× PBS buffer + Pierce Protease Inhibitors without shaking. Cells were spun at 500 g for 5 min between each wash step. To lyse cells, 70 μl of cross-linked cells were resuspended in 112.5 μl of Cell Lysis Buffer [10 mM Tris pH 8.0 (ThermoFisher), 10 mM NaCl, 0.2% IGEPAL (Sigma)] plus Protease Inhibitors and incubated on ice 10 min. Lysed cells were spun for 5 min at 500 g. Nuclei were resuspended and lysed in 1 ml of Nuclei Lysis Buffer [1% sodium dodecyl sulfate (SDS) (Sigma), 10 mM ethylenediaminetetracacetic acid (EDTA) (Fisher Scientific), 50 mM Tris-HCl pH 8.1 (Sigma)] plus Protease Inhibitors and incubated on ice for 10 min. Lysed nuclei were diluted with 0.5 ml of ChIP Dilution Buffer [1% Triton X-100 (Santa Cruz Biotech), 2 mM EDTA, 50 mM NaCl (Sigma), 20 mM Tris-HCl, pH 8.0] and split into five 300 μl-aliquots. Cells were disrupted using a Qsonica Q700A Sonicator with a 5.5 in Cup Horn. Sonicated chromatin was spun at 10 000 g for 10 min at 4 °C to remove impurities and then flash frozen at −80 °C. To confirm sonication efficiencies, 100 μl of sonicated chromatin was purified and resolved via electrophoresis to confirm ~700 bp fragments. For IPs, 50 μg of each chromatin preparation was diluted to 1 ml in dilution buffer [1% Triton X-100 (Santa Cruz Biotech), 2 mM EDTA, 150 mM

sodium chloride (NaCl) (Sigma), 20 mM Tris-HCl, pH 8.0]. Chromatin was precleared for 3 h at 4 °C with nutation with 20 μl of washed [3× PBS buffer + BSA (5 mg/ml) (Sigma)] Magna ChIP Protein A + G (Millipore). Fifty μl (20%) of precleared chromatin was frozen for input control. Chromatin from nontransfected cells was incubated with 5 μg of rabbit anti-H3K27me3 07-449 (Millipore) or 5 μg of rabbit IgG (Cell Signaling 27295) at 4 °C for 12 h with nutation. Chromatin from dCas/sgRNA plasmid-transfected cells was incubated with 40 μl of washed anti-FLAG M2 magnetic beads (M8823, Sigma) (3× with TBS (50 mM Tris HCl, 150 mM NaCl, pH 7.4) or 5 μg of rabbit IgG (Cell Signaling 27295) at 4 °C for 12 h with nutation. Chromatin-anti-FLAG-bead complexes were washed three times with TBS buffer. Chromatin-anti-H3K27me3 and chromatin-IgG samples were incubated with 20 μl Magna ChIP Protein A + G beads for 3 h at 4 °C with nutation and then washed 6 times with 10 min rotating incubations with RIPA buffer [50 mM HEPES pH 7.6 (Thermo Fisher Scientific), 1 mM EDTA, 0.7% Sodium-Deoxycholate (Sigma), 1% IGEPAL CA-630 (Sigma), 0.5 M LiCl (Sigma)] and two times with 5 min rotating incubations with tris-EDTA pH 7.6 (Sigma). Washed chromatin-antibody-bead complexes were resuspended in 100 μl of elution buffer [1% SDS, 0.1 M sodium bicarbonate (Sigma), 0.1 M NaCl]. Fifty μl inputs were brought up to 100 μl in elution buffer. IPs and inputs were nutated for 30 min at room temperature then incubated at 65 °C for 9 h to reverse cross-linking. Samples were treated for 30 min at 37 °C with 10 μg of RNase A and then for 2 h at 62 °C with 10 μg of Proteinase K. DNA from IPs and inputs was purified with Genelute PCR Cleanup Kit (Sigma) and eluted in 50 μl nuclease-free water.

2.3.7   Real-Time Quantitative PCR of ChIP-Enriched DNA

Real-time quantitative PCR reactions (15 μl each) contained SYBR Green master mix, 2 μl of immunoprecipitated (IP), IgG-IP, or input template DNA, and 2.25 pmol of primers. Input Cp values were adjusted by subtracting $\log_2 20$ from each input Cp, as 50 μl was taken from 1 ml total chromatin or ½o. % IP DNA bound was calculated as $100 \times 2^{Ct\ input - Ct\ IP}$. % IgG-IP bound ($100 \times 2^{Ct\ input - Ct\ IgGIP}$) was subtracted from % IP DNA bound to calculate % IP enrichment (minus IgG mock IP) for H3K27me3 mapping. For dCas9 enrichment, % IP enrichment (minus IgG mock IP) at site GAPDH was subtracted from % IP enrichment (minus IgG mock IP) at Site 1 to calculate % IP enrichment (minus background).

Primer sequences for site 1 were as follows:
5'–cgaccctgcataagcttgcc (forward);
5'–ccgcgtacgtgatgttcacc (reverse).
Primer sequences for site 2 were as follows:

5'–ggtgaacatcacgtacgcgg (forward);

5'–aataacgcgcccaacaccgg (reverse).

Primer sequences for site 3 were as follows:

5'–gcgcccgcgaacgacattta (forward);

5'–gagatgtgacgaacgtgtac (reverse).

Primer sequences for site 4 were as follows:

5'–ttgtaccagagtcctttgatcg (forward);

5'–ccgtgatggaatggaacaac (reverse).

Primer sequences for GAPDH were as follows:

5'–tactagcggttttacgggcg (forward);

5'–tcgaacaggaggagcagagagcga (reverse).

Statistical Analyses. For analyses of ChIP-qPCR Assay data, standard deviations were calculated for n = 3 replicate IPs from single chromatin preps. The differences of means for Luc14/GAL4EED cells and Luc14/GAL4EED + dox cells were calculated using the two sample, one-tailed Student's t test. For p < 0.05, confidence was 95% for 2 degrees of freedom and a test statistic of $t_{(0.05,2)}$ = 2.920. For p < 0.01, confidence was 99% for 2 degrees of freedom and a test statistic of $t_{(0.01,2)}$ = 6.965.

2.3.8 siRNA Transfections

At time 0 h, puromycin (puro) was removed and GAL4EED cells were induced with doxycycline (dox, Santa Cruz Biotechnology) at 1 µg/ml. At 96 h, dox was removed and media with puro was used. Cells were seeded in 12-well plates such that at 96 h, cells were at 50% confluency. One well was collected for Luciferase assay (see above). The remaining wells were used for lipid-mediated transfection with 2.5 µl of 20 µm anti-SUZ12 siRNA duplex (Dharmacon)/well and 1.5 µl Oligofectamine (Life Technologies) per manufacturer's protocol. siRNA sequence used was as follows:[53]

Sense: 5' A.A.G.C.U.G.U.U.A.C.C.A.A.G.C.U.C.C.G.U.–G.U.U 3';

Antisense: 5' C.A.C.G.G.A.G.C.U.U.G.G.U.A.A.C.A.G.–C.U.U.U.U 3'.

Mock transfected cells (water used in place of siRNA duplex) were used as a control. At 144 h, siRNA and mock transfections were repeated. At 264 h, siRNA and mock transfected cells were transfected with Cas9/sg034 (three experimental replicates) (see above). At 336 h cells were collected to determine luciferase expression, transfection efficiency, and editing efficiency (see above).

References

(*42*)   Simon, J. A., and Kingston, R. E., (2013). Occupying chromatin: Polycomb mechanisms for getting to genomic targets, stopping transcriptional traffic, and staying put. *Molecular Cell 49*, 808–824, DOI: 10.1016/j.molcel.2013.02.013.

(*50*)   Tiwari, V. K., Cope, L., McGarvey, K. M., Ohm, J. E., and Baylin, S. B., (2008). A novel 6C assay uncovers Polycomb-mediated higher order chromatin conformations. *Genome Research 18*, 1171–1179, DOI: 10.1101/gr.073452.107.

(*51*)   Bell, O., Tiwari, V. K., Thomä, N. H., and Schübeler, D., (2011). Determinants and dynamics of genome accessibility. *Nature Reviews Genetics 12*, 554–564, DOI: 10.1038/nrg3017.

(*52*)   Aoto, T., Saitoh, N., Sakamoto, Y., Watanabe, S., and Nakao, M., (2008). Polycomb group protein-associated chromatin is reproduced in post-mitotic G 1 phase and is required for S phase progression. *Journal of Biological Chemistry 283*, 18905–18915, DOI: 10.1074/jbc.M709322200.

(*53*)   Hansen, K. H., Bracken, A. P., Pasini, D., Dietrich, N., Gehani, S. S., Monrad, A., Rappsilber, J., Lerdrup, M., and Helin, K., (2008). A model for transmission of the H3K27me3 epigenetic mark. *Nature Cell Biology 10*, 1291–1300, DOI: 10.1038/ncb1787.

(*54*)   Daer, R. M., Cutts, J. P., Brafman, D. A., and Haynes, K. A., (2017). The Impact of Chromatin Dynamics on Cas9-Mediated Genome Editing in Human Cells. *ACS Synthetic Biology 6*, 428–438, DOI: 10.1021/acssynbio.5b00299.

(*55*)   Wu, X., Scott, D. A., Kriz, A. J., Chiu, A. C., Hsu, P. D., Dadon, D. B., Cheng, A. W., Trevino, A. E., Konermann, S., Chen, S., Jaenisch, R., Zhang, F., and Sharp, P. A., (2014). Genome-wide binding of the CRISPR endonuclease Cas9 in mammalian cells. *Nature Biotechnology 32*, 670–676, DOI: 10.1038/nbt.2889.

(*56*)   Kuscu, C., Arslan, S., Singh, R., Thorpe, J., and Adli, M., (2014). Genome-wide analysis reveals characteristics of off-target sites bound by the Cas9 endonuclease. *Nature Biotechnology 32*, 677–683, DOI: 10.1038/nbt.2916.

(*58*)   Singh, R., Kuscu, C., Quinlan, A., Qi, Y., and Adli, M., (2015). Cas9-chromatin binding information enables more accurate CRISPR off-target prediction. *Nucleic Acids Research 43*, e118, DOI: 10.1093/nar/gkv575.

(*59*)   Horlbeck, M. A., Witkowsky, L. B., Guglielmi, B., Replogle, J. M., Gilbert, L. A., Villalta, J. E., Torigoe, S. E., Tjian, R., and Weissman, J. S., (2016). Nucleosomes impede cas9 access to DNA in vivo and in vitro. *eLife 5*, 1–21, DOI: 10.7554/eLife.12677.

(*66*)   Isaac, R. S., Jiang, F., Doudna, J. A., Lim, W. A., Narlikar, G. J., and Almeida, R., (2016). Nucleosome breathing and remodeling constrain CRISPR-Cas9 function. *eLife 5*, 1–14, DOI: 10.7554/eLife.13450.

(*69*)   Chen, X., Rinsma, M., Janssen, J. M., Liu, J., Maggio, I., and Gonçalves, M. A., (2016). Probing the impact of chromatin conformation on genome editing tools. *Nucleic Acids Research 44*, 6482–6492, DOI: 10.1093/nar/gkw524.

(*71*)   Perez-Pinera, P., Kocak, D. D., Vockley, C. M., Adler, A. F., Kabadi, A. M., Polstein, L. R., Thakore, P. I., Glass, K. A., Ousterout, D. G., Leong, K. W., Guilak, F., Crawford, G. E., Reddy, T. E., Gersbach, C. A., Kabadi, M., Polstein, L. R., Thakore, P. I., Glass, K. A., Ousterout, D. G., Leong, K. W., Guilak, F., Crawford, G. E., Reddy, T. E., and Gersbach, C. A., (2013). RNA-guided gene activation by CRISPR-Cas9–based transcription factors. *Nature Methods 10*, 973–976, DOI: 10.1038/nmeth.2600.

(*74*)   Hsu, P. D., Scott, D. a., Weinstein, J. a., Ran, F. A., Konermann, S., Agarwala, V., Li, Y., Fine, E. J., Wu, X., Shalem, O., Cradick, T. J., Marraffini, L. a., Bao, G., and Zhang, F., (2013). DNA targeting specificity of RNA-guided Cas9 nucleases. *Nature Biotechnology 31*, 827–832, DOI: 10.1038/nbt.2647.

(*104*)   Ran, F. A., Hsu, P. D., Lin, C.-Y., Gootenberg, J. S., Konermann, S., Trevino, A. E., Scott, D. A., Inoue, A., Matoba, S., Zhang, Y., and Zhang, F., (2013). Double Nicking by RNA-Guided CRISPR Cas9 for Enhanced Genome Editing Specificity. *Cell 154*, 1380–1389, DOI: 10.1016/j.cell.2013.08.021.

(*105*)   Hsu, P. D., Lander, E. S., and Zhang, F., (2014). Development and Applications of CRISPR-Cas9 for Genome Engineering. *Cell 157*, 1262–1278, DOI: 10.1016/j.cell.2014.05.010.

(*106*)   Sánchez-Rivera, F. J., and Jacks, T., (2015). Applications of the CRISPR–Cas9 system in cancer biology. *Nature Reviews Cancer 15*, 387–395, DOI: 10.1038/nrc3950.

(*107*)   Cong, L., Ran, F. A., Cox, D., Lin, S., Barretto, R., Habib, N., Hsu, P. D., Wu, X., Jiang, W., Marraffini, L. A., and Zhang, F., (2013). Multiplex genome engineering using CRISPR/Cas systems. *Science 339*, 819–823, DOI: 10.1126/science.1231143. Multiplex.

(*108*)   Bultmann, S., Morbitzer, R., Schmidt, C. S., Thanisch, K., Spada, F., Elsaesser, J., Lahaye, T., and Leonhardt, H., (2012). Targeted transcriptional activation of silent oct4 pluripotency gene by combining designer TALEs and inhibition of epigenetic modifiers. *Nucleic Acids Research 40*, 5368–5377, DOI: 10.1093/nar/gks199.

(*109*)   Valton, J., Dupuy, A., Daboussi, F., Thomas, S., Maréchal, A., Macmaster, R., Melliand, K., Juillerat, A., and Duchateau, P., (2012). Overcoming transcription activator-like effector (TALE) DNA binding domain sensitivity to cytosine methylation. *The Journal of biological chemistry 287*, 38427–32, DOI: 10.1074/jbc.C112.408864.

(*110*)   Bernstein, B. E., Mikkelsen, T. S., Xie, X., Kamal, M., Huebert, D. J., Cuff, J., Fry, B., Meissner, A., Wernig, M., Plath, K., Jaenisch, R., Wagschal, A., Feil, R., Schreiber, S. L., and Lander, E. S., (2006). A bivalent chromatin structure marks key developmental genes in embryonic stem cells. *Cell 125*, 315–26, DOI: 10.1016/j.cell.2006.02.041.

(*111*)   Aoki, R., Chiba, T., Miyagi, S., Negishi, M., Konuma, T., Taniguchi, H., Ogawa, M., Yokosuka, O., and Iwama, A., (2010). The polycomb group gene product Ezh2 regulates proliferation and differentiation of murine hepatic stem/progenitor cells. *Journal of Hepatology 52*, 854–63, DOI: 10.1016/j.jhep.2010.01.027.

(*112*)   Xie, R., Everett, L. J., Lim, H.-W., Patel, N. A., Schug, J., Kroon, E., Kelly, O. G., Wang, A., D'Amour, K. A., Robins, A. J., Won, K.-J., Kaestner, K. H., and Sander, M., (2013). Dynamic chromatin remodeling mediated by polycomb proteins orchestrates pancreatic differentiation of human embryonic stem cells. *Cell stem cell 12*, 224–237, DOI: 10.1016/j.stem.2012.11.023.

(*113*)   Squazzo, S. L., O'Geen, H., Komashko, V. M., Krig, S. R., Jin, V. X., Jang, S.-w., Margueron, R., Reinberg, D., Green, R., and Farnham, P. J., (2006). Suz12 binds to silenced regions of the genome in a cell-type-specific manner. *Genome Research 16*, 890–900, DOI: 10.1101/gr.5306606.

(*114*)   Sparmann, A., and van Lohuizen, M., (2006). Polycomb silencers control cell fate, development and cancer. *Nature Reviews Cancer 6*, 846–856, DOI: 10.1038/nrc1991.

(*115*)   Haynes, K. A., and Silver, P. A., (2011). Synthetic reversal of epigenetic silencing. *Journal of Biological Chemistry 286*, 27176–27182, DOI: 10.1074/jbc.C111.229567.

(*116*)   Nakagawa, Y., Sakuma, T., Sakamoto, T., Ohmuraya, M., Nakagata, N., and Yamamoto, T., (2015). Production of knockout mice by DNA microinjection of various CRISPR/Cas9 vectors into freeze-thawed fertilized oocytes. *BMC Biotechnology 15*, 33, DOI: 10.1186/s12896-015-0144-x.

(*117*)   Pattanayak, V., Lin, S., Guilinger, J. P., Ma, E., Doudna, J. A., and Liu, D. R., (2013). High-throughput profiling of off-target DNA cleavage reveals RNA-programmed Cas9 nuclease specificity. *Nature Biotechnology 31*, 839–843, DOI: 10.1038/nbt.2673.

(*118*)   Cavalli, G., and Paro, R., (1999). Epigenetic inheritance of active chromatin after removal of the main transactivator. *Science 286*, 955–958, DOI: 10.1126/science.286.5441.955.

(*119*)   Tan, J., Yang, X., Zhuang, L., Jiang, X., Chen, W., Lee, P. L., Karuturi, R. M., Tan, P. B. O., Liu, E. T., and Yu, Q., (2007). Pharmacologic disruption of Polycomb-repressive complex 2-mediated gene repression selectively induces apoptosis in cancer cells. *Genes & Development 21*, 1050–1063, DOI: 10.1101/gad.1524107.

(*120*)   Kanduri, M., Sander, B., Ntoufa, S., Papakonstantinou, N., Sutton, L.-a., Stam-atopoulos, K., Kanduri, C., and Rosenquist, R., (2013). A key role for EZH2 in epigenetic silencing of HOX genes in mantle cell lymphoma. *Epigenetics 8*, 1280–1288, DOI: 10.4161/epi.26546.

(*121*)   Daer, R. M., Cutts, J. P., Brafman, D., and Haynes, K. A., Chromatin CRISPR Interference. https://benchling.com/hayneslab/f_/V1mVw1Lp-chromatin-crispr-interference/ (accessed Mar. 2015).

(*122*)   Katoh, K., and Standley, D. M., (2013). MAFFT multiple sequence alignment soft-ware version 7: improvements in performance and usability. *Molecular Biology and Evolution 30*, 772–780, DOI: 10.1093/molbev/mst010.

Chapter 3

ENHANCING CAS9 ACTIVITY IN HETEROCHROMATIN[‡]

3.1 Introduction

In chapter 2, we demonstrated that compact, gene-silencing chromatin impedes Cas9
binding and editing by making the DNA less accessible to Cas9/gRNA binding (Figure 2.3
and Figure 2.5). Our investigation of the underlying mechanism showed that disruption
of chromatin through siRNA-mediated knockdown of the Polycomb complex enhanced
CRISPR editing, but that target gene overexpression impeded CRISPR activity (Figure 2.6).
Thus, further research is needed to establish chromatin manipulation as a practical tool
for gene editing. In this chapter, we test additional approaches for improving target site
accessibility in heterochromatin. To begin, we compare two general methods for inducing
an open, non-silenced state to enhance CRISPR efficiency: chromatin-disrupting inhibitor
drugs and transient expression of site-specific chromatin-modifying proteins. We explored
the mechanism of enhanced editing at artificially opened chromatin in HEK293 cells using
deep sequencing of edited DNA and chromatin immunoprecipitation (ChIP) of histone
modifications. We demonstrate modest CRISPR enhancement with pre-treatment with
a transiently expressed site-specific fusion transcriptional activator Gal4-p65. We show
co-treatment with Gal4-p65 and the small molecule chromatin inhibitor UNC1999 do not
improve Cas9 editing. In both cases, loss of H3K27me3 was observed but was only associ-
ated with the CRISPR-permissive state in pre-treatment with a transcriptional activator.
We next tested whether delivery of a pre-assembled Cas9/sgRNA ribonucleoprotein (RNP)
with a chemically modified, degradation resistent sgRNA effects targeting in closed chro-
matin. Preliminary data suggest that synthetic guide RNAs greatly improve Cas9 editing in
heterochromatin.

3.2 Sequencing the *Luciferase* Transgene

While testing the above described approaches for improving Cas9 editing effiency, we also
further characterized the two cell lines used in our study, Luc14 and GAL4EED. To construct
the Luc14 cell line, Hansen et al. transfected the Flp-In T-REx - 293 Cell Line (Invitrogen)
with a plasmid containing the *UAS-TK-luciferase* sequence 5xGAL4TKLucNeo and selected

---

[‡] This chapter is a manuscript in preparation. See section F.2 for a discussion of authorship and contribu-
tions.
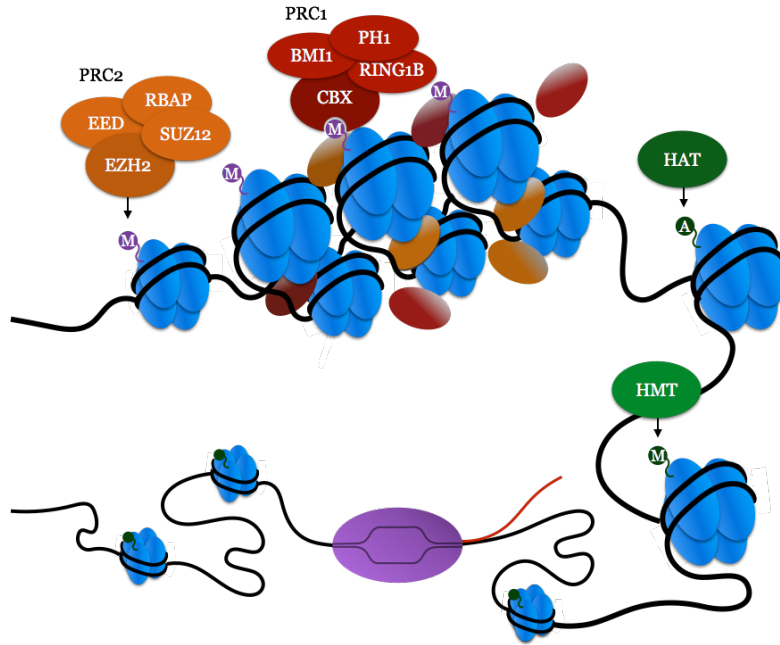
Figure 3.1. Facultative heterochromatin inhibits Cas9 editing while open chromatin is permissive to Cas9. The PRC2 (Polycomb repressive complex 2) holoenzyme (orange) writes the silencing chromatin mark H3K27me3. It is composed of SUZ12 (Suppressor of Zeste 12), EED (Embryonic ectoderm development), RbAp (Retinoblastoma-binding protein), and EZH2 (Enhancer of zeste 2).[50,52] The PRC1 (Polycomb repressive complex 1) holoenzyme (red) reads and propogates the silencing mark H3K27me3. It is composed of CBX8 (Chromobox protein homolog), RING1b (Ring finger protein 1b), and BMI1 (Polycomb group RING finger protein 4).[50,52] Localization of PRC1 and PRC2 results in histone (blue) compaction and gene silencing by preventing binding to the DNA by proteins like RNA polymerase and Cas9. HATs (Histone acetyltransferases) (dark green) add activating acetylation marks to histones, opening chromatin and activating transcription.[123] HMTs (Histone methyltransferases) (light green) add activating methylation marks to histones, opening chromatin and activating transcription.[124] These proteins write activating marks and erase silencing marks, recruiting other chromatin remodelers and loosening the local chromatin to allow for access to the DNA by RNA polymerase (purple) and other DNA binding proteins like Cas9.
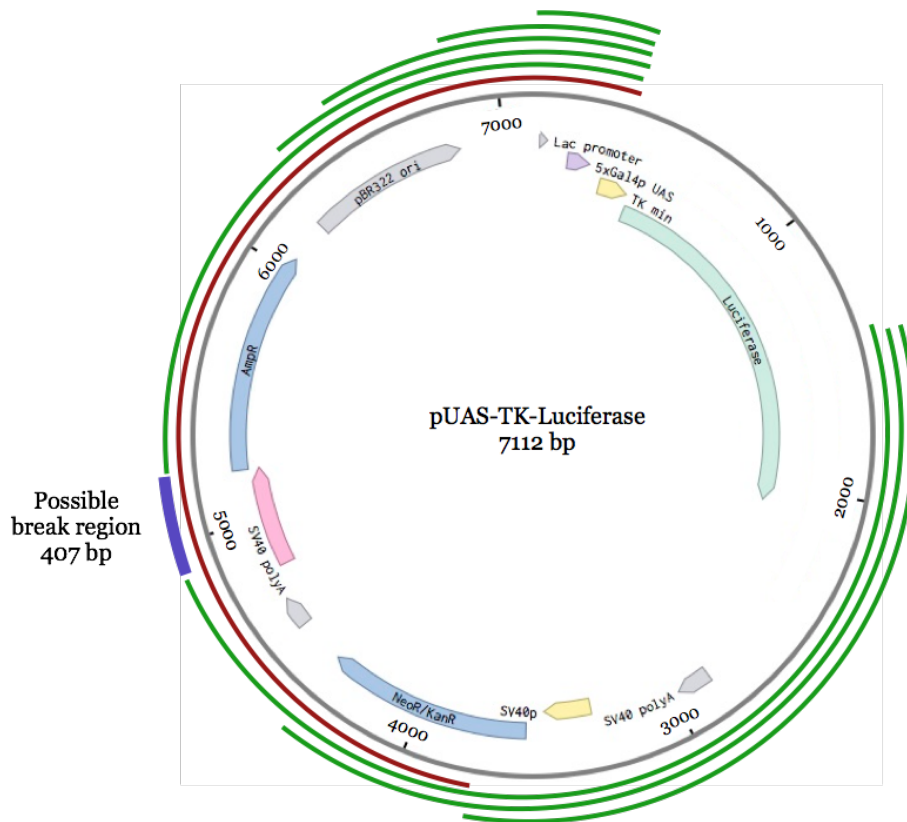
Figure 3.2. Sequencing the *luciferase* transgene. Green bands indicate the PCR produced a product with the expected length. Red bands indicate the expected PCR product from a failed reaction. Purple band indicates the probable break region. Significant plasmid features are annotated.

for stable integration.[53] The Flp-In T-REx - 293 Cell Line has a single-integrated FRT site and constitutively expresses the TetR repressor. To build the GAL4EED cell line, they used the FRT site to integrate a dox-inducible Gal4-EED fusion protein expression plasmid (pcDNA5/FRT/TO GAL4–EED) into the Luc14 parent cell line. They confirmed their system behaved as expected using ChIP for the H3K27me3 silencing mark deposited after Gal4EED recruitment to *luciferase* (see chapter 2 for a full discussion of the cell line and Figure 2.1 and Figure 2.5b for our data).[53,54] Along with generously providing us with the Luc14 and GAL4EED cell lines, Hansen et al. sent us the sequence map for the *pUAS-TK-Luciferase* plasmid. We performed Sanger sequencing to verify the plasmid sequence and have provided an updated sequence map online.We next used end point PCR to identify the location in the plasmid where it broke before insertion. This data will allow us to use ChIP-qPCR to characterize the chromatin state upstream and downstream of the *gal4* initiation site. We anchored one primer in the *pUAS-TK-Luciferase* to prevent false positives Because this cell
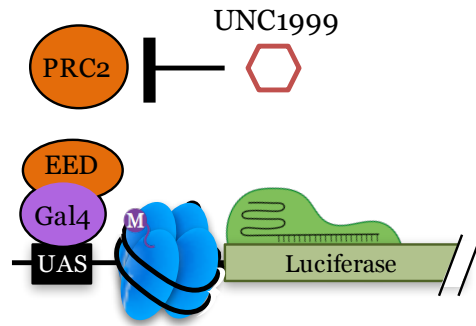
Figure 3.3. Using chromatin inhibitors to improve Cas9 editing. We are using UNC1999, a small molecule drug that inhibits the protein Enhancer of zeste 2 (EZH2), a component of the Polycomb Repressive Complex 2 (PRC2).[125] PRC2 is responsible for maintaining the repressive mark H3K27me3.[50,52]

line contains at least four transgenes, it is likely that the plasmid elements occur multiple times in the genome. We paired each anchor primer with primers moving farther away from the transgene (Figure 3.2). Only one of our PCR reactions failed leading us to identify a possible break region in the plasmid (Figure 3.2). It is important to note that we do not know whether this PCR faied because it traversed the break point or because the product was long and the reaction was inefficient. We did not have the original plasmid to be able to run a positive control. Furthermore, because the *pUAS-TK-Luciferase* plasmid randomly integrated, we do not know if it was inserted multiple times. In order to determine this, we would need to sequence the genome of the cell line.

3.3   Improving Cas9 Editing with Chromatin Inhibiting Drugs

We hypothesized that treatment with with a broad acting, chromatin inhibiting drug would allow for Cas9 to bind and edit a target site located in heterochromatin (Figure 3.3). UNC1999 is a small molecule drug that disrupts heterochromatin in mammalian cells by binding to the active site of the methyltransferase EZH2 to prevent the methylation at H3K27me3, a modification that supports Polycomb complex formation and a closed chromatin state.[125] Konze et al. demonstrated that UNC1999 effectively removed all H3K27me3 from the cell by directly inhibiting EZH2 and EZH1 in both MCF7 (a human breast cancer cell line) and HEK293T cells.[125]

UNC1999 can be diluted in media and therefore can be delivered to all cells in a culture, making it an attractive option for difficult to transfect cell lines. Konze et al. also showed that UNC1999 is effective when fed to and injected into mice with no observed toxicity.[125]

Tk-luciferase expression
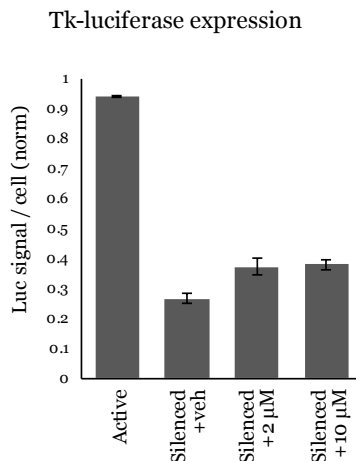
Figure 3.4. UNC1999 dose effect on Luciferase expression. (a) UNC1999 only modestly increases Luciferase expresion at 2 µM and 10 µM doses of UNC1999 over DMSO control (Silenced +veh). Experiment was done with n = 1 biological samples. Error bars indicate standard deviation of n = 3 technical replicates.

3.3.1 Determining UNC1999 Dose

To begin, we determined the toxicity of UNC1999 in our cells. Because Konze et al. tested in HEK293T cells and our experiments use HEK293 cells, we started with the dose ranges they tested. Supplemental Table C.1 shows the concentrations we tested and the resulting toxicity determined through microscopy. For our vehicle control, we added the volume of DMSO corresponding to the highest volume of UNC1999 in DMSO added to our cells, 2.5 µL. We tested both cell types, Luc14 and GAL4EED, at concentrations of 1, 2, 5, 10, 20, and 50 mM and looked for toxicity after 48 h. We did not observe any toxicity in the vehicle control. Cells grown in 1, 2, 5, and 10 mM showed growth similar to the vehicle control. Cells grown in 20 mM showed some toxicity while 50 mM was completely toxic.

We next determined if the non-toxic doses 2 µM and 10 µM increased *luciferase* expression. After 48 h, we saw very modest increases in Luciferase activity compared to vehicle control (Figure 3.4). We did not see differences between the 2 µM and 10 µM doses. Based on these results, we decided to test whether the lower dosage, 2 µM, removed the silencing mark H3K27me3 from our *luciferase* transgene via (ChIP). However, our preliminary results did not show a reduction in H3K27me3 (data not shown). For our next experiments, we tested the higher concentration of 10 µM.

51

a Tk-luciferase expression

b Tk-luciferase chromatin profile
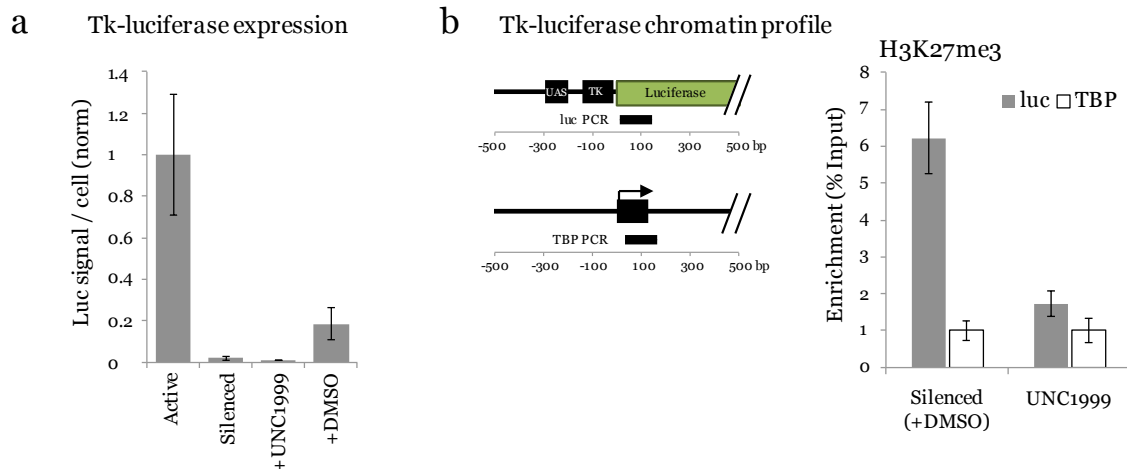
H3K27me3

Figure 3.5. UNC1999 effect on Luciferase expression and H3K27me3. GAL4EED cells were treated with doxycycline (dox) for 96 h and treated with UNC1999 for 120 h. (a) UNC1999 does not increase *luciferase* expression over the silenced state. Luciferase expression was measured 24 h post treatment with UNC1999. Error bars indicate standard deviation of $n = 3$ biological replicates. (b) ChIP assay shows that UNC1999 removes H3K27me3 at the *luciferase* transgene. Error bars indicate standard deviation of $n = 3$ replicate pulldowns from a single chromatin prep.

3.3.2 UNC1999 Removes H3K27me3 from Previously Silenced Locus

We next tested the effect of higher doses of UNC1999 on our *luciferase* transgene. We silenced the chromatin at *luciferase*, as described in chapter 2, Figure 2.1, by adding dox for 96 h. At 120 h (24 h after dox removal), we added 10 μM of UNC1999 for 120 h. At 264 h (24 h after UNC1999 removal), we measured luciferase activity and performed ChIP assay to determine H3K27me3 occupancy. Figure 3.5 shows that while UNC1999 does not significantly increase Luciferase activity, we see a significant decrease in H3K27me3 compared to the DMSO control ($p < 0.01$). We conclude that at 10 μM, UNC1999 can effectively remove the silencing mark H3K27me3 from our silenced transgene but does not initiate transcriptional activation. We proceeded to determine if this removal is sufficient to improve Cas9 editing.

3.3.3 Effect of UNC1999 on Cas9 Editing

To measure whether Cas9 editing is improved at a silenced locus after treatment with UNC1999, we followed the treatment steps described in subsection 3.3.2. At 264 h, we transfected with Cas9/sgRNA expressing plasmids with sgRNAs targeting sg046, 32, 25,
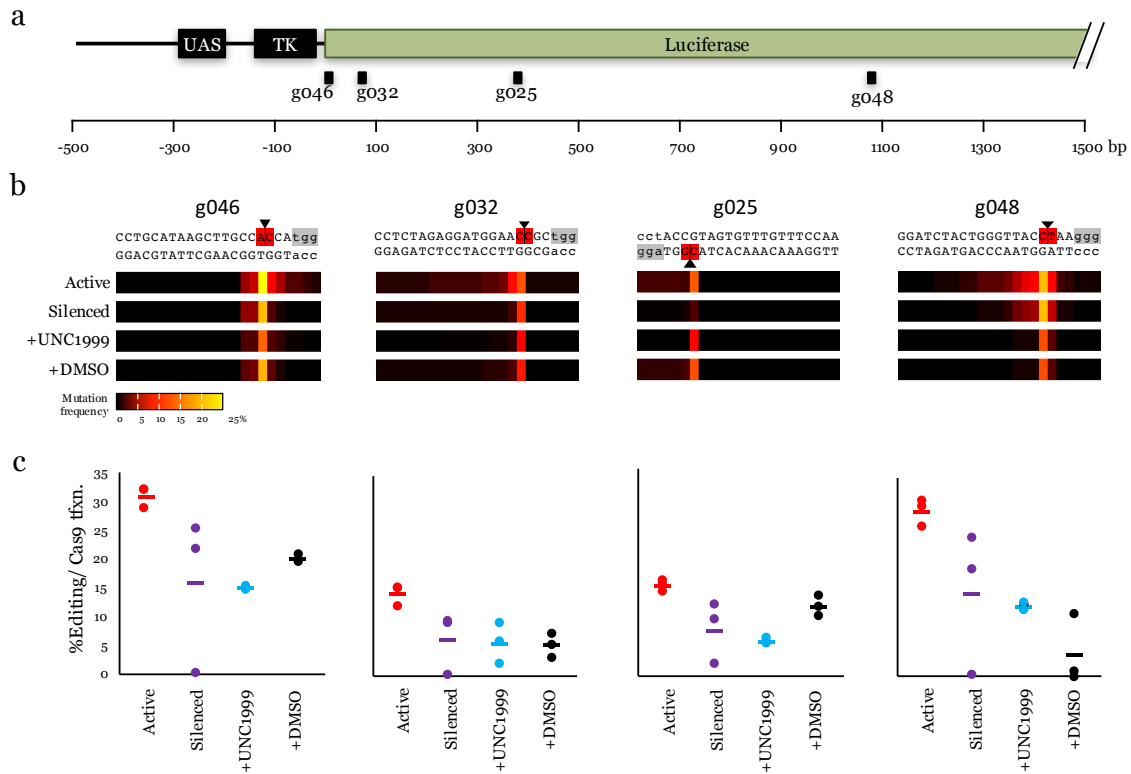
Figure 3.6. UNC1999 effect on Cas9 editing. (a) Map of the *luciferase* transgene and the sgRNA target sites. (b) Heat maps of the mutational frequency determined by deep sequencing. (c) Comparison of editing efficiencies at each sgRNA target site in each chromatin state. In (b) and (c), open chromatin (active), closed chromatin (silenced), reopened with UNC1999 (+UNC1999), and a vehicle control (+DMSO). In (c), dots indicate individual replicates and bars indicate the average of the three biological replicates.

and 48 (Figure 3.6a). In chapter 2 Figure 2.3 we showed that chromatin inhibited Cas9 at sg046 and sg032 target sites but not at sg025 or sg048.[54] At 96 h post transfection, we collected the treated cells and assayed for Cas9 editing using deep sequencing. In Figure 3.6b and c, we see that UNC1999 does not improve Cas9 editing. At sg046, we see significant inhibition of editing in the vehicle control when compared to the active state ($p < 0.001$). However, treatment with UNC1999 not only showed inhibition when compared to the active state ($p < 0.001$), we see even greater inhibition than in the vehicle control ($p < 0.001$). We see the same trend across the other three sgRNA sites. At sg032 and sg025, we see inhibition at all treatments compared to active state ($p < 0.05$ for each). At sg048, we see the same trend; editing is reduced in both the UNC1999 and DMSO treated samples ($p < 0.005$) but the difference between silenced and active is not significant ($p = 0.06$).

We conclude that UNC1999 treatment under these conditions is not effective in improving Cas9 editing at sites in heterochromatin. We hypothesize that removal of the H3K27me3 silencing mark is not sufficient to remove the nucleosomes occupying the locus. To confirm this, we will perform ChIP assay using an antibody agains unmodified H3.

We also do not observe the same inhibition pattern at these sgRNA target sites we reported in chapter 2 for our silenced state compared to the active state. For the active chromatin state, we see a close distribution of our replicates. The error for the silenced state is very large, and for each sgRNA site, there is one biological replicate that showed complete inhibition. Importantly, we see a trend of inhibition in the silenced +DMSO control state when compared to active with $p < 0.05$ for all sites. This is also inconsistent with our previously reported data in which we saw inhibition at sg046 and sg032 but not at sg025 or sg048. In those assays, we used the less sensitive Surveyor assay while in these assays, we are using deep sequencing to detect editing efficiency. We are repeating these experiments to determine whether this variability is due to an experimental error or if editing in heterochromatin is noisy.

3.4   Improving Cas9 Editing with Transcriptional Activators

Our previous work demonstrated that transcriptional activators can activate on gene expression at *luciferase* after silencing (Figure 2.6. However, we did not explore whether gene activation is associated with remodeling of the local chromatin. We hypothesize that strong polymerase recruitment using the targeted, synthetic activator, Gal4-p65, could result in nucleosome sliding away from the transgene, allowing for Cas9 to access the target site. In chapter 2, we tested this hypothesis for a single target site by co-transfecting a Gal4-p65 expressing plasmid with the Cas9/sgRNA plasmid and observed that high levels of transcriptional activation might inhibit Cas9 (Figure 2.6). We hypothesized that after initial recruitment of Gal4-p65, Cas9 is outcompeted by the transcriptional initiation complex and polymerase. Waiting several days post-treatment with Gal4-p65 before transfecting with the Cas9/sgRNA plasmid might allow for nucleosome repositioning to occur followed by plasmid dilution and slowing of transcription at the target site. To test this, we measured the change in Luciferase activity and chromatin state 9 days after treatment with the Gal4-p65 activator. We next measured how co-treatment and pre-treatment (9 days) effects Cas9 editing at a previously silenced target site.
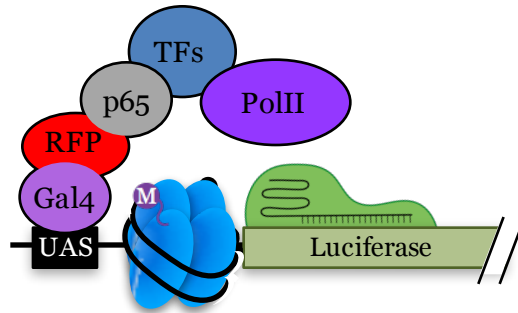
Figure 3.7. Using transcriptional activators to improve Cas9 editing. We are using a targeted transcriptional activator, Gal4-p65, to activate transcription at the previously silenced *luciferase* transgene to improve Cas9 editing.

3.4.1 Gal4-p65 Activates Transcription and Modifies Chromatin at Previously Silenced Locus

To measure the effect of our activator on heterochromatin, we induced silencing at *luciferase* in GAL4EED cells as described in chapter 2 Figure 2.1 by treating with dox for 96 h. At 24 h after dox removal, we transfected with the Gal4-p65 plasmid. After 3 days and 9 days, we collected the cells and assayed for Luciferase activity. We performed ChIP only on samples collected after 9 days.

In Figure 3.8a, we see that Gal4-p65 causes strong and sustained re-activation of *luciferase* for both 3 days and 9 days. This is consistent with our previous results (Figure 2.6).[54]

Using ChIP-qPCR, we determined the change in H3K27me3 after treatment with the Gal4-p65 activator. Similar to treatment with UNC1999, we saw a significant reduction in the amount of H3K27me3 9 days post transfection with the Gal4-p65 expressing plasmid ($p < 0.005$) (Figure 3.8b). This suggests that Gal4-p65 is either recruiting chromatin remodelers that are removing the nucleosomes or the silencing mark, or that strong recruitment of RNA polymerase is responsible for the change in chromatin.

To determine whether p65 localization results in addition of active chromatin modifications, we tested for the presence of an activating mark, H3K4me3. We saw some reduction in the mark between active and silenced though it was not significant ($p = 0.06$) (Figure 3.8b). We did observe a significant increase in the active mark between the silenced state and the reopened state ($p < 0.01$).

Interestingly, our data indicate that the active and silenced state have the H3K4me3 mark (Figure 3.8b). This mark is associated with bivalent promoters and is often seen together with H3K27me3.[110] This suggests that recruitment of PRC1 and PRC2 does not

a
Tk-luciferase expression

b
Tk-luciferase chromatin profile

H3K27me3

H3K4me3
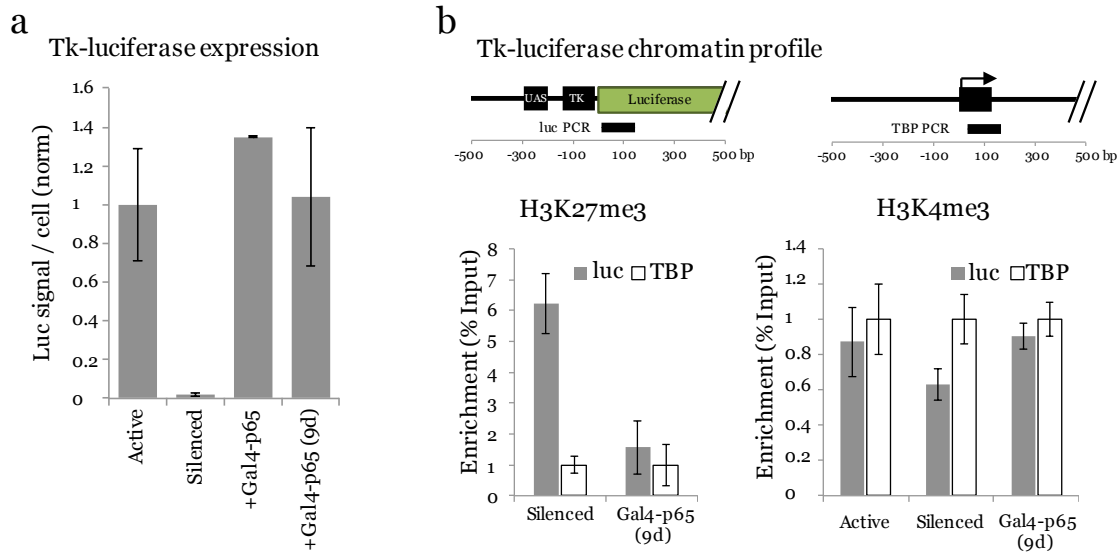
Figure 3.8. Targeted transcriptional activator Gal4-p65 increases Luciferase expression and modifies local chromatin. GAL4EED cells were treated with doxycycline (dox) for 96 h and transfected with the Gal4-p65 expressing plasmid. (a) Gal4-p65 increases gene expression at the previously silenced *luciferase* transgene. Luciferase expression was measureed after 3 days or 9 days. Error bars indicate standard deviation of n = 3 biological replicates. (b) Gal4-p65 reduces H3K27me3 at the *luciferase* transgene. H3K4me3 is present in each chromatin state but increased after treatment with Gal4-p65. Error bars indicate standard deviation of n = 3 replicate pulldowns from a single chromatin prep.

result in removal of H3K4me3 at our site. Unfortunately, the literature does not point to a single chromatin modification associated with p65. In order to determine whether recruitment of Gal4-p65 results in the addition of an activating mark, we will need to screen other activating marks.

3.4.2   Effect of Gal4-p65 on Cas9 Editing

To measure the effect of our activator on heterochromatin, we again silenced GAL4EED cells with dox for 96 h. At 24 h after dox removal, we transfected with either the Gal4-p65 plasmid and the Cas9/sgRNA plasmid (for co-treatment) or the Gal4-p65 plasmid alone (for pre-treatment). For co-treated samples, we collected to assay for editing efficiency 72 h post-transfection. For pre-treated samples, we transfected with the Cas9/sgRNA plasmid 9 days after Gal4-p65 transfection and collected to assay for editing efficiency 72 h later. We tested four sgRNA target sites: sg046, 32, 25, and 48 (Figure 3.6a).
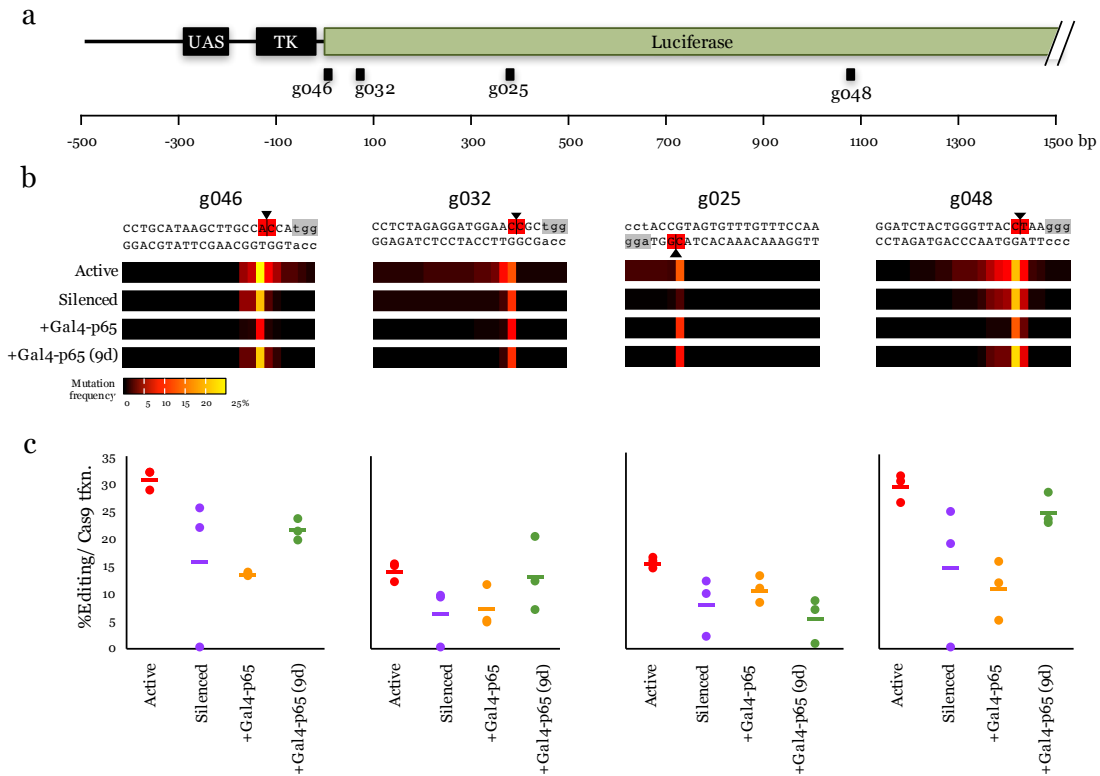
Figure 3.9. Transcriptional activator effect on Cas9 editing. (a) Map of the *luciferase* transgene and the sgRNA target sites. (b) Heat maps of the mutational frequency. (c) Comparison of editing efficiencies at each sgRNA target site in each chromatin state. In (b) and (c), open chromatin (active), closed chromatin (silenced), reopened with Gal4-p65 after 3 days (+Gal4-p65), and opened with Gal4-p65 after 9 days (+Gal4-p65 (9d)). In (c), dots indicate individual replicates and bars indicate the average of the three biological replicates. Note: "Active" and "Silenced" data are the same data presented in Figure 3.6.

Active and Silenced controls in Figure 3.9b and c are the same data presented in Figure 3.6. In subsection 3.3.3 we discuss the inconsistency with these data and the data we presented in chapter 2 Figure 2.3 and the variability observed in the Silenced controls.

For all target sites, we do not see any improvement in editing after co-treatment or pre-treatment when compared to the silenced controls. At sites sg046 and sg048, co-treated samples show significant reduction in editing when compared to pre-treated samples ($p < 0.01$). These data support our hypothesis that inhibition of Cas9 by targeted over expression diminishes with time.

While not significant, the Gal4-p65 pre-treatment data show a trend toward higher editing efficiency over the silenced state. As discussed above, the silenced state data are

noisy. However, the silenced state treated with DMSO used as the control for the UNC1999 experiments (Figure 3.6) showed significant reduction in editing when compared to the active controls for each target site. We do not expect the low volume of DMSO added to these cells is responsible for this reduction in editing and therefore are a suitable control for our pre-treatment data. We compared editing efficiencies at each target site between the silenced DMSO control and pre-treatment with Gal4-p65 (Figure 3.10). At sg046, we do not see any improvement in editing after Gal4-p65 pretreatment (Figure 3.10b). At sg032 there is a slight increase in efficiency but the data are not significant ($p = 0.07$). At sg025 and sg048, we see significant editing improvements after pre-treatment ($p < 0.05$ for sg025 and $p < 0.005$ for sg048).

While more experiments are necessary, these data begin to support our hypothesis that transient expression of transcriptional activators remodels chromatin to a more Cas9-permissive state (Figure 3.10). However, hyperactive transcription further inhibits Cas9 editing (Figure 3.8). Further exploration should include weaker transcriptional activators to balance chromatin reopening with moderate promoter activity.

3.5   Improving Cas9 Editing with Synthetic Guide RNAs

In adddition to artificially reopening silenced chromatin, we also tested whether increasing the stability of the RNP using chemically modified sgRNAs improves Cas9 editing in heterochromatin. The RNP is subject to degradation becasue of the single stranded RNA extending from the complex. If the mechanism of chromatin inhibition is reducing, but not blocking, access to target sites, increasing the stability of the RNP could keep more active Cas9 molecules in the nucleus for longer. This would increase the number of tries over the same time period and possibly increase the accumulation of edits.

We used synthetic sgRNAs modified to have greater stability from addition of 2'-O-methyl group and a sulfur atom substituted for an oxygen on the linking phosphodiester bonds between the last three nucleotide on the 5' and 3' ends of the sgRNA (Synthego).[126–128] SgRNAs modified in this way are resistant to degradation and show significantly improved editing efficiencies compared to other RNP introduction techniques.

At this time, we only have editing efficiencies for one sgRNA site, sg032 (Figure 3.11a), and only one biological replicate. In Figure 3.11b and c, we see that the RNP editing efficiency is over five times greater than the active state with plasmid delivery. These preliminary data suggest that delivery of RNP with synthetically modified sgRNAs greatly improves Cas9 editing at sites in closed chromatin.

It is important to note here that the controls we are using are not ideal and therefore cannot say what is responsible for this improvement: the methods of Cas9 delivery (pre-complexed RNP over plasmid) or increased stability of the modified sgRNA. When an RNP
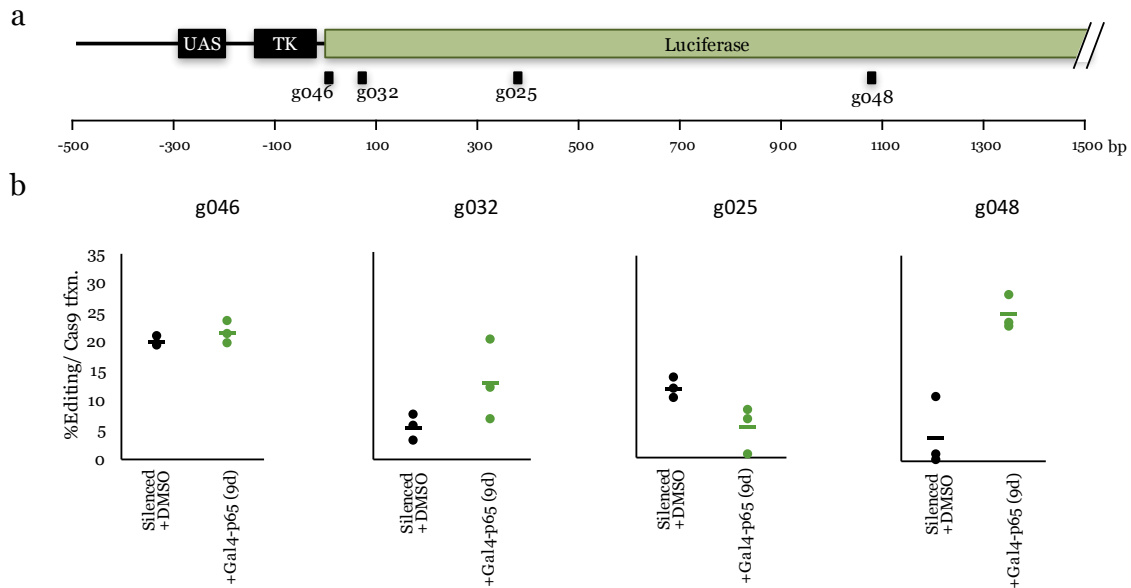
Figure 3.10. The effect of pre-treatment with transcriptional activator Cas9 editing compared to DMSO control. (a) Map of the *luciferase* transgene and the sgRNA target sites. (b) Heat maps of the mutational frequency. (c) Comparison of editing efficiencies at each sgRNA target site for silenced samples treate with DMSO vehicle control (Silenced +DMSO) or pre-treated with Gal4-p65 for 9 days (+Gal4-p65 (9d)). Dots indicate individual replicates and bars indicate the average of the three biological replicates. Note: "Silenced +DMSO" data are the same data presented in Figure 3.6.

is electroporated into the cell, it is immediately active. Cas9 delivery via plasmid requires transcription, translation, RNP complex formation, and nuclear localization before editing begins. To control for these differences, we will compare editing of RNP with modified and unmodified sgRNAs. It is also possible that RNP delivery results in much higher protein concentrations in the cell. For our plasmid experiments, we determine transfection efficiency using the EGFP reported on our plasmid. To determine protein delivery efficiency, we will perform Western blots using anti-Cas9 antibodies.

Even without knowing the mechanism, we can still conclude that RNP delivery of Cas9 with chemically modified sgRNAs is the most promising approach for improving Cas9 editing in closed chromatin.

3.6 Future Work: Gene Expression and Cas9

The data reported in Figure 3.9b and c suggested that gene over-expression inhibits Cas9 editing at some target sites. With this in mind, we designed experiments to determine
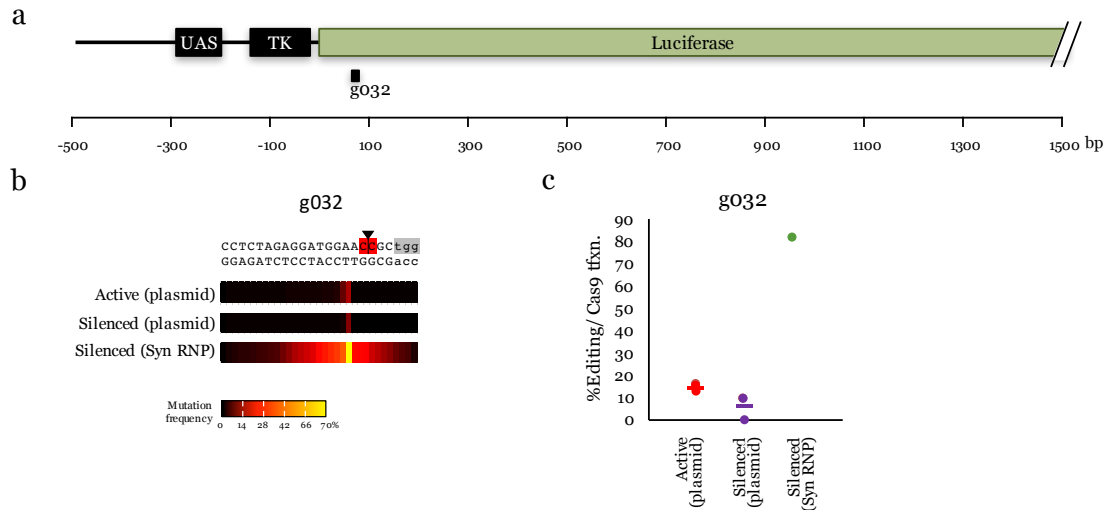
Figure 3.11. Increased RNA stability greatly increases Cas9 editing at sites in closed chromatin. (a) Map of the *luciferase* transgene and the sgRNA target sites. (b) Heat maps of the mutational frequency. (c) Comparison of editing efficiencies at each sgRNA target site in each chromatin state. In (b) and (c), open chromatin transfected with plasmid expressing Cas9/sgRNA [active (plasmid)], closed chromatin transfected with plasmid expressing Cas9/sgRNA [silenced (plasmid)], and closed chromatin electroporated with Cas9/sgRNA ribonucleoproteins (RNPs) [silenced (RNP)]. In (c), dots indicate individual replicates and bars indicate the average of the three biological replicates. Silenced (RNP) includes data from a sinle experiment. Note: "Active" and "Silenced" data are the same data presented in Figure 3.6 and Figure 3.9.

the threshold of artificial gene expression that Cas9 can tolerate. We hypothesize that while low-levels of polymerase activity maintain an open chromatin state and allow for Cas9 access, over-expression results in competition with polymerase and observed reductions in editing activity.

The Luc14 cell line used in these studies contains a constitutively expressed, genomic-integrated TetR and a Frt site (section 3.2). We designed and built a vector for Frt-mediated integration of a dox-inducible transcriptional activator system, Gal4-mCherry-p65. With this system, we would be able to gradually increase gene expression at the *luciferase* transgene and measure Cas9 inhibition.

Current progress includes construction of the integration plasmid and a kill-curve with the selection antibiotic, hygromycin. Next steps to complete this project require generation of the stable cell line, characterization of Luciferase expression in response to dox induction, and measuring Cas9 editing at different expression levels. We hypothesize that in addition

to overexpression resulting in Cas9 inhibition, distance from the transcriptional start site will also effect sensitivity to expression levels.

3.7 Discussion

Here, we investigated methods for improving Cas9 editing at sites located in silenced chromatin. First, we tested how artificial opening of closed chromatin effects CRISPR editing activity. We compared two approaches: indirect activation via the disruption of closed chromatin and fusion-mediated activation. The data presented in this chapter are preliminary and do not conclusively demonstrate that these approaches significantly improve Cas9 editing in silenced chromatin.

While UNC1999 effectively removed H3K27me3 from the Tk-luciferase transgene (Figure 3.5b), we did not see editing efficiencies similar to the active state (Figure 3.6b and c). Furthermore, UNC1999 treatment did not increase Luciferase expression to levels similar to the unsilenced state (Figure 3.5a) (Figure 4B). We hypothesize that UNC1999 removed the silencing mark but that the histone proteins remained tightly compacted and continued to inhibit Cas9. Future work should include screening other chromatin-inhibiting drugs and testing combinations of drugs.

Pre-treatment with the Gal4-p65 activator shows the most promising improvement in editing (Figure 3.10c). Co-treatment showed greater inhibition, supporting our hypothesis that high levels of transcriptional activity can impede Cas9 editing through steric hinderence. The work proposed in section 3.6 will test this hypothesis with consideration of the distance from the transcriptional start site, where transcriptional initiation complexes might increase steric competition. Future work should also include testing weaker transcriptional activators to determine if they can initiate sufficient transcription to reopen silenced chromatin without creating steric competition.

The key advantage of the activator Gal4-p65, or any fusion of a DNA binding domain with a transcriptional activator, is the ability to target a single site, presumably without disrupting the expression of other genes. Global chromatin modification by drugs like UNC1999 likely will not be tolerated in many applications. While the fusion proteins tested in this study are targeted to a Gal4 binding domain, they can be modified to be fused to dCas9 or other targetable DNA binding domains making them widely applicable.[72]

However, there are also applications in which gene activation, even if targeted, will not be acceptable. For example, if the target site is a global transcriptional activator or an oncogene that initiates apoptosis, any expression could lead to further chromatin remodeling and irreversible changes to the cell state. Chromatin remodeling without gene activation (i.e. UNC1999 treatment) would be a better approach over targeted activation. Furthermore,

broad-acting chromatin remodeling may be necessary for manipulating chromatin at multiple sites or at sites for which DNA-binding modules cannot be designed (e.g., low complexity sequences). Low molecular weight compounds do not require transfection and are easier to deliver. By exploring both strategies, our work allows researchers to choose an appropriate strategy specific to their experimental goals.

We also tested whether delivering Cas9 complexed with a chemically modified sgRNA efficiently targets Cas9 to sites in closed chromatin. The chemical modification reduces degradation of the protruding RNA from Cas9 increasing the stability of the RNP.[126–128] Although we currently have limited data, our synthetic guide RNA shows the greatest improvement in editing in heterochromatin (Figure 3.11). As presented here, these experiments are not well-controled in our current design and we cannot conclude what is responsible for the improvement; there are several differences between our current control data set and this treated sample. First, in our controls, we are transfecting plasmid DNA. We likely don't have active Cas9/sgRNA complexes until at least 24 h after transfection as we do not observe EGFP expression until 24 h. With the synthetic guide approach, we are transfecting RNPs which are likely immediately active when they enter the cell. Even with these limitations, these results are very promising, and we are performing additional experiments to determine whether this is consistent across replicates as well as target sites.

3.8 Methods

3.8.1 Cell Lines and Plasmids

For this study, we used HEK293 cells carrying a *firefly luciferase* transgene (Luc14) or the *firefly luciferase* transgene plus an inducible *tetO-Gal4EED* transgene (GAL4EED), described previously (chapter 2).[53,54] Briefly, in the GAL4EED cell line, chromatin state at the *Gal4UAS-TK-luciferase* transgene can be controlled by the addition of doxycyclin (dox); cells are open until treated with dox for 96 h.[54] The *Gal4UAS-TK-luciferase* transgene in the Luc14 cell line remains open as there is no *Gal4EED* transgene. These states have been characterized by luciferase expression assays and ChIP-qPCR.[53,54]

Cas9 was transfected using pU6-(BbsI)_CBh-Cas9-T2A-EGFP (DNASU UnSC00746685) built from pX330-U6-Chimeric_BB-CBh-hSpCas9 (a gift from Feng Zhang, Addgene plasmid #42230) (described in Daer et al.). The pU6-(BbsI)_CBh-Cas9-T2A-EGFP expresses the human optimized Cas9 protein and EGFP from the same mRNA transcript. Guide RNAs sg025, sg032, sg046, and sg048 were cloned into pU6-(BbsI)_CBh-Cas9-T2A-EGFP (described in Daer et al.). Gal4-p65 transfections were done with plasmid CMV-Gal4p65_MV1 (DNASU UnSC00746686) which expresses the Gal4-mCherry-p65 fusion protein from a CMV promoter.

Annotated sequences of the plasmids used in this study are available online.[129]

3.8.2 Cell Culturing and Transfection

Luc14 and GAL4EED were cultured using Gibco DMEM high glucose 1× (Life Technologies) with 10% Tet-free Fetal Bovine Serum (FBS) (Omega Scientific), 0.5 µg/ml puromycin (puro) and 1% penicillin streptomycin (ATCC) and grown at 37 °C in a humidified 5% CO_2 incubator. To induce chromatin silencing at *luciferase* in GAL4EED cells, puro was removed and 1 µg/ml of dox (Santa Cruz Biotechnology) was added to the media for 96 h.

For transfections, cells were seeded in 12-well plates such that 24 h later they were at 90% confluency. Lipid complexes were formed using 500 ng plasmid, 3 µl Lipofectamine LTX, and 1 µl Plus Reagent (Life Technologies) per well and diluted in Gibco Opti-MEM (Thermo-Fisher) to a final volume of 100 µl per well. Cells were collected for analyses 72 h post transfection.

For UNC1999 treatment, powdered UNC1999 (Cayman Chemical) was dissolved in DMSO to 10 mM. Toxicity was determined using a dilution curve (data not shown). Gal4EED cells were treated for 96 h with dox to induce silencing. After 24 h without dox, cells were treated with 10 mM UNC1999 by diluting 1 µl of 10 mM UNC1999 per 1 ml media for 72 h. Control cells were treated with 1 µl of DMSO (vehicle) per 1 ml media. Cells were grown for 1 day in media without UNC1999 before Luciferase assay (described below), transfection with Cas9/sgRNA plasmids (described above) or ChIP assay (described below).

3.8.3 Luciferase Assays

Cells were washed with PBS and collected with 0.2 ml of trypsin-EDTA (0.25%) (Life Technologies) and 0.5 ml DMEM. Cells were pelleted at 200 g for 5 min at room temperature, washed with PBS, pelleted again, resuspended in 1 ml of FACS buffer (1% FBS in 1× PBS), and filtered with 35 µm cell strainers (Electron Microscopy Sciences). Transfection efficiencies for each sample were determined by measuring the mCherry positive cells in 10 000 live cells with the BD Accuri C6 Flow Cytometer and accompanying software (BD Biosciences). Cell counts to normalize luciferase activity were determined by counting the number of live cells in 20 µl from each sample by flow cytometry. Luciferase assay was performed in triplicate, with 100 µl of each sample diluted in 100 µl D-luciferin diluted in buffer [Steady-Luc Firefly HTS Assay Kit (Biotium)] according to manufacturer's protocol, in CORNING and Costar 96-well Plates, black sides, clear bottom (Bioexpress). One hundred µl of FACS buffer with 100 µl of diluted D-luciferin was used as background control. The reaction incubated for 5 min at room temperature with orbital shaking and luminescence was determined

with a Synergy H1Multi-Mode Reader (Biotek). Luciferase activity normalized per cell was calculated:

$$\frac{\text{Luciferase}}{\text{cell}} = \text{Luciferase signal} - \frac{\text{background signal}}{\text{cell count in 20\,\textmu l} \times \frac{100\,\text{\textmu l}}{20\,\text{\textmu l}}}$$

3.8.4   CRISPR Activity Assays

After 72 h of growth post-transfection with pU6-(BbsI)_CBh-Cas9-T2A-EGFP (DNASU UnSC00746685) with sgRNAs sg025, sg032, sg046, and sg048,[54] cells were collected as with 0.2 ml of trypsin and 0.5 ml of DMEM and spun for 5 min at 500 g at room temperature. Supernatant was discarded and cells were resuspended in 250 µl of 1× PBS. To determine transfection efficiency, 50 µl were counted by flow cytometry, gated for live cells, and the percent of GFP positive cells was recorded. Genomic DNA was extracted from the remaining 200 µl of cells using the QIAamp DNA Mini Kit (Qiagen) and eluted in 100 µl of nuclease-free water.

PCR of gDNA was performed using GoTaq 2× mastermix (Promega) using primers P198/198 (sequences listed in Supplemental Table C.2) [95 °C for 10 min; 34 x (95 °C for 30 s; 58 °C for 30 s; 72 °C for 120 s)]. Nested PCR was performed by diluting 2 µl of PCR product into 500 µl of water and Phusion High-Fidelity DNA Polymerase (Thermo Scientific) (primers listed in Supplemental Table C.3). PCR reactions were purified using the Genelute PCR Cleanup Kit (Sigma) and submitted to the Center for Computational and Integrative Biology (CCIB) Core Facility (Massachusetts General Hospital, Cambridge, MA) according to their requirements for sequencing.

3.8.5   Crosslinked Chromatin Immunoprecipitation

For p65 co-treatment ChIPs, Luc14s and Gal4EED + dox cells were transfected with 18 µg p65 plasmid using the 100 µl Neon transfection system (Invitrogen) following the recommended protocol (1100 V pulse voltage, 20 ms pulse width, 2 pulses, with cell density 5×10^6/ml). Cells were grown at 37 °C for 72 h, fixed as described below, and sorted using the BD FACSAria II cell sorter. Lysis and sonication steps were performed same day as described below. For chromatin remodeler treatment ChIPs, Gal4EED + dox cells were transfected with 18 µg of each chromatin remodeler plasmid using the Neon transfection system as described above. For p65 pre-treatment ChIPs, Gal4EED + dox cells were transfected with Lipofectamine as described above and grown at 37 °C for 9 days.

Cells were washed and collected as described above and fixed with 1% formaldehyde (Thermo Fisher Scientific) in 1× Dulbecco's PBS for 10 min. The reaction was quenched

with 125 mM glycine (Sigma) for 5 min at room temperature with gentle rocking followed by four washes with 1× PBS and Pierce Protease Inhibitors (Thermo Fisher Scientific), two for 5 min at room temperature and two without incubation. Cells were pelleted between each wash at room temperature for 5 minute at 500 g. During the last wash step, 10 µl of cells were transferred to a new tube, diluted into 90 µl of 1× PBS, and 20 µl of cells were counted via flow cytometry. Total number of cells were calculated for each sample. Cells and nuclei were lysed with cell lysis buffer and nuclei lysis buffer. Chromatin was diluted in 500 µl of ChIP dilution buffer [1% Triton X-100 (Santa Cruz Biotech), 2 mM EDTA, 150 mM NaCl (Sigma), 20 mM Tris-HCl, pH 8.0] and split into 1.5 ml microcentrifuge tubes, 300 µl per tube. Chromatin was sonicated using the Qsonica Q700A Sonicator with a 5.5 in Cup Horn, spun for 10 min at 4 °C at 1×10^4 g, and efficiency was confirmed using the Agilent 2200 Tapestation. Sonicated chromatin from 5×10^6 cells was diluted in 1.5 ml siliconized, low-binding tubes (Sigma) in ChIP dilution buffer to 1 ml for each pulldown, except for the p65 sorted experiments where chromatin from 1.5×10^6 cells was used. Chromatin was precleared by incubation with 20 µl of Magna ChIP Protein A + G beads (Millipore) (washed 3 times with 5 mg/ml BSA (Sigma) in 1× PBS) for 3 h at 4 °C with nutation. Beads were separated and removed using a magnetic rack (Invitrogen), 50 µl from each chromatin prep was frozen for inputs, and chromatin was incubated with antibody [5 µl anti-Histone H3 antibody (ab1791, Abcam); 5 µl anti-H3K27me3 antibody (07–449, Millipore); 3 µl anti-H3K4me3 (ab8580, Abcam)] for 12 h at 4 °C with nutation. Chromatin was incubated with 20 µl washed Magna ChIP beads for 3 h at 4 °C with nutation. Beads were washed at 4 °C 3 times, first with 1 ml low salt buffer [20 mM Tris-HCl, 2 mM EDTA, 1% Triton X-100, 0.1% SDS (Sigma), 150 mM NaCl (Sigma)], 1 ml high salt buffer [20 mM Tris-HCl, 2 mM EDTA, 1% Triton X-100, 0.1% SDS, 500 mM NaCl], and 1 ml tris-EDTA pH 7.6 (Sigma) with 10 min incubations with nutation between each wash. Beads were resuspended in 100 µl elution buffer [1% SDS, 0.1 M NaHCO$_3$ (Sigma), 0.1 M NaCl], inputs were thawed and diluted with 50 µl elution buffer, and all samples were incubated for 30 min at room temperature with nutation. Samples were incubated at 65 °C for 7 h for uncrosslinking, at 45 °C for 14 h with 20 µg of Proteinase K (Thermo-Fisher), and eluted in 50 µl nuclease-free water using the Genelute PCR Cleanup Kit (Sigma).

3.8.6   Quantitative PCR of ChIP DNA

Relative quantification of ChIP samples was performed using real-time quantitative PCR and SYBR Green I master mix (Roche) as previously described.[54] To adjust for input dilution, $\log_2 20$ was subtracted from input Cp values.

% IP DNA bound was calculated as $100 \times 2^{\text{Ct input} - \text{Ct IP}}$. % IgG-IP bound ($100 \times 2^{\text{Ct input} - \text{Ct IgGIP}}$) was subtracted from % IP DNA bound to calculate % IP enrichment for H3K27me3 and H3K4me3 ChIP samples.

Primer sequences for site 1 were as follows:
5'–CGGCGCCATTCTATCCTCTA (forward);
5'–ATTCCGCGTACGTGATGTTC (reverse).
Primer sequences for TBP were as follows:
5'–CAGGGGTTCAGTGAGGTCG (forward);
5'–CCCTGGGTCACTGCAAAGAT (reverse).

3.8.7   RNP Electroporation

Synthetic guide RNAs and purified Cas9 protein were generous gifts from Synthego. RNP complex formation and electroporation were performed following manufacturer protocols. Briefly, 1 pmol of Cas9 protein and 9 pmol synthetic sgRNAs were complexed together. Cells were prepared for electroporation as described previously.[54] RNP complexes were electroporated into cells using the Neon Transfection system (Life Technologies) and the 10 μL tips. Neon settings were as follows: pulse voltage 1500 V; pulse width 30 ms; 1 pulse; with cell density 5×10^6/ml.

3.8.8   Statistical Analyses

The percentage of edited reads was normalized to transfection efficiency for each sample. Averages and standard deviations were calculated for each of $n = 3$ biological replicates.

To analyze ChIP-qPCR Assay data, averages and standard deviations were calculated for each of $n = 3$ replicate IPs from a single chromatin preparation. For each cell/treatment data set, percent IP DNA for site 1 and TBP were normaized to percent IP DNA for TBP.

The differences of means to compare cell/treatment data sets for both editing and ChIP experiments were calculated using the two sample, one-tailed Student's t test. For $p < 0.05$, 95% confidence with 2 degrees of freedom and a test statistic of $t_{(0.05,2)} = 2.920$. For $p < 0.01$, 99% confidence with 2 degrees of freedom and a test statistic of $t_{(0.01,2)} = 6.965$.

References

(*50*)   Tiwari, V. K., Cope, L., McGarvey, K. M., Ohm, J. E., and Baylin, S. B., (2008). A novel 6C assay uncovers Polycomb-mediated higher order chromatin conformations. *Genome Research 18*, 1171–1179, DOI: 10.1101/gr.073452.107.

(*52*)   Aoto, T., Saitoh, N., Sakamoto, Y., Watanabe, S., and Nakao, M., (2008). Polycomb group protein-associated chromatin is reproduced in post-mitotic G 1 phase and is required for S phase progression. *Journal of Biological Chemistry 283*, 18905–18915, DOI: 10.1074/jbc.M709322200.

(*53*)   Hansen, K. H., Bracken, A. P., Pasini, D., Dietrich, N., Gehani, S. S., Monrad, A., Rappsilber, J., Lerdrup, M., and Helin, K., (2008). A model for transmission of the H3K27me3 epigenetic mark. *Nature Cell Biology 10*, 1291–1300, DOI: 10.1038/ncb1787.

(*54*)   Daer, R. M., Cutts, J. P., Brafman, D. A., and Haynes, K. A., (2017). The Impact of Chromatin Dynamics on Cas9-Mediated Genome Editing in Human Cells. *ACS Synthetic Biology 6*, 428–438, DOI: 10.1021/acssynbio.5b00299.

(*72*)   Polstein, L. R., Perez-pinera, P., Kocak, D. D., Vockley, M., Bledsoe, P., Song, L., Safi, A., Crawford, G. E., Reddy, T. E., Gersbach, C. a., Carolina, N., and Surgery, O., (2015). Genome-wide specificity of DNA binding , gene regulation , and chromatin remodeling by TALE- and CRISPR / Cas9-based transcriptional activators. *Genome research 25*, 1158–1169, DOI: 10.1101/gr.179044.114..

(*110*)   Bernstein, B. E., Mikkelsen, T. S., Xie, X., Kamal, M., Huebert, D. J., Cuff, J., Fry, B., Meissner, A., Wernig, M., Plath, K., Jaenisch, R., Wagschal, A., Feil, R., Schreiber, S. L., and Lander, E. S., (2006). A bivalent chromatin structure marks key developmental genes in embryonic stem cells. *Cell 125*, 315–26, DOI: 10.1016/j.cell.2006.02.041.

(*123*)   Racey, L. A., and Byvoet, P., (1971). Histone acetyltransferase in chromatin. Evidence for in vitro enzymatic transfer of acetate from acetyl-coenzyme A to histones. *Experimental Cell Research 64*, 366–370, DOI: 10.1016/0014-4827(71)90089-9.

(*124*)   Rea, S., Eisenhaber, F., O'Carroll, D., Strahl, B. D., Sun, Z. W., Schmid, M., Opravil, S., Mechtler, K., Ponting, C. P., Allis, C. D., and Jenuwein, T., (2000). Regulation of chromatin structure by site-specific histone H3 methyltransferases. *Nature 406*, 593–599, DOI: 10.1038/35020506.

(*125*)   Konze, K. D., Ma, A., Li, F., Barsyte-Lovejoy, D., Parton, T., MacNevin, C. J., Liu, F., Gao, C., Huang, X.-p., Kuznetsova, E., Rougie, M., Jiang, A., Pattenden, S. G., Norris, J. L., James, L. I., Roth, B. L., Brown, P. J., Frye, S. V., Arrowsmith, C. H., Hahn, K. M., Wang, G. G., Vedadi, M., and Jin, J., (2013). An Orally Bioavailable Chemical Probe of the Lysine Methyltransferases EZH2 and EZH1. *ACS Chemical Biology 8*, 1324–1334, DOI: 10.1021/cb400133j.

(*126*) Holden, K., Maures, T., Walker, J., Miano, J., Seclen, E., Christian, M., Bak, R., Goodwin, M., and Hazelbaker, D., Use of Synthetic sgRNAs for Highly Efficient CRISPR Editing in Various Cell Types., Poster presented at the 2017 meeting on Genome Engineering: The CRISPR-Cas Revolution, Cold Spring Harbor, 2017.

(*127*) Hendel, A., Bak, R. O., Clark, J. T., Kennedy, A. B., Ryan, D. E., Roy, S., Steinfeld, I., Lunstad, B. D., Kaiser, R. J., Wilkens, A. B., Bacchetta, R., Tsalenko, A., Dellinger, D., Bruhn, L., and Porteus, M. H., (2015). Chemically modified guide RNAs enhance CRISPR-Cas genome editing in human primary cells. *Nature Biotechnology 33*, 985–989, DOI: 10.1038/nbt.3290.

(*128*) Dever, D. P., Bak, R. O., Reinisch, A., Camarena, J., Washington, G., Nicolas, C. E., Pavel-Dinu, M., Saxena, N., Wilkens, A. B., Mantri, S., Uchida, N., Hendel, A., Narla, A., Majeti, R., Weinberg, K. I., and Porteus, M. H., (2016). CRISPR/Cas9 β-globin gene targeting in human haematopoietic stem cells. *Nature 539*, 384–389, DOI: 10.1038/nature20134.

(*129*) Daer, R. M., Barrett, C. M., and Haynes, K. A., Gal4 DNA-binding Fusion Transcription Regulators. https://benchling.com/hayneslab/f_/5wovkOaK-gal4-dna-binding-fusion-transcription-regulators/ (accessed Sept. 9, 2017).

Chapter 4

CAN THE NATURAL DIVERSITY OF QUORUM-SENSING ADVANCE SYNTHETIC BIOLOGY?[§]

Quorum-sensing networks enable bacteria to sense and respond to chemical signals produced by neighboring bacteria. They are widespread: over 100 morphologically and genetically distinct species of eubacteria are known to use quorum sensing to control gene expression. This diversity suggests the potential to use natural protein variants to engineer parallel, input-specific, cell–cell communication pathways. However, only three distinct signaling pathways, Lux, Las, and Rhl, have been adapted for and broadly used in engineered systems. The paucity of unique quorum-sensing systems and their propensity for crosstalk limits the usefulness of our current quorum-sensing toolkit. This review discusses the need for more signaling pathways, roadblocks to using multiple pathways in parallel, and strategies for expanding the quorum-sensing toolbox for synthetic biology.

4.1 Modules from Natural Quorum-Sensing Networks Can Be Decoupled and Integrated into Synthetic Systems

Scientists first explored the genetic circuitry of a quorum-sensing system through basic research of *Vibrio fischeri*, a symbiotic microbe that populates the light organ of the bobtail squid, *Euprymna scolopes*. Researchers identified an operon called "Lux" that allowed individual *V. fischeri* cells to produce a glowing phenotype by expressing Luciferase specifically in dense bacterial populations.[75] Explorations of other microbial genomes revealed dozens of Lux homologs that are collectively known as HSL quorum-sensing networks.[77−79] In addition to bioluminescence, they found that these bacteria use quorum sensing to couple population density with the onset of group behaviors such as virulence, biofilm formation, sporulation, competence, and disruption of neighboring bacterial biofilms.[76]

Homoserine lactones networks are more commonly known as N-acyl homoserine lactone (AHL) quorum-sensing networks. However, our discussion includes LuxI-like synthases that produce compounds with a homoserine lactone ring but groups other than the acyl tail. In this review, we will consider homoserine lactone (HSL) to include AHLs as well as non-acyl tail compounds. We will refer to HSL with an acyl tail as acyl-HSL.

a Natural Quorum Sensing

b Engineered Quorum Sensing
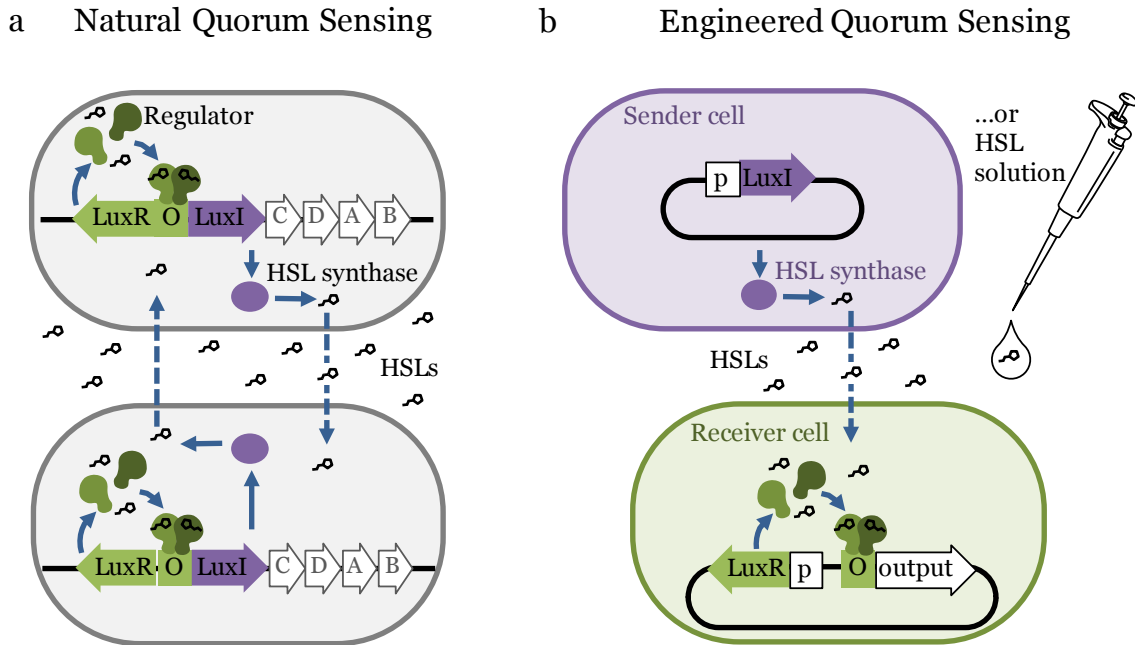
Figure 4.1. The structure of natural and artificial homoserine lactone (HSL) networks. (a) Natural HSL quorum-sensing networks such as the luciferase expression system in *Vibrio fischeri* regulate the expression of gene clusters (e.g., *LuxR, I, C, D, A,* and *B*). (b) Quorum-sensing networks have been decoupled and used to build engineered, synthetic systems to control the expression of any gene of interest (output). O = "Operator" binding site for the regulator protein, p = constitutive promoter.

Homoserine lactones quorum-sensing networks generally consist of an HSL synthase LuxI-like protein, an HSL-binding LuxR-like regulator, and promoters that are regulated by LuxR-like/HSL complexes. The LuxI-like HSL synthase enzyme produces chemical signals called HSLs.[82,83] Most HSLs diffuse passively across the cell membrane, while some require active transport. Quorum sensing is triggered when high external HSL concentrations drive net influx, allowing HSLs to bind and activate a LuxR-like regulator. The activated LuxR-like/HSL complex binds to a 20 base pair inverted repeat known as a Lux-like-box and regulates expression of downstream genes (Figure 4.1A). Synthases from various species of bacteria produce different HSL signals, and their corresponding regulators generally bind their cognate HSL with varying levels of specificity.

Researchers have also identified two other families of cell–cell communication networks: autoinducer-2 (AI-2) networks[130,131] and autoinducing peptides (AIPs), also called peptide pheromone networks.[131,132] While AI-2 and AIP networks may be used in engineered systems, the molecular components of HSL networks are simpler, more diverse, and require little modification to function as expected when they are transferred into new host cells.

These characteristics of the HSL family of quorum-sensing networks are well suited for building sophisticated, multi-component, synthetic systems. Therefore, we focus primarily on the HSL networks in this review.

Synthetic biologists and genetic engineers often use HSL quorum-sensing pathways to engineer novel behaviors in prokaryotic microorganisms. In these engineered systems, quorum-sensing pathways are used as a set of decoupled components where the HSL synthase is the "Sender" component and the regulator and promoter are collectively the "Receiver" component (Figure 4.1B).[85] They can be employed as "genetic wires" linking the functional elements of multi-component biological systems.[133,134] The wires connect circuit components within a cell or across a population of single or multiple strains. The Sender converts an input stimulus into a transmittable signal, the HSL, which activates the Receiver. The Receiver modulates expression of an output as designated by the designer (Figure 4.2A). This input stimulus may be anything that activates a promoter, including heavy metals,[135,136] specific wavelengths of light,[90] biochemical signals secreted by pathogens,[98,137] the hypoxic microenvironment surrounding a tumor,[138] and HSLs from tandem quorum-sensing networks.[133] The output may be any gene controlled by a Lux-like promoter, such as a visible reporter,[90,97,133] cell motility,[139] antimicrobial proteins,[98,137] and anti-cancer drugs.[138]

The simplicity of these networks allows researchers to model how quorum-sensing-controlled gene expression is regulated in response to HSL signal concentration.[140–142] These models can inform how a quorum-sensing network should be implemented in a synthetic circuit to achieve the desired behavior.[140,141] Furthermore, dry lab researchers have used modeling to demonstrate how quorum-sensing systems control group response in the presence of noisy signal concentrations, supporting their use in synthetic biology as robust circuit components.[143,144]

Incorporating quorum-sensing networks into production strains has advanced the field of metabolic engineering. Quorum sensing has been used to synchronize gene expression across a population to reduce cell-to-cell variability and to increase yields in engineered strains.[135,145–147] For example, by linking a Lux-based genetic oscillator with a gas phase signal oscillator, researchers coordinated gene expression among 2.5 million cells across 5 mm of space with minimal noise.[135,145,146] Anesiadis et al. employed this type of circuit in a production strain, where they engineered a cell-density-dependent switch using the Lux system to control production of serine in an *Escherichia coli* knockout strain.[147] Group-controlled gene expression implemented by an HSL quorum-sensing network leads to overall higher serine production.

Quorum-sensing networks are also used in genetic circuits to perform computation. Tabor et al. took advantage of the diffusibility of HSL through agar to build a bacterial edge detector using the Lux network.[90] They demonstrated that stationary physical spacing of

71
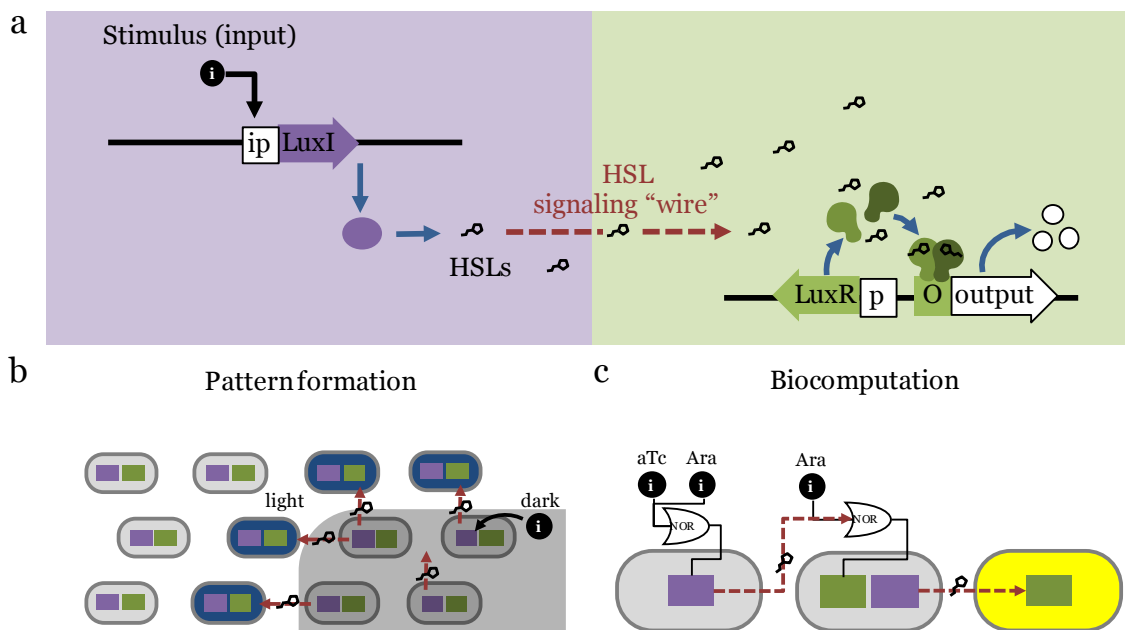
Figure 4.2. Homoserine lactone (HSL)-based genetic wiring supports the function of sophisticated synthetic systems. (a) Quorum-sensing pathways used as wires to link an input stimulus with expression of an output gene. (b) An edge detector expressed as Light L Neighboring Dark. The absence of light (dark) allows HSL production to activate LacZ (blue) in neighboring light-exposed cells.[90] (c) Biocomputational systems implement complex Boolean expressions by linking combinations of small molecule inputs (e.g., tetracycline aTc and arabinose Ara) to outputs (e.g., yellow fluorescence) using HSL signaling.[133]

bacteria relative to different inputs drives controlled expression of an output. The circuit was designed such that bacteria exposed to darkness expressed HSLs but no output (LacZ). The circuit allowed only bacteria that were both adjacent to HSL-producers and exposed to light to express LacZ, which resulted in a pigmented outline at the edges of a light-masked region (Figure 4.2B). While most biocomputation is digital, Daniel et al. showed the versatility of quorum-sensing networks by demonstrating analog computation using the Lux network; their circuit converts logarithmic HSL input into linear fluorescent output over a large range of HSL concentrations.[89] Thus far, engineered biocomputation has used monolayers of cells. Three-dimensional (3D) colony-printing techniques will increase the sophistication of these systems.[148] Controlled spacing of colonies based on HSL-diffusion rates could allow engineering a temporal element into a split circuit.

In the preceding examples, the cells in each system are expressing the same circuit. However, engineers may also coordinate gene circuits distributed among multiple populations. Brenner et al. used the Rhl and Las networks from *Pseudomonas aeruginosa* to build

two strains of *E. coli* that form a biofilm together once both populations reach a threshold density.[91] Balagaddé et al. used components from the Lux and Las networks to engineer a predator–prey relationship between *E. coli* strains.[149] High predator population density induces cell death in the prey strain, while high prey population density supports survival of the predator strain. You et al. placed a cell death gene under the control of the Lux promoter and built a bistable system that maintains a population density of a defined range.[150] At high cell density, the Lux network activates a cell death. At decreased cell density, the cell death gene is inactive and the population begins to grow again. Computation may be split across multiple strains, distributing the energy demands of a complex computation that are too great for a single cell (Figure 4.2A).[151,152] Wang et al. built a two-strain, three-input biosensor in *E. coli* that produces RFP only in the presence of three heavy metal contaminants: arsenic, mercury, and copper.[136] Cell 1 produces LuxI after exposure to arsenic and mercury; Cell 2 expresses RFP in response to *N*-(3-oxo-hexanoyl)-L-homoserine lactone (3O-C6-HSL) produced by Cell 1 and copper. Tamsir et al. linked circuits expressed in multiple cell populations using two quorum-sensing networks derived from P. aeruginosa, Rhl and Las (Figure 4.2C).[133] They implemented complex Boolean expressions using different spatial arrangements on agar plates. Their system is built with the functionally completed NOR operator and can implement any Boolean expression.

4.2 Crosstalk Between Quorum-Sensing Pathways Challenges the Development of Synthetic Genetic Circuits

Attempts to isolate, study, and apply quorum-sensing pathways for bioengineering is often thwarted by unexpected crosstalk. Quorum sensing is a popular tool among synthetic biologists for designing multicellular systems, but widely utilized HSL quorum-sensing networks are currently limited to three pathways: Lux, Las, and Rhl. These networks all exhibit crosstalk with each other, complicating the design of complex genetic systems implemented with quorum-sensing networks.

For instance, a single regulator can be activated by multiple acyl-HSL-class molecules, resulting in cross-activation of regulators from different species of bacteria. This phenomenon was observed in a proof-of-concept system designed by Canton et al. wherein an output gene for green fluorescent protein (GFP) was placed under the control of a LuxR receiver module.[97,100] Four chemically distinct acyl-HSLs, *N*-hexanoyl-L-homoserine lactone (C6-HSL), *N*-heptanoyl-L-homoserine lactone (C7-HSL), *N*-(3-oxo-octanoyl)-L-homoserine lactone (3O-C8-HSL) and, at higher concentrations, *N*-octanoyl-L-homoserine lactone (C8-HSL), all activated expression of GFP at levels comparable to or even greater than the cognate LuxI acyl-HSL, 3O-C6-HSL.[97] Many different HSL synthases, including EsaI, ExpI, and

AhlI, produce the same major cognate acyl-HSL as LuxI, suggesting that these pathways would have high levels of crosstalk if built into the same network.[85,153] In the report of their predator–prey, two-strain system, Balagaddé et al. discussed low-level crosstalk between LuxI and LasR,[149] which was recently confirmed by observing LuxI and LasR interactions in a single-strain system /.[100] However, Balagadde's system functioned such that crosstalk was apparently below the threshold for altering intended behavior.[149] Interestingly, this type of crosstalk is also observed in nature.[77] For example, two opportunistic pathogens, *Burkholderia cepacia* and *P. aeruginosa*, are known to co-infect patients with cystic fibrosis.[95] Each pathogen's quorum-sensing regulators respond to the other's HSLs, resulting in coordination of virulence-gene expression.

Crosstalk can also occur at the level of the target, or "output," gene; similarities between promoter sequences and the DNA-binding domains within the regulator proteins contribute to crosstalk between quorum-sensing pathways. The acyl-HSL-activated LuxR regulator stimulates transcription at its cognate promoter as well as the Esa promoter, while acyl-HSL-activated LasR, EsaR, and ExpR regulators are also capable of initiating transcription at the Lux promoter.[84,98,99] While this type of crosstalk can be avoided by using only one regulator per strain, they will not behave as two orthogonal wires within a single cell.

4.3 Expanding the Set of Orthogonal Quorum-Sensing Pathways Enables Design of Complex Genetic Circuits

Synthetic circuits may be engineered to detect specific combinations of input signals so long as each sensing pathway functions independently (orthogonally) without undesired intercommunication (crosstalk). Genetic circuits designed to respond to complex combinations of environmental conditions must distinguish and integrate multiple distinct input signals. Orthogonal quorum-sensing pathways are necessary to implement complex circuits that respond to signals produced by living cells, rather than requiring synthetic, exogenous inputs. Engineered division of labor is a major research area in metabolic engineering;[154,155] orthogonal quorum-sensing modules will enable further development of cell-autonomous metabolic regulation in multi-strain bioreactor systems. Quorum-sensing circuits could be used to engineer multi-strain, self-monitoring microbial populations that perform energetically expensive metabolic processes in a single culture. Multiple co-cultured strains could be designed to monitor and maintain a target population ratio, or steps in a metabolic process could be timed for accumulation of precursors.[133]

Circuit sophistication is limited by metabolic capacity, transcription and translation resources, and crosstalk within the cell. Moon et al. pushed the bounds of single-cell computational capability by building a four input AND gate in *E. coli*.[156] Their complex logic gate

allows living bacterial cells to express GFP in the presence of four exogenous compounds and no fewer. Transcription activator complexes were decoupled and placed under the control of distinct inducible promoters that respond to the presence of soluble compounds (arabinose, IPTG, tetracycline, and the acyl-HSL 3O-C6-HSL) in the cell culture medium. More complex circuits could be implemented by replacing the exogenous inputs in the Moon et al. system with quorum-sensing wires linking cells performing independent computation.[156] Scaling can be achieved through modularity by building complex computational systems with simple independent components. By designing the components in separate strains and connecting them with orthogonal quorum-sensing wires, computational steps can be performed independently without exhausting cellular resources.

Connecting complex circuits requires orthogonal HSL networks to independently signal each strain's computation. However, using even two quorum-sensing networks in parallel is constrained by crosstalk. To our knowledge, there is no published demonstration of three or more orthogonal quorum-sensing networks in a single system. The complexity of multi-input integration circuits remains constrained by reliance on exogenous signals and by the limited number of orthogonal input–output pathways.

4.4 Strategies for Minimizing Crosstalk

Promiscuous interactions between HSLs and regulators, as well as between regulators and promoters, prevent many quorum-sensing systems from operating independently and in parallel. Some have used gene-network engineering approaches to mitigate crosstalk.[91,100,133,149] For instance, Brenner et al. engineered their system to avoid crosstalk between the Las and Rhl networks.[91] They split the networks between two strains to eliminate promoter–regulator crosstalk and controlled HSL synthase production via a positive feedback loop to achieve a two-strain, biofilm-forming consortium.

Another approach to eliminate crosstalk between signaling pathways is using quorum-sensing pathways from distinct families (the aforementioned HSL, AI-2, and AIP pathways). Significant variance in the chemistry of the signaling molecules suggests that cross-reactivity is unlikely: HSLs contain a lactone ring with a hydrocarbon acyl or aryl tail, AI-2 is a furanosyl borate diester composed of two five-membered rings stabilized by a boron atom, and AIPs are relatively large circular peptides composed of amino acids.[157,158] However, this approach may be limited in its flexibility since both AI-2 and AIP require active transport and multiple proteins to generate and detect the signals. With a few exceptions, HSL networks require only two proteins and one promoter. While AI-2 quorum sensing is limited to only one signaling molecule, multiple AIP pathways may exist that do not have cross-reactivity. Marchand et al. recently demonstrated modularity and orthogonality of two AIP signals

from *Staphylococcus aureus*.[158] In their system, *E. coli* was the AIP sender, producing and secreting two AIPs, and two engineered strains of *Bacillus megaterium* each received one of the signals but not the other. While the ability to use two AIPs in a single cell was not explored, this is a promising result and further research could demonstrate orthogonality between AIPs and HSL quorum sensing.

Directed evolution could also be used to generate regulator proteins that specifically respond to any desired HSL. Mutational analyses and 3D protein structure data have helped to identify key amino acid residues that govern the interaction between regulators and acyl-HSL ligands. Using positive and negative selection, Collins et al. generated a LuxR mutant that no longer responds to the cognate 3O-C6-HSL but gained responsiveness to *N*-decanoyl-ʟ-homoserine lactone (C10-HSL), to which wild-type LuxR does not respond.[159] They then demonstrated the orthogonality of LuxR wild type versus the mutant. However, directed evolution of regulator proteins to generate novel orthogonality is technically daunting and only generates mutants with minor changes to the wild-type binding pocket, limiting the range of possible novel behaviors. Furthermore, they bind to and activate the same promoter and, while this feature could be leveraged to build OR gates, they cannot be used as orthogonal networks in the same cell without further mutagenesis to alter promoter-binding specificity.

Finally, scientists could explore other microbial genomes for quorum-sensing homologs that have not yet been exploited for synthetic biology. Comparative genomics has identified dozens of HSL family (Lux-like) homologs in divergent species.[80] A major advantage of exploring wild-type homologs over directed evolution is that natural evolution has already "discovered" functional regulators in a very broad exploration space of amino acid sequences. Evolution has selected for regulator proteins of significantly different sizes, as opposed to artificial selection techniques that, due to practical constraints, do not deviate significantly from pre-existing primary structures.

4.5   The Basis of Specificity in the HSL Signaling Family

Investigations of microbial quorum-sensing pathways have revealed molecular characteristics that underlie the diversity of HSL signaling pathways in different species. These signaling pathways have been distinguished on the basis of the operator binding sites at promoters elsewhere.[160] In this review, we focus on diversity in the geometries of HSL signaling molecules and the HSL-binding pockets within the regulator proteins.

The extensive molecular diversity of naturally occurring HSL signaling molecules suggests that many functionally distinct HSLs, and thus orthogonal pathways, may exist. HSLs vary in the R-group, an acyl or aryl tail that extends from a homoserine lactone head (Figure 4.3).[79] HSL synthases have been reported to generate HSLs of varying carbon chain
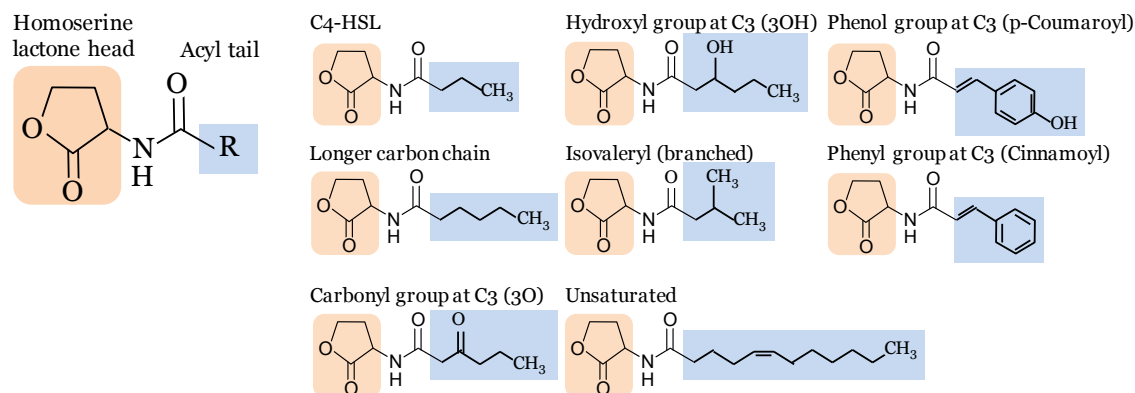
Figure 4.3. Structural diversity of homoserine lactone (HSL) signaling molecules that are produced by bacteria. Representative variants are shown.

lengths, branching functional groups, and hydrocarbon saturation (Figure 4.4). Straight-chain acyl R-groups vary by chain lengths (e.g., *N*-butyryl-L-homoserine lactone (C4-HSL) versus C6-HSL in Figure 4.3) from 4 to 18 carbon atoms. Some acyl R-groups carry side-group replacements at the third or fourth carbon in the chain: a carbonyl group at C3 (e.g., 3O-C6-HSL), a hydroxyl group at C4 (e.g., *N*-(3-hydroxy-hexanoyl)-L-homoserine lactone (3-OH-C6-HSL)), or a methyl group at C3 (e.g., branched-chain isovaleryl-HSL). Aryl R-groups have a phenol group at C4 (*N*-(p-Coumaroyl)-L-homoserine lactone (pC-HSL)), or a phenyl group at C4 (cinnamoyl-HSL). R-groups also differ by the degree of saturation in the carbon chain (e.g., monounsaturated 3OH-C14:1); unsaturation results in a carbon–carbon double bond, which changes the shape of the acyl tail, compared to the saturated form.

In some instances, a single synthase can produce two or more HSL variants. This variety arises from the species-specific combination of acyl tails that are carried into the HSL synthesis pathway by acyl-carrier proteins (ACPs) or aryl-CoA.[163] Some HSL synthases display promiscuity in ACP or CoA-binding affinity and can catalyze formation of several different HSL molecules. Other HSL molecules show no overlap across species, suggesting that the cognate regulators may have evolved to respond specifically to certain HSLs, and orthogonal quorum-sensing systems may exist in nature.

Regulator proteins from the HSL quorum-sensing family (LuxR homologs) consist of two major domains: an N-terminal autoinducer (HSL) binding region and a C-terminal region that binds DNA (Figure 4.5). To visually compare the topologies of functional regions in different regulators, we have generated scaled protein domain maps using descriptions from the literature[164–167] and annotations from protein domain-scanning databases Uniprot,[168] Prosite,[169] InterPro,[170] and the Protein Data Bank (Figure 4.5).[171] Autoinducer-binding regions (InterPro IPR005143) contain roughly six alpha helices and six beta strands. Published 3D structures for TraR (PDB 1L3L),[165] LasR (PDB 2UV0),[166] CviR (PDB 3QP6),[167]
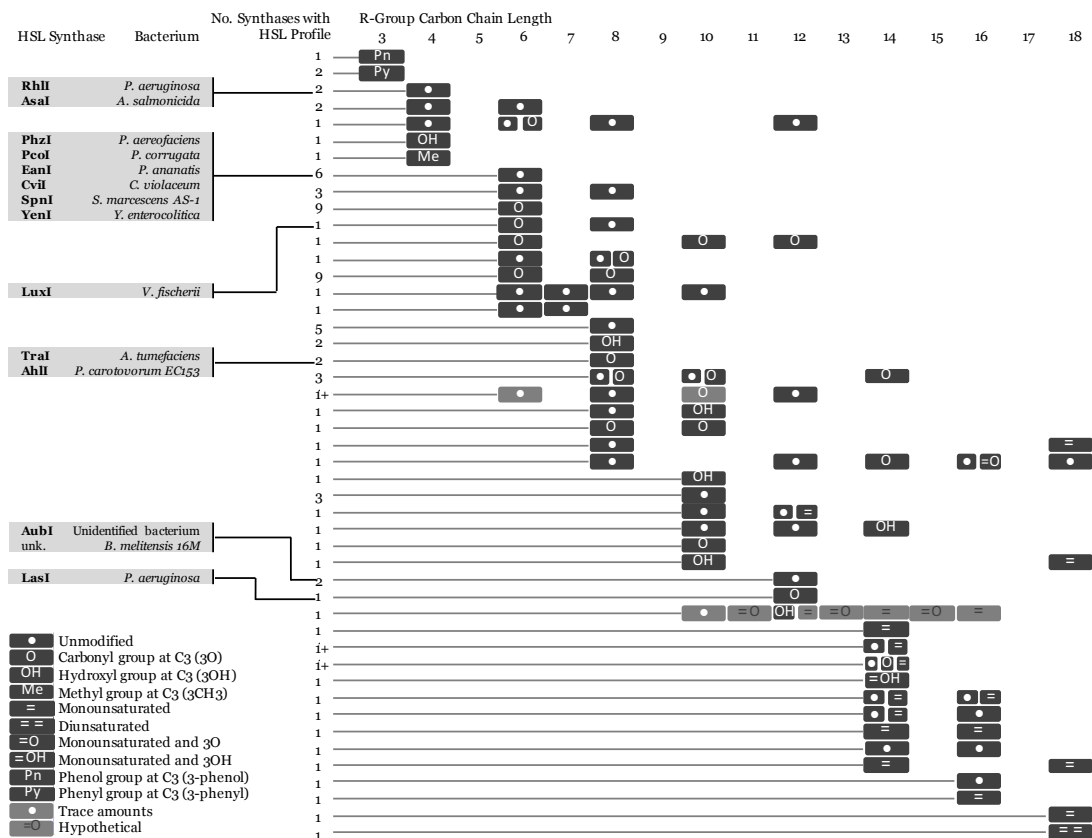
Figure 4.4. Diversity in homoserine lactone (HSL) produced by synthases across bacterial species. Select synthases and representative species are shown in gray boxes. Each row represents one or several HSLs produced by one or more synthase. The number of synthases with each HSL profile is indicated. A (1+) indicates that the exact number of synthases is not known. A comprehensive chart with referenced literature is provided as Supplemental Material in Figure E.1 in Appendix E. Hypothetical = cases where one of two molecules with identical mass [i.e., 3O-C(n)-HSL and C(n + 1)-HSL] might be produced by the bacterium, but the molecules could not be resolved with mass spectrometry. * The hypothetical monounsaturated N-dodecanoyl-L-homoserine lactone (C12-HSL) produced by AbaI is not shown here.

and SdiA[172] reveal that a five-strand beta sheet is sandwiched between two three-helix bundles. The C-terminal DNA-binding domains are characterized as "helix−turn−helix" (HTH) regions (Prosite PS50043) that consist of four alpha helices. The second and third helices within the HTH region are often identified as a conserved H−T−H motif (Prosite PRU00411); the third helix has been characterized as the DNA recognition helix in TraR.[165] When HSL molecules bind to their corresponding quorum-sensing regulator, they often
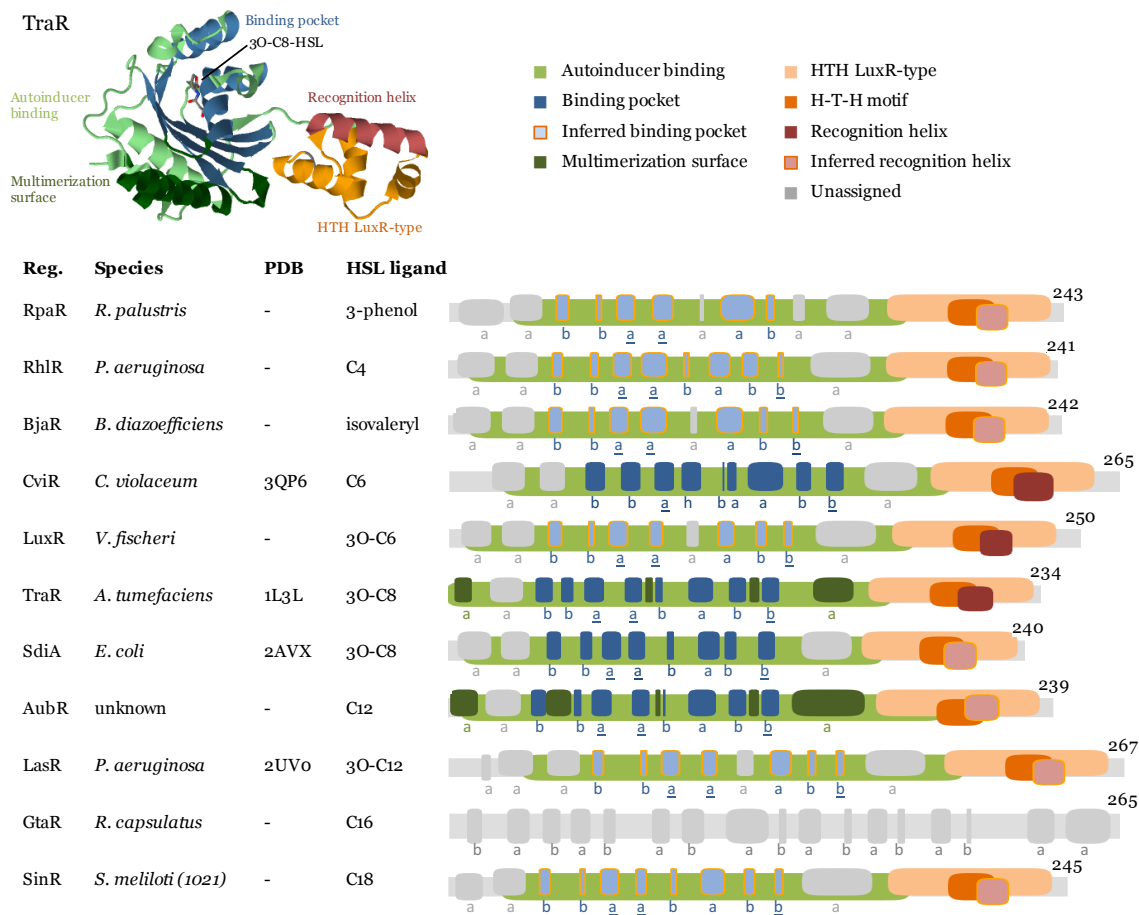
Figure 4.5. Comparison of protein motifs in select regulators. [This figure contains an error regarding GtaR and is correctly described in Appendix D.] The three-dimensional (3D) structure of TraR is shown as an example of how domains and the homoserine lactone (HSL) ligand are typically positioned in space. The underlined letters in the b−b−a−a−b−a−b−b secondary structure motif indicate the location of highly conserved amino acids that form hydrogen bonds with the homoserine lactone head of HSLs. Published 3D structure data (Protein Data Bank) are listed where available ("−" = not available). Abbreviations used are: Reg. = regulator protein, H−T−H = helix−turn−helix, a = alpha helix, b = beta strand, h = 3/10 helix. Database entries for conserved motifs are: autoinducer binding = IPR005143, HTH LuxR-type = PS50043. Inferred binding pockets are patterns of secondary structures that are similar to the TraR binding pocket. Inferred recognition helices are the second alpha helix from the C-terminus. Secondary structures for proteins with no available 3D structure data were mapped using the Jpred prediction tool.[161] Maps were generated using DomainDraw.[162]

induce multimerization of regulator proteins. This multimeric state is the active form, capable of binding an inverted DNA sequence repeat at the target promoter and inducing transcription of downstream genes.

Analysis of the HSL-regulator binding pockets suggests that the shape, size, hydrophobicity, and functionalization determine the binding affinity of a regulator for a specific HSL. This implies that comparison of known HSL–regulator interactions may identify likely candidates for orthogonal quorum-sensing networks. For example, it has been hypothesized that quorum-sensing systems that produce long, straight-chain acyl-HSLs have regulators with longer binding pockets; likewise, a system that uses acyl-HSL molecules with branching functional groups will have regulators with binding pockets that accommodate the branches.[166] Thus, taking sterics into account, a quorum-sensing system that uses HSL molecules with a relatively short hydrocarbon tail and bulky functional groups may be orthogonal to a system that uses long-chain, non-branched HSL molecules.

Hydrophobic interactions between the HSL tail and amino acid residues within the binding pocket suggest that these binding interactions are dominated by van der Waals forces (Figure 4.3).[166] Because the HSL tail is buried within the binding pocket, the hydrophobicity of each component also determines the entropic stability, with a predominantly hydrophobic tail pairing stably with a predominantly hydrophobic binding pocket and less hydrophobic tail pairing stably with a less hydrophobic binding pocket. Therefore, HSL tail and binding pocket hydrophobicity may be a predictor of orthogonality between quorum-sensing pathways.

Pharmacophore models for HSL-regulator binding developed by Geske et al. support the idea that functionalization of the HSL molecule underlies binding pocket selectivity.[173] Their models are based on the response of Tra, Las, and Lux regulators to libraries of HSLs and synthetic analogs in a system that used beta-galactosidase as the output gene. Comparison of the atomic geometries of ligands reveals three general properties linked with HSL efficacy: spacing of hydrophobic regions, hydrogen bond donor regions, and hydrogen bond acceptor regions within the R-group attached to the lactone ring. For instance, TraR shows the greatest response to a group of ligands in which the acyl tail contains one hydrogen bond donor region followed by two hydrogen bond acceptor regions arranged in trans and ended in a hydrophobic region.[173]

Conservation and divergence in the conformation of regulator N-terminal HSL-binding regions support the idea that variation in HSL R-groups coordinates selective regulator–ligand interactions. Here, we explore whether motifs in the protein structures of regulators provide insight into the underlying mechanism of HSL-binding selectivity. Primary sequence alignments show 10% to 25% identity in regulator homologs[166] and therefore provide very limited information. We have attempted a more coarse-grained approach on a select set

of well-characterized regulators by annotating secondary structures that correspond to the TraR binding pocket. For regulators that lack published 3D structure data, we have annotated secondary structures as hypothetical HSL-binding pockets (Figure 4.5).

The autoinducer-binding region contains two functional domains in its tertiary structure: the multimerization surface and the HSL-binding pocket. The multimerization surface of the TraR homodimer consists primarily of alpha helices a1 and a6,[166] plus other residues within loops that link helices and beta strands (Figure 4.5). The HSL-binding pocket binds a single HSL molecule in the space between a five-strand antiparallel beta sheet and a three-helix bundle.[166] In the primary structure of TraR, these secondary structures are arranged in the order of b–b–a–a–b–a–b–b. The first and second alpha helix and the last beta strand of this motif (underlined in Figure 4.5) contain the amino acids that form hydrogen bonds with the homoserine lactone head of the HSL ligand. These residues are highly conserved in LuxR protein homologs, reflecting a common binding mechanism at the non-variable head regions of HSL molecules. In contrast, the variable acyl tail extends into the region of the binding pocket that is formed by residues that show less conservation in LuxR homologs, suggesting a mechanism for HSL selectivity.[166]

TraR and SdiA are most responsive to the ligand 3O-C8-HSL.[173,174] These regulators contain the same b–b–a–a–b–a–b–b pattern of secondary structures in their HSL-binding pocket domains (Figure 4.5). This pair of regulators fits the attractive idea that binding pockets with similar secondary structures may prefer the same HSL ligands. However, comparisons of other regulators challenge this idea. While some regulators that respond to HSLs with smaller or larger R-groups deviate from the b–b–a–a–b–a–b–b motif, there are others, i.e., RhlR, LasR, and SinR, which contain the same motif yet respond to different ligands: C4-HSL, *N*-(3-oxo-dodecanoyl)-L-homoserine lactone (3O-C12-HSL), and *N*-octadecanoyl-L-homoserine lactone (C18-HSL), respectively.[173,175,176] It is possible that variations in specific residues in RhlR, LasR, and SinR account for their preferences for different ligands. AubR contains a substitution of the third beta strand with an alpha helix in the b–b–a–a–b–a–b–b motif, similar to LuxR and BjaR. LuxR and BjaR respond to 3O-C6-HSL[97] and isovaleryl-HSL,[163] respectively. Assuming that the ligand for AubR is *N*-dodecanoyl-L-homoserine lactone (C12-HSL) (produced by AubI[81]), AubR, LuxR, and BjaR represent another set of regulators where similarities in secondary structures do not appear to correspond to similar ligands. Exploration of the range of HSL-responsiveness of these regulators may provide more insight into their structure–function relationships.

Interestingly, no HSL-regulator protein-related motifs appear in GtaR. Leung et al. reported that GtaR regulates its target promoter (a Lux promoter homolog) in response to *N*-hexadecanoyl-L-homoserine lactone (C16-HSL) and cell-free growth medium collected from HSL-producing strains.[177] GatR shows sequence conservation with the TatD family of

deoxyribonuclease proteins. Like the LuxR homologs, TatD proteins contain interspersed beta strands and alpha helices. Here, we have annotated predicted secondary structures within GtaR; these domains are inferred from comparisons of GatR with closely related TatD proteins that have published 3D structures. Given its distinct arrangement of secondary structures, GtaR might represent a unique class of HSL-responsive regulator proteins. [This text contains an error regarding GtaR and is correctly described in Appendix D.]

4.6   Conclusion and Discussion

The information we present here on the diversity of HSL molecules and regulator proteins is insufficient to conclude that the structures of regulator binding pockets and the atomic geometries of the HSL ligands imply orthogonality. Regulators that respond to distinct HSL ligands show different protein folding patterns in some cases but similar structures in others. With limited data on regulator promiscuity, secondary structure alone cannot predict HSL ligand preference; thus, interaction between specific amino acid residues and atoms within the HSL molecule may need to be considered. This investigation is limited by the lack of 3D structure data for LuxR homologs.

Many gaps in knowledge remain in understanding the extent of orthogonality or interaction between the homologous pathways in living cells. To date, the published functional studies of the quorum-sensing homologs in synthetic circuits (HSL synthases, regulators, and promoters) include just three homologous quorum-sensing pathways, or they use purified compounds to stimulate one or a few regulators. Furthermore, the available 3D structure data for regulator proteins is sparse compared to the total number of putative regulator homologs that have been identified via metagenomic analysis.[81] More comprehensive analyses to study the responses of regulator proteins to different HSLs, such as that of Geske et al., may enable us to predict and select orthogonal pathways for use in complex synthetic systems.[173] For instance, *E. coli* could be used as a universal host to carry dozens of decoupled sender and receiver components (Figure 4.1), derived from the genomes of various bacterial species. Culture media from sender strains could be used to stimulate receiver strains carrying a reporter driven by a receiver system (regulator protein and its corresponding promoter).

The discovery of novel orthogonal quorum-sensing pathways will provide metabolic engineers and synthetic biologists with HSL signaling wires that do not cross-react. Using these insulated, independently functioning pathways, synthetic circuits could be designed to detect distinct combinations of multiple input signals and scale simple single-cell components to sophisticated multi-strain circuits. It is imperative to continue research on quorum-sensing pathway behavior across multiple disciplines, including crystallography,

molecular biology, microbiology, metabolic engineering, and synthetic biology, to fill critical gaps in knowledge that have prevented us from engineering highly sophisticated biological systems.

References

(*75*)   Ruby, E. G., and Nealson, K. H., (1976). Symbiotic Association of Photobacterium Fischeri with the Marine Luminous Fish Monocentris Japonica: A Model Of Symbiosis Based on Bacterial Studies. *The Biological Bulletin 151*, 574–586, DOI: 10.2307/1540507.

(*76*)   Eberl, L., (1999). N-acyl homoserinelactone-mediated gene regulation in gram-negative bacteria. *Systematic and applied microbiology 22*, 493–506, DOI: 10.1016/S0723-2020(99)80001-0.

(*77*)   Fuqua, C., Winans, S. C., and Greenberg, E. P., (1996). Census and consensus in bacterial ecosystems: the LuxR-LuxI family of quorum-sensing transcriptional regulators. *Annual review of microbiology 50*, 727–51, DOI: 10.1146/annurev.micro.50.1.727.

(*78*)   Williams, P., Winzer, K., Chan, W. C., and Camara, M., (2007). Look who's talking: communication and quorum sensing in the bacterial world. *Philosophical Transactions of the Royal Society B: Biological Sciences 362*, 1119–1134, DOI: 10.1098/rstb.2007.2039.

(*79*)   Dickschat, J. S., (2010). Quorum sensing and bacterial biofilms. *Natural product reports 27*, 343–69, DOI: 10.1039/b804469b.

(*80*)   Case, R. J., Labbate, M., and Kjelleberg, S., (2008). AHL-driven quorum-sensing circuits: their frequency and function among the Proteobacteria. *The ISME journal 2*, 345–9, DOI: 10.1038/ismej.2008.13.

(*81*)   Nasuno, E., Kimura, N., Fujita, M. J., Nakatsu, C. H., Kamagata, Y., and Hanada, S., (2012). Phylogenetically Novel LuxI/LuxR-Type Quorum Sensing Systems Isolated Using a Metagenomic Approach. *Applied and Environmental Microbiology 78*, 8067–8074, DOI: 10.1128/AEM.01442-12.

(*82*)   Engebrecht, J., and Silverman, M., (1984). Identification of genes and gene products necessary for bacterial bioluminescence. *Proceedings of the National Academy of Sciences of the United States of America 81*, 4154–8.

(*83*)   Kaplan, H. B., and Greenberg, E. P., (1987). Overproduction and purification of the luxR gene product: Transcriptional activator of the Vibrio fischeri luminescence system. *Proceedings of the National Academy of Sciences of the United States of America 84*, 6639–43.

(*84*) von Bodman, S., Ball, J., Faini, M., Herrera, C., Minogue, T., Urbanowski, M., and Stevens, A., (2003). The quorum sensing negative regulators EsaR and ExpREcc, homologues within the LuxR family, retain the ability to function as activators of transcription. *Journal of bacteriology 185*, 7001–7007, DOI: 10.1128/JB.185.23.7001.

(*85*) Miller, M. B., and Bassler, B. L., (2001). Quorum sensing in bacteria. *Annual review of microbiology 55*, 165–99, DOI: 10.1146/annurev.micro.55.1.165.

(*89*) Daniel, R., Rubens, J. R., Sarpeshkar, R., and Lu, T. K., (2013). Synthetic analog computation in living cells. *Nature 497*, 619–23, DOI: 10.1038/nature12148.

(*90*) Tabor, J. J., Salis, H. M., Simpson, Z. B., Chevalier, A. a., Levskaya, A., Marcotte, E. M., Voigt, C. a., and Ellington, A. D., (2009). A Synthetic Genetic Edge Detection Program. *Cell 137*, 1272–1281, DOI: 10.1016/j.cell.2009.04.048.

(*91*) Brenner, K., Karig, D. K., Weiss, R., and Arnold, F. H., (2007). Engineered bidi-rectional communication mediates a consensus in a microbial biofilm consortium. *Proceedings of the National Academy of Sciences of the United States of America 104*, 17300–4, DOI: 10.1073/pnas.0704256104.

(*92*) Davis, R. M., Muller, R. Y., and Haynes, K. A., (2015). Can the Natural Diversity of Quorum-Sensing Advance Synthetic Biology? *Frontiers in Bioengineering and Biotechnology 3*, 1–10, DOI: 10.3389/fbioe.2015.00030.

(*95*) Lewenza, S., Visser, M. B., and Sokol, P. a., (2002). Interspecies communication between Burkholderia cepacia and Pseudomonas aeruginosa. *Canadian Journal of Microbiology 48*, 707–716, DOI: 10.1139/w02-068.

(*97*) Canton, B., Labno, A., and Endy, D., (2008). Refinement and standardization of synthetic biological parts and devices. *Nature biotechnology 26*, 787–93, DOI: 10.1038/nbt1413.

(*98*) Saeidi, N., Wong, C. K., Lo, T.-M., Nguyen, H. X., Ling, H., Leong, S. S. J., Poh, C. L., and Chang, M. W., (2011). Engineering microbes to sense and eradicate Pseudomonas aeruginosa, a human pathogen. *Molecular systems biology 7*, 1–11, DOI: 10.1038/msb.2011.55.

(*99*) Shong, J., Huang, Y.-M., Bystroff, C., and Collins, C. H., (2013). Directed evolution of the quorum-sensing regulator EsaR for increased signal sensitivity. *ACS Chemical Biology 8*, 789–95, DOI: 10.1021/cb3006402.

(*100*) Wu, F., Menn, D. J., and Wang, X., (2014). Article Circuits : From Unimodality to Trimodality. *Chemistry & Biology 21*, 1629–1638, DOI: 10.1016/j.chembiol.2014.10.008.

(*130*) Vendeville, A., Winzer, K., Heurlier, K., Tang, C. M., and Hardie, K. R., (2005). Making 'sense' of metabolism: autoinducer-2, LUXS and pathogenic bacteria. *Nature Reviews Microbiology 3*, 383–396, DOI: 10.1038/nrmicro1146.

(*131*)   Reading, N. C., and Sperandio, V., (2006). Quorum sensing: the many languages of bacteria. *FEMS microbiology letters 254*, 1–11, DOI: 10.1111/j.1574-6968.2005. 00001.x.

(*132*)   Kleerebezem, M., Quadri, L. E., Kuipers, O. P., and de Vos, W. M., (1997). Quorum sensing by peptide pheromones and two-component signal-transduction systems in Gram-positive bacteria. *Molecular microbiology 24*, 895–904.

(*133*)   Tamsir, A., Tabor, J., and Voigt, C., (2011). Robust multicellular computing using genetically encoded NOR gates and chemical 'wires'. *Nature 469*, 212–215, DOI: 10.1038/nature09565.Robust.

(*134*)   Goñi-Moreno, A., Amos, M., and de la Cruz, F., (2013). Multicellular computing using conjugation for wiring. *PLOS ONE 8*, e65986, DOI: 10.1371/journal.pone. 0065986.

(*135*)   Prindle, A., Samayoa, P., Razinkov, I., Danino, T., Tsimring, L. S., and Hasty, J., (2011). A sensing array of radically coupled genetic 'biopixels'. *Nature 481*, 39–44, DOI: 10.1038/nature10722.

(*136*)   Wang, B., Barahona, M., and Buck, M., (2013). A modular cell-based biosensor using engineered genetic logic circuits to detect and integrate multiple environmental signals. *Biosensors & bioelectronics 40*, 368–76, DOI: 10.1016/j.bios.2012.08.011.

(*137*)   Gupta, S., Bram, E. E., and Weiss, R., (2013). Genetically programmable pathogen sense and destroy. *ACS Synthetic Biology 2*, 715–23, DOI: 10.1021/sb4000417.

(*138*)   Anderson, J. C., Clarke, E. J., Arkin, A. P., and Voigt, C. a., (2006). Environmentally controlled invasion of cancer cells by engineered bacteria. *Journal of molecular biology 355*, 619–27, DOI: 10.1016/j.jmb.2005.10.076.

(*139*)   Liu, C., Fu, X., Liu, L., Ren, X., Chau, C. K. L., Li, S., Xiang, L., Zeng, H., Chen, G., Tang, L.-H., Lenz, P., Cui, X., Huang, W., Hwa, T., and Huang, J.-D., (2011). Sequential establishment of stripe patterns in an expanding cell population. *Science 334*, 238–41, DOI: 10.1126/science.1209042.

(*140*)   McMillen, D., Kopell, N., Hasty, J., and Collins, J. J., (2002). Synchronizing genetic relaxation oscillators by intercell signaling. *Proceedings of the National Academy of Sciences of the United States of America 99*, 679–84, DOI: 10.1073/pnas. 022642299.

(*141*)   Pai, A., and You, L., (2009). Optimal tuning of bacterial sensing potential. *Molecular systems biology 5*, DOI: 10.1038/msb.2009.43.

(*142*)   Pai, A., Srimani, J. K., Tanouchi, Y., and You, L., (2014). Generic Metric to Quantify Quorum Sensing Activation Dynamics. *ACS Synthetic Biology 3*, 220–227, DOI: 10.1021/sb400069w.

(*143*) Koseska, A., Zaikin, A., Kurths, J., and García-Ojalvo, J., (2009). Timing cellular decision making under noise via cell-cell communication. *PLOS ONE 4*, e4872, DOI: 10.1371/journal.pone.0004872.

(*144*) Weber, M., and Buceta, J., (2013). Dynamics of the quorum sensing switch: stochastic and non-stationary effects. *BMC systems biology 7*, 1–15, DOI: 10.1186/1752-0509-7-6.

(*145*) Danino, T., Mondragón-Palomino, O., Tsimring, L., and Hasty, J., (2010). A synchronized quorum of genetic clocks. *Nature 463*, 326–330, DOI: 10.1038/nature08753. A.

(*146*) Prindle, A., Selimkhanov, J., Danino, T., Samayoa, P., Goldberg, A., Bhatia, S., and Hasty, J., (2012). Genetic circuits in Salmonella typhimurium. *ACS Synthetic Biology 1*, 458–464, DOI: 10.1021/sb300060e.

(*147*) Anesiadis, N., Kobayashi, H., Cluett, W. R., and Mahadevan, R., (2013). Analysis and design of a genetic circuit for dynamic metabolic engineering. *ACS Synthetic Biology 2*, 442–52, DOI: 10.1021/sb300129j.

(*148*) Connell, J. L., Ritschdorff, E. T., Whiteley, M., and Shear, J. B., (2013). 3D printing of microscopic bacterial communities. *Proceedings of the National Academy of Sciences of the United States of America 110*, 18380–5, DOI: 10.1073/pnas.1309729110.

(*149*) Balagaddé, F. K., Song, H., Ozaki, J., Collins, C. H., Barnet, M., Arnold, F. H., Quake, S. R., and You, L., (2008). A synthetic Escherichia coli predator-prey ecosystem. *Molecular systems biology 4*, DOI: 10.1038/msb.2008.24.

(*150*) You, L., Cox, R., Weiss, R., and Arnold, F., (2004). Programmed population control by cell–cell communication and regulated killing. *Nature 428*, 868–71, DOI: 10.1038/nature02468.1..

(*151*) Ji, W., Shi, H., Zhang, H., Sun, R., Xi, J., Wen, D., Feng, J., Chen, Y., Qin, X., Ma, Y., Luo, W., Deng, L., Lin, H., Yu, R., and Ouyang, Q., (2013). A formalized design process for bacterial consortia that perform logic computing. *PLOS ONE 8*, e57482, DOI: 10.1371/journal.pone.0057482.

(*152*) Payne, S., and You, L., (2014). Engineered cell-cell communication and its applications. *Advances in biochemical engineering/biotechnology 146*, 97–121, DOI: 10.1007/10_2013_249.

(*153*) Põllumaa, L., Alamäe, T., and Mäe, A., (2012). Quorum Sensing and Expression of Virulence in Pectobacteria. *Sensors 12*, 3327–3349, DOI: 10.3390/s120303327.

(*154*) Bernstein, H., Paulson, S., and Carlson, R., (2012). Synthetic Escherichia coli consortia engineered for syntrophy demonstrate enhanced biomass productivity. *Journal of biotechnology 157*, 159–166, DOI: 10.1016/j.jbiotec.2011.10.001.

(*155*)   Vinuselvi, P., and Lee, S. K., (2012). Engineered Escherichia coli capable of co-utilization of cellobiose and xylose. *Enzyme and microbial technology 50*, 1–4, DOI: 10.1016/j.enzmictec.2011.10.001.

(*156*)   Moon, T., Lou, C., Tamsir, A., Stanton, B., and Voigt, C., (2012). Genetic programs constructed from layered logic gates in single cells. *Nature 491*, 249–253, DOI: 10.1038/nature11516.Genetic.

(*157*)   Chen, X., Schauder, S., Potier, N., Van Dorsselaer, A., Pelczer, I., Bassler, B. L. B., and Hughson, F. F. M., (2002). Structural identification of a bacterial quorum-sensing signal containing boron. *Nature 415*, 545–549, DOI: 10.1038/415545a.

(*158*)   Marchand, N., and Collins, C. H., (2013). Peptide-based communication system enables Escherichia coli to Bacillus megaterium interspecies signaling. *Biotechnology and bioengineering 110*, 3003–12, DOI: 10.1002/bit.24975.

(*159*)   Collins, C. H., Leadbetter, J. R., and Arnold, F. H., (2006). Dual selection enhances the signaling specificity of a variant of the quorum-sensing transcriptional activator LuxR. *Nature biotechnology 24*, 708–12, DOI: 10.1038/nbt1209.

(*160*)   Vannini, A., (2002). The crystal structure of the quorum sensing protein TraR bound to its autoinducer and target DNA. *The EMBO Journal 21*, 4393–4401, DOI: 10.1093/emboj/cdf459.

(*161*)   Cole, C., Barber, J. D., and Barton, G. J., (2008). The Jpred 3 secondary structure prediction server. *Nucleic Acids Research 36*, W197–W201, DOI: 10.1093/nar/gkn238.

(*162*)   Fink, J. L., and Hamilton, N., (2007). DomainDraw: a macromolecular feature drawing program. *In silico biology 7*, 145–50.

(*163*)   Lindemann, A., Pessi, G., Schaefer, A., Mattmann, M., Christensen, Q., Kessler, A., Hennecke, H., Blackwell, H., Greenberg, E., and Harwood, C., (2011). Isovaleryl-homoserine lactone, an unusual branched-chain quorum-sensing signal from the soybean symbiont Bradyrhizobium japonicum. *Proceedings of the National Academy of Sciences 108*, 16765–70, DOI: 10.1073/pnas.1114125108.

(*164*)   Egland, K., and Greenberg, E., (2001). Quorum sensing in Vibrio fischeri- Analysis of the LuxR DNA binding region by alanine-scanning mutagenesis. *Journal of bacteriology 183*, 382–386, DOI: 10.1128/JB.183.1.382–386.2001.

(*165*)   Zhang, R.-g., Pappas, K. M., Pappas, T., Brace, J. L., Miller, P. C., Oulmassov, T., Molyneaux, J. M., Anderson, J. C., Bashkin, J. K., Winans, S. C., and Joachimiak, A., (2002). Structure of a bacterial quorum-sensing transcription factor complexed with pheromone and DNA. *Nature 417*, 971–4, DOI: 10.1038/nature00833.

(*166*)   Bottomley, M. J., Muraglia, E., Bazzo, R., and Carfi, A., (2007). Molecular insights into quorum sensing in the human pathogen Pseudomonas aeruginosa from the structure of the virulence regulator LasR bound to its autoinducer. *The Journal of biological chemistry 282*, 13592–600, DOI: 10.1074/jbc.M700556200.

(*167*)   Chen, G., Swem, L. R., Swem, D. L., Stauff, D. L., O'Loughlin, C. T., Jeffrey, P. D., Bassler, B. L., and Hughson, F. M., (2011). A strategy for antagonizing quorum sensing. *Molecular cell 42*, 199–209, DOI: 10.1016/j.molcel.2011.04.003.

(*168*)   UniProt Consortium, (2014). Activities at the Universal Protein Resource (UniProt). *Nucleic acids research 42*, D191–8, DOI: 10.1093/nar/gkt1140.

(*169*)   Sigrist, C., de Castro, E., Cerutti, L., Cuche, B., Hulo, N., Bridge, A., Bougueleret, L., and Xenarios, I., (2013). New and continuing developments at PROSITE. *Nucleic acids research 41*, D344–7, DOI: 10.1093/nar/gks1067.

(*170*)   Mitchell, A., Chang, H.-Y., Daugherty, L., Fraser, M., Hunter, S., Lopez, R., McAnulla, C., McMenamin, C., Nuka, G., Pesseat, S., Sangrador-Vegas, A., Scheremetjew, M., Rato, C., Yong, S.-Y., Bateman, A., Punta, M., Attwood, T. K., Sigrist, C. J. a., Redaschi, N., Rivoire, C., Xenarios, I., Kahn, D., Guyot, D., Bork, P., Letunic, I., Gough, J., Oates, M., Haft, D., Huang, H., Natale, D. a., Wu, C. H., Orengo, C., Sillitoe, I., Mi, H., Thomas, P. D., and Finn, R. D., (2015). The InterPro protein families database: the classification resource after 15 years. *Nucleic acids research 43*, D213–D221, DOI: 10.1093/nar/gku1241.

(*171*)   Berman, H. M., Westbrook, J., Feng, Z., Gilliland, G., Bhat, T. N., Weissig, H., Shindyalov, I. N., and Bourne, P. E., (2000). The Protein Data Bank www.rcsb.org. *Nucleic acids research 28*, 235–242, DOI: 10.1093/nar/28.1.235.

(*172*)   Yao, Y., Martinez-Yamout, M. a., Dickerson, T. J., Brogan, A. P., Wright, P. E., and Dyson, H. J., (2006). Structure of the Escherichia coli quorum sensing protein SdiA: activation of the folding switch by acyl homoserine lactones. *Journal of molecular biology 355*, 262–73, DOI: 10.1016/j.jmb.2005.10.041.

(*173*)   Geske, G. D. G., Mattmann, M. M. E., and Blackwell, H. E., (2008). Evaluation of a focused library of N-aryl L-homoserine lactones reveals a new set of potent quorum sensing modulators. *Bioorganic & medicinal chemistry letters 18*, 5978–81, DOI: 10.1128/JB.183.1.382–386.2001.

(*174*)   Michael, B., Smith, J., Swift, S., Heffron, F., and Ahmer, B., (2001). SdiA of Salmonella enterica is a LuxR homolog that detects mixed microbial communities. *Journal of bacteriology 183*, 5733–42, DOI: 10.1128/JB.183.19.5733–5742.2001.

(*175*)   Llamas, I., Keshavan, N., and González, J., (2004). Use of Sinorhizobium meliloti as an indicator for specific detection of long-chain N-acyl homoserine lactones. *Applied and Environmental Microbiology 70*, 3715–3723, DOI: 10.1128/AEM.70.6.3715–3723.2004.

(*176*)   Kumari, A., Pasini, P., Deo, S. K., Flomenhoft, D., Shashidhar, H., and Daunert, S., (2006). Biosensing systems for the detection of bacterial quorum signaling molecules. *Analytical chemistry 78*, 7603–9, DOI: 10.1021/ac061421n.

(*177*) Leung, M., Brimacombe, C., Spiegelman, G., and Beatty, J., (2012). The GtaR protein negatively regulates transcription of the gtaRI operon and modulates gene transfer agent (RcGTA) expression in Rhodobacter capsulatus. *Molecular microbiology 83*, 759–774, DOI: 10.1111/j.1365-2958.2011.07963.x.

Chapter 5

CHARACTERIZATION OF DIVERSE HOMOSERINE LACTONE SYNTHASES IN *ESCHERICHIA COLI* USING THE LUX QUORUM SENSING REGULATOR[¶]

Quorum sensing is used by over 100 bacterial species to regulate group behaviors, such as bioluminescence, virulence, and biofilm formation, by sending and receiving small molecules called HSLs. Bioengineers have incorporated quorum sensing networks into genetic circuits using HSLs as chemical wires to connect logical operations. However, the development of higher-order genetic circuitry is inhibited by crosstalk, in which one QS network responds to HSLs produced by a different network. We selected ten synthases with narrow yet diverse HSL production profiles to employ as our sender devices. Here, we use decoupled sender and receiver systems to demonstrate the sensitivity of one receiver, the commonly used Lux system, to HSLs from ten distinct synthases. This work represents the most extensive comparison of QS networks to date and greatly expands the bacterial signaling toolkit.

5.1 Introduction

As described in chapter 1 and chapter 4, there are many examples of researchers incorporating quorum sensing networks into genetic circuits with increasing complexity. However, in almost all cases, they use synthetic HSL molecules as the input. To continue pushing the complexity of these engineered systems, researchers will need to spread components across cells, which will require multiple, non-overlapping quorum sensing networks. There are multiple levels of crosstalk between quorum sensing networks: synthase, regulator, and promoter (Figure 1.6). This works addresses crosstalk due to synthase promiscuity: when a synthase produces multiple HSLs (Figure 5.1). Recent efforts have led to identification and engineering of regulators that respond to narrow ranges of HSL molecules (discussed in chapter 1).[87,88,102] In order to implement these tools in biological circuits, we will require complementary synthases with narrow HSL production profiles.

We aimed to expand the quorum sensing toolbox by characterizing synthases novel to engineered systems. Here we have characterized ten HSL synthases by their induction of a popular receiver, BBa_F2620 in a commonly used lab chassis, *Escherichia coli* BL21. Each synthase selected produces a narrow profile of HSLs while the set covers a wide variety of tail lengths and modifications. We have submitted these parts to the iGEM Registry of Standard Biological Parts so they can be accessed by anyone interested in utilizing them.

[¶] This chapter is a manuscript in preparation. See section F.4 for a discussion of authorship and contributions.
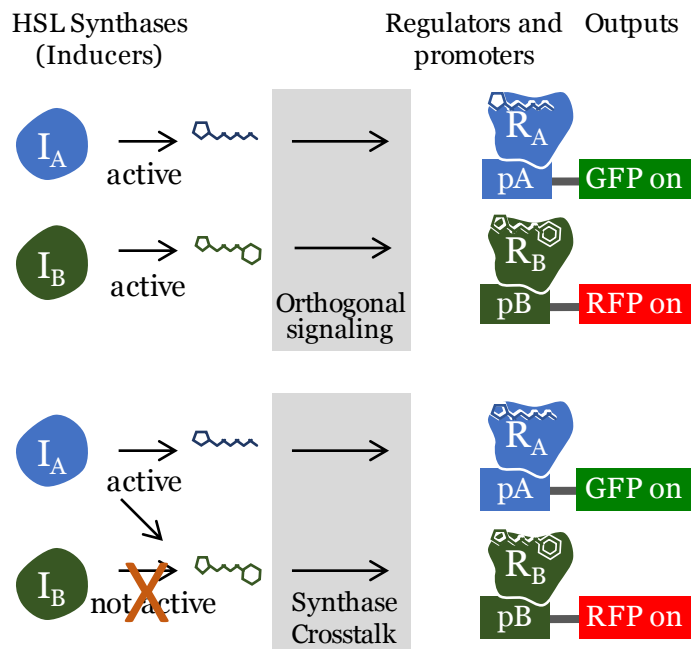
Figure 5.1. Synthase crosstalk in engineered systems. Synthases that produce narrow HSL profiles induce regulators with complementary narrow response profiles. Promiscuous synthases cross-induce multiple receivers resulting in network crosstalk. Figure modified from Figure 1.6 in chapter 1.

5.2 Justification for Sender Media over Synthetic HSLs

Inducing with synthetic HSLs is a useful method for testing functionality of a receiver and initial screening of potential orthogonality[88,97] and has also been used to induce circuits containing quorum sensing regulators (discussed in chapter 4). However, circuits utilizing quorum sensing networks for practical applications depend on induction with HSLs produced by a synthase protein and not exogenously added synthetic HSLs. The HSL profile of a synthase depends on the promiscuity of the enzyme for other substrates and the availability of the on and off-target substrates. Thus, inducing with a single HSL, even if it is the primary HSL produced by a synthase, will not provide the full picture of how a receiver responds to a sender profile composed of multiple HSL species.

Synthase proteins catalyze the production of HSL molecules by facilitating lactone ring formation from S-adenosyl methionine and attaching a tail to the lactone ring from one of two donors. The most commonly observed donors are acyl carrier proteins (ACPs), while a few synthases are known to accept from coenzyme A (CoA). ACP and CoA are involved in many important pathways including fatty acid biosynthesis and degradation and thus carry a wide variety of tails with different lengths, modifications, and levels of saturation.
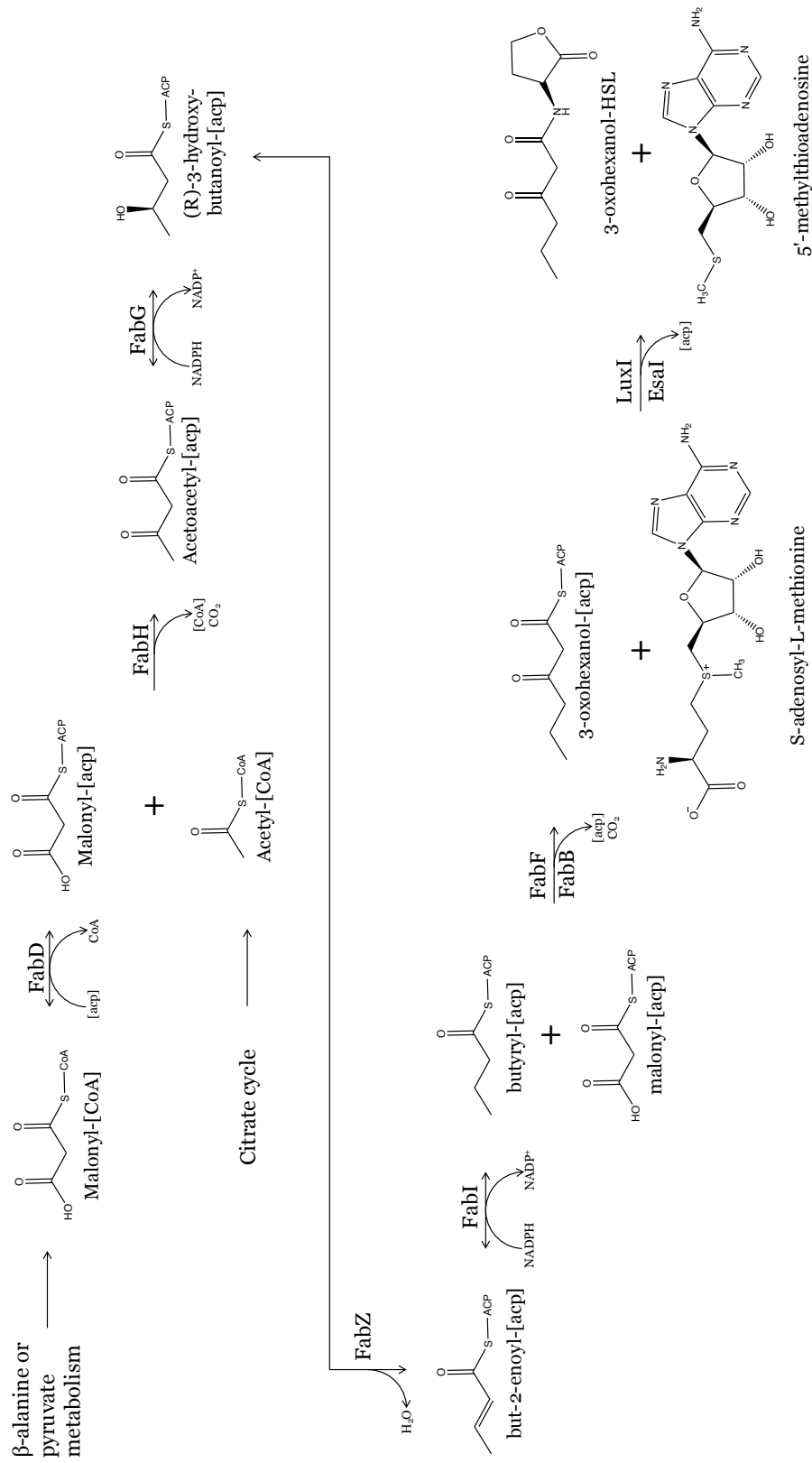
Figure 5.2. 3-oxo-C6-Homoserine lactone synthesis pathway in *Escherichia coli*. The fatty acid biosynthesis enzymes in each reaction and their references are listed in Table 5.1.

Table 5.1. Fatty Acid Biosynthesis Enzymes from *Escherichia coli*

Protein		Gene
ACP	Acyl carrier protein[181]	*acpP*
ACC	Acetyl-CoA carboxylase[182]	*acca−d*
FabD	ACP S-malonyltransferase[183]	*fabD*
FabH	3-oxoacyl-ACP synthase III[184]	*fabH*
FabG	3-oxoacyl-ACP reductase[185]	*fabG*
FabA	3-hydroxyacyl-ACP dehydratase[179,186]	*fabA*
FabZ	3-hydroxyacyl-ACP dehydratase[179]	*fabZ*
FabI	Enoyl-ACP reductase I[184]	*fabI*
FabB	3-oxoacyl-ACP synthase I[187,188]	*fabB*
FabF	3-oxoacyl-ACP synthase II[187,188]	*fabF*

In *E. coli*, ACPs comprise 0.25% of all soluble protein, but the availability of an ACP species with a particular tail within that population depends on the set of enzymes listed in Table 5.1[178] These enzymes are responsible for modifying and lengthening the tails on ACPs. In Figure 5.2 we show the synthesis pathway for the commonly used LuxI precursor HSL, 3-oxo-C6-HSL. As shown in chapter 4 Figure 4.4, HSLs can be much more complex, with tails as long as 18 carbons with varying degrees of saturation and types of modifications. Each of these modifications requires an additional enzymatic step, and thus the population of acyl-ACPs varies across bacterial species and growth conditions. In *E. coli* there are many enzymes involved in modifying ACPs (Figure 5.2 and Table 5.1). Most of the reactions catalyzed by these enzymes are bidirectional, and their activities depend on the concentrations of the products, allowing for self-regulation of the biosynthesis pathway. Further pathway control comes from high levels of competition for substrates between enzymes and negative feedback of enzymes by acyl-ACPs.[178] Furthermore, many of these enzymes have reduced specificity for longer-chain substrates. FabA and FabZ, which catalyze the dehydration of ACP chains by introducing a cis unsaturated bond at C2, have a ~5−fold reduction in specificity for chains longer than ten carbons.[179] Because of this, long-tail ACPs are found at much lower concentrations in *E. coli*.[180] It is possible that synthases which depend on long-tail ACPs for synthesis of HSLs will produce them at low levels or will show higher levels of promiscuity in the absence of their preferred substrate.

Previous work provides evidence for the dependence of synthase behavior on the chassis. In Figure 5.3, we present data we estimated or extracted from three published studies by Gould et al., Beck von Bodman et al., and Ortori et al. Gould et al. expressed LasI in *E. coli*, measured HSL expression profiles, and found that LasI produced multiple HSLs in *E. coli*, suggesting LasI can use multiple acyl-[acp] subtrates (Figure 5.3a and c).[189] Ortori

et al. characterized the LasI HSL production profile in *Pseudomonas aeruginosa* but, as the multiple quorum sensing networks in this species are interdependent, it is difficult to determine which HSLs are produced by which synthase. They generated knockout strains but their data suggest that LasI does not function properly without RhlI and vise versa. While we cannot say from their data which HSLs are produced by LasI in *P. aeruginosa*, we can conclude that LasI generates a different profile of HSLs when expressed in *E. coli*. In *E. coli*, 20% of the HSL molecules produced by LasI were not measured in any of the wildtype (WT) or knockout conditions in *P. aeruginosa* (Figure 5.3a and c).[189,191] These include six HSL molecules, with *N*-(3-oxo-undecanoyl)-L-homoserine lactone (3-oxo-C11-HSL) measured above 10% and small amounts of 3-oxo-C6-HSL, 3-oxo-C8-HSL, *N*-(3-oxo-nonanoyl)-L-homoserine lactone (3-oxo-C9-HSL), C12-HSL, and *N*-(3-oxo-tridecanoyl)-L-homoserine lactone (3-oxo-C13-HSL) (Figure 5.3a and c). These data suggest that not only does LasI have promiscuous substrate specificity, the species-dependent population of available acyl-[acp] species influences the LasI HSL production profile. In contrast, EsaI expressed only 3-oxo-C6-HSL in both *E. coli*[189] and in its native species *Erwinia stewartii* (Figure 5.3b and c).[84]

Taken together, these data suggest that in order to understand the relationship between a sender module and a receiver module, they must be tested together in the chassis of interest. This is the approach we take in this study.

5.3 Initial Synthase Screen

We began by measuring the degree to which a small set of senders induced the Biobrick part Bba_F2620, designed and thoroughly characterized by Canton et al.[97] Canton et al. measured how a LuxR receiver responds to induction by synthetic HSLs.[97] In contrast, we chose to measure the LuxR receiver response to HSLs produced by bacteria expressing HSL synthase proteins (discussed above). F2620 constitutively expresses the LuxR regulator protein and contains the inducible pLux promoter.[97] We cloned EGFP (BBa_E0240) downstream of pLux so that upon addition of a compatible HSL, LuxR will bind the pLux promoter and induce EGFP expression. As discussed above, in contrast to Canton et al., we induced F2620 with media from *E. coli* BL21 expressing HSL synthases from a sender plasmid (Figure 5.4a). The Lux system is known for its promiscuity and is often used to test for the presence of HSLs in bacterial supernatants and therefore is a suitable receiver for testing sender functionality. We built a modular sender vector into which we could easily clone different synthase genes (Figure 5.4a). It also contains the pTet promoter, BBa_R0040, which will allow users to switch to a drug-inducible system by using a chassis with the TetR protein.[192] Using this vector, we constructed a small library of senders, LuxI from *Vibrio*
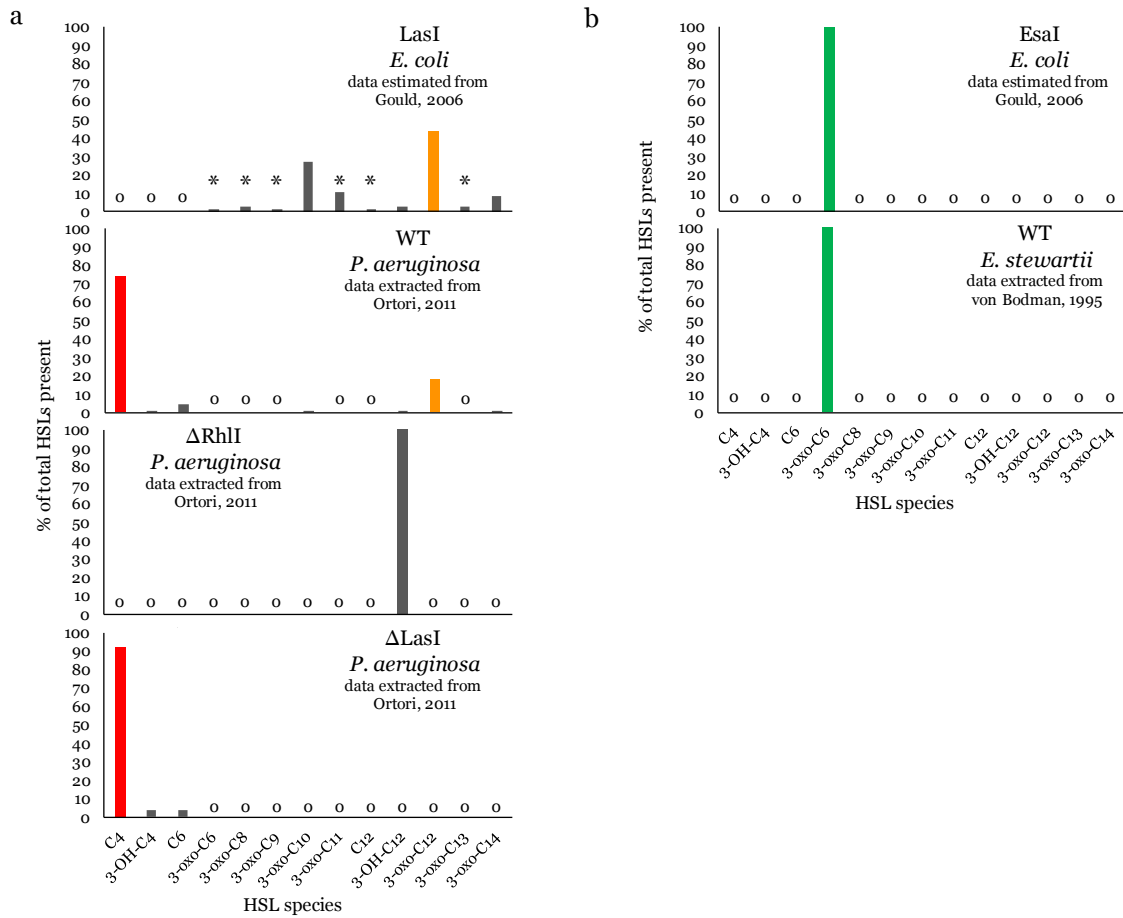
Figure 5.3. Homoserine lactone (HSL) profiles of synthase proteins depend on host (chassis). Data estimated from Gould et al. and extracted from Beck von Bodman et al., Ortori et al. (a) LasI expressed in *Escherichia coli* produces HSLs not measured in LasI-expressing *Pseudomonas aeruginosa*. (b) EsaI produces the same single HSL, 3-oxo-C6-HSL in *E. coli* and its native organism, *Erwinia stewartii*. * Indicates HSLs measured in *E. coli* but not in *P. aeruginosa*.

c

HSL species	LasI[α] *E. coli*	WT[β] *P. aeruginosa*	ΔRhlI[β] *P. aeruginosa*	ΔLasI[β] *P. aeruginosa*	EsaI[α] *E. coli*	WT[χ] *E. stewartii*
C4	n.m	73.79	n.m	92.26	n.m	n.m
3-OH-C4	n.m	1.18	n.m	3.87	n.m	n.m
C6	n.m	4.85	n.m	3.87	n.m	n.m
3-oxo-C6	~1.09*	n.m	n.m	n.m	100.00	100.00
3-oxo-C8	~2.72*	n.m	n.m	n.m	n.m	n.m
3-oxo-C9	~1.09*	n.m	n.m	n.m	n.m	n.m
3-oxo-C10	~27.21	0.39	n.m	n.m	n.m	n.m
3-oxo-C11	~10.88*	n.m	n.m	n.m	n.m	n.m
C12	~1.09*	n.m.	n.m	n.m	n.m	n.m
3-OH-C12	~2.72	0.66	100.00	n.m	n.m	n.m
3-oxo-C12	~43.54	18.09	n.m	n.m	n.m	n.m
3-oxo-C13	~2.72*	n.m.	n.m	n.m	n.m	n.m
3-oxo-C14	~8.16	1.05	n.m	n.m	n.m	n.m

α data estimated from Gould, 2006
β data extracted from Ortori, 2011
χ data extracted from von Bodman, 1995

Figure 5.3. Continued. (c) Estimated and extracted values from Gould et al. and Beck von Bodman et al., Ortori et al. expressed as precentages of total HSLs measured by solid-phase extraction (SPE) liquid chromatography tandem mass spectrometry LC/MS/MS,[189] fast atom bombardment (FAB) MS-MS,[190] or LC-MS/MS.[191] * Indicates HSLs measured in *E. coli* but not in *P. aeruginosa*.

fischeri, LasI and RhlI from *P. aeruginosa*, and EsaI from *E. stewartii* (Figure 5.4b). We transformed a common lab chassis, *E.coli* BL21 with F2620_EGFP for our receiver device and with each of the sender plasmids for our senders. We grew the senders and receivers separately, collected and filtered sender media containing HSLs, and induced our receiver device with dilutions of sender media (Figure 5.4c). We measured GFP and optical density (OD) over time for each dilution using a plate reader.

In order to understand how each sender behaves with F2620, we measured GFP production over time for several dilutions of media containing HSLs produced by our synthases. We calculated the rate of GFP production for each concentration and fit those values with the Hill function. In Figure 5.5a–d, we have plotted the Hill functions for each of the synthases inducing F2620. As expected, the LuxI sender efficiently induces F2620 (Figure 5.5a). Consistent with previously published studies in *E. coli*, LasI did not induce LuxR (Figure 5.5b).[149] As shown in Figure 5.3a and c, LasI expressed in *E. coli* produced mostly long-chain 3-oxo HSLs.[189] Canton et al. did not test any of these HSL species but Balagaddé et al. was able to build a predator-prey system based on orthogonality between the Las and

a

Synthase gene insertion site

RBS

mCherry

Term
Term

RBS
pTet

pMB1 origin of replication

Ampicillin resistance

Synthase gene insertion site

```
AAAGAGGAGAAAtactGAGACGcacaccaGAGACGaacattactagAAAGAGGAGAAA
TTTCTCCTCTTTatgaCTCTGCgtgtggtCTCTGCttgtaatgatcTTTCTCCTCTTT
```

RBS B0034   BsmBI site   BsmBI site   RBS B0034

b

Synthase	HSL profile in native organism	Reference	HSL profile in *E. coli*	Reference
LuxI	3-oxo-C6-HSL C8-HSL	Eberhard 1981	n.d.	N/A
LasI	3-oxo-C12-HSL	Fuqua 2002	3-oxo-C6-HSL 3-oxo-C8-HSL 3-oxo-C9-HSL 3-oxo-C11-HSL C12-HSL 3-oxo-C13-HSL	Gould 2006
RhlI	C4-HSL	Fuqua 2002	n.d.	N/A
EsaI	3-oxo-C6-HSL	von Bodman 1995	3oxo-C6-HSL	Gould 2006

c

LuxR / pLux — GFP off — Bba_F2620

LuxR / pLux — GFP on — Bba_F2620

S   R

1. Grow Sender and Receiver bacteria separately

2. Pellet Senders, filter-purify AHL-enriched medium, add to Receivers

3. Measure Receiver induction

Figure 5.4. Initial screen: Modular sender plasmid, synthases, and experimental approach.

Figure 5.4. Continued. (a) Modular sender plasmid used in this study. BsmBI cloning sites downstream of the pTet promoter and strong ribosome binding site (RBS) allow for drop-in of any synthase gene. Downstream from the cloning site is a second RBS and an mCherry gene for expression of a fluorescent reporter off the same mRNA transcript. (b) Chart of the synthases used in these experiments with the HSL profiles they are known to express in their native organism as well as *Escherichia coli* when available. n.d. no data available. (c) Cartoon of our experimental approach. *E. coli* BL21 expressing synthase proteins (senders) or F2620 (receiver) were grown separately. Senders were pelleted and the media containing HSLs was removed, filtered, and diluted. Receivers were grown with the filtered and diluted sender media and optical density (OD) and GFP expression were measured to determine rates of induction for each concentration of sender media.

Lux networks.[149] RhlI did induce F2620 but only at higher concentrations (Figure 5.5c). We expect RhlI to produce mostly C4-HSL which Canton et al. found only induced F2620 at high concentrations.[97] However, Ortori et al. found that *P. auruginosa* only expressing RhlI produced small amounts of C6-HSL and 3-oxo-C6-HSL.[191] This suggests that RhlI is capable of catalyzing the formation of these HSL species which are known to induce LuxR.[97] We hypothesize that RhlI produces C6-HSL and 3-oxo-C6-HSL at high enough concentrations in *E. coli* BL21 to induce F2620. EsaI, which produces the same HSL as LuxI, also induces F2620 (Figure 5.5d).

The Hill function provides us with additional information about the interactions between F2620 and each synthase. Figure 5.5e shows a heatmap comparing the Hill function values from our data set. Each of these values describes a different facet of the relationship between sender and receiver. GFP_{max} tells us the maximum GFP expression F2620 produced. The heat map quickly shows us that LuxI induces the highest expression levels but not much higher than RhlI and EsaI. We also see that LasI did not induce above background. V_{max} tells us the maximum production rate. For a receiver device, this is the fastest rate a synthase can turn the receiver on. All of the synthases but LasI can quickly switch F2620 to an active expression state. K_d tells us the concentration of diluted media that corresponds to the half-maximal GFP production rate. This can be thought of as how sensitive the receiver is to the synthase media. The higher the value, the less sensitive the receiver is to that synthase. Interestingly, even though LuxI induces F2620 to express the highest levels of GFP, it requires higher concentrations of sender media to do so. It is possible that EsaI is more efficient at catalyzing the formation of HSLs. Finally, n tells us how fast the switching from uninduced to induced happens as concentrations of synthase media increase. In this context, an n greater than 1 could mean that the regulator is unstable at low concentrations of synthase media but is stabilized by binding an HSL molecule. Below that concentration, regulator protein is degraded and there is little induction. Once the concentration threshold is crossed, stabilized regulator accumulates and induces GFP production.

a

LuxI -> LuxR

GFP Production rate (A.U. / hour)

Media percentage ($\log_{10}$)

General Hill equation

$$\frac{dGFP}{dt} = \frac{V_{max}\,[HSL]^n}{K_d^{\,n} + [HSL]^n}$$

$$\frac{dGFP}{dt} = \frac{6189\,[HSL]^{1.0}}{2.2^{1.0} + [HSL]^{1.0}}$$

$GFP_{max} = 25490$ A.U.

b

LasI -> LuxR

GFP Production rate (A.U. / hour)

Media percentage ($\log_{10}$)

General Hill equation

$$\frac{dGFP}{dt} = \frac{V_{max}\,[HSL]^n}{K_d^{\,n} + [HSL]^n}$$

$$\frac{dGFP}{dt} = 0$$

$GFP_{max} = 547$ A.U.

c

RhlI -> LuxR

GFP Production rate (A.U. / hour)

Media percentage ($\log_{10}$)

General Hill equation

$$\frac{dGFP}{dt} = \frac{V_{max}\,[HSL]^n}{K_d^{\,n} + [HSL]^n}$$

$$\frac{dGFP}{dt} = \frac{5774\,[HSL]^{0.5}}{0.3^{0.5} + [HSL]^{0.5}}$$

$GFP_{max} = 19329$ A.U.

d

EsaI -> LuxR

GFP Production rate (A.U. / hour)

Media percentage ($\log_{10}$)

General Hill equation

$$\frac{dGFP}{dt} = \frac{V_{max}\,[HSL]^n}{K_d^{\,n} + [HSL]^n}$$

$$\frac{dGFP}{dt} = \frac{6077\,[HSL]^{5.1}}{0.1^{5.1} + [HSL]^{5.1}}$$

$GFP_{max} = 19329$ A.U.

f

General Hill equation

$$\frac{dGFP}{dt} = \frac{V_{max}\,[HSL]^n}{K_d^{\,n} + [HSL]^n}$$

0   max

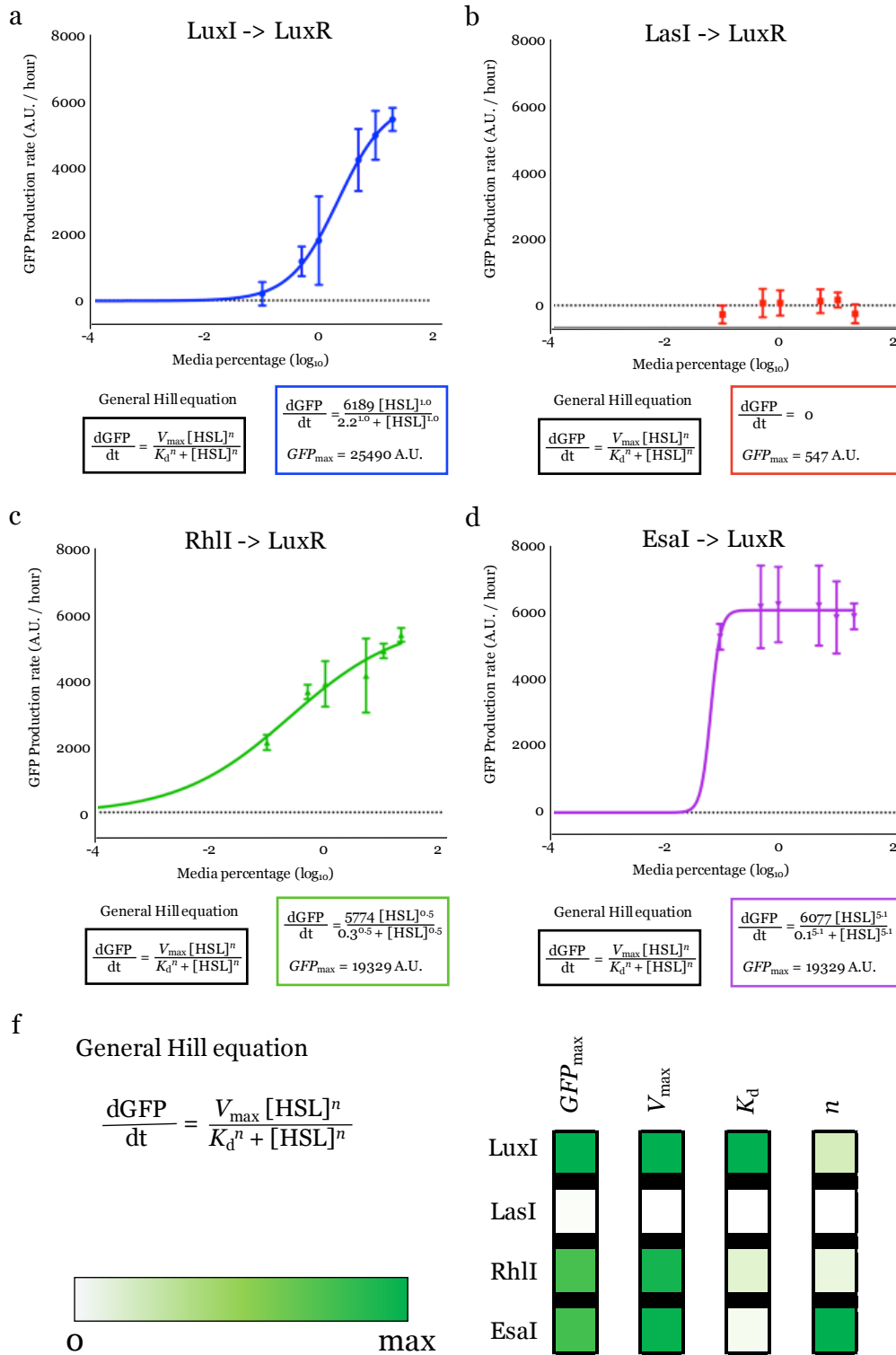|	GFP_{max}	V_{max}	K_d	n
LuxI				
LasI				
RhlI				
EsaI				

Figure 5.5. Synthases induce LuxR receiver device.

99

Figure 5.5. Continued. (a) LuxI induces the LuxR receiver device. (b) LasI does not induce LuxR above background. (c) RhlI induces LuxR but at a relatively lower level than LuxI and EsaI. (d) EsaI induces the LuxR receiver device similarly to LuxI. (e) Heat map of values from Hill equations fit to data in (a) through (d). GFP_{max} is the maximum level of GFP expression measured. V_{max} is the maximum GFP production rate. K_d is the concentration corresponding to half-maximal GFP production rate. n is cooperativity of the regulator and HSL molecules. GFP production rate = maximum value from the derivative of each dilution curve. Dilution curves (not shown) were normalized to OD. Error bars in (a) through (d) indicate s.d. of three biological replicates.

Presenting the data in this way allows readers to make comparative decisions about which synthase might be most appropriate for a specific application. For example, one might want very fast, concentration-sensitive switching with low total expression of the output to prevent stress on the chassis. One could quickly compare each sender and select a synthase with relatively high V_{max}, low n, and low GFP_{max}. The success of these preliminary sender experiments encouraged us to expand our sender library.

5.4   Designing the Senders

We hypothesized that by building a library of senders with narrow HSL profiles, each producing one or two unique HSLs, we would enable genetic engineers to build complex circuits utilizing multiple quorum sensing networks without crosstalk. Several recent studies have engineered or identified receiver modules that respond to non-overlapping HSL profiles. In order to fully take advantage of these new tools, we will need senders that produce complementary non-overlapping profiles. For example, Tashiro et al. evolved LuxR to respond only to either 3-oxo-C6-HSL or 3-oxo-C8-HSL.[102] Complementary senders would include one synthase that produces 3-oxo-C6-HSL but not 3-oxo-C8-HSL and a second that produces 3-oxo-C8-HSL but not 3-oxo-C6-HSL.

With these goals in mind, we selected ten synthase proteins to characterize. We considered the length of the acyl chain, the chain saturation, and the number of different HSLs produced by a single sender. As described in chapter 4, we searched the literature for all known synthases and the HSL profiles they produce (Appendix E Figure E.1). From these, we selected the following HSL synthases: RpaI, BraI, RhlI, BjaI, EsaI, LuxI, AubI, LasI, and CerI. As shown in Figure 5.6a, this synthase set produces a wide range of HSLs with chain lengths from 3 to 18 carbons and modifications such as phenol, phenyl, carbonyl, and methyl groups. We include Lux as it is the most commonly used network and the cognate sender to our F2620 receiver device. Also including EsaI may seem redundant as they both produce 3-oxo-C6-HSL as their major HSL. However, Gould et al. showed that EsaI only

produces 3-oxo-C6-HSL in *E. coli* and therefore may have a narrower HSL profile than LuxI. We also included SinI despite its promiscuity because of the unique HSLs it catalyzes, including the unsaturated 3-oxo-7,8-cis-C16-HSL and the long chain C18-HSL.[193]

As discussed above, it is possible that some of these synthase proteins will produce different HSL profiles in *E. coli* than their native species. Figure 5.6b shows the predicted ACP substrates for each of the HSLs produced by the seven synthases that use ACP substrates (RpaI, BraI, and BjaI use coenzyme A substrates Lindemann et al.). Figure 5.6c shows the fatty acid synthesis pathway for *E. coli*. Colored boxes indicate when each substrate is produced in the pathway. It is clear from this chart that longer chain HSLs require many more enzymatic steps. For example, catalyzing the formation of *N*-(3-oxo-dodecanoyl)-L-homoserine lactone (3-oxo-C12-HSL) from 3-oxo-C6-HSL requires 12 additional steps while C18-HSL requires 27 additional steps. It is possible that synthases that produce longer chain HSLs will produce lower concentrations than the shorter chain enzymes or that their activity will be more promiscuous as is seen with LasI (Figure 5.3a).
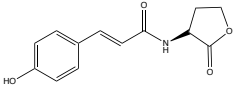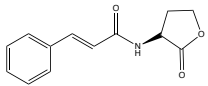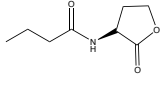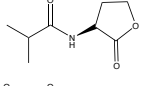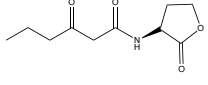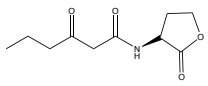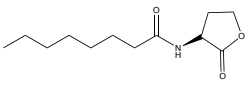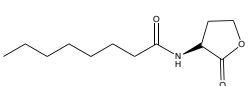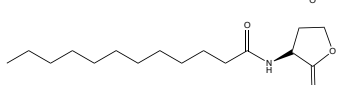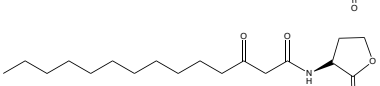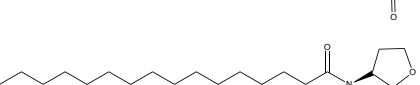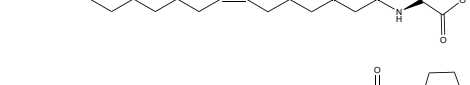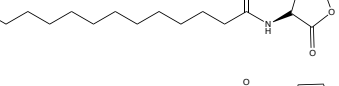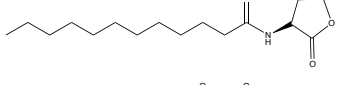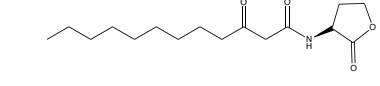
5.5   Testing the Senders: Plate Reader Experiments

For these experiments, we modified the modular sender vector to have the cloning sites EcoRI and XbaI (Figure 5.7. We followed the same approach illustrated in Figure 5.4c, inducing F2620_EGFP with dilutions of sender media but induced at higher concentrations than in the previous experiments.

We found that F2620 had a measurable response to all but one of our senders (Figure 5.8. We can conclude from these data that we successfully expressed all senders but SinI in *E. coli* BL21. Consistent with our previous results, RhlI, LuxI, and EsaI induce LuxR. LuxR is highly responsive even at low doses to those synthases as well as BraI and BjaI suggesting these enzymes are functional in our chassis. LasI, AubI, CerI, and RpaI show induction above background at all doses but LuxR is less sensitive to these synthases at low concentrations. This could be due to LuxR insensitivity to the HSLs produced or low activity of these enzymes in our chassis. To determine whether senders SinI, AubI, CerI, RpaI, and LasI are functional, we will need to test these senders inducing their cognate receiver or a promiscuous receiver sensitive to longer chain HSLs.

In our earlier data (Figure 5.5b), we did not see induction by LasI. However, in these experiments, we see induction at our highest tested concentration, 50%. Balagaddé et al. demonstrated functional orthogonality between the the Las and Lux networks. This suggests that complete orthogonality is not necessary for functional orthogonality. If only high concentrations of sender media are able to induce a receiver module, adjustments to synthase expression levels by changing promoter and RBS strengths could be sufficient to

Table 5.2. Homoserine lactone (HSL) Production Profiles and acyl carrier protein (ACP) Substrates for the Synthases Used in this Study

Synthase	HSL Species	ACP Species Substrate	
RpaI		[CoA substrate]	
BraI		[CoA substrate]	
RhlI		N-C4-enoyl-[acp]	▭
BjaI		[CoA substrate]	
EsaI		3-oxo-C6-enoyl-[acp]	▭
LuxI		3-oxo-C6-enoyl-[acp]	▭
SinI		N-C8-enoyl-[acp]	▭
		N-C8-enoyl-[acp]	▭
		N-C12-enoyl-[acp]	▭
		3-oxo-C14-enoyl-[acp]	▭
		N-C16-enoyl-[acp]	▭
		3-oxo-7-cis-C14-enoyl-[acp]	▭
		N-C18-enoyl-[acp]	▭
AubI		N-C12-enoyl-[acp]	▭
LasI		3-oxo-C12-enoyl-[acp]	▭
CerI		7-cis-C14-enoyl-[acp]	▭

102
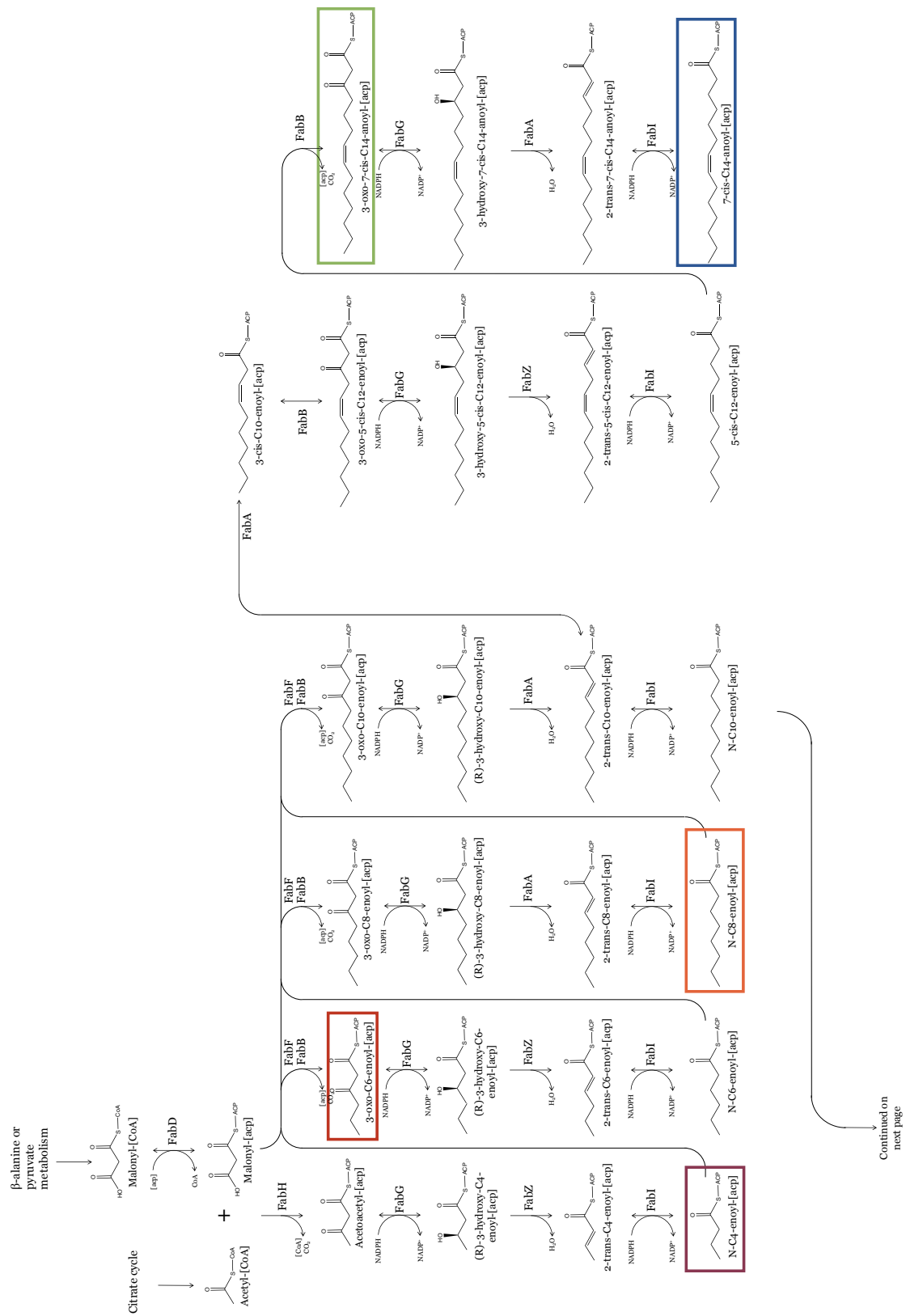
Figure 5.6. Fatty acid biosynthesis pathway in *Escherichia coli*. Colored boxes correspond to the colored boxes in Table 5.2 and indicate the ACP substrates we expect these synthases to use.
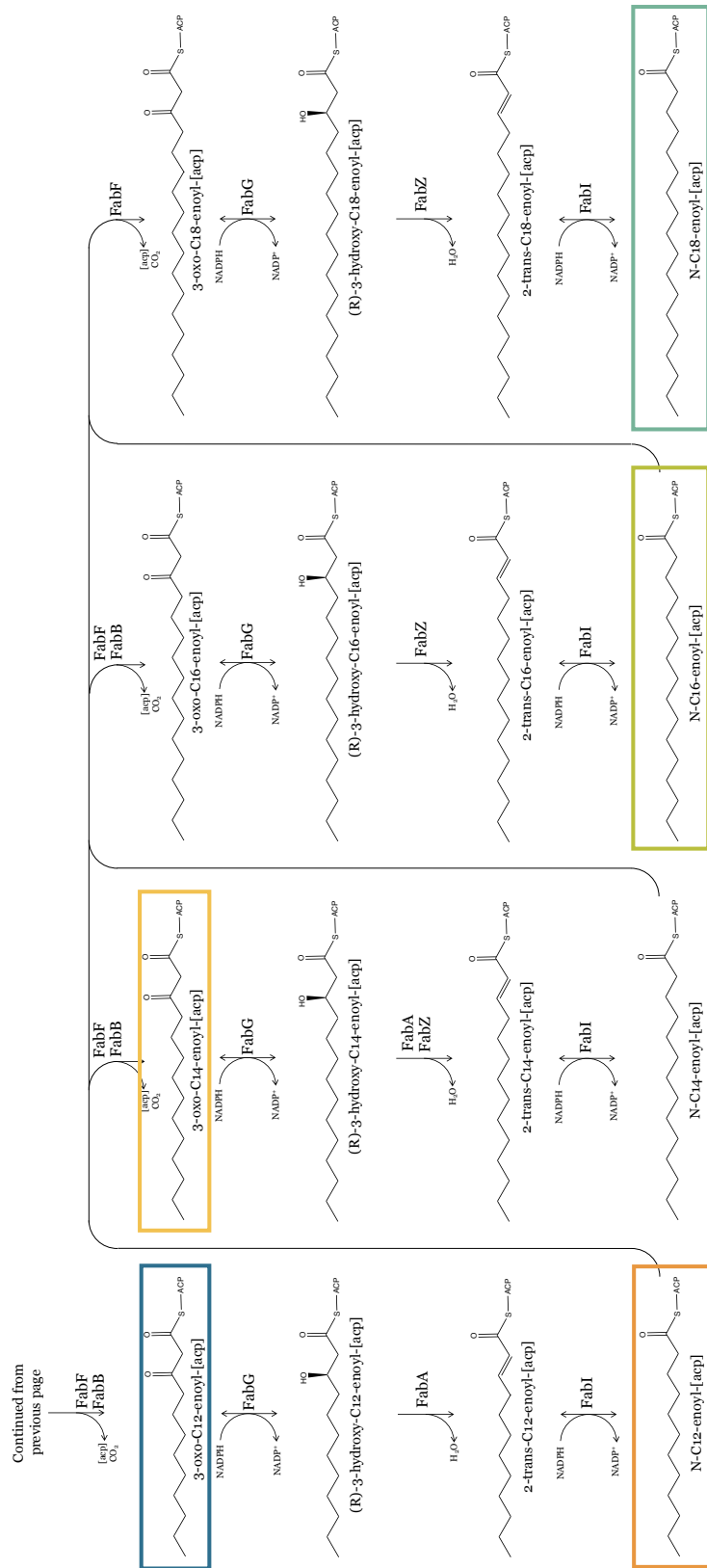
Figure 5.6. Continued.
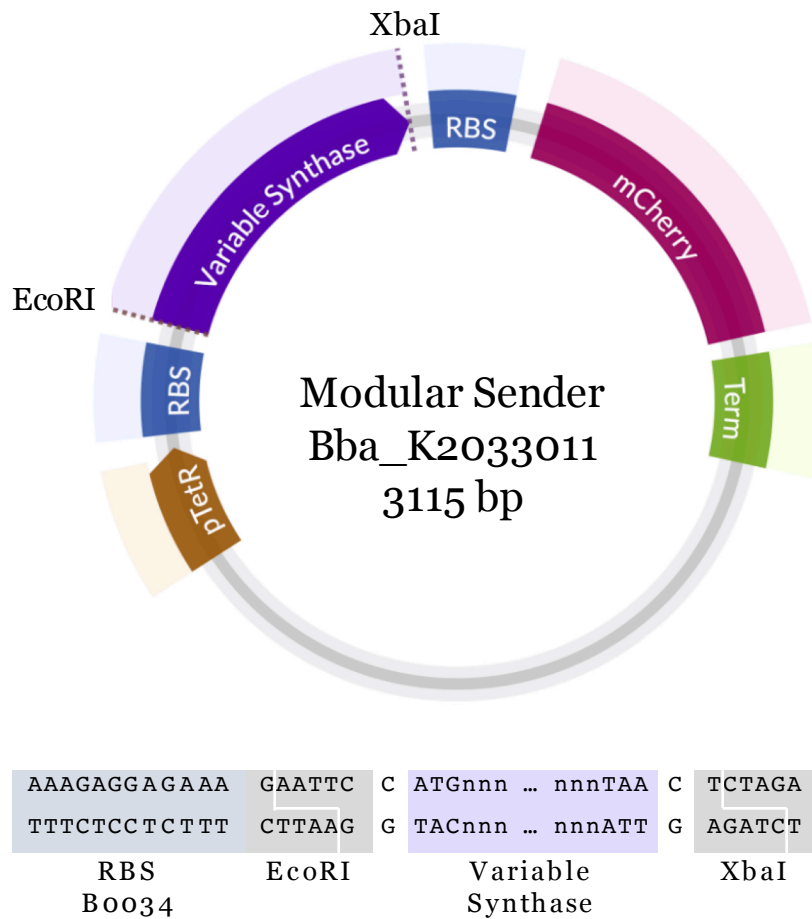
Figure 5.7. Updated modular sender vector. This sender vector was updated from the vector shown in Figure 5.4 a. It includes XbaI and EcoRI restriction sites to clone in the variable synthase proteins.

prevent crosstalk. Additionally, low level expression of a lactonase could be used to prevent accumulation of the HSLs.

Recently, Scott et al. found that RpaI did not induce LuxR and built a network based on their orthogonality.[101] This further supports the hypothesis that full orthogonality is not necessary for functional orthogonality. Importantly, Scott et al., built their system in *Salmonella typhimurium*. It is also possible that RpaI does not produce the same HSL profile in the two chassis. These data further emphasize the importance of testing quorum sensing networks under relevant conditions for each application.

We attempted to fit Hill functions to each sender inducing the LuxR receiver device (Figure 5.9). However, with only four doses, 0%, 10%, 25%, or 50% (Figure 5.8), the resulting Hill equations are not representative of the behavior of the device. For senders
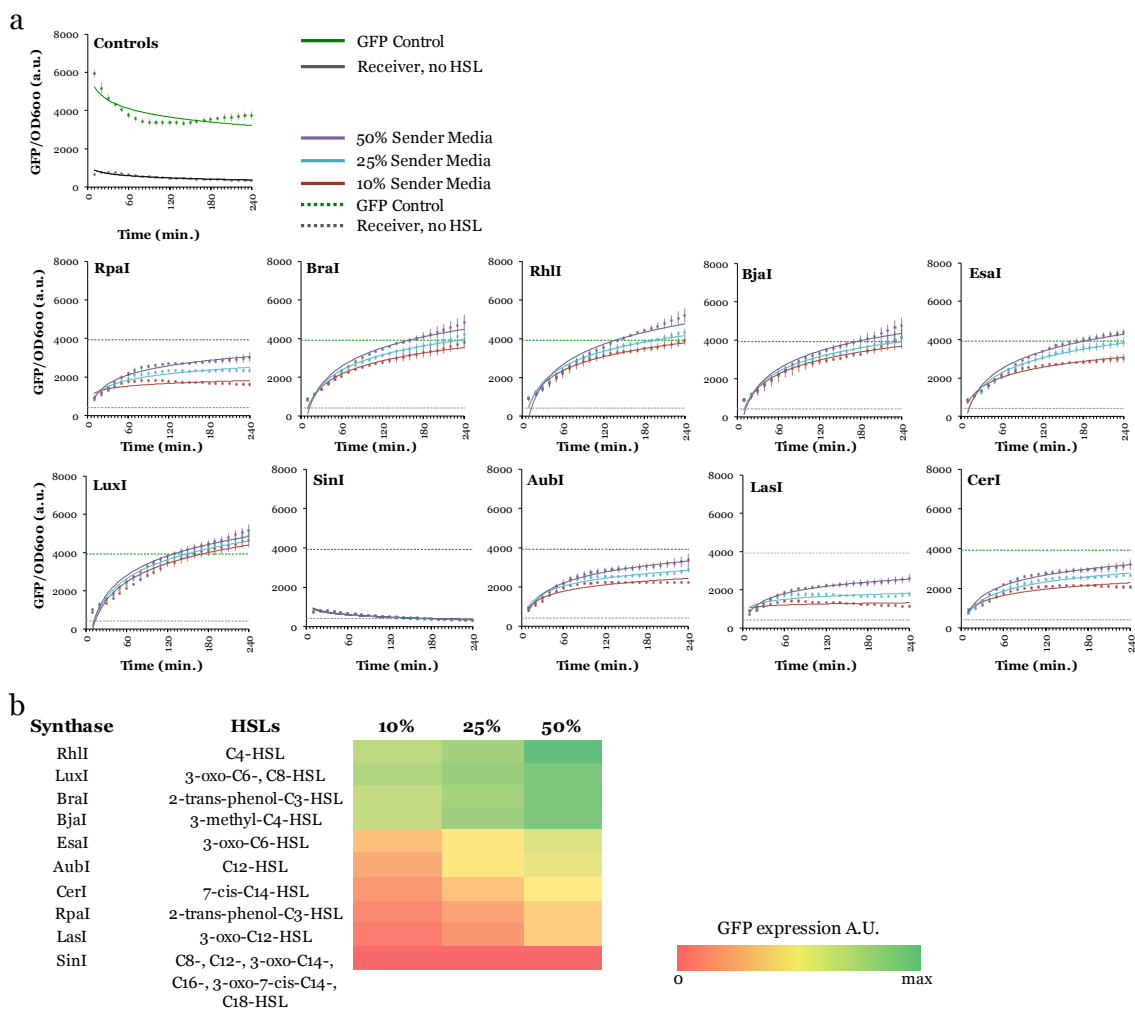
Figure 5.8. Induction of F2620 LuxR receiver device with ten synthases. (a) GFP control plasmid (green) and LuxR receiver grown in the absence of sender media (grey). LuxR receiver device GFP production over time grown in 10% (purple), 25% (blue), or 50% (red) dilutions of sender media for each of ten sender devices. Dotted green line and grey line on each graph indicates the maximum GFP expression seen in the corresponding control in the Control graph. Bars indicate standard deviation of three biological replicates. (b) Heat map shows relative GFP_{max} of the LuxR receiver induced by each sender at three concentrations.
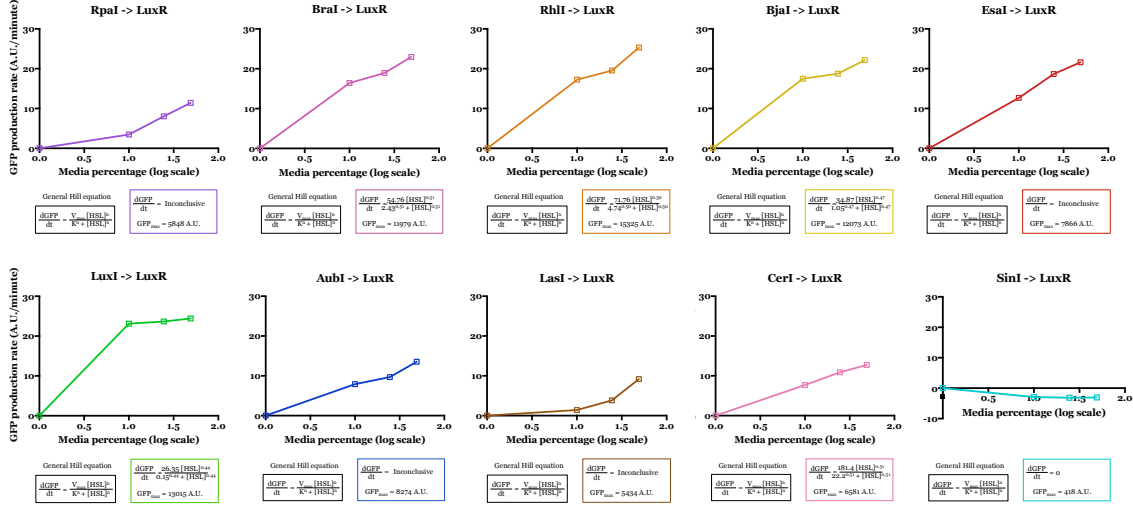
Figure 5.9. Dose response curves for ten senders inducing LuxR receiver. Hill functions were fit to the maximum induction rates (V_{max}) for each media dilution for each sender inducing the LuxR receiver device. Insufficient data points resulted in unreliable fit curves.

BraI, RhlI, BjaI, EsaI, and LuxI, the receiver is at close to V_{max} at the lowest tested dilution of 10%. Several dilutions below 10% should be tested to better understand the dose responses. For senders RpaI, AubI, LasI, and CerI, the tested dilutions do not reach a production rate plateau, suggesting these should be tested at higher concentrations.

5.6   Designing the Receivers

To complement our sender library, we also began the design work for constructing a library of receivers. We decided to base our receivers on the Biobrick part F2620 with some important changes. First, F2620 has very leaky expression of GFP in the absence of sender media (data not shown). We suspect this is due to two reasons: read-through by polymerase on the plasmid and LuxR regulator over-expression. The organization of the genes could allow for read through from the strong constitutive Tet promoter across the two transcriptional terminators. To address this issue, we reversed the order of the *pTet_Receiver_T_T* and *pInd_GFP_T_T* (Figure 5.10). LuxR and most other quorum sensing regulators are unstable and degraded in the absence of a compatible HSL.[194] In the presence of 3-oxo-C6-HSL, LuxR dimerizes and can bind its cognate DNA domain. However, it is possible that over-expression of the Lux regulator protein allows the LuxR dimer to form in the absence of the HSL and activate the promoter, resulting in high background GFP expression. We therefore decided to use the RBS B0032 from the Biobrick registry which is weaker RBS than used in F2620 Figure 5.10.[195]
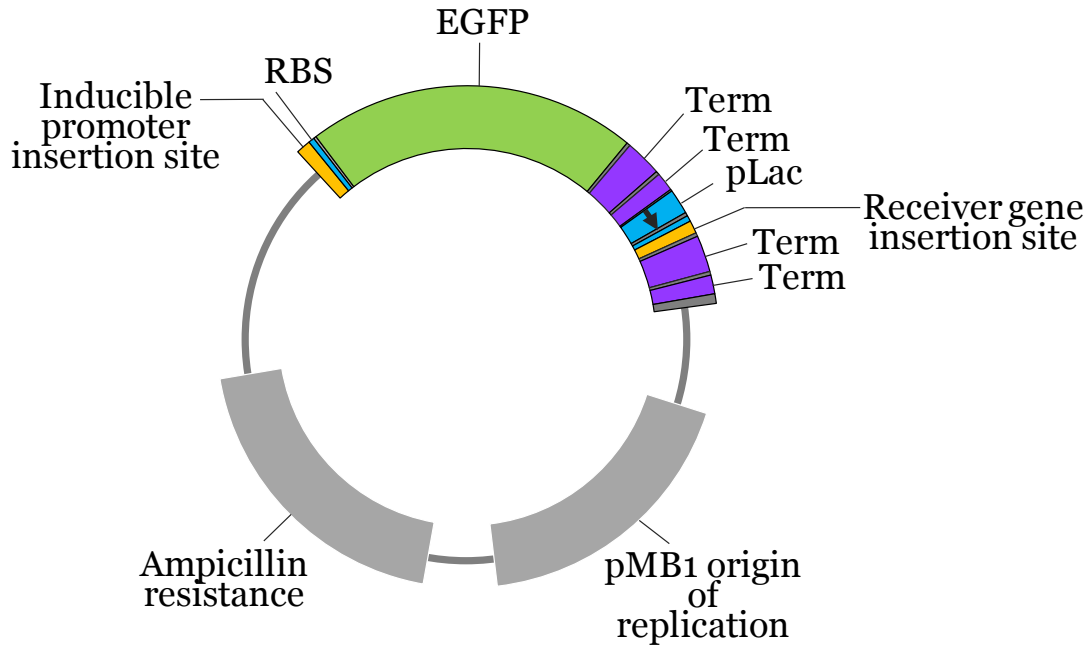
Inducible promoter insertion site

```
GATCTAGTGGaatttaGTCTTCggtaccGAAGACaactaggTCACACAGGAAAG
CTAGATCACCttaaatCAGAAGgtgtggtCTTCTGttgatgAGTGTGTCCTTTC
```

| Backbone | BbsI site | BbsI site | RBS B0032 |

Receiver gene insertion site

```
TCACACAGGAAAGGAATTCgcggccgcttCTAGAactagCCAGGCATCAAATAAA
AGTGTGTCCTTTCCTTAAGcgccggcgaAGATCTtgatcGGTCCGTAGTTTATTT
```

| RBS B0032 | EcoRI site | XbaI site | Terminator B0010 |

Figure 5.10. Modular receiver vector. The modular receiver vector has BbsI cloning sites to drop in inducible promoters and EcoRI and XbaI cloning sites to drop in the receiver genes.

For our initial screening and induction characterization experiments, we want constitutive expression of all genes. Looking ahead to future applications of these parts, we provide the option of independently inducible senders and receivers. We chose to make the senders tetracycline (tet) inducible under control of the pTet promoter and the receiver regulator IPTG inducible using the pLac promoter.[192]

We retained the HSL-inducible promoter structure used in F2620 for our new receivers. Specifically, including the 20 bp palindromic regulator binding site upstream of the *V. fischeri* Lux promoter -35 region.

Receiver construction and characterization is ongoing in our lab. Preliminary results confirm this receiver design is functional for other quorum sensing networks. Future work will include induction tests with each new receiver and our library of senders.

Scott et al. built a similar library of receivers including LuxR, LasR, RhlR, Tra, Rpa, Ahy, Sma, Cer, and Exp, but found that several of them were not functional in *E. coli*. They hypothesized that the regulators were unable to properly interact with the *E. coli* sigma factor. They found that mutating one amino acid in the Tra regulator resulted in a functional TraR receiver in *E. coli*. After initial testing of our receiver library, we will similarly do protein alignments on any regulators that do not respond to their cognate senders.

5.7   Preliminary Receiver Tests Confirm Sender Functionality

To validate the design of our receivers, we constructed a LasR device and tested its response to the long chain synthases SinI, AubI, CerI, RpaI, and LasI. In Figure 5.11 we see that LasI and AubI induces LasR at both low and high concentrations validating our receiver design and LasI and AubI functionality in our chassis. LasR sensitivity to RpaI and CerI is similar to LuxR: we see induction at high concentration at ~50% of LasI-LasR induction but little induction at low concentrations. We can confirm that these synthases are functional in *E. coli* but we will need to induce their cognate receiver to understand if they are producing low levels or if they are potentially functionally orthogonal to both LuxR and LasR. Finally, SinI shows induction of LasI above background at high concentrations but these data suggest that SinI is not very functional in *E. coli*.

5.8   Methods

5.8.1   Construction of the LuxR Receiver

An inducible LuxR receiver, F2620_EGFP, was built from with the plasmids BBa_-F2620 and BBa_E0240 (both gifts from iGEM Headquarters). BBa_F2620 contains the
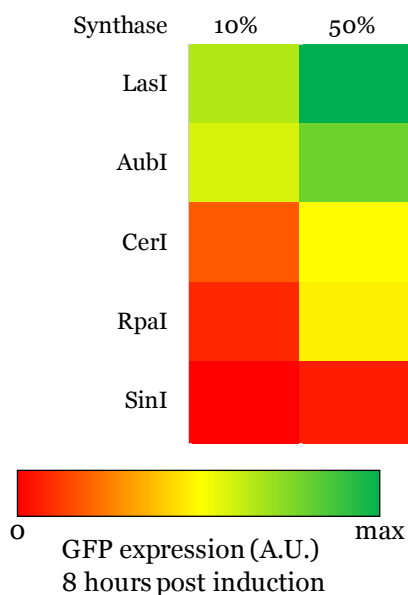
Figure 5.11. LasR receiver is sensitive to long chain synthases. The LasR receiver device was induced with purified media from senders SinI, AubI, CerI, RpaI, and LasI. Heat map represents GFP expression (A.U.) minus background (LasR with negative sender media) at 8 h post induction.

promoter p(TetR) controlling expression of the LuxR regulator and the LuxR-HSL regulated promoter p(LuxR). BBa_E0240 contains an RBS, GFP, and two transcriptional terminators. BBa_F2620 was cut downstream of p(LuxR) with SpeI (Thermo Fisher Scientific) and PstI (Thermo Fisher Scientific). The RBS-GFP-Terminator insert was cut from BBa_E0240 with XbaI (Thermo Fisher Scientific) and PstI and ligated into BBa_F2620.

5.8.2 Construction of the Modular Sender Vector

The modular sender vector was constructed from the vector pSB1A3 (a gift from iGEM Headquarters). Using Phusion-based PCR, an insert was constructed that allows for modular cloning of synthase sequences into the vector via the standard BioBrick cloning method. The insert contains the promoter p(TetR) (BBa_R0040), followed by a multiple cloning site (EcoRI, NotI, XbaI, and SpeI), a strong ribosome binding site (BBa_B0034), an mCherry open reading frame (BBa_J06504), and two terminators (BBa_B0010 and BBa_B0012). The insert was constructed by using Phusion polymerase (New England Biolabs) to amplify the RBS-mCherry-terminators insert from the plasmid BBa_J06702 (a gift from iGEM Headquarters). The promoter sequence was ligated with the remainder of the construct

using T4 ligase (New England Biolabs). This final insert was cloned into the pSB1A3 vector using the restriction enzymes EcoRI and PstI (Thermo Fisher Scientific). This vector was used as the negative sender plasmid.

5.8.3   Cloning of HSL Synthase Homologs

The coding regions for the following HSL synthases were synthesized as double-stranded oligos (IDT) with an EcoRI binding site upstream and a XbaI cut site downstream: AubI, BjaI, BraI, CerI, EsaI, LasI, LuxI, RhlI, RpaI, and SinI. The Modular Sender Vector and each HSL synthase oligo were cut with EcoRI and XbaI (Thermo Fisher Scientific) and ligated using T4 ligase (New England Biolabs). Plasmids containing synthases not already in the iGEM registry were submitted with the following identification keys: AubI BBa_K2033000, BjaI BBa_K2033002, BraI BBa_K2033004, CerI BBa_K2033006, SinI BBa_K2033008. The negative sender vector is the

5.8.4   Microplate Reader Induction Assay

Microplate reader induction assays were used to determine RFP 580 nm to 610 nm, GFP 485 nm to 515 nm, and absorbance (OD600) of *E. coli* BL21 (New England Biolabs) cells induced with media expressed by sender construct cells.

5.8.4.1   Receiver Culture Preparation

Single colonies of *E. coli* BL21 cells transformed with F2620_EGFP or GFP positive plasmid (pTrc99A vector expressing GFP from the pLac promoter) were inoculated in 3 ml of LB broth [25 g Acros LB broth Lennox granules (Sigma) in 1000 mL water] with 5 μg/ml ampicillin (VWR) and grown for 16 h at 37 °C with shaking. OD600 values of the F2620 receiver and GFP positive control cultures were recorded. New cultures from each of culture were seeded to OD600 = 0.05 and grown at 37 °C with shaking OD600 = 0.8. Cultures were spun at 4500 g for 5 min. Supernatants were discarded and cells were resuspended in fresh LB with ampicillin to obtain final culture concentrations of OD600 = 0.8.

5.8.4.2   Sender Media Preparation

Single colonies of *E. coli* BL21 cells transformed with sender plasmids or negative sender plasmid were inoculated in 3 ml of LB with 5 μg/ml ampicillin (VWR) and grown for 16 h at 37 °C with shaking. Sender and negative sender cultures were spun at 4500 g for 5 min.

Table 5.3. Culture and Media Dilutions for Plate Reader Assays

Sender Dilution	Spent media (µL)			Receiver Culture (µL)
	Sender	Negative Sender	Total	
0 %	0	150	150	150
10 %	30	120	150	150
25 %	75	75	150	150
50 %	150	0	150	150

Supernatants were filtered with 0.22 µm nylon filters (VWR International) to remove any remaining cells.

5.8.4.3 Plate Reader Setup

Corning Black Costar Clear Bottom 96 Well Plates (Fisher Scientific) were loaded with a total volume of 300 µl per well with a final $OD600$ of 0.4. Varying concentrations of sender and negative sender media were used to ensure the same total volume of spent media per well (Table 5.3). In addition to a total of 150 µl spent media, 150 µl of working receiver stock was added per well.

Plates were run on a Biotek Synergy H1 Microplate Reader, measuring RFP, GFP, and $OD600$ every 10 min for 8 h at 37 °C with shaking. Automatic gain adjustment was set to scale to the lowest detected well values for each measurement.

5.8.5 Induction Curve and Heat Map Analysis

Triplicate GFP signal (A.U.) for each sample (by sender type and concentration) was divide by triplicate $OD600$ measurements at each time point. Mean $GFP/OD600$ was calculated and plotted against time from 0 min to 240 min using Microsoft Excel 2016 (error = standard deviation). Logarithmic curves of best fit were added to each data set (by sender type and concentration).

To generate the heatmap, maximum mean $GFP/OD600$ for each sample type (by sender and concentration) was determined regardless of time, although in most cases the maximum value was at the final time point. Maximum mean $GFP/OD600$ values were conditionally formatted to visually indicate lowest to highest values colorimetrically.

5.8.6 Hill Function Analysis

For each sender type and concentration, the slope of the line tangent to the curve was determined at 60 min from the equations given for logarithmic curves of best fit determined in the induction curve analysis (described above). This time point was chosen as the cultures had all reached mid-log phase at this point. These slope values represent the rate of GFP production V for each concentration of sender media by sender media type. GFP production rate was plotted against log_{10} sender media percentages using GraphPad Prism software. GraphPad Prism was used to determine the *HillSlope*, V_{max}, and K_d values. A non-linear regression analysis was used to graph media dilution vs. normalized response with a variable slope.

References

(*84*) von Bodman, S., Ball, J., Faini, M., Herrera, C., Minogue, T., Urbanowski, M., and Stevens, A., (2003). The quorum sensing negative regulators EsaR and ExpREcc, homologues within the LuxR family, retain the ability to function as activators of transcription. *Journal of bacteriology 185*, 7001–7007, DOI: 10.1128/JB.185.23.7001.

(*87*)   Chen, Y., Kim, J. K., Hirning, A. J., and Bennett, Matthew, R., (2016). Emergent genetic oscillations in a synthetic microbial consortium. *Science 349*, 986–989, DOI: 10.1126/science.aaa3794.Emergent.

(*88*)   Scott, S. R., and Hasty, J., (2016). Quorum Sensing Communication Modules for Microbial Consortia. *ACS Synthetic Biology 5*, 969–977, DOI: 10.1021/acssynbio.5b00286.

(*97*)   Canton, B., Labno, A., and Endy, D., (2008). Refinement and standardization of synthetic biological parts and devices. *Nature biotechnology 26*, 787–93, DOI: 10.1038/nbt1413.

(*101*)   Scott, S. R., Din, M. O., Bittihn, P., Xiong, L., Tsimring, L. S., and Hasty, J., (2017). A stabilized microbial ecosystem of self-limiting bacteria using synthetic quorum-regulated lysis. *Nature Microbiology 2*, 17083, DOI: 10.1038/nmicrobiol.2017.83.

(*102*)   Tashiro, Y., Kimura, Y., Furubayashi, M., Tanaka, A., Terakubo, K., Saito, K., Kawai-Noma, S., and Umeno, D., (2016). Directed evolution of the autoinducer selectivity of Vibrio fischeri LuxR. *The Journal of General and Applied Microbiology 247*, 1–8, DOI: 10.2323/jgam.2016.04.005.

(*149*)   Balagaddé, F. K., Song, H., Ozaki, J., Collins, C. H., Barnet, M., Arnold, F. H., Quake, S. R., and You, L., (2008). A synthetic Escherichia coli predator-prey ecosystem. *Molecular systems biology 4*, DOI: 10.1038/msb.2008.24.

(*163*)   Lindemann, A., Pessi, G., Schaefer, A., Mattmann, M., Christensen, Q., Kessler, A., Hennecke, H., Blackwell, H., Greenberg, E., and Harwood, C., (2011). Isovaleryl-homoserine lactone, an unusual branched-chain quorum-sensing signal from the soybean symbiont Bradyrhizobium japonicum. *Proceedings of the National Academy of Sciences 108*, 16765–70, DOI: 10.1073/pnas.1114125108.

(*178*)   Byers, D. M., and Gong, H., (2007). Acyl carrier protein: structure-function relationships in a conserved multifunctional protein family. *Biochemistry and cell biology = Biochimie et biologie cellulaire 85*, 649–662, DOI: 10.1139/o07-109.

(*179*)   Heath, R. J., and Rock, C. O., (1996). Roles of the FabA and FabZ beta-hydroxyacyl-acyl carrier protein dehydratases in Escherichia coli fatty acid biosynthesis. *The Journal of biological chemistry 271*, 27795–27801, DOI: 10.1074/jbc.271.44.27795.

(*180*)   Rock, C. O., and Jackowski, S., (1982). Regulation of phospholipid synthesis in Escherichia coli. Composition of the acyl-acyl carrier protein pool in vivo. *The Journal of biological chemistry 257*, 10759–65.

(*181*)   Majerus, P. W., Alberts, A. W., and Vagelos, P. R., (1964). The Acyl Carrier Protein of Fatty Acid Synthesis: Purification, Physical Properties, and Substrate Binding Site. *Proceedings of the National Academy of Sciences of the United States of America 51*, 1231–8.

(*182*)   Polakis, S. E., Guchhait, R. B., Zwergel, E. E., Lane, M. D., and Cooper, T. G., (1974). Acetyl coenzyme A carboxylase system of Escherichia coli. Studies on the mechanisms of the biotin carboxylase- and carboxyltransferase-catalyzed reactions. *The Journal of biological chemistry 249*, 6657–67.

(*183*)   Magnuson, K., Carey, M. R., and Cronan, J. E., (1995). The putative fabJ gene of Escherichia coli fatty acid synthesis is the fabF gene. *Journal of bacteriology 177*, 3593–5.

(*184*)   Heath, R. J., and Rock, C. O., (1996). Regulation of Fatty Acid Elongation and Initiation by Acyl-Acyl Carrier Protein in Escherichia coli. *The Journal of biological chemistry 271*, 1833–1836, DOI: 10.1074/jbc.271.4.1833.

(*185*)   Heath, R. J., and Rock, C. O., (1995). Enoyl-acyl carrier protein reductase (fabI) plays a determinant role in completing cycles of fatty acid elongation in Escherichia coli. *Journal of Biological Chemistry 270*, 26538–26542, DOI: 10.1074/jbc.270.44.26538.

(*186*)   Feng, Y., and Cronan, J. E., (2009). Escherichia coli Unsaturated Fatty Acid Synthesis. *Journal of Biological Chemistry 284*, 29526–29535, DOI: 10.1074/jbc.M109.023440.

(*187*)   D'Agnolo, G., Rosenfeld, I. S., and Vagelos, P. R., (1975). Multiple Forms of ß-Ketoacyl-Acyl Synthetase in Escherichia coli. *Journal of Biological Chemistry 250*, 5289–5294.

(*188*)   Janßen, H., and Steinbüchel, A., (2014). Fatty acid synthesis in Escherichia coli and its applications towards the production of fatty acid based biofuels. *Biotechnology for Biofuels 7*, 7, DOI: 10.1186/1754-6834-7-7.

(*189*)   Gould, T. a., Herman, J., Krank, J., Murphy, R. C., and Churchill, M. E. a., (2006). Specificity of Acyl-Homoserine Lactone Synthases Examined by Mass Spectrometry. *Journal of Bacteriology 188*, 773–783, DOI: 10.1128/JB.188.2.773-783.2006.

(*190*)   Beck von Bodman, S., and Farrand, S. K., (1995). Capsular polysaccharide biosynthesis and pathogenicity in Erwinia stewartii require induction by an N-acylhomoserine lactone autoinducer. *Journal of bacteriology 177*, 5000–8.

(*191*)   Ortori, C. A., Dubern, J. F., Chhabra, S. R., Cámara, M., Hardie, K., Williams, P., and Barrett, D. A., (2011). Simultaneous quantitative profiling of N-acyl-l-homoserine lactone and 2-alkyl-4(1H)-quinolone families of quorum-sensing signaling molecules using LC-MS/MS. *Analytical and Bioanalytical Chemistry 399*, 839–850, DOI: 10.1007/s00216-010-4341-0.

(*192*)   Lutz, R., and Bujard, H., (1997). Independent and tight regulation of transcriptional units in Escherichia coli via the LacR/O, the TetR/O and AraC/I1-I2 regulatory elements. *Nucleic acids research 25*, 1203–10, DOI: 10.1093/nar/25.6.1203.

(*193*)   Marketon, M. M., Gronquist, M. R., Eberhard, A., and González, J. E., (2002). Characterization of the Sinorhizobium meliloti sinR/sinI locus and the production of novel N-acyl homoserine lactones. *Journal of bacteriology 184*, 5686–95, DOI: 10.1128/JB.184.20.5686.

(*194*)   Tsai, C.-S., and Winans, S. C., (2010). LuxR-type quorum-sensing regulators that are detached from common scents. *Molecular Microbiology 77*, 1072–1082, DOI: 10.1111/j.1365-2958.2010.07279.x.

(*195*)   Gardner, T. S., Cantor, C. R., and Collins, J. J., (2000). Construction of a genetic toggle switch in Escherichia coli. *Nature 403*, 339–42, DOI: 10.1038/35002131.

Chapter 6

DISCUSSION

6.1   Improving Cas9 Editing in Heterochromatin

The CRISPR/Cas9 system is a powerful tool that allows genetic engineers to make precise modifications to virtually any genomic locus.[48] The list of applications continues to grow, from high-throughput mammalian genome editing to targeted transcriptional control to in vivo chromosomal tracking.[49,61,196] Until recently, however, it was unclear whether the bacterially-derived Cas9 protein could efficiently target loci in heterochromatin, the DNA-protein complex that controls gene expression and nuclear organization in eukaryotic cells.[50–52] Our work presented in chapter 2 demonstrated that facultative heterochromatin inhibits Cas9 binding and editing at some sites and is supported by other recent publications.[54,69] To continue advancing its applications in eukaryotic genomes, we will need to identify methods for improving Cas9 activity in heterochromatin.

In chapter 3 we investigated strategies for enhancing Cas9 editing at target sites located in silenced chromatin. We used a small molecule drug and a targeted transcriptional activator to artificially reopen silenced chromatin (Figure 3.3). We found that the drug UNC1999 removed the silencing mark without increasing target gene expression (Figure 3.5). However, our preliminary data do not indicate that it effectively improves Cas9 editing (Figure 3.6). We next tested whether targeting a strong transcriptional activator, Gal4-p65, to our transgene pushes the chromatin to a more permissive state, allowing Cas9 editing to occur (Figure 3.7). We found that co-treatment and pre-treatment with the Gal4-p65 activator increases target gene expression and removes the silencing mark (Figure 3.8). Our preliminary data show that pre-treatment with our targeted transcriptional activator improves Cas9 editing at some of the sgRNA sites tested (Figure 3.9 and Figure 3.10). However, co-treatment did not improve editing and showed significantly reduced editing when compared to the preteated cells (Figure 3.9). In section 3.6, we propose experiments to determine how hyperactive gene expression affects Cas9 activity. Future work will include further characterization of the effect of transcriptional activators and chromatin-modifying drugs on Cas9 editing.

Finally, we found that delivery of Cas9 complexed with a degradation-resistent synthetic sgRNA greatly increased editing in silenced chromatin, even over editing at the active state. These early results are very promising and our future work will determine whether this approach will provide consistent improvement of editing across many target sites. While our data show editing improvement, we cannot conclude what is responsible for the increased editing. We hypothesize that several factors contribute to Cas9 editing efficiency in

116

chromatin. Our data suggest that heterochromatin inhibits, but does block, Cas9 editing. We propose that subtle factors which impact Cas9 activity, such as RNP stability, time, and sgRNA binding efficiency, are amplified when the Cas9 target site is occluded. This would explain how tightly clustered target sites show different levels of inhibition by heterochromatin (Figure 2.3). We hypothesize that sites that are not sensitive to heterochromatin have increased stability and binding affinity. Future work will involve computational prediction of gRNA stability to identify correlation with sensitivity to chromatin state.

Taken together, the work presented in chapter 2 and chapter 3 advances the field of genetic engineering by providing methods for improving Cas9 targeting in difficult-to-access sites in heterochromatin.

6.2 Quorum Sensing

Quorum sensing networks have been widely implemented in engineered circuits as genetic wires that use small molecules, commonly HSLs, to signal information.[92] The full potential of these networks has been hampered by crosstalk among them. To overcome this limitation, we must identify and characterize orthogonal networks. Nature has provided us with over 100 quorum sensing networks, but only four have been extensively used in synthetic biology. A series of recent publications has greatly expanding the number of receiver devices available to genetic engineers: Scott et al. and Chen et al. built and characterized RpaR, TraR, and CinR devices;[87,88] Tashiro et al. mutated the promiscuous LuxR receiver to respond to a single HSL, either 3-oxo-C6-HSL or 3-oxo-C8-HSL;[102] Grant et al. reduced off-target binding of the LasR regulator to the LuxR binding domain.[103] Our work to build a library of senders with narrow HSL profiles complements these efforts and enables researchers to build more complex networks with minimal crosstalk. Our data presentation allows for direct comparison of sender devices based on parameters such as sensitivity, total output, and rate of induction.

All but one of the synthases we tested induced our LuxR receiver device, including LasI and RpaI. Previous studies have demonstrated the orthogonality of LasI/LuxR and RpaI/LuxR and implemented circuits without crosstalk.[101,149] We hypothesize that quorum sensing networks do not need to be completely orthogonal in order to be functionally orthogonal. In our study, LuxR was insensitive to LasI and RpaI at low concentrations. Synthase expression could be controlled by using weak promoters and ribosome binding sites and by limiting HSL accumulation with lactonases to avoid crosstalk in a circuit. In addition to these two synthases, AubI, CerI, and SinI induced LuxR at high concentrations but not at lower concentrations. We propose these senders as potential functionally-orthogonal synthases to the LuxR receiver.

Our work also demonstrates the importance of testing quorum sensing networks in the chassis of interest. Published mass spectrometry data show that LasI produces a different HSL profile in *Escherichia coli* than in its native organism *Pseudomonas aeruginosa*.[189,191] Furthermore, the RpaI/LuxR orthogonality observed by Scott et al. can also be explained by having using different species for our experiments.[101] Scott et al. used *Salmonella typhimurium* whereas we used *E. coli* BL21. As discussed above, the abundance and diversity of acyl carrier proteins and, in the case of RpaI, coenzyme A species will likely determine the HSL expression profile for each sender. It is possible that RpaI produces different ratios of HSLs in *S. typhimurium* and *E. coli* BL21. This can be determined using mass spectrometry[189–191]

In addition to expanding the set of functionally orthogonal quorum sensing networks, our work also allows for greater diversity of device behaviors. We observed a wide range of sensitivities and production levels in the nine of ten synthases that induced the LuxR receiver. By reporting their Hill function parameters, we allow researchers to directly compare senders and select those which fit the profile for their application, enabling the design of more complex circuits. These parameters can be incorporated into a computational model of a circuit in order to determine the possible circuit behaviors and inform identification of networks to test.

In addition to synthetic biology and engineering, our library of senders has applications in medicine. *P. aeruginsa* has been found in the microenvironment of certain breast cancers.[197] Zhao et al. and Balhouse et al. found that the major HSL produced by the Las quorum sensing network in *P. auruginosa* can inhibit tumor growth.[197,198] Researchers can express additional senders in the BSL1 *E. coli* and screen for tumor suppression activity.

Complete characterization of this library will require testing of how each sender induces our library of receivers as well as measuring its HSL profile in *E. coli* BL21 by mass spectrometry. As described in chapter 5, receiver devices are under construction and we are gathering induction data for more sender/receiver pairs. Mass spectrometry will confirm whether our senders have narrow HSL profiles and are capable of selectively inducing a single receiver device. In tandem with the newly published selective receivers, our work will significantly expand the number and diversity of engineering-ready sender and receiver devices.

References

(*48*)   Jinek, M., Chylinski, K., Fonfara, I., Hauer, M., Doudna, J. a., and Charpentier, E., (2012). A Programmable Dual-RNA-Guided DNA Endonuclease in Adaptive Bacterial Immunity. *Science 337*, 816–821, DOI: 10.1126/science.1225829.

(*49*)   Gilbert, L. A., Larson, M. H., Morsut, L., Liu, Z., Brar, G. A., Torres, S. E., Stern-Ginossar, N., Brandman, O., Whitehead, E. H., Doudna, J. A., Lim, W. A., Weissman, J. S., and Qi, L. S., (2013). CRISPR-Mediated Modular RNA-Guided Regulation of Transcription in Eukaryotes. *Cell 154*, 442–451, DOI: 10.1016/j.cell.2013.06.044.

(*50*)   Tiwari, V. K., Cope, L., McGarvey, K. M., Ohm, J. E., and Baylin, S. B., (2008). A novel 6C assay uncovers Polycomb-mediated higher order chromatin conformations. *Genome Research 18*, 1171–1179, DOI: 10.1101/gr.073452.107.

(*51*)   Bell, O., Tiwari, V. K., Thomä, N. H., and Schübeler, D., (2011). Determinants and dynamics of genome accessibility. *Nature Reviews Genetics 12*, 554–564, DOI: 10.1038/nrg3017.

(*52*)   Aoto, T., Saitoh, N., Sakamoto, Y., Watanabe, S., and Nakao, M., (2008). Polycomb group protein-associated chromatin is reproduced in post-mitotic G 1 phase and is required for S phase progression. *Journal of Biological Chemistry 283*, 18905–18915, DOI: 10.1074/jbc.M709322200.

(*54*)   Daer, R. M., Cutts, J. P., Brafman, D. A., and Haynes, K. A., (2017). The Impact of Chromatin Dynamics on Cas9-Mediated Genome Editing in Human Cells. *ACS Synthetic Biology 6*, 428–438, DOI: 10.1021/acssynbio.5b00299.

(*61*)   Radzisheuskaya, A., Shlyueva, D., Müller, I., and Helin, K., (2016). Optimizing sgRNA position markedly improves the efficiency of CRISPR/dCas9-mediated transcriptional repression. *Nucleic Acids Research 44*, DOI: 10.1093/nar/gkw583.

(*69*)   Chen, X., Rinsma, M., Janssen, J. M., Liu, J., Maggio, I., and Gonçalves, M. A., (2016). Probing the impact of chromatin conformation on genome editing tools. *Nucleic Acids Research 44*, 6482–6492, DOI: 10.1093/nar/gkw524.

(*87*)   Chen, Y., Kim, J. K., Hirning, A. J., and Bennett, Matthew, R., (2016). Emergent genetic oscillations in a synthetic microbial consortium. *Science 349*, 986–989, DOI: 10.1126/science.aaa3794.Emergent.

(*88*)   Scott, S. R., and Hasty, J., (2016). Quorum Sensing Communication Modules for Microbial Consortia. *ACS Synthetic Biology 5*, 969–977, DOI: 10.1021/acssynbio.5b00286.

(*92*)   Davis, R. M., Muller, R. Y., and Haynes, K. A., (2015). Can the Natural Diversity of Quorum-Sensing Advance Synthetic Biology? *Frontiers in Bioengineering and Biotechnology 3*, 1–10, DOI: 10.3389/fbioe.2015.00030.

(*101*)   Scott, S. R., Din, M. O., Bittihn, P., Xiong, L., Tsimring, L. S., and Hasty, J., (2017). A stabilized microbial ecosystem of self-limiting bacteria using synthetic quorum-regulated lysis. *Nature Microbiology 2*, 17083, DOI: 10.1038/nmicrobiol.2017.83.

(*102*)   Tashiro, Y., Kimura, Y., Furubayashi, M., Tanaka, A., Terakubo, K., Saito, K., Kawai-Noma, S., and Umeno, D., (2016). Directed evolution of the autoinducer selectivity of Vibrio fischeri LuxR. *The Journal of General and Applied Microbiology 247*, 1–8, DOI: 10.2323/jgam.2016.04.005.

(*103*) Grant, P. K., Dalchau, N., Brown, J. R., Federici, F., Rudge, T. J., Yordanov, B., Patange, O., Phillips, A., and Haseloff, J., (2016). Orthogonal intercellular signaling for programmed spatial behavior. *Molecular Systems Biology 12*, 849–849, DOI: 10.15252/msb.20156590.

(*149*) Balagaddé, F. K., Song, H., Ozaki, J., Collins, C. H., Barnet, M., Arnold, F. H., Quake, S. R., and You, L., (2008). A synthetic Escherichia coli predator-prey ecosystem. *Molecular systems biology 4*, DOI: 10.1038/msb.2008.24.

(*189*) Gould, T. a., Herman, J., Krank, J., Murphy, R. C., and Churchill, M. E. a., (2006). Specificity of Acyl-Homoserine Lactone Synthases Examined by Mass Spectrometry. *Journal of Bacteriology 188*, 773–783, DOI: 10.1128/JB.188.2.773-783.2006.

(*190*) Beck von Bodman, S., and Farrand, S. K., (1995). Capsular polysaccharide biosynthesis and pathogenicity in Erwinia stewartii require induction by an N-acylhomoserine lactone autoinducer. *Journal of bacteriology 177*, 5000–8.

(*191*) Ortori, C. A., Dubern, J. F., Chhabra, S. R., Cámara, M., Hardie, K., Williams, P., and Barrett, D. A., (2011). Simultaneous quantitative profiling of N-acyl-l-homoserine lactone and 2-alkyl-4(1H)-quinolone families of quorum-sensing signaling molecules using LC-MS/MS. *Analytical and Bioanalytical Chemistry 399*, 839–850, DOI: 10.1007/s00216-010-4341-0.

(*196*) Chen, B., Gilbert, L. A., Cimini, B. A., Schnitzbauer, J., Zhang, W., Li, G.-w., Park, J., Blackburn, E. H., Weissman, J. S., Qi, L. S., and Huang, B., (2013). Dynamic Imaging of Genomic Loci in Living Human Cells by an Optimized CRISPR/Cas System. *Cell 155*, 1479–1491, DOI: 10.1016/j.cell.2013.12.001.

(*197*) Balhouse, B. N., Patterson, L., Schmelz, E. M., Slade, D. J., and Verbridge, S. S., (2017). N-(3-oxododecanoyl)-L-homoserine lactone interactions in the breast tumor microenvironment: Implications for breast cancer viability and proliferation in vitro. *PLOS ONE 12*, ed. by Singh, P. K., DOI: 10.1371/journal.pone.0180372.

(*198*) Zhao, G., Neely, A. M., Schwarzer, C., Lu, H., Whitt, A. G., Stivers, N. S., Burlison, J. A., White, C., Machen, T. E., and Li, C., (2016). N-(3-oxo-acyl) homoserine lactone inhibits tumor growth independent of Bcl-2 proteins. *Oncotarget 7*, 5924–42, DOI: 10.18632/oncotarget.6827.

REFERENCES

(*1*)   Flemming, W., (1879). Beitrage zur kenntnis der zelle und ihrer lebenserscheinungen I. *Archiv für mikroskopische Anatomie 16*, 302–436.

(*2*)   Paweletz, N., (2001). Walther Flemming: pioneer of mitosis research. *Nature reviews. Molecular cell biology 2*, 72–75, DOI: 10.1038/35048077.

(*3*)   Schuettengruber, B., Bourbon, H. M., Di Croce, L., and Cavalli, G., (2017). Genome regulation by Polycomb and Trithorax: 70 years and counting. *Cell 171*, 34–57, DOI: 10.1016/j.cell.2017.08.002.

(*4*)   Lewis, P., (1947). New mutants report. *Drosophila Information Service 21*, 69.

(*5*)   Lewis, E., (1978). A gene complex controlling segmentation in Drosophila. *Nature 276*, 565–570.

(*6*)   Ingham, P. W., (1983). Differential expression of bithorax complex genes in the absence of the extra sex combs and trithorax genes. *Nature 306*, 591–593, DOI: 10.1038/306591a0.

(*7*)   Ingham, P. W., (1985). Genetic control of the spatial pattern of selector gene expression in Drosophila. *Cold Spring Harbor Symposia on Quantitative Biology 50*, 201–208.

(*8*)   Struhl, G., and Akam, M., (1985). Altered distributions of Ultrabithorax transcripts in extra sex combs mutant embryos of Drosophila. *The EMBO journal 4*, 3259–3264.

(*9*)   Kennison, J. A., and Tamkun, J. W., (1988). Dosage-dependent modifiers of polycomb and antennapedia mutations in Drosophila. *Proceedings of the National Academy of Sciences 85*, 8136–8140, DOI: 10.1073/pnas.85.21.8136.

(*10*)   Ingham, P. W., (1985). A clonal analysis of the requirement for the trithorax gene in the diversification of segments in Drosophila. *Journal of embryology and experimental morphology 89*, 349–365.

(*11*)   van der Lugt, N. M., Domen, J., Linders, K., van Roon, M., Robanus-Maandag, E., te Riele, H., van der Valk, M., Deschamps, J., Sofroniew, M., and van Lohuizen, M., (1994). Posterior transformation, neurological abnormalities, and severe hematopoietic defects in mice with a targeted deletion of the bmi-1 proto-oncogene. *Genes & Development 8*, 757–69.

(*12*)   Coré, N., Bel, S., Gaunt, S. J., Aurrand-Lions, M., Pearce, J., Fisher, A., and Djabali, M., (1997). Altered cellular proliferation and mesoderm patterning in Polycomb-M33-deficient mice. *Development 124*, 721–729, DOI: 10.1038/374724a0.

(*13*)   Jacobs, J. J., Kieboom, K., Marino, S., DePinho, R. A., and van Lohuizen, M., (1999). The oncogene and Polycomb-group gene bmi-1 regulates cell proliferation and senescence through the ink4a locus. *Nature 397*, 164–168, DOI: 10.1038/16476.

(*14*)   van Lohuizen, M., Frasch, M., Wientjens, E., and Berns, A., (1991). Sequence similarity between the mammalian bmi-1 proto-oncogene and the Drosophila regulatory genes Psc and Su(z)2. *Nature 353*, 353–355, DOI: 10.1038/353353a0.

(*15*)   Djabali, M., Selleri, L., Parry, P., Bower, M., Young, B. D., and Evans, G. a., (1992). A trithorax-like gene is interrupted by chromosome 11q23 translocations in acute leukaemias. *Nature genetics 2*, 113–118, DOI: 10.1038/ng1092-113.

(*16*)   Jacobs, J. L., Scheijen, B., Voncken, J. W., Kieboom, K., Berns, A., and van Lohuizen, M., (1999). Bmi-1 collaborates with c-Mycin tumorigenesis by inhibiting c-Myc-induced apoptosis via INK4a/ARF. *Genes {&} Development*, 2678–2690, DOI: 10.1101/gad.13.20.2678.

(*17*)   Cao, R., Wang, L., Wang, H., Xia, L., Erdjument-Bromage, H., Tempst, P., Jones, R. S., and Zhang, Y., (2002). Role of histone H3 lysine 27 methylation in Polycomb-group silencing. *Science 298*, 1039–1043, DOI: 10.1126/science.1076997.

(*18*)   Czermin, B., Melfi, R., McCabe, D., Seitz, V., Imhof, A., and Pirrotta, V., (2002). Drosophila enhancer of Zeste/ESC complexes have a histone H3 methyltransferase activity that marks chromosomal Polycomb sites. *Cell 111*, 185–196, DOI: 10.1016/S0092-8674(02)00975-3.

(*19*)   Kuzmichev, A., Nishioka, K., Erdjument-Bromage, H., Tempst, P., and Reinberg, D., (2002). Histone methyltransferase activity associated with a human multiprotein complex containing the Enhancer of Zeste protein. *Genes & Development 16*, 2893–2905, DOI: 10.1101/gad.1035902.

(*20*)   Müller, J., Hart, C. M., Francis, N. J., Vargas, M. L., Sengupta, A., Wild, B., Miller, E. L., O'Connor, M. B., Kingston, R. E., and Simon, J. A., (2002). Histone methyl-transferase activity of a Drosophila Polycomb group repressor complex. *Cell 111*, 197–208, DOI: 10.1016/S0092-8674(02)00976-5.

(*21*)   Fischle, W., Wang, Y., Jacobs, S. A., Kim, Y., Allis, C. D., and Khorasanizadeh, S., (2003). Molecular basis for the discrimination of repressive methyl-lysine marks in histone H3 by Polycomb and HP1 chromodomains. *Genes & Development 17*, 1870–1881, DOI: 10.1101/gad.1110503.

(*22*)   Cooper, S., Dienstbier, M., Hassan, R., Schermelleh, L., Sharif, J., Blackledge, N. P., De Marco, V., Elderkin, S., Koseki, H., Klose, R., Heger, A., and Brockdorff, N., (2014). Targeting Polycomb to pericentric heterochromatin in embryonic stem cells reveals a role for H2AK119u1 in PRC2 recruitment. *Cell Reports 7*, 1456–1470, DOI: 10.1016/j.celrep.2014.04.012.

(*23*)   Blackledge, N. P., Rose, N. R., and Klose, R. J., (2015). Targeting Polycomb systems to regulate gene expression: modifications to a complex story. *Nature Reviews Molecular Cell Biology 16*, 643–649, DOI: 10.1038/nrm4067.

(*24*)   Schaaf, C. A., Misulovin, Z., Gause, M., Koenig, A., Gohara, D. W., Watson, A., and Dorsett, D., (2013). Cohesin and Polycomb proteins functionally interact to control transcription at silenced and active genes. *PLoS Genetics 9*, DOI: 10.1371/journal.pgen.1003560.

(*25*)   Loubiere, V., Delest, A., Thomas, A., Bonev, B., Schuettengruber, B., Sati, S., Martinez, A.-M., and Cavalli, G., (2016). Coordinate redeployment of PRC1 proteins suppresses tumor formation during Drosophila development. *Nature Genetics 48*, 1436–1442, DOI: 10.1038/ng.3671.

(*26*)   Margueron, R., Li, G., Sarma, K., Blais, A., Zavadil, J., Woodcock, C. L., Dynlacht, B. D., and Reinberg, D., (2008). Ezh1 and Ezh2 maintain repressive chromatin through different mechanisms. *Molecular Cell 32*, 503–518, DOI: 10.1016/j.molcel.2008.11.004.

(*27*)   Osborne, C. S., Chakalova, L., Brown, K. E., Carter, D., Horton, A., Debrand, E., Goyenechea, B., Mitchell, J. A., Lopes, S., Reik, W., and Fraser, P., (2004). Active genes dynamically colocalize to shared sites of ongoing transcription. *Nature Genetics 36*, 1065–1071, DOI: 10.1038/ng1423.

(*28*)   Simonis, M., Klous, P., Splinter, E., Moshkin, Y., Willemsen, R., de Wit, E., van Steensel, B., and de Laat, W., (2006). Nuclear organization of active and inactive chromatin domains uncovered by chromosome conformation capture–on-chip (4C). *Nature Genetics 38*, 1348–1354, DOI: 10.1038/ng1896.

(*29*)   Buchenau, P., Hodgson, J., Strutt, H., and Arndt-Jovin, D. J., (1998). The distribution of Polycomb-group proteins during cell division and development in Drosophila embryos- Impact on models for silencing. *Cell 141*, 469–481, DOI: 10.1083/jcb.141.2.469.

(*30*)   Saurin, A. J., Shiels, C., Williamson, J., Satijn, D. P., Otte, A. P., Sheer, D., and Freemont, P. S., (1998). The human Polycomb group complex associates with pericentromeric heterochromatin to form a novel nuclear domain. *Journal of Cell Biology 142*, 887–898, DOI: 10.1083/jcb.142.4.887.

(*31*)   Denholtz, M., Bonora, G., Chronis, C., Splinter, E., de Laat, W., Ernst, J., Pellegrini, M., and Plath, K., (2013). Long-range chromatin contacts in embryonic stem cells reveal a role for pluripotency factors and Polycomb proteins in genome organization. *Cell Stem Cell 13*, ed. by Nixon, A. E., 602–616, DOI: 10.1016/j.stem.2013.08.013.

(*32*)   Vieux-Rochas, M., Fabre, P. J., Leleu, M., Duboule, D., and Noordermeer, D., (2015). Clustering of mammalian Hox genes with other H3K27me3 targets within an active nuclear domain. *Proceedings of the National Academy of Sciences 112*, 4672–4677, DOI: 10.1073/pnas.1504783112.

(*33*) Wijchers, P. J., Krijger, P. H., Geeven, G., Zhu, Y., Denker, A., Verstegen, M. J., Valdes-Quezada, C., Vermeulen, C., Janssen, M., Teunissen, H., Anink-Groenen, L. C., Verschure, P. J., and de Laat, W., (2016). Cause and consequence of tethering a SubTAD to different nuclear compartments. *Molecular Cell 61*, 461−473, DOI: 10.1016/j.molcel.2016.01.001.

(*34*) Entrevan, M., Schuettengruber, B., and Cavalli, G., (2016). Regulation of genome architecture and function by Polycomb proteins. *Trends in Cell Biology 26*, 511−525, DOI: 10.1016/j.tcb.2016.04.009.

(*35*) Wani, A. H., Boettiger, A. N., Schorderet, P., Ergun, A., Münger, C., Sadreyev, R. I., Zhuang, X., Kingston, R. E., and Francis, N. J., (2016). Chromatin topology is coupled to Polycomb group protein subnuclear organization. *Nature Communications 7*, 10291, DOI: 10.1038/ncomms10291.

(*36*) Schoenfelder, S., Sugar, R., Dimond, A., Javierre, B.-m., Armstrong, H., Mifsud, B., Dimitrova, E., Matheson, L., Tavares-Cadete, F., Furlan-Magaril, M., Segonds-Pichon, A., Jurkowski, W., Wingett, S. W., Tabbada, K., Andrews, S., Herman, B., LeProust, E., Osborne, C. S., Koseki, H., Fraser, P., Luscombe, N. M., and Elderkin, S., (2015). Polycomb repressive complex PRC1 spatially constrains the mouse embryonic stem cell genome. *Nature Genetics 47*, 1179−1186, DOI: 10.1038/ng.3393.

(*37*) Kundu, S., Ji, F., Sunwoo, H., Jain, G., Lee, J. T., Sadreyev, R. I., Dekker, J., and Kingston, R. E., (2017). Polycomb Repressive Complex 1 generates discrete compacted domains that change during differentiation. *Molecular Cell 65*, 432−446.e5, DOI: 10.1016/j.molcel.2017.01.009.

(*38*) Isono, K., Endo, T. A., Ku, M., Yamada, D., Suzuki, R., Sharif, J., Ishikura, T., Toyoda, T., Bernstein, B. E., and Koseki, H., (2013). SAM domain polymerization links subnuclear clustering of PRC1 to gene silencing. *Developmental Cell 26*, 565−577, DOI: 10.1016/j.devcel.2013.08.016.

(*39*) Simon, J., Chiang, A., Bender, W., Shimell, M. J., and O'Connor, M., Elements of the Drosophila bithorax complex that mediate repression by Polycomb group products., 1993, DOI: 10.1006/dbio.1993.1174.

(*40*) Fauvarque, M.-o., and Dura, J.-m., (1993). Polyhomeotic regulatory sequences induce developmental regulator- dependent variegation and targeted P- element insertions in Drosophila. *Genes & Development 7*, 1508−1520.

(*41*) Müller, J., and Bienz, M., (1991). Long range repression conferring boundaries of Ultrabithorax expression in the Drosophila embryo. *The EMBO journal 10*, 3147−3155.

(*42*) Simon, J. A., and Kingston, R. E., (2013). Occupying chromatin: Polycomb mechanisms for getting to genomic targets, stopping transcriptional traffic, and staying put. *Molecular Cell 49*, 808−824, DOI: 10.1016/j.molcel.2013.02.013.

(*43*)   Plath, K., Fang, J., Mlynarczyk-Evans, S., Cao, R., Worringer, K., Wang, H., de la Cruz, C., Otte, A., Panning, B., and Zhang, Y., (2003). Role of histone H3 lysine 27 methylation in X inactivation. *Science 300*, 131–135, DOI: 10.1126/science.1084274.

(*44*)   Mendenhall, E. M., Koche, R. P., Truong, T., Zhou, V. W., Issac, B., Chi, A. S., Ku, M., and Bernstein, B. E., (2010). GC-rich sequence elements recruit PRC2 in mammalian ES cells. *PLoS Genetics 6*, ed. by Madhani, H. D., e1001244, DOI: 10.1371/journal.pgen.1001244.

(*45*)   Blackledge, N. P., Farcas, A. M., Kondo, T., King, H. W., McGouran, J. F., Hanssen, L. L., Ito, S., Cooper, S., Kondo, K., Koseki, Y., Ishikura, T., Long, H. K., Sheahan, T. W., Brockdorff, N., Kessler, B. M., Koseki, H., and Klose, R. J., (2014). Variant PRC1 complex-dependent H2A ubiquitylation drives PRC2 recruitment and Polycomb domain formation. *Cell 157*, 1445–1459, DOI: 10.1016/j.cell.2014.05.004.

(*46*)   Illingworth, R. S., Moffat, M., Mann, A. R., Read, D., Hunter, C. J., Pradeepa, M. M., Adams, I. R., and Bickmore, W. A., (2015). The E3 ubiquitin ligase activity of RING1B is not essential for early mouse development. *Genes & Development 29*, 1897–1902, DOI: 10.1101/gad.268151.115.

(*47*)   Pengelly, A. R., Kalb, R., Finkl, K., and Müller, J., (2015). Transcriptional repression by PRC1 in the absence of H2A monoubiquitylation. *Genes & Development 29*, 1487–1492, DOI: 10.1101/gad.265439.115.

(*48*)   Jinek, M., Chylinski, K., Fonfara, I., Hauer, M., Doudna, J. a., and Charpentier, E., (2012). A Programmable Dual-RNA-Guided DNA Endonuclease in Adaptive Bacterial Immunity. *Science 337*, 816–821, DOI: 10.1126/science.1225829.

(*49*)   Gilbert, L. A., Larson, M. H., Morsut, L., Liu, Z., Brar, G. A., Torres, S. E., Stern-Ginossar, N., Brandman, O., Whitehead, E. H., Doudna, J. A., Lim, W. A., Weissman, J. S., and Qi, L. S., (2013). CRISPR-Mediated Modular RNA-Guided Regulation of Transcription in Eukaryotes. *Cell 154*, 442–451, DOI: 10.1016/j.cell.2013.06.044.

(*50*)   Tiwari, V. K., Cope, L., McGarvey, K. M., Ohm, J. E., and Baylin, S. B., (2008). A novel 6C assay uncovers Polycomb-mediated higher order chromatin conformations. *Genome Research 18*, 1171–1179, DOI: 10.1101/gr.073452.107.

(*51*)   Bell, O., Tiwari, V. K., Thomä, N. H., and Schübeler, D., (2011). Determinants and dynamics of genome accessibility. *Nature Reviews Genetics 12*, 554–564, DOI: 10.1038/nrg3017.

(*52*)   Aoto, T., Saitoh, N., Sakamoto, Y., Watanabe, S., and Nakao, M., (2008). Polycomb group protein-associated chromatin is reproduced in post-mitotic G 1 phase and is required for S phase progression. *Journal of Biological Chemistry 283*, 18905–18915, DOI: 10.1074/jbc.M709322200.

(*53*)   Hansen, K. H., Bracken, A. P., Pasini, D., Dietrich, N., Gehani, S. S., Monrad, A., Rappsilber, J., Lerdrup, M., and Helin, K., (2008). A model for transmission of the H3K27me3 epigenetic mark. *Nature Cell Biology 10*, 1291–1300, DOI: 10.1038/ncb1787.

(*54*)   Daer, R. M., Cutts, J. P., Brafman, D. A., and Haynes, K. A., (2017). The Impact of Chromatin Dynamics on Cas9-Mediated Genome Editing in Human Cells. *ACS Synthetic Biology 6*, 428–438, DOI: 10.1021/acssynbio.5b00299.

(*55*)   Wu, X., Scott, D. A., Kriz, A. J., Chiu, A. C., Hsu, P. D., Dadon, D. B., Cheng, A. W., Trevino, A. E., Konermann, S., Chen, S., Jaenisch, R., Zhang, F., and Sharp, P. A., (2014). Genome-wide binding of the CRISPR endonuclease Cas9 in mammalian cells. *Nature Biotechnology 32*, 670–676, DOI: 10.1038/nbt.2889.

(*56*)   Kuscu, C., Arslan, S., Singh, R., Thorpe, J., and Adli, M., (2014). Genome-wide analysis reveals characteristics of off-target sites bound by the Cas9 endonuclease. *Nature Biotechnology 32*, 677–683, DOI: 10.1038/nbt.2916.

(*57*)   O'Geen, H., Henry, I. M., Bhakta, M. S., Meckler, J. F., and Segal, D. J., (2015). A genome-wide analysis of Cas9 binding specificity using ChIP-seq and targeted sequence capture. *Nucleic Acids Research 43*, 3389–3404, DOI: 10.1093/nar/gkv137.

(*58*)   Singh, R., Kuscu, C., Quinlan, A., Qi, Y., and Adli, M., (2015). Cas9-chromatin binding information enables more accurate CRISPR off-target prediction. *Nucleic Acids Research 43*, e118, DOI: 10.1093/nar/gkv575.

(*59*)   Horlbeck, M. A., Witkowsky, L. B., Guglielmi, B., Replogle, J. M., Gilbert, L. A., Villalta, J. E., Torigoe, S. E., Tjian, R., and Weissman, J. S., (2016). Nucleosomes impede cas9 access to DNA in vivo and in vitro. *eLife 5*, 1–21, DOI: 10.7554/eLife.12677.

(*60*)   Horlbeck, M. A., Gilbert, L. A., Villalta, J. E., Adamson, B., Pak, R. A., Chen, Y., Fields, A. P., Park, C. Y., Corn, J. E., Kampmann, M., and Weissman, J. S., (2016). Compact and highly active next-generation libraries for CRISPR-mediated gene repression and activation. *eLife 5*, 1–20, DOI: 10.7554/eLife.19760.

(*61*)   Radzisheuskaya, A., Shlyueva, D., Müller, I., and Helin, K., (2016). Optimizing sgRNA position markedly improves the efficiency of CRISPR/dCas9-mediated transcriptional repression. *Nucleic Acids Research 44*, DOI: 10.1093/nar/gkw583.

(*62*)   Smith, J. D., Suresh, S., Schlecht, U., Wu, M., Wagih, O., Peltz, G., Davis, R. W., Steinmetz, L. M., Parts, L., and St.Onge, R. P., (2016). Quantitative CRISPR interference screens in yeast identify chemical-genetic interactions and new rules for guide RNA design. *Genome Biology 17*, 45, DOI: 10.1186/s13059-016-0900-9.

(*63*)   Chari, R., Mali, P., Moosburner, M., and Church, G. M., (2015). Unraveling CRISPR-Cas9 genome engineering parameters via a library-on-library approach. *Nature Methods 12*, 823–826, DOI: 10.1038/nmeth.3473.

(*64*)   Jensen, K. T., Fløe, L., Petersen, T. S., Huang, J., Xu, F., Bolund, L., Luo, Y., and Lin, L., (2017). Chromatin accessibility and guide sequence secondary structure affect CRISPR-Cas9 gene editing efficiency. *FEBS Letters 591*, 1892–1901, DOI: 10.1002/1873-3468.12707.

(*65*)   Hinz, J. M., Laughery, M. F., and Wyrick, J. J., (2015). Nucleosomes Inhibit Cas9 Endonuclease Activity in Vitro. *Biochemistry 54*, 7063–7066, DOI: 10.1021/acs.biochem.5b01108.

(*66*)   Isaac, R. S., Jiang, F., Doudna, J. A., Lim, W. A., Narlikar, G. J., and Almeida, R., (2016). Nucleosome breathing and remodeling constrain CRISPR-Cas9 function. *eLife 5*, 1–14, DOI: 10.7554/eLife.13450.

(*67*)   Anderson, J., and Widom, J., (2000). Sequence and position-dependence of the equilibrium accessibility of nucleosomal DNA target sites 1 1Edited by T. Richmond. *Journal of Molecular Biology 296*, 979–987, DOI: 10.1006/jmbi.2000.3531.

(*68*)   Partensky, P. D., and Narlikar, G. J., (2009). Chromatin Remodelers Act Globally, Sequence Positions Nucleosomes Locally. *Journal of Molecular Biology 391*, 12–25, DOI: 10.1016/j.jmb.2009.04.085.

(*69*)   Chen, X., Rinsma, M., Janssen, J. M., Liu, J., Maggio, I., and Gonçalves, M. A., (2016). Probing the impact of chromatin conformation on genome editing tools. *Nucleic Acids Research 44*, 6482–6492, DOI: 10.1093/nar/gkw524.

(*70*)   Yang, L., Guell, M., Byrne, S., Yang, J. L., De Los Angeles, A., Mali, P., Aach, J., Kim-Kiselak, C., Briggs, A. W., Rios, X., Huang, P. Y., Daley, G., and Church, G., (2013). Optimization of scarless human stem cell genome editing. *Nucleic Acids Research 41*, 9049–9061, DOI: 10.1093/nar/gkt555.

(*71*)   Perez-Pinera, P., Kocak, D. D., Vockley, C. M., Adler, A. F., Kabadi, A. M., Polstein, L. R., Thakore, P. I., Glass, K. A., Ousterout, D. G., Leong, K. W., Guilak, F., Crawford, G. E., Reddy, T. E., Gersbach, C. A., Kabadi, M., Polstein, L. R., Thakore, P. I., Glass, K. A., Ousterout, D. G., Leong, K. W., Guilak, F., Crawford, G. E., Reddy, T. E., and Gersbach, C. A., (2013). RNA-guided gene activation by CRISPR-Cas9–based transcription factors. *Nature Methods 10*, 973–976, DOI: 10.1038/nmeth.2600.

(*72*)   Polstein, L. R., Perez-pinera, P., Kocak, D. D., Vockley, M., Bledsoe, P., Song, L., Safi, A., Crawford, G. E., Reddy, T. E., Gersbach, C. a., Carolina, N., and Surgery, O., (2015). Genome-wide specificity of DNA binding , gene regulation , and chromatin remodeling by TALE- and CRISPR / Cas9-based transcriptional activators. *Genome research 25*, 1158–1169, DOI: 10.1101/gr.179044.114..

(*73*)   Knight, S. C., Xie, L., Deng, W., Guglielmi, B., Witkowsky, L. B., Bosanac, L., Zhang, E. T., El Beheiry, M., Masson, J.-B., Dahan, M., Liu, Z., Doudna, J. A., and Tjian, R., (2015). Dynamics of CRISPR-Cas9 genome interrogation in living cells. *Science 350*, 823–826, DOI: 10.1126/science.aac6572.

(*74*)   Hsu, P. D., Scott, D. a., Weinstein, J. a., Ran, F. A., Konermann, S., Agarwala, V., Li, Y., Fine, E. J., Wu, X., Shalem, O., Cradick, T. J., Marraffini, L. a., Bao, G., and Zhang, F., (2013). DNA targeting specificity of RNA-guided Cas9 nucleases. *Nature Biotechnology 31*, 827–832, DOI: 10.1038/nbt.2647.

(*75*)   Ruby, E. G., and Nealson, K. H., (1976). Symbiotic Association of Photobacterium Fischeri with the Marine Luminous Fish Monocentris Japonica: A Model Of Symbiosis Based on Bacterial Studies. *The Biological Bulletin 151*, 574–586, DOI: 10.2307/1540507.

(*76*)   Eberl, L., (1999). N-acyl homoserinelactone-mediated gene regulation in gram-negative bacteria. *Systematic and applied microbiology 22*, 493–506, DOI: 10.1016/S0723-2020(99)80001-0.

(*77*)   Fuqua, C., Winans, S. C., and Greenberg, E. P., (1996). Census and consensus in bacterial ecosystems: the LuxR-LuxI family of quorum-sensing transcriptional regulators. *Annual review of microbiology 50*, 727–51, DOI: 10.1146/annurev.micro.50.1.727.

(*78*)   Williams, P., Winzer, K., Chan, W. C., and Camara, M., (2007). Look who's talking: communication and quorum sensing in the bacterial world. *Philosophical Transactions of the Royal Society B: Biological Sciences 362*, 1119–1134, DOI: 10.1098/rstb.2007.2039.

(*79*)   Dickschat, J. S., (2010). Quorum sensing and bacterial biofilms. *Natural product reports 27*, 343–69, DOI: 10.1039/b804469b.

(*80*)   Case, R. J., Labbate, M., and Kjelleberg, S., (2008). AHL-driven quorum-sensing circuits: their frequency and function among the Proteobacteria. *The ISME journal 2*, 345–9, DOI: 10.1038/ismej.2008.13.

(*81*)   Nasuno, E., Kimura, N., Fujita, M. J., Nakatsu, C. H., Kamagata, Y., and Hanada, S., (2012). Phylogenetically Novel LuxI/LuxR-Type Quorum Sensing Systems Isolated Using a Metagenomic Approach. *Applied and Environmental Microbiology 78*, 8067–8074, DOI: 10.1128/AEM.01442-12.

(*82*)   Engebrecht, J., and Silverman, M., (1984). Identification of genes and gene products necessary for bacterial bioluminescence. *Proceedings of the National Academy of Sciences of the United States of America 81*, 4154–8.

(*83*)   Kaplan, H. B., and Greenberg, E. P., (1987). Overproduction and purification of the luxR gene product: Transcriptional activator of the Vibrio fischeri luminescence system. *Proceedings of the National Academy of Sciences of the United States of America 84*, 6639–43.

(*84*)   von Bodman, S., Ball, J., Faini, M., Herrera, C., Minogue, T., Urbanowski, M., and Stevens, A., (2003). The quorum sensing negative regulators EsaR and ExpREcc, homologues within the LuxR family, retain the ability to function as activators of

transcription. *Journal of bacteriology 185*, 7001–7007, DOI: 10.1128/JB.185.23.7001.

(*85*) Miller, M. B., and Bassler, B. L., (2001). Quorum sensing in bacteria. *Annual review of microbiology 55*, 165–99, DOI: 10.1146/annurev.micro.55.1.165.

(*86*) Gupta, A., Reizman, I. M. B., Reisch, C. R., and Prather, K. L. J., (2017). Dynamic regulation of metabolic flux in engineered bacteria using a pathway-independent quorum-sensing circuit. *Nature Biotechnology 35*, 273–279, DOI: 10.1038/nbt.3796.

(*87*) Chen, Y., Kim, J. K., Hirning, A. J., and Bennett, Matthew, R., (2016). Emergent genetic oscillations in a synthetic microbial consortium. *Science 349*, 986–989, DOI: 10.1126/science.aaa3794.Emergent.

(*88*) Scott, S. R., and Hasty, J., (2016). Quorum Sensing Communication Modules for Microbial Consortia. *ACS Synthetic Biology 5*, 969–977, DOI: 10.1021/acssynbio.5b00286.

(*89*) Daniel, R., Rubens, J. R., Sarpeshkar, R., and Lu, T. K., (2013). Synthetic analog computation in living cells. *Nature 497*, 619–23, DOI: 10.1038/nature12148.

(*90*) Tabor, J. J., Salis, H. M., Simpson, Z. B., Chevalier, A. a., Levskaya, A., Marcotte, E. M., Voigt, C. a., and Ellington, A. D., (2009). A Synthetic Genetic Edge Detection Program. *Cell 137*, 1272–1281, DOI: 10.1016/j.cell.2009.04.048.

(*91*) Brenner, K., Karig, D. K., Weiss, R., and Arnold, F. H., (2007). Engineered bidirectional communication mediates a consensus in a microbial biofilm consortium. *Proceedings of the National Academy of Sciences of the United States of America 104*, 17300–4, DOI: 10.1073/pnas.0704256104.

(*92*) Davis, R. M., Muller, R. Y., and Haynes, K. A., (2015). Can the Natural Diversity of Quorum-Sensing Advance Synthetic Biology? *Frontiers in Bioengineering and Biotechnology 3*, 1–10, DOI: 10.3389/fbioe.2015.00030.

(*93*) Hudaiberdiev, S., Choudhary, K. S., Vera Alvarez, R., Gelencsér, Z., Ligeti, B., Lamba, D., and Pongor, S., (2015). Census of solo LuxR genes in prokaryotic genomes. *Frontiers in cellular and infection microbiology 5*, 20, DOI: 10.3389/fcimb.2015.00020.

(*94*) Passos da Silva, D., Patel, H. K., González, J. F., Devescovi, G., Meng, X., Covaceuszach, S., Lamba, D., Subramoni, S., and Venturi, V., (2015). Studies on synthetic LuxR solo hybrids. *Frontiers in cellular and infection microbiology 5*, 52, DOI: 10.3389/fcimb.2015.00052.

(*95*) Lewenza, S., Visser, M. B., and Sokol, P. a., (2002). Interspecies communication between Burkholderia cepacia and Pseudomonas aeruginosa. *Canadian Journal of Microbiology 48*, 707–716, DOI: 10.1139/w02-068.

(*96*)   Chandler, J. R., Heilmann, S., Mittler, J. E., and Greenberg, E. P., (2012). Acyl-homoserine lactone-dependent eavesdropping promotes competition in a laboratory co-culture model. *The ISME journal 6*, 1–10, DOI: 10.1038/ismej.2012.69.

(*97*)   Canton, B., Labno, A., and Endy, D., (2008). Refinement and standardization of synthetic biological parts and devices. *Nature biotechnology 26*, 787–93, DOI: 10.1038/nbt1413.

(*98*)   Saeidi, N., Wong, C. K., Lo, T.-M., Nguyen, H. X., Ling, H., Leong, S. S. J., Poh, C. L., and Chang, M. W., (2011). Engineering microbes to sense and eradicate Pseudomonas aeruginosa, a human pathogen. *Molecular systems biology 7*, 1–11, DOI: 10.1038/msb.2011.55.

(*99*)   Shong, J., Huang, Y.-M., Bystroff, C., and Collins, C. H., (2013). Directed evolution of the quorum-sensing regulator EsaR for increased signal sensitivity. *ACS Chemical Biology 8*, 789–95, DOI: 10.1021/cb3006402.

(*100*)   Wu, F., Menn, D. J., and Wang, X., (2014). Article Circuits : From Unimodality to Trimodality. *Chemistry & Biology 21*, 1629–1638, DOI: 10.1016/j.chembiol.2014.10.008.

(*101*)   Scott, S. R., Din, M. O., Bittihn, P., Xiong, L., Tsimring, L. S., and Hasty, J., (2017). A stabilized microbial ecosystem of self-limiting bacteria using synthetic quorum-regulated lysis. *Nature Microbiology 2*, 17083, DOI: 10.1038/nmicrobiol.2017.83.

(*102*)   Tashiro, Y., Kimura, Y., Furubayashi, M., Tanaka, A., Terakubo, K., Saito, K., Kawai-Noma, S., and Umeno, D., (2016). Directed evolution of the autoinducer selectivity of Vibrio fischeri LuxR. *The Journal of General and Applied Microbiology 247*, 1–8, DOI: 10.2323/jgam.2016.04.005.

(*103*)   Grant, P. K., Dalchau, N., Brown, J. R., Federici, F., Rudge, T. J., Yordanov, B., Patange, O., Phillips, A., and Haseloff, J., (2016). Orthogonal intercellular signaling for programmed spatial behavior. *Molecular Systems Biology 12*, 849–849, DOI: 10.15252/msb.20156590.

(*104*)   Ran, F. A., Hsu, P. D., Lin, C.-Y., Gootenberg, J. S., Konermann, S., Trevino, A. E., Scott, D. A., Inoue, A., Matoba, S., Zhang, Y., and Zhang, F., (2013). Double Nicking by RNA-Guided CRISPR Cas9 for Enhanced Genome Editing Specificity. *Cell 154*, 1380–1389, DOI: 10.1016/j.cell.2013.08.021.

(*105*)   Hsu, P. D., Lander, E. S., and Zhang, F., (2014). Development and Applications of CRISPR-Cas9 for Genome Engineering. *Cell 157*, 1262–1278, DOI: 10.1016/j.cell.2014.05.010.

(*106*)   Sánchez-Rivera, F. J., and Jacks, T., (2015). Applications of the CRISPR–Cas9 system in cancer biology. *Nature Reviews Cancer 15*, 387–395, DOI: 10.1038/nrc3950.

(*107*)   Cong, L., Ran, F. A., Cox, D., Lin, S., Barretto, R., Habib, N., Hsu, P. D., Wu, X., Jiang, W., Marraffini, L. A., and Zhang, F., (2013). Multiplex genome engineering using CRISPR/Cas systems. *Science 339*, 819–823, DOI: 10.1126/science.1231143. Multiplex.

(*108*)   Bultmann, S., Morbitzer, R., Schmidt, C. S., Thanisch, K., Spada, F., Elsaesser, J., Lahaye, T., and Leonhardt, H., (2012). Targeted transcriptional activation of silent oct4 pluripotency gene by combining designer TALEs and inhibition of epigenetic modifiers. *Nucleic Acids Research 40*, 5368–5377, DOI: 10.1093/nar/gks199.

(*109*)   Valton, J., Dupuy, A., Daboussi, F., Thomas, S., Maréchal, A., Macmaster, R., Melliand, K., Juillerat, A., and Duchateau, P., (2012). Overcoming transcription activator-like effector (TALE) DNA binding domain sensitivity to cytosine methyla-tion. *The Journal of biological chemistry 287*, 38427–32, DOI: 10.1074/jbc.C112. 408864.

(*110*)   Bernstein, B. E., Mikkelsen, T. S., Xie, X., Kamal, M., Huebert, D. J., Cuff, J., Fry, B., Meissner, A., Wernig, M., Plath, K., Jaenisch, R., Wagschal, A., Feil, R., Schreiber, S. L., and Lander, E. S., (2006). A bivalent chromatin structure marks key developmental genes in embryonic stem cells. *Cell 125*, 315–26, DOI: 10.1016/ j.cell.2006.02.041.

(*111*)   Aoki, R., Chiba, T., Miyagi, S., Negishi, M., Konuma, T., Taniguchi, H., Ogawa, M., Yokosuka, O., and Iwama, A., (2010). The polycomb group gene product Ezh2 regulates proliferation and differentiation of murine hepatic stem/progenitor cells. *Journal of Hepatology 52*, 854–63, DOI: 10.1016/j.jhep.2010.01.027.

(*112*)   Xie, R., Everett, L. J., Lim, H.-W., Patel, N. A., Schug, J., Kroon, E., Kelly, O. G., Wang, A., D'Amour, K. A., Robins, A. J., Won, K.-J., Kaestner, K. H., and Sander, M., (2013). Dynamic chromatin remodeling mediated by polycomb proteins orches-trates pancreatic differentiation of human embryonic stem cells. *Cell stem cell 12*, 224–237, DOI: 10.1016/j.stem.2012.11.023.

(*113*)   Squazzo, S. L., O'Geen, H., Komashko, V. M., Krig, S. R., Jin, V. X., Jang, S.-w., Margueron, R., Reinberg, D., Green, R., and Farnham, P. J., (2006). Suz12 binds to silenced regions of the genome in a cell-type-specific manner. *Genome Research 16*, 890–900, DOI: 10.1101/gr.5306606.

(*114*)   Sparmann, A., and van Lohuizen, M., (2006). Polycomb silencers control cell fate, development and cancer. *Nature Reviews Cancer 6*, 846–856, DOI: 10.1038/ nrc1991.

(*115*)   Haynes, K. A., and Silver, P. A., (2011). Synthetic reversal of epigenetic silencing. *Journal of Biological Chemistry 286*, 27176–27182, DOI: 10.1074/jbc.C111. 229567.

(*116*)   Nakagawa, Y., Sakuma, T., Sakamoto, T., Ohmuraya, M., Nakagata, N., and Ya-mamoto, T., (2015). Production of knockout mice by DNA microinjection of various CRISPR/Cas9 vectors into freeze-thawed fertilized oocytes. *BMC Biotechnology 15*, 33, DOI: 10.1186/s12896-015-0144-x.

(*117*)   Pattanayak, V., Lin, S., Guilinger, J. P., Ma, E., Doudna, J. A., and Liu, D. R., (2013). High-throughput profiling of off-target DNA cleavage reveals RNA-programmed Cas9 nuclease specificity. *Nature Biotechnology 31*, 839–843, DOI: 10.1038/nbt.2673.

(*118*)   Cavalli, G., and Paro, R., (1999). Epigenetic inheritance of active chromatin after removal of the main transactivator. *Science 286*, 955–958, DOI: 10.1126/science.286.5441.955.

(*119*)   Tan, J., Yang, X., Zhuang, L., Jiang, X., Chen, W., Lee, P. L., Karuturi, R. M., Tan, P. B. O., Liu, E. T., and Yu, Q., (2007). Pharmacologic disruption of Polycomb-repressive complex 2-mediated gene repression selectively induces apoptosis in cancer cells. *Genes & Development 21*, 1050–1063, DOI: 10.1101/gad.1524107.

(*120*)   Kanduri, M., Sander, B., Ntoufa, S., Papakonstantinou, N., Sutton, L.-a., Stam-atopoulos, K., Kanduri, C., and Rosenquist, R., (2013). A key role for EZH2 in epigenetic silencing of HOX genes in mantle cell lymphoma. *Epigenetics 8*, 1280–1288, DOI: 10.4161/epi.26546.

(*121*)   Daer, R. M., Cutts, J. P., Brafman, D., and Haynes, K. A., Chromatin CRISPR Interference. https://benchling.com/hayneslab/f_/V1mVw1Lp-chromatin-crispr-interference/ (accessed Mar. 2015).

(*122*)   Katoh, K., and Standley, D. M., (2013). MAFFT multiple sequence alignment soft-ware version 7: improvements in performance and usability. *Molecular Biology and Evolution 30*, 772–780, DOI: 10.1093/molbev/mst010.

(*123*)   Racey, L. A., and Byvoet, P., (1971). Histone acetyltransferase in chromatin. Evi-dence for in vitro enzymatic transfer of acetate from acetyl-coenzyme A to histones. *Experimental Cell Research 64*, 366–370, DOI: 10.1016/0014-4827(71)90089-9.

(*124*)   Rea, S., Eisenhaber, F., O'Carroll, D., Strahl, B. D., Sun, Z. W., Schmid, M., Opravil, S., Mechtler, K., Ponting, C. P., Allis, C. D., and Jenuwein, T., (2000). Regulation of chromatin structure by site-specific histone H3 methyltransferases. *Nature 406*, 593–599, DOI: 10.1038/35020506.

(*125*)   Konze, K. D., Ma, A., Li, F., Barsyte-Lovejoy, D., Parton, T., MacNevin, C. J., Liu, F., Gao, C., Huang, X.-p., Kuznetsova, E., Rougie, M., Jiang, A., Pattenden, S. G., Norris, J. L., James, L. I., Roth, B. L., Brown, P. J., Frye, S. V., Arrowsmith, C. H., Hahn, K. M., Wang, G. G., Vedadi, M., and Jin, J., (2013). An Orally Bioavailable Chemical Probe of the Lysine Methyltransferases EZH2 and EZH1. *ACS Chemical Biology 8*, 1324–1334, DOI: 10.1021/cb400133j.

(*126*)   Holden, K., Maures, T., Walker, J., Miano, J., Seclen, E., Christian, M., Bak, R., Goodwin, M., and Hazelbaker, D., Use of Synthetic sgRNAs for Highly Efficient CRISPR Editing in Various Cell Types., Poster presented at the 2017 meeting on Genome Engineering: The CRISPR-Cas Revolution, Cold Spring Harbor, 2017.

(*127*)   Hendel, A., Bak, R. O., Clark, J. T., Kennedy, A. B., Ryan, D. E., Roy, S., Steinfeld, I., Lunstad, B. D., Kaiser, R. J., Wilkens, A. B., Bacchetta, R., Tsalenko, A., Dellinger, D., Bruhn, L., and Porteus, M. H., (2015). Chemically modified guide RNAs enhance CRISPR-Cas genome editing in human primary cells. *Nature Biotechnology 33*, 985–989, DOI: 10.1038/nbt.3290.

(*128*)   Dever, D. P., Bak, R. O., Reinisch, A., Camarena, J., Washington, G., Nicolas, C. E., Pavel-Dinu, M., Saxena, N., Wilkens, A. B., Mantri, S., Uchida, N., Hendel, A., Narla, A., Majeti, R., Weinberg, K. I., and Porteus, M. H., (2016). CRISPR/Cas9 β-globin gene targeting in human haematopoietic stem cells. *Nature 539*, 384–389, DOI: 10.1038/nature20134.

(*129*)   Daer, R. M., Barrett, C. M., and Haynes, K. A., Gal4 DNA-binding Fusion Transcription Regulators. https://benchling.com/hayneslab/f_/5wovkOaK-gal4-dna-binding-fusion-transcription-regulators/ (accessed Sept. 9, 2017).

(*130*)   Vendeville, A., Winzer, K., Heurlier, K., Tang, C. M., and Hardie, K. R., (2005). Making 'sense' of metabolism: autoinducer-2, LUXS and pathogenic bacteria. *Nature Reviews Microbiology 3*, 383–396, DOI: 10.1038/nrmicro1146.

(*131*)   Reading, N. C., and Sperandio, V., (2006). Quorum sensing: the many languages of bacteria. *FEMS microbiology letters 254*, 1–11, DOI: 10.1111/j.1574-6968.2005.00001.x.

(*132*)   Kleerebezem, M., Quadri, L. E., Kuipers, O. P., and de Vos, W. M., (1997). Quorum sensing by peptide pheromones and two-component signal-transduction systems in Gram-positive bacteria. *Molecular microbiology 24*, 895–904.

(*133*)   Tamsir, A., Tabor, J., and Voigt, C., (2011). Robust multicellular computing using genetically encoded NOR gates and chemical 'wires'. *Nature 469*, 212–215, DOI: 10.1038/nature09565.Robust.

(*134*)   Goñi-Moreno, A., Amos, M., and de la Cruz, F., (2013). Multicellular computing using conjugation for wiring. *PLOS ONE 8*, e65986, DOI: 10.1371/journal.pone.0065986.

(*135*)   Prindle, A., Samayoa, P., Razinkov, I., Danino, T., Tsimring, L. S., and Hasty, J., (2011). A sensing array of radically coupled genetic 'biopixels'. *Nature 481*, 39–44, DOI: 10.1038/nature10722.

(*136*)   Wang, B., Barahona, M., and Buck, M., (2013). A modular cell-based biosensor using engineered genetic logic circuits to detect and integrate multiple environmental signals. *Biosensors & bioelectronics 40*, 368–76, DOI: 10.1016/j.bios.2012.08.011.

(*137*)   Gupta, S., Bram, E. E., and Weiss, R., (2013). Genetically programmable pathogen sense and destroy. *ACS Synthetic Biology 2*, 715–23, DOI: 10.1021/sb4000417.

(*138*)   Anderson, J. C., Clarke, E. J., Arkin, A. P., and Voigt, C. a., (2006). Environmentally controlled invasion of cancer cells by engineered bacteria. *Journal of molecular biology 355*, 619–27, DOI: 10.1016/j.jmb.2005.10.076.

(*139*)   Liu, C., Fu, X., Liu, L., Ren, X., Chau, C. K. L., Li, S., Xiang, L., Zeng, H., Chen, G., Tang, L.-H., Lenz, P., Cui, X., Huang, W., Hwa, T., and Huang, J.-D., (2011). Sequential establishment of stripe patterns in an expanding cell population. *Science 334*, 238–41, DOI: 10.1126/science.1209042.

(*140*)   McMillen, D., Kopell, N., Hasty, J., and Collins, J. J., (2002). Synchronizing genetic relaxation oscillators by intercell signaling. *Proceedings of the National Academy of Sciences of the United States of America 99*, 679–84, DOI: 10.1073/pnas.022642299.

(*141*)   Pai, A., and You, L., (2009). Optimal tuning of bacterial sensing potential. *Molecular systems biology 5*, DOI: 10.1038/msb.2009.43.

(*142*)   Pai, A., Srimani, J. K., Tanouchi, Y., and You, L., (2014). Generic Metric to Quantify Quorum Sensing Activation Dynamics. *ACS Synthetic Biology 3*, 220–227, DOI: 10.1021/sb400069w.

(*143*)   Koseska, A., Zaikin, A., Kurths, J., and García-Ojalvo, J., (2009). Timing cellular decision making under noise via cell-cell communication. *PLOS ONE 4*, e4872, DOI: 10.1371/journal.pone.0004872.

(*144*)   Weber, M., and Buceta, J., (2013). Dynamics of the quorum sensing switch: stochastic and non-stationary effects. *BMC systems biology 7*, 1–15, DOI: 10.1186/1752-0509-7-6.

(*145*)   Danino, T., Mondragón-Palomino, O., Tsimring, L., and Hasty, J., (2010). A synchronized quorum of genetic clocks. *Nature 463*, 326–330, DOI: 10.1038/nature08753. A.

(*146*)   Prindle, A., Selimkhanov, J., Danino, T., Samayoa, P., Goldberg, A., Bhatia, S., and Hasty, J., (2012). Genetic circuits in Salmonella typhimurium. *ACS Synthetic Biology 1*, 458–464, DOI: 10.1021/sb300060e.

(*147*)   Anesiadis, N., Kobayashi, H., Cluett, W. R., and Mahadevan, R., (2013). Analysis and design of a genetic circuit for dynamic metabolic engineering. *ACS Synthetic Biology 2*, 442–52, DOI: 10.1021/sb300129j.

(*148*)   Connell, J. L., Ritschdorff, E. T., Whiteley, M., and Shear, J. B., (2013). 3D printing of microscopic bacterial communities. *Proceedings of the National Academy of Sciences of the United States of America 110*, 18380–5, DOI: 10.1073/pnas.1309729110.

(*149*)   Balagaddé, F. K., Song, H., Ozaki, J., Collins, C. H., Barnet, M., Arnold, F. H., Quake, S. R., and You, L., (2008). A synthetic Escherichia coli predator-prey ecosystem. *Molecular systems biology 4*, DOI: 10.1038/msb.2008.24.

(*150*)   You, L., Cox, R., Weiss, R., and Arnold, F., (2004). Programmed population control by cell–cell communication and regulated killing. *Nature 428*, 868–71, DOI: 10.1038/nature02468.1..

(*151*)   Ji, W., Shi, H., Zhang, H., Sun, R., Xi, J., Wen, D., Feng, J., Chen, Y., Qin, X., Ma, Y., Luo, W., Deng, L., Lin, H., Yu, R., and Ouyang, Q., (2013). A formalized design process for bacterial consortia that perform logic computing. *PLOS ONE 8*, e57482, DOI: 10.1371/journal.pone.0057482.

(*152*)   Payne, S., and You, L., (2014). Engineered cell-cell communication and its applications. *Advances in biochemical engineering/biotechnology 146*, 97–121, DOI: 10.1007/10_2013_249.

(*153*)   Põllumaa, L., Alamäe, T., and Mäe, A., (2012). Quorum Sensing and Expression of Virulence in Pectobacteria. *Sensors 12*, 3327–3349, DOI: 10.3390/s120303327.

(*154*)   Bernstein, H., Paulson, S., and Carlson, R., (2012). Synthetic Escherichia coli consortia engineered for syntrophy demonstrate enhanced biomass productivity. *Journal of biotechnology 157*, 159–166, DOI: 10.1016/j.jbiotec.2011.10.001.

(*155*)   Vinuselvi, P., and Lee, S. K., (2012). Engineered Escherichia coli capable of co-utilization of cellobiose and xylose. *Enzyme and microbial technology 50*, 1–4, DOI: 10.1016/j.enzmictec.2011.10.001.

(*156*)   Moon, T., Lou, C., Tamsir, A., Stanton, B., and Voigt, C., (2012). Genetic programs constructed from layered logic gates in single cells. *Nature 491*, 249–253, DOI: 10.1038/nature11516.Genetic.

(*157*)   Chen, X., Schauder, S., Potier, N., Van Dorsselaer, A., Pelczer, I., Bassler, B. L. B., and Hughson, F. F. M., (2002). Structural identification of a bacterial quorum-sensing signal containing boron. *Nature 415*, 545–549, DOI: 10.1038/415545a.

(*158*)   Marchand, N., and Collins, C. H., (2013). Peptide-based communication system enables Escherichia coli to Bacillus megaterium interspecies signaling. *Biotechnology and bioengineering 110*, 3003–12, DOI: 10.1002/bit.24975.

(*159*)   Collins, C. H., Leadbetter, J. R., and Arnold, F. H., (2006). Dual selection enhances the signaling specificity of a variant of the quorum-sensing transcriptional activator LuxR. *Nature biotechnology 24*, 708–12, DOI: 10.1038/nbt1209.

(*160*)   Vannini, A., (2002). The crystal structure of the quorum sensing protein TraR bound to its autoinducer and target DNA. *The EMBO Journal 21*, 4393–4401, DOI: 10.1093/emboj/cdf459.

(*161*)   Cole, C., Barber, J. D., and Barton, G. J., (2008). The Jpred 3 secondary structure prediction server. *Nucleic Acids Research 36*, W197–W201, DOI: 10.1093/nar/gkn238.

(*162*)   Fink, J. L., and Hamilton, N., (2007). DomainDraw: a macromolecular feature drawing program. *In silico biology 7*, 145–50.

(*163*)   Lindemann, A., Pessi, G., Schaefer, A., Mattmann, M., Christensen, Q., Kessler, A., Hennecke, H., Blackwell, H., Greenberg, E., and Harwood, C., (2011). Isovaleryl-homoserine lactone, an unusual branched-chain quorum-sensing signal from the soybean symbiont Bradyrhizobium japonicum. *Proceedings of the National Academy of Sciences 108*, 16765–70, DOI: 10.1073/pnas.1114125108.

(*164*)   Egland, K., and Greenberg, E., (2001). Quorum sensing in Vibrio fischeri- Analysis of the LuxR DNA binding region by alanine-scanning mutagenesis. *Journal of bacteriology 183*, 382–386, DOI: 10.1128/JB.183.1.382–386.2001.

(*165*)   Zhang, R.-g., Pappas, K. M., Pappas, T., Brace, J. L., Miller, P. C., Oulmassov, T., Molyneaux, J. M., Anderson, J. C., Bashkin, J. K., Winans, S. C., and Joachimiak, A., (2002). Structure of a bacterial quorum-sensing transcription factor complexed with pheromone and DNA. *Nature 417*, 971–4, DOI: 10.1038/nature00833.

(*166*)   Bottomley, M. J., Muraglia, E., Bazzo, R., and Carfi, A., (2007). Molecular insights into quorum sensing in the human pathogen Pseudomonas aeruginosa from the structure of the virulence regulator LasR bound to its autoinducer. *The Journal of biological chemistry 282*, 13592–600, DOI: 10.1074/jbc.M700556200.

(*167*)   Chen, G., Swem, L. R., Swem, D. L., Stauff, D. L., O'Loughlin, C. T., Jeffrey, P. D., Bassler, B. L., and Hughson, F. M., (2011). A strategy for antagonizing quorum sensing. *Molecular cell 42*, 199–209, DOI: 10.1016/j.molcel.2011.04.003.

(*168*)   UniProt Consortium, (2014). Activities at the Universal Protein Resource (UniProt). *Nucleic acids research 42*, D191–8, DOI: 10.1093/nar/gkt1140.

(*169*)   Sigrist, C., de Castro, E., Cerutti, L., Cuche, B., Hulo, N., Bridge, A., Bougueleret, L., and Xenarios, I., (2013). New and continuing developments at PROSITE. *Nucleic acids research 41*, D344–7, DOI: 10.1093/nar/gks1067.

(*170*)   Mitchell, A., Chang, H.-Y., Daugherty, L., Fraser, M., Hunter, S., Lopez, R., McAnulla, C., McMenamin, C., Nuka, G., Pesseat, S., Sangrador-Vegas, A., Scheremetjew, M., Rato, C., Yong, S.-Y., Bateman, A., Punta, M., Attwood, T. K., Sigrist, C. J. a., Redaschi, N., Rivoire, C., Xenarios, I., Kahn, D., Guyot, D., Bork, P., Letunic, I., Gough, J., Oates, M., Haft, D., Huang, H., Natale, D. a., Wu, C. H., Orengo, C., Sillitoe, I., Mi, H., Thomas, P. D., and Finn, R. D., (2015). The InterPro protein families database: the classification resource after 15 years. *Nucleic acids research 43*, D213–D221, DOI: 10.1093/nar/gku1241.

(*171*)   Berman, H. M., Westbrook, J., Feng, Z., Gilliland, G., Bhat, T. N., Weissig, H., Shindyalov, I. N., and Bourne, P. E., (2000). The Protein Data Bank www.rcsb.org. *Nucleic acids research 28*, 235–242, DOI: 10.1093/nar/28.1.235.

(*172*)   Yao, Y., Martinez-Yamout, M. a., Dickerson, T. J., Brogan, A. P., Wright, P. E., and Dyson, H. J., (2006). Structure of the Escherichia coli quorum sensing protein SdiA: activation of the folding switch by acyl homoserine lactones. *Journal of molecular biology 355*, 262–73, DOI: 10.1016/j.jmb.2005.10.041.

(*173*)   Geske, G. D. G., Mattmann, M. M. E., and Blackwell, H. E., (2008). Evaluation of a focused library of N-aryl L-homoserine lactones reveals a new set of potent quorum sensing modulators. *Bioorganic & medicinal chemistry letters 18*, 5978–81, DOI: 10.1128/JB.183.1.382–386.2001.

(*174*)   Michael, B., Smith, J., Swift, S., Heffron, F., and Ahmer, B., (2001). SdiA of Salmonella enterica is a LuxR homolog that detects mixed microbial communities. *Journal of bacteriology 183*, 5733–42, DOI: 10.1128/JB.183.19.5733–5742.2001.

(*175*)   Llamas, I., Keshavan, N., and González, J., (2004). Use of Sinorhizobium meliloti as an indicator for specific detection of long-chain N-acyl homoserine lactones. *Applied and Environmental Microbiology 70*, 3715–3723, DOI: 10.1128/AEM.70. 6.3715–3723.2004.

(*176*)   Kumari, A., Pasini, P., Deo, S. K., Flomenhoft, D., Shashidhar, H., and Daunert, S., (2006). Biosensing systems for the detection of bacterial quorum signaling molecules. *Analytical chemistry 78*, 7603–9, DOI: 10.1021/ac061421n.

(*177*)   Leung, M., Brimacombe, C., Spiegelman, G., and Beatty, J., (2012). The GtaR protein negatively regulates transcription of the gtaRI operon and modulates gene transfer agent (RcGTA) expression in Rhodobacter capsulatus. *Molecular microbiology 83*, 759–774, DOI: 10.1111/j.1365-2958.2011.07963.x.

(*178*)   Byers, D. M., and Gong, H., (2007). Acyl carrier protein: structure-function relationships in a conserved multifunctional protein family. *Biochemistry and cell biology = Biochimie et biologie cellulaire 85*, 649–662, DOI: 10.1139/o07-109.

(*179*)   Heath, R. J., and Rock, C. O., (1996). Roles of the FabA and FabZ beta-hydroxyacyl-acyl carrier protein dehydratases in Escherichia coli fatty acid biosynthesis. *The Journal of biological chemistry 271*, 27795–27801, DOI: 10.1074/jbc.271.44. 27795.

(*180*)   Rock, C. O., and Jackowski, S., (1982). Regulation of phospholipid synthesis in Escherichia coli. Composition of the acyl-acyl carrier protein pool in vivo. *The Journal of biological chemistry 257*, 10759–65.

(*181*)   Majerus, P. W., Alberts, A. W., and Vagelos, P. R., (1964). The Acyl Carrier Protein of Fatty Acid Synthesis: Purification, Physical Properties, and Substrate Binding Site. *Proceedings of the National Academy of Sciences of the United States of America 51*, 1231–8.

(*182*)   Polakis, S. E., Guchhait, R. B., Zwergel, E. E., Lane, M. D., and Cooper, T. G., (1974). Acetyl coenzyme A carboxylase system of Escherichia coli. Studies on the mechanisms of the biotin carboxylase- and carboxyltransferase-catalyzed reactions. *The Journal of biological chemistry 249*, 6657–67.

(*183*)   Magnuson, K., Carey, M. R., and Cronan, J. E., (1995). The putative fabJ gene of Escherichia coli fatty acid synthesis is the fabF gene. *Journal of bacteriology 177*, 3593–5.

(*184*)   Heath, R. J., and Rock, C. O., (1996). Regulation of Fatty Acid Elongation and Initiation by Acyl-Acyl Carrier Protein in Escherichia coli. *The Journal of biological chemistry 271*, 1833–1836, DOI: 10.1074/jbc.271.4.1833.

(*185*)   Heath, R. J., and Rock, C. O., (1995). Enoyl-acyl carrier protein reductase (fabI) plays a determinant role in completing cycles of fatty acid elongation in Escherichia coli. *Journal of Biological Chemistry 270*, 26538–26542, DOI: 10.1074/jbc.270.44.26538.

(*186*)   Feng, Y., and Cronan, J. E., (2009). Escherichia coli Unsaturated Fatty Acid Synthesis. *Journal of Biological Chemistry 284*, 29526–29535, DOI: 10.1074/jbc.M109.023440.

(*187*)   D'Agnolo, G., Rosenfeld, I. S., and Vagelos, P. R., (1975). Multiple Forms of ß-Ketoacyl-Acyl Synthetase in Escherichia coli. *Journal of Biological Chemistry 250*, 5289–5294.

(*188*)   Janßen, H., and Steinbüchel, A., (2014). Fatty acid synthesis in Escherichia coli and its applications towards the production of fatty acid based biofuels. *Biotechnology for Biofuels 7*, 7, DOI: 10.1186/1754-6834-7-7.

(*189*)   Gould, T. a., Herman, J., Krank, J., Murphy, R. C., and Churchill, M. E. a., (2006). Specificity of Acyl-Homoserine Lactone Synthases Examined by Mass Spectrometry. *Journal of Bacteriology 188*, 773–783, DOI: 10.1128/JB.188.2.773-783.2006.

(*190*)   Beck von Bodman, S., and Farrand, S. K., (1995). Capsular polysaccharide biosynthesis and pathogenicity in Erwinia stewartii require induction by an N-acylhomoserine lactone autoinducer. *Journal of bacteriology 177*, 5000–8.

(*191*)   Ortori, C. A., Dubern, J. F., Chhabra, S. R., Cámara, M., Hardie, K., Williams, P., and Barrett, D. A., (2011). Simultaneous quantitative profiling of N-acyl-l-homoserine lactone and 2-alkyl-4(1H)-quinolone families of quorum-sensing signaling molecules using LC-MS/MS. *Analytical and Bioanalytical Chemistry 399*, 839–850, DOI: 10.1007/s00216-010-4341-0.

(*192*)   Lutz, R., and Bujard, H., (1997). Independent and tight regulation of transcriptional units in Escherichia coli via the LacR/O, the TetR/O and AraC/I1-I2 regulatory elements. *Nucleic acids research 25*, 1203–10, DOI: 10.1093/nar/25.6.1203.

(*193*)   Marketon, M. M., Gronquist, M. R., Eberhard, A., and González, J. E., (2002). Characterization of the Sinorhizobium meliloti sinR/sinI locus and the production of novel N-acyl homoserine lactones. *Journal of bacteriology 184*, 5686–95, DOI: 10.1128/JB.184.20.5686.

(*194*)   Tsai, C.-S., and Winans, S. C., (2010). LuxR-type quorum-sensing regulators that are detached from common scents. *Molecular Microbiology 77*, 1072–1082, DOI: 10.1111/j.1365-2958.2010.07279.x.

(*195*)   Gardner, T. S., Cantor, C. R., and Collins, J. J., (2000). Construction of a genetic toggle switch in Escherichia coli. *Nature 403*, 339–42, DOI: 10.1038/35002131.

(*196*)   Chen, B., Gilbert, L. A., Cimini, B. A., Schnitzbauer, J., Zhang, W., Li, G.-w., Park, J., Blackburn, E. H., Weissman, J. S., Qi, L. S., and Huang, B., (2013). Dynamic Imaging of Genomic Loci in Living Human Cells by an Optimized CRISPR/Cas System. *Cell 155*, 1479–1491, DOI: 10.1016/j.cell.2013.12.001.

(*197*)   Balhouse, B. N., Patterson, L., Schmelz, E. M., Slade, D. J., and Verbridge, S. S., (2017). N-(3-oxododecanoyl)-L-homoserine lactone interactions in the breast tumor microenvironment: Implications for breast cancer viability and proliferation in vitro. *PLOS ONE 12*, ed. by Singh, P. K., DOI: 10.1371/journal.pone.0180372.

(*198*)   Zhao, G., Neely, A. M., Schwarzer, C., Lu, H., Whitt, A. G., Stivers, N. S., Burlison, J. A., White, C., Machen, T. E., and Li, C., (2016). N-(3-oxo-acyl) homoserine lactone inhibits tumor growth independent of Bcl-2 proteins. *Oncotarget 7*, 5924–42, DOI: 10.18632/oncotarget.6827.

(*199*)   Jackson, V., (1978). Studies on histone organization in the nucleosome using formaldehyde as a reversible cross-linking agent. *Cell 15*, 945–954.

(*200*)   Gilmour, D. S., and Lis, J. T., (1984). Detecting protein-DNA interactions in vivo: Distribution of RNA polymerase on specific bacterial genes. *Proceedings of the National Academy of Sciences 81*, 4275–4279.

(*201*)   Gilmour, D. S., and Lis, J. T., (1985). In vivo interactions of RNA polymerase II with genes of Drosophila melanogaster. *Molecular and cellular biology 5*, 2009–18.

(*202*)   Saiki, R. K., Scharf, S., Faloona, F., Mullis, K. B., Horn, G. T., Erlich, H. A., and Arnheim, N., (1985). Enzymatic amplification of beta-globin genomic sequences and restriction site analysis for diagnosis of sickle cell anemia. *Science 230*, 1350–1354.

(*203*)   Solomon, M. J., Larsen, P. L., and Varshavsky, A., (1988). Mapping protein-DNA interactions in vivo with formaldehyde- Evidence that histone H4 is retained on a highly transcribed gene. *Cell 53*, 937–947.

(*204*)   Higuchi, R., Fockler, C., Dollinger, G., and Watson, R., (1993). Kinetic PCR analysis: Real-time monitoring of DNA amplification reactions. *Nature Biotechnology 11*, 1026–1030, DOI: 10.1038/nbt0993-1026.

(*205*) Kuo, M.-H., and Allis, C., (1999). In vivo cross-linking and immunoprecipitation for studying dynamic Protein-DNA associations in a chromatin environment. *Methods 19*, 425–433, DOI: 10.1006/meth.1999.0879.

(*206*) Blat, Y., and Kleckner, N., (1999). Cohesins bind to preferential sites along yeast chromosome III, with differential regulation along arms versus the centric region. *Cell 98*, 249–259, DOI: 10.1016/S0092-8674(00)81019-3.

(*207*) Barski, A., Cuddapah, S., Cui, K., Roh, T.-y., Schones, D. E., Wang, Z., Wei, G., Chepelev, I., and Zhao, K., (2007). High-resolution profiling of histone methylations in the human genome. *Cell 129*, 823–837, DOI: 10.1016/j.cell.2007.05.009.

(*208*) Albert, I., Mavrich, T. N., Tomsho, L. P., Qi, J., Zanton, S. J., Schuster, S. C., and Pugh, B. F., (2007). Translational and rotational settings of H2A.Z nucleosomes across the Saccharomyces cerevisiae genome. *Nature 446*, 572–576, DOI: 10.1038/nature05632.

(*209*) Johnson, D. S., Mortazavi, A., Myers, R. M., and Wold, B., (2007). Genome-wide mapping of in vivo protein-DNA interactions. *Science 316*, 1497–1502, DOI: 10.1126/science.1141319.

(*210*) Mikkelsen, T. S., Ku, M., Jaffe, D. B., Issac, B., Lieberman, E., Giannoukos, G., Alvarez, P., Brockman, W., Kim, T.-k., Koche, R. P., Lee, W., Mendenhall, E., O'Donovan, A., Presser, A., Russ, C., Xie, X., Meissner, A., Wernig, M., Jaenisch, R., Nusbaum, C., Lander, E. S., and Bernstein, B. E., (2007). Genome-wide maps of chromatin state in pluripotent and lineage-committed cells. *Nature 448*, 553–560, DOI: 10.1038/nature06008.

(*211*) Hoffman, E. A., Frey, B. L., Smith, L. M., and Auble, D. T., (2015). Formaldehyde crosslinking: A tool for the study of chromatin complexes. *Journal of Biological Chemistry 290*, 26404–26411, DOI: 10.1074/jbc.R115.651679.

(*212*) Davis, R. M., Muller, R. Y., and Haynes, K. A., (2015). Corrigendum: Can the Natural Diversity of Quorum-Sensing Advance Synthetic Biology? *Frontiers in Bioengineering and Biotechnology 3*, DOI: 10.3389/fbioe.2015.00099.

(*213*) Schultz, J., Milpetz, F., Bork, P., and Ponting, C. P., (1998). SMART, a simple modular architecture research tool: Identification of signaling domains. *Proceedings of the National Academy of Sciences 95*, 5857–5864, DOI: 10.1073/pnas.95.11.5857.

(*214*) Letunic, I., Doerks, T., and Bork, P., (2014). SMART: recent updates, new developments and status in 2015. *Nucleic Acids Research 43*, D257–D260, DOI: 10.1093/nar/gku949.

(*215*) Ahlgren, N. a., Harwood, C. S., Schaefer, A. L., Giraud, E., and Greenberg, E. P., (2011). Aryl-homoserine lactone quorum sensing in stem-nodulating photosynthetic bradyrhizobia. *Proceedings of the National Academy of Sciences 108*, 7183–7188, DOI: 10.1073/pnas.1103821108.

(*216*)   Chandler, J., Duerkop, B., Hinz, A., West, T., Herman, J., Churchill, M., Skerrett, S., and Greenberg, E., (2009). Mutational Analysis of Burkholderia thailandensis Quorum Sensing and Self-Aggregation. *Journal of bacteriology 191*, 5901–9, DOI: 10.1128/JB.00591-09.

(*217*)   Conway, B., and Greenberg, E., (2002). Quorum-Sensing Signals and Quorum-Sensing Genes in Burkholderia vietnamiensis. *Journal of bacteriology 184*, 1187–91, DOI: 10.1128/JB.184.4.1187–1191.2002.

(*218*)   Dulla, G. F. J., and Lindow, S. E., (2009). Acyl-homoserine lactone-mediated cross talk among epiphytic bacteria modulates behavior of Pseudomonas syringae on leaves. *The ISME journal 3*, 825–34, DOI: 10.1038/ismej.2009.30.

(*219*)   Eberhard, A., Burlingame, A. L., Eberhard, C., Kenyon, G. L., Nealson, K. H., and Oppenheimer, N. J., (1981). Structural identification of autoinducer of Photobacterium fischeri luciferase. *Biochemistry 20*, 2444–2449, DOI: 10.1021/bi00512a013.

(*220*)   Fuqua, C., and Greenberg, E. P., (2002). Signalling: Listening in on bacteria: acyl-homoserine lactone signalling. *Nature Reviews Molecular Cell Biology 3*, 685–695, DOI: 10.1038/nrm907.

(*221*)   Galloway, W. R. J. D., Hodgkinson, J. T., Bowden, S. D., Welch, M., and Spring, D. R., (2011). Quorum Sensing in Gram-Negative Bacteria: Small-Molecule Modulation of AHL and AI-2 Quorum Sensing Pathways. *Chemical reviews 111*, 28–67, DOI: 10.1021/cr100109t..

(*222*)   Iida, A., Ohnishi, Y., and Horinouchi, S., (2008). An OmpA family protein, a target of the GinI/GinR quorum-sensing system in Gluconacetobacter intermedius, controls acetic acid fermentation. *Journal of bacteriology 190*, 5009–19, DOI: 10.1128/JB.00378-08.

(*223*)   Khajanchi, B. K., Kirtley, M. L., Brackman, S. M., and Chopra, A. K., (2011). Immunomodulatory and protective roles of quorum-sensing signaling molecules N-acyl homoserine lactones during infection of mice with Aeromonas hydrophila. *Infection and immunity 79*, 2646–57, DOI: 10.1128/IAI.00096-11.

(*224*)   Lewenza, S., Conway, B., Greenberg, E. P., and Sokol, P. A., (1999). Quorum sensing in Burkholderia cepacia: identification of the LuxRI homologs CepRI. *Journal of bacteriology 181*, 748–56.

(*225*)   Licciardello, G., Bertani, I., Steindler, L., Bella, P., Venturi, V., and Catara, V., (2007). Pseudomonas corrugata contains a conserved N-acyl homoserine lactone quorum sensing system; its role in tomato pathogenicity and tobacco hypersensitivity response. *FEMS microbiology ecology 61*, 222–34, DOI: 10.1111/j.1574-6941.2007.00338.x.

(*226*)   Llamas, I., Quesada, E., Martínez-Cánovas, M. J., Gronquist, M., Eberhard, A., and González, J. E., (2005). Quorum sensing in halophilic bacteria: detection of N-acyl-homoserine lactones in the exopolysaccharide-producing species of Halomonas.

Extremophiles : life under extreme conditions 9, 333–41, DOI: 10.1007/s00792-005-0448-1.

(*227*)   Malott, R. J., Baldwin, A., Mahenthiralingam, E., and Sokol, P. A., (2005). Characterization of the cciIR quorum-sensing system in Burkholderia cenocepacia. *Infection and immunity 73*, 4982–92, DOI: 10.1128/IAI.73.8.4982-4992.2005.

(*228*)   Mastroleo, F., Van Houdt, R., Atkinson, S., Mergeay, M., Hendrickx, L., Wattiez, R., and Leys, N., (2013). Modelled microgravity cultivation modulates N-acylhomoserine lactone production in Rhodospirillum rubrum S1H independently of cell density. *Microbiology (Reading, England) 159*, 2456–66, DOI: 10.1099/mic.0.066415-0.

(*229*)   Mcclean, K. H., Winson, M. K., Fish, L., Taylor, A., Chhabra, S. R., Camara, M., Daykin, M., Lamb, J. H., Swift, S., Bycroft, B. W., Stewart, G. S. A. B., and Williams, P., (1997). Quorum sensing and Chromobacterium violaceum: exploitation of violacein production and inhibition for the detection of N-acyl homoserine lactones. *Microbiology (Reading, England) 143*, 3703–3711, DOI: 10.1099/00221287-143-12-3703.

(*230*)   Moré, M. I., Finger, L. D., Stryker, J. L., Fuqua, C., Eberhard, A., and Winans, S. C., (1996). Enzymatic Synthesis of a Quorum-Sensing Autoinducer Through Use of Defined Substrates. *Science 272*, 1655–1658, DOI: 10.1126/science.272.5268.1655.

(*231*)   Morohoshi, T., Nakamura, Y., Yamazaki, G., Ishida, A., N, K., and Ikeda, T., (2007). The Plant Pathogen Pantoea ananatis Produces N-Acylhomoserine Lactone and Causes Center Rot Disease of Onion by Quorum Sensing. *Journal of bacteriology 189*, 8333–8, DOI: 10.1128/JB.01054-07.

(*232*)   Niu, C., Clemmer, K., Bonomo, R., and Rather, P., (2008). Isolation and Characterization of an Autoinducer Synthase from Acinetobacter baumannii. *Journal of bacteriology 190*, 3386–92, DOI: 10.1128/JB.01929-07.

(*233*)   Pontes, M., Babst, M., Lochhead, R., Oakeson, K., Smith, K., and Dale, C., (2008). Quorum Sensing Primes the Oxidative Stress Response in the Insect Endosymbiont, Sodalis glossinidius. *PLOS ONE 3*, e3541, DOI: 10.1371/journal.pone.0003541.

(*234*)   Rodelas, B., Lithgow, J. K., Wisniewski-Dye, F., Hardman, A., Wilkinson, A., Economou, A., Williams, P., and Downie, J. A., (1999). Analysis of quorum-sensing-dependent control of rhizosphere-expressed (rhi) genes in Rhizobium leguminosarum bv. viciae. *Journal of bacteriology 181*, 3816–23.

(*235*)   Schaefer, A. L., Greenberg, E. P., Oliver, C. M., Oda, Y., Huang, J. J., Bittan-Banin, G., Peres, C. M., Schmidt, S., Juhaszova, K., Sufrin, J. R., and Harwood, C. S., (2008). A new class of homoserine lactone quorum-sensing signals. *Nature 454*, 595–9, DOI: 10.1038/nature07088.

(*236*)   Schaefer, A., Taylor, T., Beatty, J., and Greenberg, E., (2002). Long-Chain Acyl-Homoserine Lactone Quorum-Sensing Regulation of Rhodobacter capsulatus Gene Transfer Agent Production. *Journal of Bacteriology 184*, 6515–6521, DOI: 10.1128/JB.184.23.6515-6521.2002.

(*237*)   Schripsema, J., de Rudder, K. E., van Vliet, T. B., Lankhorst, P. P., de Vroom, E., Kijne, J. W., and van Brussel, A. A., (1996). Bacteriocin small of Rhizobium leguminosarum belongs to the class of N-acyl-L-homoserine lactone molecules, known as autoinducers and as quorum sensing co-transcription factors. *Journal of bacteriology 178*, 366–71.

(*238*)   Tahrioui, A., Quesada, E., and Llamas, I., (2011). The hanR/hanI quorum-sensing system of Halomonas anticariensis, a moderately halophilic bacterium. *Microbiology (Reading, England) 157*, 3378–87, DOI: 10.1099/mic.0.052167-0.

(*239*)   Ulrich, R. L., Deshazer, D., Brueggemann, E., Hines, H., Oyston, P., and Jeddeloh, J., (2004). Role of quorum sensing in the pathogenicity of Burkholderia pseudomallei. *Journal of Medical Microbiology 53*, 1053–1064, DOI: 10.1099/jmm.0.45661-0.

(*240*)   Vial, L., Cuny, C., Gluchoff-Fiasson, K., Comte, G., Oger, P. M., Faure, D., Dessaux, Y., Bally, R., and Wisniewski-Dyé, F., (2006). N-acyl-homoserine lactone-mediated quorum-sensing in Azospirillum: an exception rather than a rule. *FEMS microbiology ecology 58*, 155–68, DOI: 10.1111/j.1574-6941.2006.00153.x.

(*241*)   Wagner-Döbler, I., Thiel, V., Eberl, L., Allgaier, M., Bodor, A., Meyer, S., Ebner, S., Hennig, A., Pukall, R., and Schulz, S., (2005). Discovery of complex mixtures of novel long-chain quorum sensing signals in free-living and host-associated marine alphaproteobacteria. *Chembiochem : a European journal of chemical biology 6*, 2195–206, DOI: 10.1002/cbic.200500189.

APPENDIX A

SUPPORTING INFORMATION FOR THE IMPACT OF CHROMATIN DYNAMICS ON CAS9-MEDIATED GENOME EDITING IN HUMAN CELLS

This appendix was previously published as supporting information for Davis et al.[92]
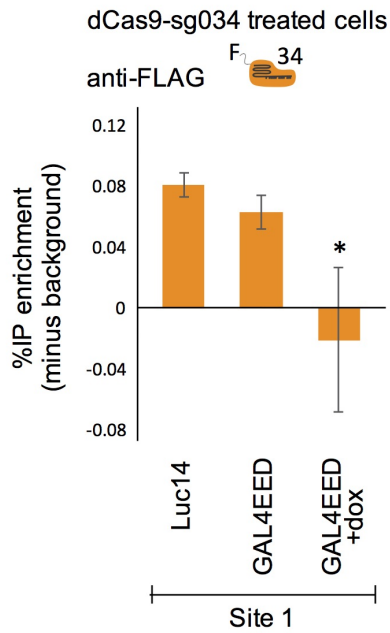
Figure A.1.   Chromatin mapping data show differential enrichment of dCas9/sg034 at *luciferase* in the open, partially closed, and closed chromatin states. Cross-linked, sheared chromatin was prepared from Luc14 (unsilenced), GAL4EED (partially silenced), or GAL4EED + dox (fully silenced) cells. An anti-FLAG antibody was used to IP chromatin from dCas9_gRNA-transfected cells. Quantitative PCR (qPCR) was used to measure IP'ed DNA. Primer set Site 1 described in Methods. A primer pair located at the constitutively active GAPDH promoter was used as a negative control to determine off-target binding. Enrichment shown as percentages of input minus background (IgG mock IP and GAPDH).

Table A.1. List of sgRNAs

sgRNA name	Target Sequence	Distance from translational start site (bp)	Editing efficiency	Off-target score[*]
sg023	ATAAATAACGCGCCCAACAC	276	21.74	92
sg025	TTGGAAACAAACACTACGGT	372	25.08	84
sg029	CATAGCTTCTGCCAACCGAA	184	15.47	86
sg030	TTCATTATAAATGTCGTTCG	316	22.72	86
sg031	CGAGGTGAACATCACGTACG	157	38.59	92
sg032	CCTCTAGAGGATGGAACCGC	62	16.03	91
sg033	GGCTATGAAGAGATACGCCC	100	19.28	89
sg034	AAGAGATACGCCCTGGTTCC	107	25.14	78
sg036	CGCTGGAGAGCAACTGCATA	79	6.01	76
sg040	CAAGCTTATGCAGGGTCGCT	-22	15.55	91
sg041	ATAATAATTTTCTGGATTAT	435	9.83	38
sg042	GGATTCTAAAACGGATTACC	472	14.18	92
sg043	TGTACATCGACTGAAATCCC	479	12.35	82
sg044	GTCACATCTCATCTACCTCC	518	20.96	66
sg045	GCAGGGTCGCTCGGTGTTCG	-31	10.38	88
sg046	CCTGCATAAGCTTGCCACCA	-3	3.86	74
sg048	GGATCTACTGGGTTACCTAA	614	24.38	88
sg051	AATCCAGAAAATTATTATCA	451	11.39	34
sg052	AATCCATGATAATAATTTTC	443	0.00	34
sg053	CAAAAACATAAAGAAAGGCC	28	7.74	35
sg054	TCTGTAAAAGCAATTGTTCC	114	16.09	37
sg055	CGGGCCTTTCTTTATGTTTT	16	8.78	42
sg056	TTTTGGCAATCAAATCATTC	694	0.00	35

Table A.2. List of Primers for Nested PCR of Genomic DNA from Cas9/sgRNA Treated Samples

sgRNA name	Forward primer	Reverse primer
sg023	P149	P215
sg025	P159	P215
sg029	P149	P174
sg030	P159	P215
sg031	P149	P174
sg032	P149	P174
sg033	P149	P176
sg034	P163	P215
sg036	P149	P174
sg040	P163	P160
sg041	P175	P214
sg042	P213	P214
sg043	P213	P214
sg044	P213	P214
sg045	P151	P160
sg046	P153	P160
sg048	P213	P214
sg051	P175	P214
sg052	P175	P214
sg053	P153	P160
sg054	P149	P162
sg055	P153	P160
sg056	P216	P217

Table A.3. List of Primers with Their Sequences

Primer name	Sequence
P149	AAGGTGACGCGTGTGGCCTC
P151	TCGCCCGGGGATCCGACTAG
P153	GCAAATGCAGTCGGGGCGGC
P159	CGCCCTGGTTCCTGGAACAA
P160	TCTGCCAACCGAACGGACAT
P162	TAAATGTCGTTCGCGGGCGC
P163	CAAACCCCGCCCAGCGTCTT
P174	GCGCCCAACACCGGCATAAA
P175	TCTTTATGCCGGTGTTGGGC
P176	AAACACTACGGTAGGCTGCG
P213	CGCAGCCTACCGTAGTGTTT
P214	CCGTGATGGAATGGAACAAC
P215	GACTGAAATCCCTGGTAATCCG
P216	CGGATTACCAGGGATTTCAGTC

Table A.4. List of Primers for ChIP-qPCR

qPCR target site	Primer name	Primer sequence
Site 1 F	P313	CGACCCTGCATAAGCTTGCC
Site 1 R	P311	CCGCGTACGTGATGTTCACC
Site 2 F	P173	GGTGAACATCACGTACGCGG
Site 2 R	P323	AATAACGCGCCCAACACCGG
Site 3 F	P331	GCGCCCGCGAACGACATTTA
Site 3 R	P329	GAGATGTGACGAACGTGTAC
Site 4 F	P316	TTGTACCAGAGTCCTTTGATCG
Site 4 R	P214	CCGTGATGGAATGGAACAAC
GAPDH F	P333	TACTAGCGGTTTTACGGGCG
GAPDH R	P334	TCGAACAGGAGGAGCAGAGAGCGA

APPENDIX B

CHROMATIN IMMUNOPRECIPITATION ASSAY DEVELOPMENT

B.1 Introduction to ChIP Assay

B.1.1 Brief History of the ChIP Assay

In the 1970's, researchers were experimenting with different methods of crosslinking to understand protein-protein interactions.[199] They would covalently link proteins, either through chemical crosslinking or other methods, and deduce which proteins were closely interacting or binding to each other.

In the mid 1980's, Gilmour et al. were the first to crosslink DNA and protein and use an antibody to pull down a specific protein. They used UV to covalently link the DNA and protein to map RNA polymerase to E coli genome in 1984[200] and then to the *Drosophila* genome the following year.[201] However, as PCR was only invented the year before,[202] early ChIP assays used hybridization probes to detect the precipitated DNA sequences. Soon after, Solomon et al. used formaldehyde to crosslink and pulldown.[203]

After the development and subsequent commercialization of real time PCR in 1993 and 1996 respectively,[204] it was applied to quantifying ChIP'd DNA.[205] With the development of more antibodies, especially those directed to histone modifications, ChIP was becoming a popular tool to understand the relationship of proteins and genomes.[205] However, genome-wide mapping of proteins was more relevant so most published ChIP data utilized ChIP-chip where the DNA was hybridized to microarrays with many target sequences.[206] Finally, with the development of deep sequencing technology, true genome-wide mapping became possible with ChIP-seq, which was demonstrated in parallel by four different labs.[207−210]

ChIP assay allows us to answer two questions: 1. Where in the genome is my protein bound and 2. How much of my protein is bound there? For question 1, we can ask if it is bound at a particular location or set of locations by using ChIP paired with quantitative PCR (qPCR). Alternatively, we can see all of the locations our protein is bound by using ChIP paired with deep sequencing or ChIP paired with a microarray. For question 2, the above assays are quantitative. In order to be able to perform a ChIP, you will need a ChIP-grade antibody against your protein of interest.

ChIP assays have a reputation for being challenging because they require extensive optimization, are sensitive to protocol deviations, and are tedious and long relative to most protocols. Here, I will introduce the steps of the assay, describe the optimization I performed, and include the detailed protocol optimized for our lab.

B.2 Overview of ChIP Steps

As shown in Figure B.1, ChIP is composed of several steps across multiple days. I have chosen to break the protocol into 9 steps, each illustrated as a separate tube in Figure B.1.

Step 0: Step 1 can be performed on adherent cells in the flask they've been grown in. However, some people prefer to collect the cells before fixation. Therefore, I have included a Step 0 for possible cell preparation.

Step 1: Fixation. This can be done chemically with something like formaldehyde. In this step, any DNA-protein or protein-protein complexes are chemically fixed together. Notably, for some applications, such as identifying histones, you do not need to fix. In this case, you would not sonicate, but would fragment the chromatin using enzymatic digestion. Optimization discussed further in subsection B.4.1.

Step 2: Lyse cells and nuclei to release the chromatin, which contains the gDNA fixed to all the associated proteins.

Step 3: Separate the chromatin by centrifugation and remove cellular debris.

Step 4: Fragment the chromatin via sonication. This step requires significant optimization to ensure the DNA fragments are of appropriate size for your downstream assays. You must also ensure that you did not over-sonicate and destroy the epitopes on the proteins. Optimization discussed further in subsection B.4.2.

Step 5: Incubate your sonicated chromatin with an antibody against your protein of interest.

Step 6: Incubate your antibody-chromatin sample with a secondary antibody against your primary antibody from step 5. It should be appropriate for the animal your primary antibody was produced in and conjugated to something that allows you to separate it from the rest of the sample. I used secondary antibodies conjugated to magnetic beads.

Step 7: Isolate your secondary antibody, which is bound to your primary antibody, which is bound to your protein of interest. Some of your protein of interest will likely be bound to DNA.

Step 8: Wash everything else away. ChIP wash steps are very diverse and thus you should try a few methods to identify a wash sequence that removes enough background without washing away your signal. It is important to make sure your wash buffers do not contain anything that will denature proteins.

Step 9: The only DNA that should be present in your sample is that which was closely associated with your protein of interest. Before you can identify and quantify it, you must remove the antibodies, protein, and beads by reversing the crosslinking and treating with a proteinase. Some people purify the DNA using columns while others do phenyl-chloroform extractions.

Now your DNA is ready to be characterized.
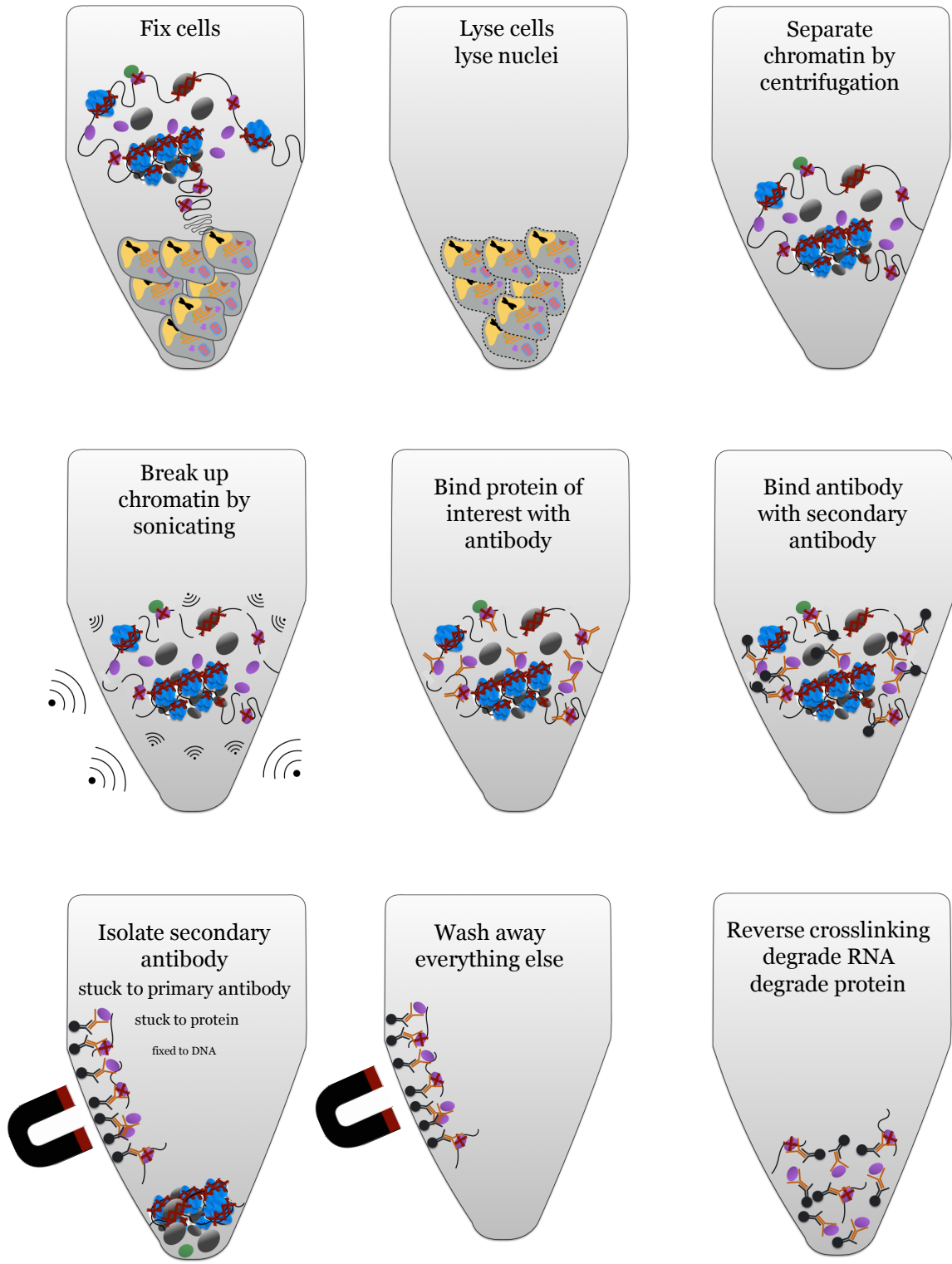
Figure B.1. Steps in chromatin immunoprecipitation.

a

ChIP-seq

What sequences are here?
Where in the genome does my
protein bind?

IP'd DNA

Sequence

ATGTGCCTGGATGCATCGTACG   CTAGCTGCTCGATACGATCGC

Map
sequences
back to the
genome

GTGCGCTAGACTGCTACGTA

b

ChIP-qPCR

Is my sequence here?
Does my protein bind at this site?

Design primers to amplify site of interest

Run qPCR with IP'd DNA and primer set(s)

IP'd DNA
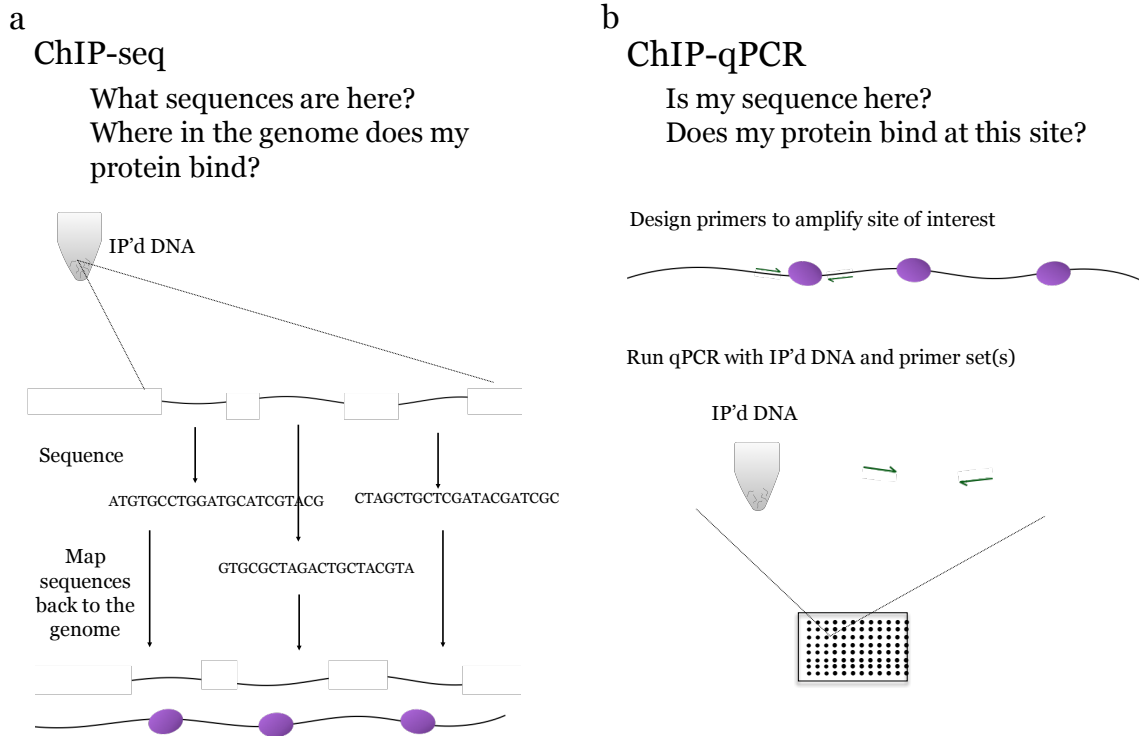
Figure B.2. Steps to identify and quantify immunoprecipitated DNA. (a) Overview of using deep sequencing to identify and map all the sites the protein of interest was bound. (b) Overview of using quantitative real time PCR (qPCR) to identify whether the protein of interest was bound at a specific location in the genome.

B.3   Identify and Quantify DNA

After purifying the DNA, you are ready to identify and quantify it. This can be done in a number of ways, the most common two being deep sequencing and qPCR. ChIP followed by deep sequencing, also called ChIP-seq, will tell you all of the DNA sequences in your sample as well as how frequently they occur Figure B.2 a. Those sequences are computationally mapped back to a reference genome using a series of algorithms. ChIP followed by qPCR (Chip-qPCR) tells you whether your protein was bound to a specific sequence Figure B.2 b. You first design qPCR primers that amplify the genomic region or regions of interest. This step takes considerable optimization, as discussed in subsection B.4.3. Next, you perform qPCR to determine if your target sequence was pulled down and how much of it was present.

B.4 Optimization

While developing the ChIP assay in my lab, I did considerable optimization. Below are some of the optimization steps and subsequent data collected during this time.

B.4.1 Fixation

Fixation is the step where proteins bound to DNA are chemical fixed together. There are different fixation agents that can be used. Some chemicals fix proteins to DNA while others fix proteins to proteins. They can be used together to pull down a protein associated with a protein bound to DNA. The concentration and fixation time should be optimized for each cell type and application. In my work, I used formaldehyde, which has a fixation length of $2\,\text{Å}$ to $3\,\text{Å}$.[211] Figure B.3 illustrates some of the issues that can arise from improper fixation.

B.4.2 Digestion

There are several methods you can employ to digest chromatin after fixation. I tested two ways: MNase digestion and sonication.

B.4.2.1 MNase Digestion

MNase digestion was used during optimization of NChIP, which does not involve fixation. MNase is an endonuclease that will digest any DNA that isn't protected by nucleosomes. The leftover, undigested DNA can be analyzed by sequencing or qPCR. Figure B.4 shows the agarose gel for different amounts of MNase enzyme amounts. Unlike with sonication, the digested fragments are quantized: each band corresponds to an integer times the length of DNA wrapped around a single nucleosome, 147 basepair.

B.4.2.2 Sonication

Extensive sonication optimization was done by my colleague, Josh Cutts. He recommended the intensity setting sonication power for the machine we used. He also advised me on how to perform this optimization experiment.

To determine the appropriate number of cycles before I saw sufficient digestion of my sample, I prepared chromatin samples and sonicated between 15 and 135 cycles, taking an aliquot every 15 cycles to analyze. I uncrosslinked the chromatin and ran the DNA on an Agilent TapeStation. Figure B.5 shows the resulting chromatograph. The chromatin looks appropriately sheared between 60 and 75 cycles at these settings.

a

Over-fixation

Too long, too strong

Nearby, unassociated proteins are chemically linked to DNA

Result: Pull down unrelated proteins
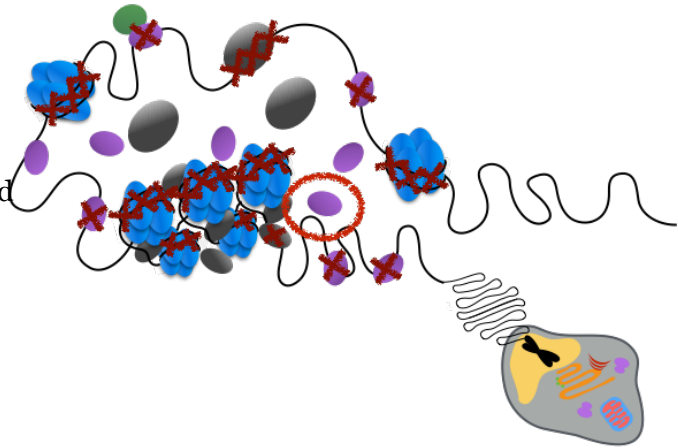
b

Under-fixation

Not long enough, too weak

Associated proteins aren't chemical linked to DNA

Result: Bound proteins aren't pulled down
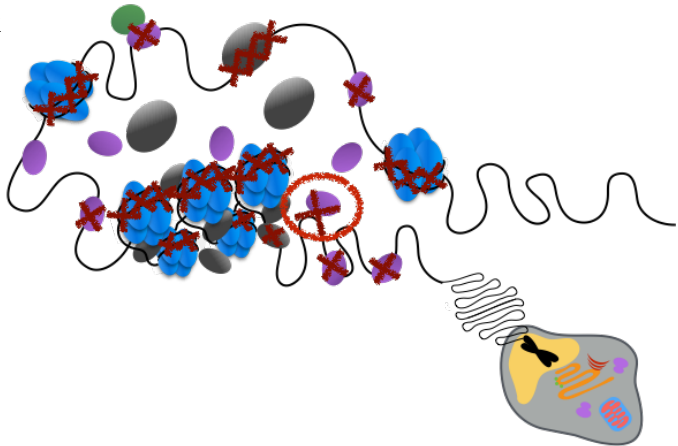
Figure B.3. Issues with fixation. (a) Results of over-fixing. (b) Results of under-fixing.
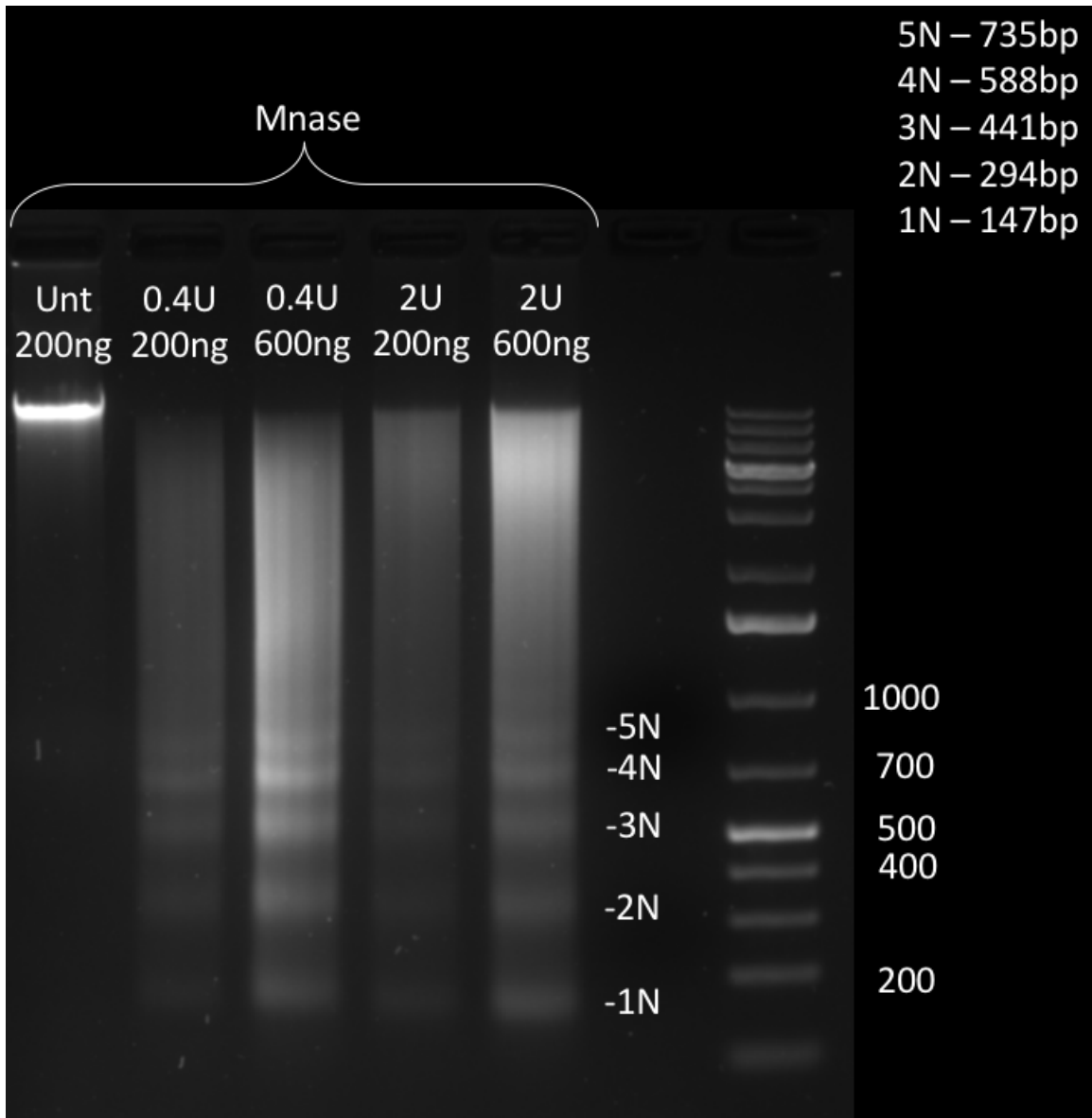
Figure B.4. Digestion of Luc14 chromatin with MNase. Ladder included on the right. Unt = untreated with nuclease. U = units of nuclease. N = nucleosome(s).
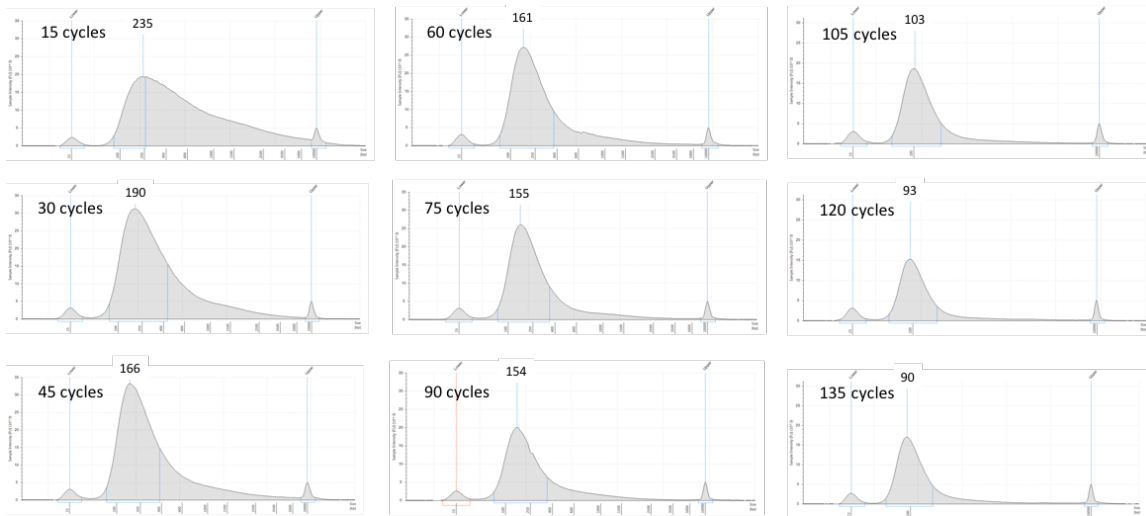
Figure B.5. Chromatograph of sonicated chromatin. Chromatin was sonicated for an increasing number of rounds and run on a bioanalyzer to determine size and amount of DNA.

B.4.3 Quantitative PCR

In order to determine the chromatin state at my target site, I wanted to perform qPCR on my immunoprecipitated DNA. We use Sybr green dye without probes so I first needed to design primer sets against my target sequence and confirm on-target amplification, single product, and primer efficiencies.

B.4.3.1 Design

My first step is to design the primers. Because I have such specific requirements for the sequence I want to amplify, I design primer sets manually, selecting sequences between 20 bp to 25 bp with melting temperatures between 60 °C to 63 °C and no more than 3 °C apart. The primers walk across the indicated sequence range in Figure B.6 a. After designing primer sets, I checked to see if they would amplify any off-target genomic sequences using the NCBI PrimerBLAST tool. Figure B.6 b shows a chart with all of the primer sets and some important sequence characteristics.

B.4.3.2 End-Point PCR

My next step is to perform end-point PCR and run the amplicons on an agarose gel (Figure B.7). This allows me to quickly exclude any primer sets that have additional products.

a

b

Primer pair designation	5' of F primer pos rel to TSS	F primer	F Primer GC%	R primer	R primer GC%	Amplicon length	Ampllicon GC%	Position
1	-430	P197	60	P351	65	144	47.92	Upstream of 5xGal
2	-306	P350	65	P353	65	117	63.25	5xGal
3	-306	P350	65	P352	65	148	62.84	5xGal
4	-209	P165	65	P166	60	126	58.73	Upstream and TK promoter
5	-140	P163	65	P358	55	135	60	TK promoter
6	-140	P163	65	P349	60	137	60.58	TK promoter
7	-129	P359	55	P358	55	124	58.87	TK promoter
8	-129	P359	55	P349	60	126	59.52	TK promoter
9	-114	P357	50	P358	55	109	60.55	TK promoter
10	-114	P357	50	P349	60	111	61.26	TK promoter
11	-99	P153	70	P349	60	96	62.5	TK promoter
12	-99	P153	70	P358	55	94	61.7	TK promoter
13	-75	P355	55	P356	55	144	54.86	TK promoter
14	-33	P149	65	P150	60	132	78.3	across TSS
15	-3	P313	60	P150	60	102	76.1	across TSS
16	-3	P313	60	P348	60	141	51.77	across TSS
17	+12	P308	60	P348	60	126	50.79	just downstream of TSS
18	+18	P227	60	P311	60	145	49.66	just downstream of TSS
19	+23	P309	65	P311	60	140	51.43	just downstream of TSS
20	+31	P360	55	P361	50	135	49.63	just downstream of TSS
21	+31	P360	55	P311	60	132	50.76	just downstream of TSS

Figure B.6.   Primer design steps. (a) qPCR primers were within the region indicated on the *luciferase* transgene map. (b) Primer sets designed for this study.

As you can see in Figure B.7, we can exclude primer sets 3, 11, 12, and 14. However, it is important to note that this will not resolve any primer pairs that have multiple amplicons of similar lengths as those will appear as a single band on the gel.

B.4.3.3   qPCR Dilution Curve

The next step is running qPCR with primers, Sybr, and different dilutions of template DNA, in this case gDNA from Luc14 cells (Figure B.8 a). This test will tell us the sensitivity and efficiency of the primer sets. We also include a melt curve step in our qPCR protocol so we can determine if there are any off-target amplicons and significant primer dimer in the no-template control. While this has higher resolution than the agarose gel step, it still will not tell us if there are multiple amplicons with very similar melting temperatures. The only way to determine this for certain is to clone the amplicons into a plasmid and sequence them.

158
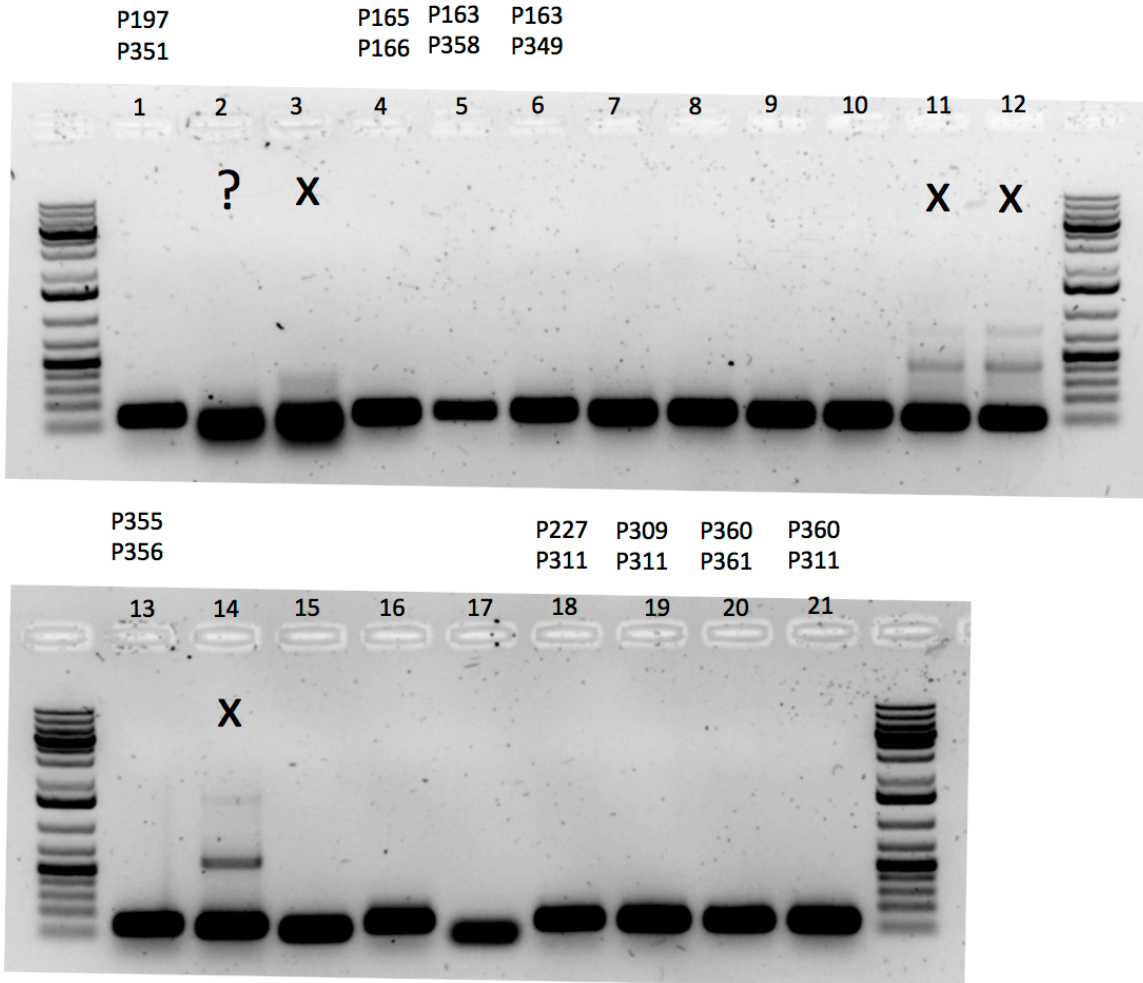
Figure B.7. Agarose gel of end-point PCR products. Primer sets 3, 11, 12, and 14 have multiple products and are thus excluded from further characterization.

Figure B.8 b illustrates part of the concept behind the dilution curve. For primer sets with 100% efficiency and an amplification factor of 2, each round will double the number of amplicons. As it is unlikely that any designed primer set will have 100% efficiency, we calculate the actual efficiency to determine whether the set is appropriate to use for an application as sensitive as qPCR. With a set of known dilutions of starting gDNA, one can calculate the primer efficiency and the amplification factor by graphing the log base 10 of the dilution against the Cp value:

$$\text{Amplification factor} = 10^{\frac{-1}{slope}}$$

$$\text{Efficiency} = (Amplification factor - 1) \times 100$$

Efficiency should be between 90% to 110%.

Figure B.8 illustrates some example curves for different gDNA dilutions. Figure B.8 a shows a primer pair that is not sensitive enough for our application. For ChIP assay, we will be precipitating low concentrations of DNA and thus need very sensitive primers. The three lowest dilutions show the same Cp value of 40, meaning we did not detect a difference in concentration for those three dilutions. Figure B.8 b shows a primer set that is too efficient, meaning it more than doubles the number of amplicons with each cycle. This is apparent after calculating the amplification factor and efficiency. The amplification factor is greater than 2 (2.23) and the efficiency is 123%, outside of our recommended range of 90% to 110%. Figure B.8 c shows a primer set that is under efficient, with amplification factor below 2 and efficiency of 82%. In Figure B.8 d we see three examples of sensitive primers with efficiencies within the acceptable range.

As mentioned above, this step not only tells us the efficiency and sensitivity, but also give a higher-resolution look at any off target amplicons and no-template control amplicons. For off target amplicons, we look for single curves in the melt curve analysis. If we see multiple curves, this means that our primer set is producing multiple products and Cp value will not reflect the concentration of only our desired product; our results will skew to reporting incorrectly higher amounts of starting DNA. For the no-template control, we look to the reported Cp value as well as the melt curve analysis. Interpretation of these results can be a bit more nuanced, depending on the researcher. For some, any product in the no template control is enough to reject a primer set. For others, it may be acceptable to use a primer set that gives a product in the no-template control. For example, say a primer set gives a great dilution curve, with near-perfect efficiency and high sensitivity. The melt curve analysis shows a single product around 86 °C. The no-template control has a Cp value of 40 and a peak in the melt-curve at 54 °C. One could conclude that primer dimer occurs only when no template is present and that any results obtained with only a single peak 86 °C in the melt curve reflect the concentration of the desired product. Any results with two peaks or a single peak at 54 °C should be discarded. In my case, I decided to be more lenient with the no template control products because, with the *luciferase* transgene, there are not many primer sets that meet the other requirements.

B.4.3.4   End-Point PCR with Target-Negative DNA

As I have mentioned above, these tests will not tell you for certain whether you have a single product. It is possible that you have multiple products with overlapping size and melting temperature. For most situations, in order to know for certain that you have a single product, you will need to clone and sequence the PCR products. However, because I am amplifying a transgene and I have the parent cell line that has the identical gDNA
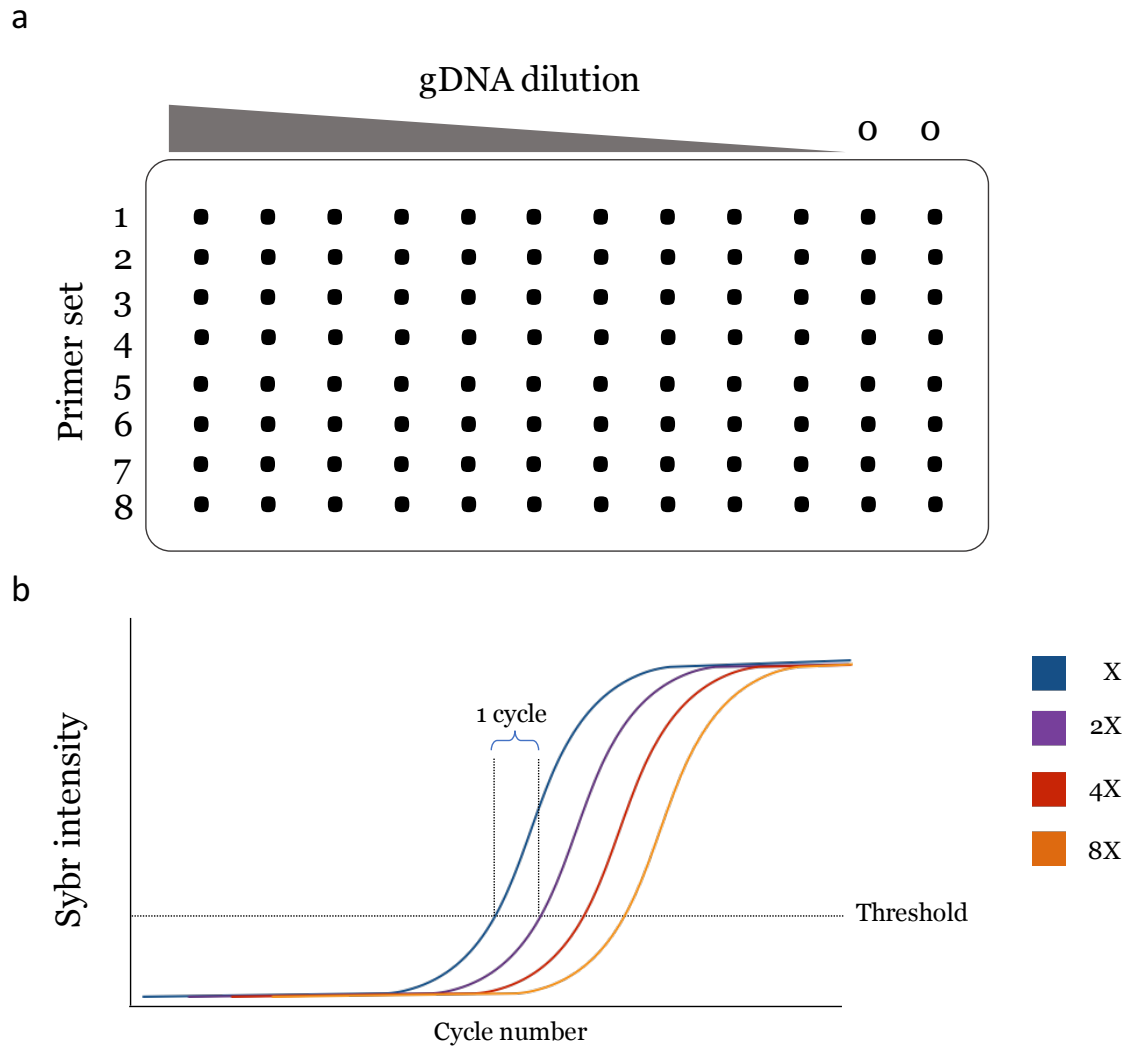
Figure B.8. qPCR dilution curve design. (a) General plate layout for a dilution curve to determine qPCR primer set efficiency. (b) Example curves for different dilutions of gDNA template.
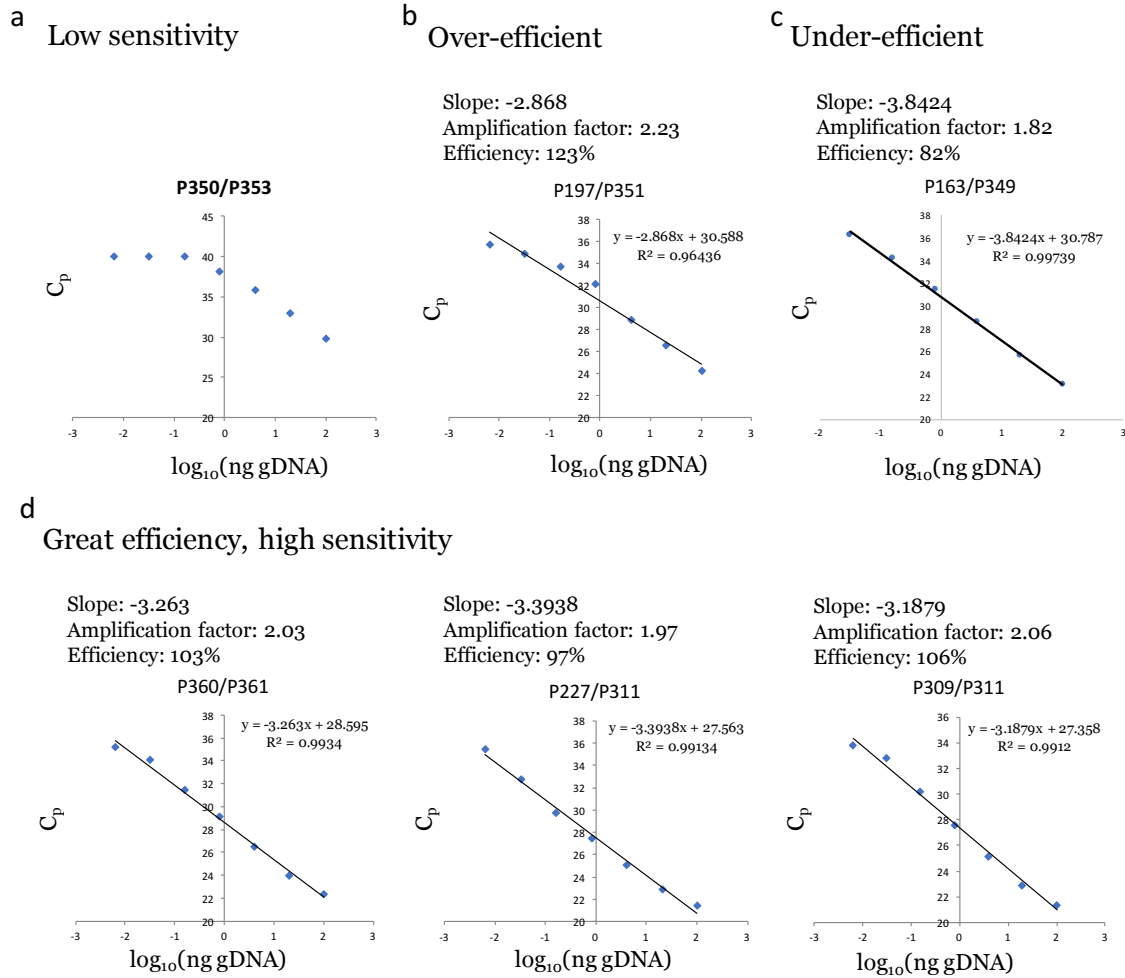
Figure B.9. Subset of primer set dilution curves. (a) This primer set does not detect the lowest dilutions of gDNA and are therefore not sensitive enough. (b) This primer set is over efficient, which means with each cycle, it more than doubles the number of amplicons. This is indicated by the amplification factor of 2.23. (c) This primer set is under efficient. This means with each amplification, it does not double the number of amplicons, as indicated by the amplification factor of 1.82. (d) These three primer sets have ideal efficiency (between 90 percent to 110 percent) and are sensitive to the lowest dilution of gDNA.

Primer #	5' of F primer pos rel to TSS	F primer	R primer	Amplicon length	Amplicon GC%	Position	Taq endpoint PCR gel results (no. of bands)	Efficiency	Extra product Sybr	Sensitivity (Cp at lowest dilution)	Neg ctrl
1	-430	P197	P351	144	47.92	Upstream of 5xGal	1	123.19%	no	high (35)	
2	-306	P350	P353	117	63.25	5xGal	1	-	no	v low (40, 40, 40)	
3	-209	P165	P166	126	58.73	Upstream and TK promoter	1	110.56%	no	high (34.5)	
4	-140	P163	P358	135	60	TK promoter	1	87.85%	no	low (40)	
5	-140	P163	P349	137	60.58	TK promoter	1	82.08%	no	low (no value)	
6	-129	P359	P358	124	58.87	TK promoter	1	-	no	low (40, 40)	
7	-129	P359	P349	126	59.52	TK promoter	1	67.28%	no	low (40, no val)	
8	-114	P357	P358	109	60.55	TK promoter	1	-	yes	-	
9	-114	P357	P349	111	61.26	TK promoter	1	68.01%	no	low (40, 40)	
10	-75	P355	P356	144	54.86	TK promoter	1	76.22%	no	low (40, 40)	
11	-3	P313	P150	102	76.1	across TSS	1	-	yes	-	
12	-3	P313	P348	141	51.77	across TSS	1	weird	probably	-	
13	+12	P308	P348	126	50.79	>TSS	1	-	yes	-	peak
14	+18	P227	P311	145	49.66	>TSS	1	97.09%	no	high (35.5)	maybe
15	+23	P309	P311	140	51.43	>TSS	1	105.91%	no	high (33.78)	
16	+31	P360	P361	135	49.63	>TSS	1	102.52%	no	high (35.16)	peak
17	+31	P360	P311	132	50.76	>TSS	1	107.36%	no	33 then 0	no

Figure B.10. Summary of results after dilution curve test. This chart includes details about each primer pair as well as a summary of the results from the tests performed.

missing only the *luciferase* transgene, I can perform end-point PCR with my primers using the parent cell line gDNA as my template. If I have a product the same band size as my expected amplicon, then I cannot be sure that this amplicon is not present when I amplify gDNA containing the *luciferase* transgene. Figure B.11 shows my end-point PCR results for the subset of primers that showed promising results from the above experiments. Primer sets 1-9 are shown as well as three internal control primer sets. The internal control primers show strong amplification, as expected. Worryingly, many of my *luciferase*-specific primer sets show small products when no *luciferase* DNA is present, most obviously primer sets 2, 3, and 4.

Figure B.12 includes the summary of the results for the subset of the primer sets that passed the initial Taq screen for multiple products. From the original 21 designed primer sets (Figure B.6 b), I am confident in using one primer set, 8. This is not a common outcome but this should demonstrate the importance of testing your primers before proceeding to qPCR.
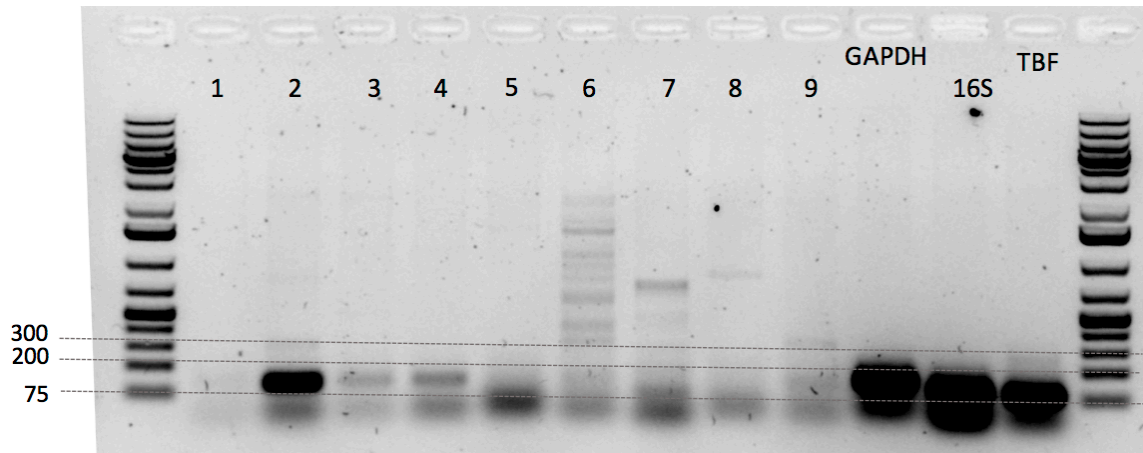
Figure B.11. Agarose gel of PCR with *luciferase*-negative gDNA. End point PCR of primer sets 1-9 with gDNA from the parent cell line for Luc14. Primer pairs for internal control genomic targets GAPDH, 16S, and TBP are also included.

Primer #	smallish amplicon from HEK293 gDNA?	5' of F primer pos rel to TSS	F primer	R primer	Amplicon length	Position	Efficiency	Extra product Sybr	Sensitivity (Cp at lowest dilution)	Neg ctrl
~~1~~	~~no~~	~~-430~~	~~P197~~	~~P351~~	~~144~~	~~Upstream of 5xGal~~	~~123.19%~~	~~no~~	~~high (35)~~	~~no~~
2	yes	-209	P165	P166	126	Upstream and TK	110.56%	no	high (34.5)	yes
3	yes	-140	P163	P358	135	TK promoter	87.85%	no	low (40)	yes
4	yes	-140	P163	P349	137	TK promoter	82.08%	no	low (no value)	yes
5	no	-75	P355	P356	144	TK promoter	76.22%	no	low (40, 40)	no
6	yes	+18	P227	P311	145	just dstream of TSS	97.09%	no	high (35.5)	maybe
7	yes	+23	P309	P311	140	just dstream of TSS	105.91%	no	high (33.78)	maybe
8	no	+31	P360	P361	135	just dstream of TSS	102.52%	no	high (35.16)	no
9	yes	+31	P360	P311	132	just dstream of TSS	107.36%	no	33 then no val	no

Figure B.12. Summary of results after all optimization tests. This chart includes details about each primer pair as well as a summary of the results from all the tests described in this section.

APPENDIX C

SUPPLEMENTAL MATERIAL FOR CHAPTER 3:
ENHANCING CAS9 ACTIVITY IN HETEROCHROMATIN

Table C.1. UNC1999 Kill Curve

Concentration (μM)	Toxicity
0 vehicle	None
1	None
2	None
5	None
10	None
20	Some
50	Toxic

Table C.2. List of Primers for PCR of Genomic DNA from Cas9/sgRNA Treated Samples

Forward Primer		Reverse Primer	
Name	Sequence	Name	Sequence
P197	ctcactcattaggcacccc	P198	cgttggtcgcttccggat

Table C.3. List of Primers for Nested PCR of Genomic DNA from Cas9/sgRNA Treated Samples

gRNA	RNA Site	Forward Primer	Reverse Primer
g046	5'−CCTGCATAAGCTTGCCA | CCA tgg−3'	P355	P311
g032	5'−CCTCTAGAGGATGGAAC | CGC tgg−3'	P163	P348
g025	5'−cct ACC | GTAGTGTTTGTTTCCAA−3'	P332	P330
	3'−TTGGAAACAAACACTAC | GGT agg−5'		
g048	5'−GGATCTACTGGGTTACC | TAA ggg−3'	P314	P318

Table C.4. Sequences for Primers for Nested PCR of Genomic DNA from Cas9/sgRNA Treated Samples

Primer Name	Sequence
P163	CAAACCCCGCCCAGCGTCTTA
P311	CCGCGTACGTGATGTTCACC
P314	CGTTCGTCACATCTCATCTACC
P318	TCCGGAATGATTTGATTGCC
P330	TAGATGAGATGTGACGAACGTG
P332	CGCCCGCGAACGACATTTATAATG
P348	TTGTTCCAGGAACCAGGGCG
P355	TCCGAGGTCCACTTCGCATA

Table C.5. List of Primers for ChIP-qPCR

| qPCR Target Site | Forward Primer | | Reverse Primer | |
	Name	Sequence	Name	Sequence
Luciferase	P360	CGGCGGCCATTCTATCCTCTA	P361	ATTCCGCGTACGTGATGTTC
TBP	P363	CAGGGGTTCAGTGAGGTCG	P364	CCCTGGGTCACTGCAAAGAT

APPENDIX D

CORRIGENDUM: CAN THE NATURAL DIVERSITY OF QUORUM-SENSING ADVANCE SYNTHETIC BIOLOGY?

A corrigendum on Davis, R. M., et al. (2015). Can the Natural Diversity of Quorum-Sensing Advance Synthetic Biology? *Frontiers in Bioengineering and Biotechnology 3*, 1–10, DOI: 10.3389/fbioe.2015.00030.

The gene WP_023917333 was incorrectly used to generate the GtaR protein motif map in Figure 5 of the original publication, which led us to publish erroneous conclusions about GtaR structure and function. At the time this manuscript was published, the gene WP_023917333 was incorrectly titled "LuxR family transcriptional regulator *Rhodobacter capsulatus*" in the NCBI database. Analysis of the correct GtaR protein sequence (WP_013066073) does not show "sequence conservation with TatD family of deoxyribonuclease proteins" nor does it lead us to conclude that GtaR "might represent a unique class of HSL-responsive regulator proteins."

Analysis of the correct protein sequence (WP_013066073) shows GtaR contains the same b–b–a–a–b–a–b–b motif as RhlR, LasR, and SinR. All four regulator proteins, RhlR, LasR, GtaR, and SinR, respond to different ligands: C4-HSL, 3O-C12-HSL, C16-HSL, and C18-HSL, respectively.[173,175–177] We surmise that variations in specific residues may account for the regulator proteins' preferences for different ligands.

The GtaR C-terminus does not match the HTH LuxR-type motif (Prosite PS50043) originally annotated in Figure 5 but does match an "HTH_LuxR" DNA binding motif designated as SMART motif SM00421[213,214] at amino acids 140–197. This motif is present in all the regulators analyzed. Figure 5 now illustrates HTH LuxR regions (SMART SM00421) instead of PS50043. Furthermore, in the original publication the protein motif maps were switched between LasR and AubR, and the SidA map was scaled incorrectly. We have corrected these errors in a new version of Figure 5, shown here.
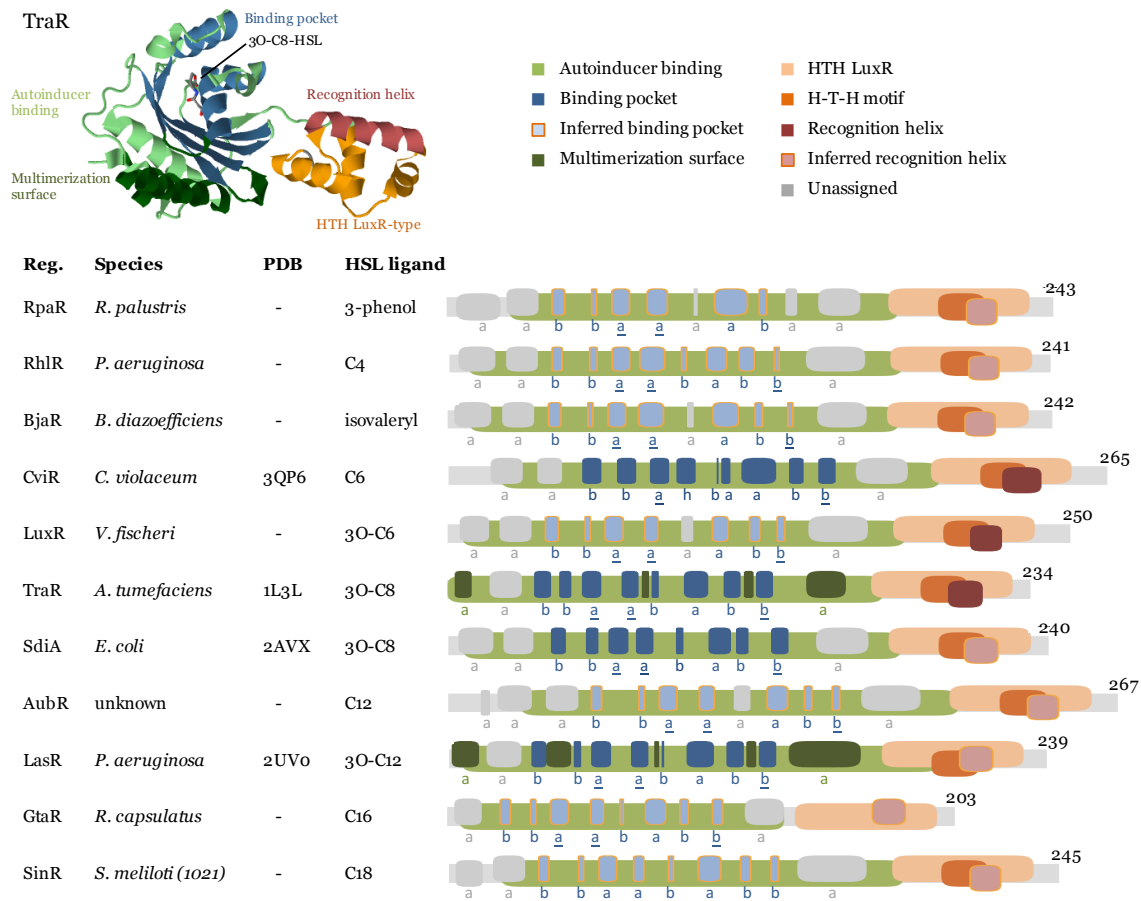
Figure D.1. Comparison of protein motifs in select regulators. The three-dimensional (3D) structure of TraR is shown as an example of how domains and the homoserine lactone (HSL) ligand are typically positioned in space. The underlined letters in the b–b–a–a–b–a–b–b secondary structure motif indicate the location of highly conserved amino acids that form hydrogen bonds with the homoserine lactone head of HSLs. Published 3D structure data (Protein Data Bank) are listed where available ("–" = not available). Abbreviations used are: Reg. = regulator protein, H−T−H = helix−turn−helix, a = alpha helix, b = beta strand, h = 3/10 helix. Database entries for conserved motifs are: autoinducer binding = IPR005143, HTH LuxR = SM00421.[213,214] Inferred binding pockets are patterns of secondary structures that are similar to the TraR binding pocket. Inferred recognition helices are the second alpha helix from the C-terminus. Secondary structures for proteins with no available 3D structure data were mapped using the Jpred prediction tool.[161] Maps were generated using DomainDraw.[162]

170

References

(*92*)   Davis, R. M., Muller, R. Y., and Haynes, K. A., (2015). Can the Natural Diversity of Quorum-Sensing Advance Synthetic Biology? *Frontiers in Bioengineering and Biotechnology 3*, 1–10, DOI: 10.3389/fbioe.2015.00030.

(*161*)   Cole, C., Barber, J. D., and Barton, G. J., (2008). The Jpred 3 secondary structure prediction server. *Nucleic Acids Research 36*, W197–W201, DOI: 10.1093/nar/gkn238.

(*162*)   Fink, J. L., and Hamilton, N., (2007). DomainDraw: a macromolecular feature drawing program. *In silico biology 7*, 145–50.

(*173*)   Geske, G. D. G., Mattmann, M. M. E., and Blackwell, H. E., (2008). Evaluation of a focused library of N-aryl L-homoserine lactones reveals a new set of potent quorum sensing modulators. *Bioorganic & medicinal chemistry letters 18*, 5978–81, DOI: 10.1128/JB.183.1.382–386.2001.

(*175*)   Llamas, I., Keshavan, N., and González, J., (2004). Use of Sinorhizobium meliloti as an indicator for specific detection of long-chain N-acyl homoserine lactones. *Applied and Environmental Microbiology 70*, 3715–3723, DOI: 10.1128/AEM.70.6.3715–3723.2004.

(*176*)   Kumari, A., Pasini, P., Deo, S. K., Flomenhoft, D., Shashidhar, H., and Daunert, S., (2006). Biosensing systems for the detection of bacterial quorum signaling molecules. *Analytical chemistry 78*, 7603–9, DOI: 10.1021/ac061421n.

(*177*)   Leung, M., Brimacombe, C., Spiegelman, G., and Beatty, J., (2012). The GtaR protein negatively regulates transcription of the gtaRI operon and modulates gene transfer agent (RcGTA) expression in Rhodobacter capsulatus. *Molecular microbiology 83*, 759–774, DOI: 10.1111/j.1365-2958.2011.07963.x.

(*212*)   Davis, R. M., Muller, R. Y., and Haynes, K. A., (2015). Corrigendum: Can the Natural Diversity of Quorum-Sensing Advance Synthetic Biology? *Frontiers in Bioengineering and Biotechnology 3*, DOI: 10.3389/fbioe.2015.00099.

(*213*)   Schultz, J., Milpetz, F., Bork, P., and Ponting, C. P., (1998). SMART, a simple modular architecture research tool: Identification of signaling domains. *Proceedings of the National Academy of Sciences 95*, 5857–5864, DOI: 10.1073/pnas.95.11.5857.

(*214*)   Letunic, I., Doerks, T., and Bork, P., (2014). SMART: recent updates, new developments and status in 2015. *Nucleic Acids Research 43*, D257–D260, DOI: 10.1093/nar/gku949.

APPENDIX E

SUPPLEMENTARY MATERIAL FOR CHAPTER 4:
DIVERSITY IN HOMOSERINE LACTONES PRODUCED BY
SYNTHASES ACROSS BACTERIAL SPECIES.

This chart was previously published as supplementary material to Davis et al.[92] It expands on Figure 4.4 in chapter 4.

Figure E.1. Diversity in homoserine lactone (HSL) produced by synthases across bacterial species. Select synthases and representative species are shown in gray boxes. Each row represents one or several HSLs produced by one or more synthase. The number of synthases with each HSL profile is indicated. A (1+) indicates that the exact number of synthases is not known. Hypothetical = cases where one of two molecules with identical mass [i.e., 3O-C(n)-HSL and C(n + 1)-HSL] might be produced by the bacterium, but the molecules could not be resolved with mass spectrometry. * The hypothetical monounsaturated N-dodecanoyl-L-homoserine lactone (C12-HSL) produced by AbaI is not shown here.

Legend

- • Unmodified
- O Carbonyl group at C3 (3O)
- OH Hydroxyl group at C3 (3OH)
- Me Methyl group at C3 (3CH3)
- = Monounsaturated
- == Diunsaturated
- =O Monounsaturated and 3O
- =OH Monounsaturated and 3OH
- Pn Phenol group at C3 (3-phenol)
- Py Phenyl group at C3 (3-phenyl)
- • Trace amounts
- =O Hypothetical

Carbon Chain Length (columns): 3, 4, 5, 6, 7, 8, 9, 10, 11, 12, 13, 14, 15, 16, 17, 18

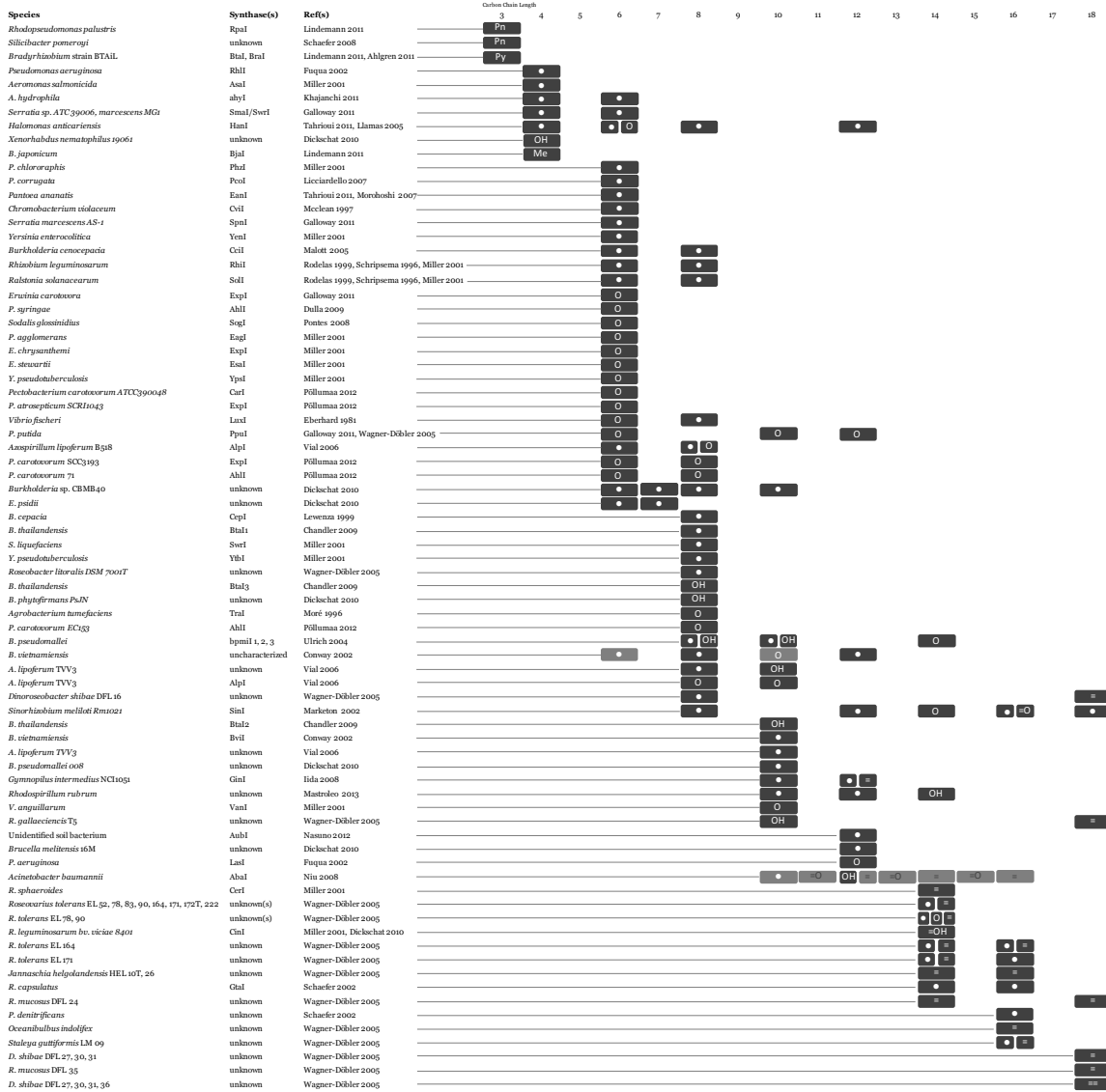| Species	Synthase(s)	Ref(s)
Rhodopseudomonas palustris	RpaI	Lindemann 2011
Silicibacter pomeroyi	unknown	Schaefer 2008
Bradyrhizobium strain BTAi1	BtaI, BraI	Lindemann 2011, Ahlgren 2011
Pseudomonas aeruginosa	RhlI	Fuqua 2002
Aeromonas salmonicida	AsaI	Miller 2001
A. hydrophila	ahyI	Khajanchi 2011
Serratia sp. ATC 39006, marcescens MG1	SmaI/SwrI	Galloway 2011
Halomonas anticariensis	HanI	Tahrioui 2011, Llamas 2005
Xenorhabdus nematophilus 19061	unknown	Dickschat 2010
B. japonicum	BjaI	Lindemann 2011
P. chlororaphis	PhzI	Miller 2001
P. corrugata	PcoI	Licciardello 2007
Pantoea ananatis	EanI	Tahrioui 2011, Morohoshi 2007
Chromobacterium violaceum	CviI	Mcclean 1997
Serratia marcescens AS-1	SpnI	Galloway 2011
Yersinia enterocolitica	YenI	Miller 2001
Burkholderia cenocepacia	CciI	Malott 2005
Rhizobium leguminosarum	RhiI	Rodelas 1999, Schripsema 1996, Miller 2001
Ralstonia solanacearum	SolI	Rodelas 1999, Schripsema 1996, Miller 2001
Erwinia carotovora	ExpI	Galloway 2011
P. syringae	AhlI	Dulla 2009
Sodalis glossinidius	SogI	Pontes 2008
P. agglomerans	EagI	Miller 2001
E. chrysanthemi	ExpI	Miller 2001
E. stewartii	EsaI	Miller 2001
Y. pseudotuberculosis	YpsI	Miller 2001
Pectobacterium carotovorum ATCC390048	CarI	Põllumaa 2012
P. atrosepticum SCRI1043	ExpI	Põllumaa 2012
Vibrio fischeri	LuxI	Eberhard 1981
P. putida	PpuI	Galloway 2011, Wagner-Döbler 2005
Azospirillum lipoferum B518	AlpI	Vial 2006
P. carotovorum SCC3193	ExpI	Põllumaa 2012
P. carotovorum 71	AhlI	Põllumaa 2012
Burkholderia sp. CBMB40	unknown	Dickschat 2010
E. psidii	unknown	Dickschat 2010
B. cepacia	CepI	Lewenza 1999
B. thailandensis	BtaI1	Chandler 2009
S. liquefaciens	SwrI	Miller 2001
Y. pseudotuberculosis	YtbI	Miller 2001
Roseobacter litoralis DSM 7001T	unknown	Wagner-Döbler 2005
B. thailandensis	BtaI3	Chandler 2009
B. phytofirmans PsJN	unknown	Dickschat 2010
Agrobacterium tumefaciens	TraI	Moré 1996
P. carotovorum EC153	AhlI	Põllumaa 2012
B. pseudomallei	bpmiI 1, 2, 3	Ulrich 2004
B. vietnamiensis	uncharacterized	Conway 2002
A. lipoferum TVV3	unknown	Vial 2006
A. lipoferum TVV3	AlpI	Vial 2006
Dinoroseobacter shibae DFL 16	unknown	Wagner-Döbler 2005
Sinorhizobium meliloti Rm1021	SinI	Marketon 2002
B. thailandensis	BtaI2	Chandler 2009
B. vietnamiensis	BviI	Conway 2002
A. lipoferum TVV3	unknown	Vial 2006
B. pseudomallei o08	unknown	Dickschat 2010
Gymnopilus intermedius NCI1051	GinI	Iida 2008
Rhodospirillum rubrum	unknown	Mastroleo 2013
V. anguillarum	VanI	Miller 2001
R. gallaeciencis T5	unknown	Wagner-Döbler 2005
Unidentified soil bacterium	AubI	Nasuno 2012
Brucella melitensis 16M	unknown	Dickschat 2010
P. aeruginosa	LasI	Fuqua 2002
Acinetobacter baumannii	AbaI	Niu 2008
R. sphaeroides	CerI	Miller 2001
Roseovarius tolerans EL 52, 78, 83, 90, 164, 171, 172T, 222	unknown(s)	Wagner-Döbler 2005
R. tolerans EL 78, 90	unknown(s)	Wagner-Döbler 2005
R. leguminosarum bv. viciae 8401	CinI	Miller 2001, Dickschat 2010
R. tolerans EL 164	unknown	Wagner-Döbler 2005
R. tolerans EL 171	unknown	Wagner-Döbler 2005
Jannaschia helgolandensis HEL 10T, 26	unknown	Wagner-Döbler 2005
R. capsulatus	GtaI	Schaefer 2002
R. mucosus DFL 24	unknown	Wagner-Döbler 2005
P. denitrificans	unknown	Schaefer 2002
Oceanibulbus indolifex	unknown	Wagner-Döbler 2005
Staleya guttiformis LM 09	unknown	Wagner-Döbler 2005
D. shibae DFL 27, 30, 31	unknown	Wagner-Döbler 2005
R. mucosus DFL 35	unknown	Wagner-Döbler 2005
D. shibae DFL 27, 30, 31, 36	unknown	Wagner-Döbler 2005

Figure E.1. Continued.

References

(*80*) Case, R. J., Labbate, M., and Kjelleberg, S., (2008). AHL-driven quorum-sensing circuits: their frequency and function among the Proteobacteria. *The ISME journal 2*, 345–9, DOI: 10.1038/ismej.2008.13.

(*81*) Nasuno, E., Kimura, N., Fujita, M. J., Nakatsu, C. H., Kamagata, Y., and Hanada, S., (2012). Phylogenetically Novel LuxI/LuxR-Type Quorum Sensing Systems Isolated Using a Metagenomic Approach. *Applied and Environmental Microbiology 78*, 8067–8074, DOI: 10.1128/AEM.01442-12.

(*92*) Davis, R. M., Muller, R. Y., and Haynes, K. A., (2015). Can the Natural Diversity of Quorum-Sensing Advance Synthetic Biology? *Frontiers in Bioengineering and Biotechnology 3*, 1–10, DOI: 10.3389/fbioe.2015.00030.

(*193*) Marketon, M. M., Gronquist, M. R., Eberhard, A., and González, J. E., (2002). Characterization of the Sinorhizobium meliloti sinR/sinI locus and the production of novel N-acyl homoserine lactones. *Journal of bacteriology 184*, 5686–95, DOI: 10.1128/JB.184.20.5686.

(*215*) Ahlgren, N. a., Harwood, C. S., Schaefer, A. L., Giraud, E., and Greenberg, E. P., (2011). Aryl-homoserine lactone quorum sensing in stem-nodulating photosynthetic bradyrhizobia. *Proceedings of the National Academy of Sciences 108*, 7183–7188, DOI: 10.1073/pnas.1103821108.

(*216*) Chandler, J., Duerkop, B., Hinz, A., West, T., Herman, J., Churchill, M., Skerrett, S., and Greenberg, E., (2009). Mutational Analysis of Burkholderia thailandensis Quorum Sensing and Self-Aggregation. *Journal of bacteriology 191*, 5901–9, DOI: 10.1128/JB.00591-09.

(*217*) Conway, B., and Greenberg, E., (2002). Quorum-Sensing Signals and Quorum-Sensing Genes in Burkholderia vietnamiensis. *Journal of bacteriology 184*, 1187–91, DOI: 10.1128/JB.184.4.1187–1191.2002.

(*218*) Dulla, G. F. J., and Lindow, S. E., (2009). Acyl-homoserine lactone-mediated cross talk among epiphytic bacteria modulates behavior of Pseudomonas syringae on leaves. *The ISME journal 3*, 825–34, DOI: 10.1038/ismej.2009.30.

(*219*) Eberhard, A., Burlingame, A. L., Eberhard, C., Kenyon, G. L., Nealson, K. H., and Oppenheimer, N. J., (1981). Structural identification of autoinducer of Photobacterium fischeri luciferase. *Biochemistry 20*, 2444–2449, DOI: 10.1021/bi00512a013.

(*220*) Fuqua, C., and Greenberg, E. P., (2002). Signalling: Listening in on bacteria: acyl-homoserine lactone signalling. *Nature Reviews Molecular Cell Biology 3*, 685–695, DOI: 10.1038/nrm907.

(*221*)   Galloway, W. R. J. D., Hodgkinson, J. T., Bowden, S. D., Welch, M., and Spring, D. R., (2011). Quorum Sensing in Gram-Negative Bacteria: Small-Molecule Modulation of AHL and AI-2 Quorum Sensing Pathways. *Chemical reviews 111*, 28–67, DOI: 10.1021/cr100109t..

(*222*)   Iida, A., Ohnishi, Y., and Horinouchi, S., (2008). An OmpA family protein, a target of the GinI/GinR quorum-sensing system in Gluconacetobacter intermedius, controls acetic acid fermentation. *Journal of bacteriology 190*, 5009–19, DOI: 10.1128/JB.00378-08.

(*223*)   Khajanchi, B. K., Kirtley, M. L., Brackman, S. M., and Chopra, A. K., (2011). Immunomodulatory and protective roles of quorum-sensing signaling molecules N-acyl homoserine lactones during infection of mice with Aeromonas hydrophila. *Infection and immunity 79*, 2646–57, DOI: 10.1128/IAI.00096-11.

(*224*)   Lewenza, S., Conway, B., Greenberg, E. P., and Sokol, P. A., (1999). Quorum sensing in Burkholderia cepacia: identification of the LuxRI homologs CepRI. *Journal of bacteriology 181*, 748–56.

(*225*)   Licciardello, G., Bertani, I., Steindler, L., Bella, P., Venturi, V., and Catara, V., (2007). Pseudomonas corrugata contains a conserved N-acyl homoserine lactone quorum sensing system; its role in tomato pathogenicity and tobacco hypersensitivity response. *FEMS microbiology ecology 61*, 222–34, DOI: 10.1111/j.1574-6941.2007.00338.x.

(*226*)   Llamas, I., Quesada, E., Martínez-Cánovas, M. J., Gronquist, M., Eberhard, A., and González, J. E., (2005). Quorum sensing in halophilic bacteria: detection of N-acyl-homoserine lactones in the exopolysaccharide-producing species of Halomonas. *Extremophiles : life under extreme conditions 9*, 333–41, DOI: 10.1007/s00792-005-0448-1.

(*227*)   Malott, R. J., Baldwin, A., Mahenthiralingam, E., and Sokol, P. A., (2005). Characterization of the cciIR quorum-sensing system in Burkholderia cenocepacia. *Infection and immunity 73*, 4982–92, DOI: 10.1128/IAI.73.8.4982-4992.2005.

(*228*)   Mastroleo, F., Van Houdt, R., Atkinson, S., Mergeay, M., Hendrickx, L., Wattiez, R., and Leys, N., (2013). Modelled microgravity cultivation modulates N-acylhomoserine lactone production in Rhodospirillum rubrum S1H independently of cell density. *Microbiology (Reading, England) 159*, 2456–66, DOI: 10.1099/mic.0.066415-0.

(*229*)   Mcclean, K. H., Winson, M. K., Fish, L., Taylor, A., Chhabra, S. R., Camara, M., Daykin, M., Lamb, J. H., Swift, S., Bycroft, B. W., Stewart, G. S. A. B., and Williams, P., (1997). Quorum sensing and Chromobacterium violaceum: exploitation of violacein production and inhibition for the detection of N-acyl homoserine lactones. *Microbiology (Reading, England) 143*, 3703–3711, DOI: 10.1099/00221287-143-12-3703.

(*230*)   Moré, M. I., Finger, L. D., Stryker, J. L., Fuqua, C., Eberhard, A., and Winans, S. C., (1996). Enzymatic Synthesis of a Quorum-Sensing Autoinducer Through Use of Defined Substrates. *Science 272*, 1655–1658, DOI: 10.1126/science.272.5268.1655.

(*231*)   Morohoshi, T., Nakamura, Y., Yamazaki, G., Ishida, A., N, K., and Ikeda, T., (2007). The Plant Pathogen Pantoea ananatis Produces N-Acylhomoserine Lactone and Causes Center Rot Disease of Onion by Quorum Sensing. *Journal of bacteriology 189*, 8333–8, DOI: 10.1128/JB.01054-07.

(*232*)   Niu, C., Clemmer, K., Bonomo, R., and Rather, P., (2008). Isolation and Characterization of an Autoinducer Synthase from Acinetobacter baumannii. *Journal of bacteriology 190*, 3386–92, DOI: 10.1128/JB.01929-07.

(*233*)   Pontes, M., Babst, M., Lochhead, R., Oakeson, K., Smith, K., and Dale, C., (2008). Quorum Sensing Primes the Oxidative Stress Response in the Insect Endosymbiont, Sodalis glossinidius. *PLOS ONE 3*, e3541, DOI: 10.1371/journal.pone.0003541.

(*234*)   Rodelas, B., Lithgow, J. K., Wisniewski-Dye, F., Hardman, A., Wilkinson, A., Economou, A., Williams, P., and Downie, J. A., (1999). Analysis of quorum-sensing-dependent control of rhizosphere-expressed (rhi) genes in Rhizobium leguminosarum bv. viciae. *Journal of bacteriology 181*, 3816–23.

(*235*)   Schaefer, A. L., Greenberg, E. P., Oliver, C. M., Oda, Y., Huang, J. J., Bittan-Banin, G., Peres, C. M., Schmidt, S., Juhaszova, K., Sufrin, J. R., and Harwood, C. S., (2008). A new class of homoserine lactone quorum-sensing signals. *Nature 454*, 595–9, DOI: 10.1038/nature07088.

(*236*)   Schaefer, A., Taylor, T., Beatty, J., and Greenberg, E., (2002). Long-Chain Acyl-Homoserine Lactone Quorum-Sensing Regulation of Rhodobacter capsulatus Gene Transfer Agent Production. *Journal of Bacteriology 184*, 6515–6521, DOI: 10.1128/JB.184.23.6515-6521.2002.

(*237*)   Schripsema, J., de Rudder, K. E., van Vliet, T. B., Lankhorst, P. P., de Vroom, E., Kijne, J. W., and van Brussel, A. A., (1996). Bacteriocin small of Rhizobium leguminosarum belongs to the class of N-acyl-L-homoserine lactone molecules, known as autoinducers and as quorum sensing co-transcription factors. *Journal of bacteriology 178*, 366–71.

(*238*)   Tahrioui, A., Quesada, E., and Llamas, I., (2011). The hanR/hanI quorum-sensing system of Halomonas anticariensis, a moderately halophilic bacterium. *Microbiology (Reading, England) 157*, 3378–87, DOI: 10.1099/mic.0.052167-0.

(*239*)   Ulrich, R. L., Deshazer, D., Brueggemann, E., Hines, H., Oyston, P., and Jeddeloh, J., (2004). Role of quorum sensing in the pathogenicity of Burkholderia pseudomallei. *Journal of Medical Microbiology 53*, 1053–1064, DOI: 10.1099/jmm.0.45661-0.

(*240*)   Vial, L., Cuny, C., Gluchoff-Fiasson, K., Comte, G., Oger, P. M., Faure, D., Dessaux, Y., Bally, R., and Wisniewski-Dyé, F., (2006). N-acyl-homoserine lactone-mediated quorum-sensing in Azospirillum: an exception rather than a rule. *FEMS microbiology ecology 58*, 155–68, DOI: 10.1111/j.1574-6941.2006.00153.x.

(*241*)   Wagner-Döbler, I., Thiel, V., Eberl, L., Allgaier, M., Bodor, A., Meyer, S., Ebner, S., Hennig, A., Pukall, R., and Schulz, S., (2005). Discovery of complex mixtures of novel long-chain quorum sensing signals in free-living and host-associated marine alphaproteobacteria. *Chembiochem : a European journal of chemical biology 6*, 2195–206, DOI: 10.1002/cbic.200500189.

APPENDIX F

AUTHORSHIP AND CONTRIBUTIONS TO CHAPTERS 2, 3, 4, AND 5

F.1 Chapter 2: The Impact of Chromatin Dynamics on Cas9-Mediated Genome Editing in Human Cells
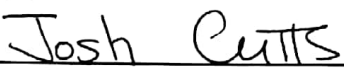
Authors of the published manuscript: René Daer (RMD), Josh Cutts (JPC), David Brafman (DAB), Karmella Haynes (KAH)

I grant René Daer permission to use our published manuscript titled, *The impact of chromatin dynamics on Cas9-mediated genome editing in human cells* as a chapter in her thesis.
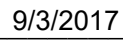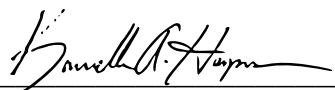
_____
Signature

_____Josh Cutts_____
Name

_____9/7/17_____
Date

I grant René Daer permission to use our published manuscript titled, *The impact of chromatin dynamics on Cas9-mediated genome editing in human cells* as a chapter in her thesis.

_____
Signature

_____David Brafman_____
Name

_____9/3/2017_____
Date

I grant René Daer permission to use our published manuscript titled, *The impact of chromatin dynamics on Cas9-mediated genome editing in human cells* as a chapter in her thesis.

(signature)

Signature

Karmella A. Haynes

Name

09/10/17

Date

F.2 Chapter 3: Enhancing Cas9 Activity in Heterochromatin

René Daer - RMD Karmella Haynes - KAH

RMD produced all the data in this chapter. RMD and KAH analyzed the data and composed the figures and text.

F.3 Chapter 4: Can the Natural Diversity of Quorum-Sensing Advance Synthetic Biology?

Authors of the published manuscript: René Davis (Daer) (RMD), Ryan Muller (RYM), Karmella Haynes (KAH).

RMD, RYM, and KAH analyzed the data and composed the figures and text.

I grant René Daer permission to use our published manuscript titled, *Can the natural diversity of quorum-sensing advance synthetic biology?* as a chapter in her thesis.
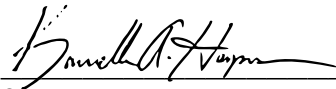
_____
Signature

Ryan Muller
_____
Name

Sept. 02, 2017
_____
Date

I grant René Daer permission to use our published manuscript titled, *Can the natural diversity of quorum-sensing advance synthetic biology?* as a chapter in her thesis.

_____
Signature

Karmella A. Haynes
_____
Name

09/10/17
_____
Date

F.4   Chapter 5: Diverse Acyl-homoserine Lactone Synthases Activate the Lux Quorum Sensing Regulator in *Escherichia coli*

René Daer (RMD), Cassandra Barrett (CMB), Ernesto Luna (EL), Jiaqi Wu (JW), Stefan Tekel (ST), Ryan Muller (RYM), Karmella Haynes (KAH)

RMD and KAH conceived of the project. RMD and CMB managed the project. RMD, CMB, and KAH analyzed the data and prepared the figures and manuscript. RMD, CMB, EL, JW, and ST designed the experiments. RMD, CMB, JW, and RYM cloned the plasmids. The data in Figure 5.8, Figure 5.9, and Figure 5.11 were produced by ST. All other data were produced or gathered from the literature by RMD.